THE SIGNIFICANCE OF MITOGENOMICS IN MYCOLOGY

EDITED BY: Tomasz Kulik, Anne D. Van Diepeningen and Georg Hausner
PUBLISHED IN: Frontiers in Microbiology

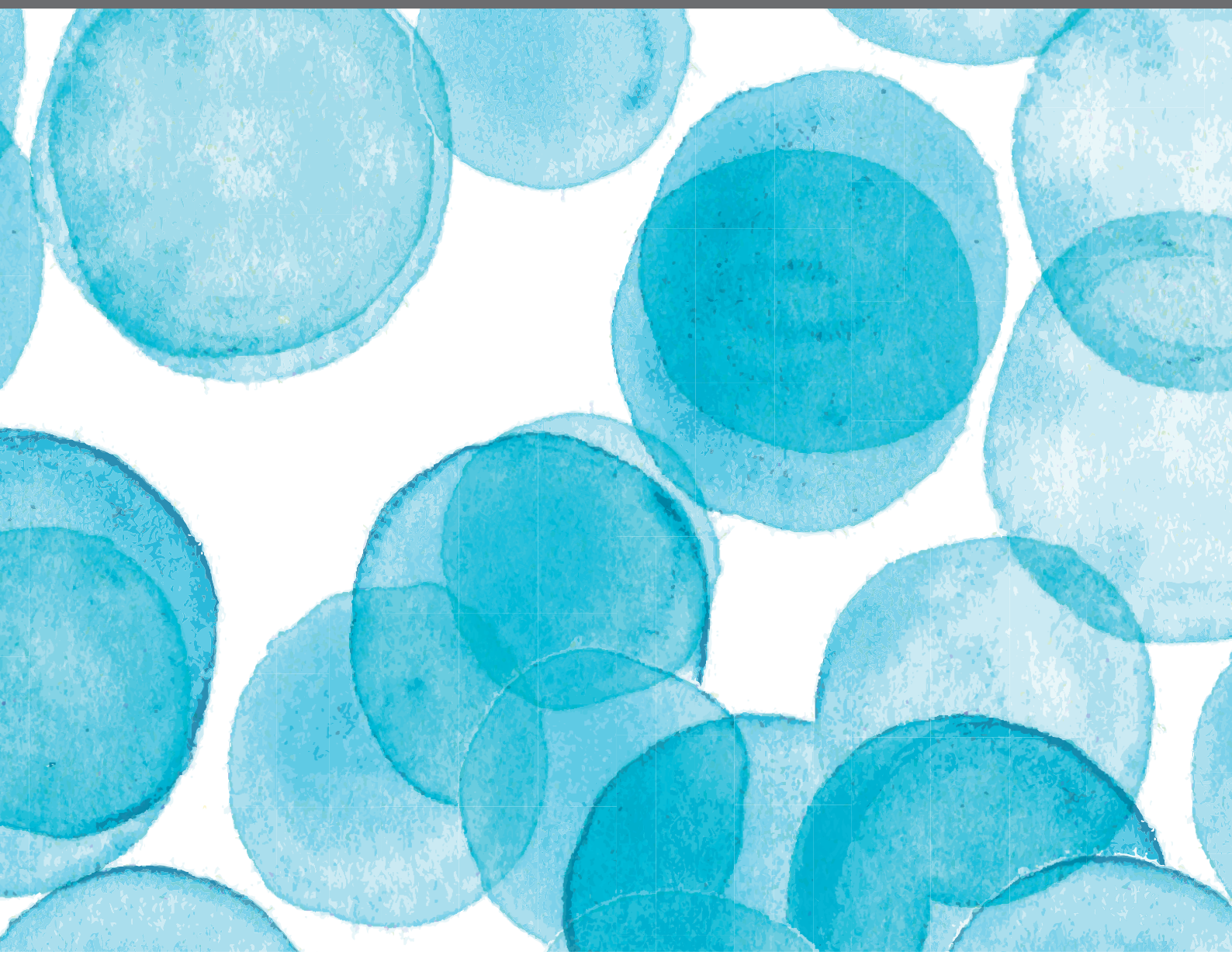

frontiers Research Topics

frontiers

ISSN 1664-8714
ISBN 978-2-88966-479-5
DOI 10.3389/978-2-88966-479-5

About Frontiers

Frontiers is more than just an open-access publisher of scholarly articles: it is a pioneering approach to the world of academia, radically improving the way scholarly research is managed. The grand vision of Frontiers is a world where all people have an equal opportunity to seek, share and generate knowledge. Frontiers provides immediate and permanent online open access to all its publications, but this alone is not enough to realize our grand goals.

Frontiers Journal Series

The Frontiers Journal Series is a multi-tier and interdisciplinary set of open-access, online journals, promising a paradigm shift from the current review, selection and dissemination processes in academic publishing. All Frontiers journals are driven by researchers for researchers; therefore, they constitute a service to the scholarly community. At the same time, the Frontiers Journal Series operates on a revolutionary invention, the tiered publishing system, initially addressing specific communities of scholars, and gradually climbing up to broader public understanding, thus serving the interests of the lay society, too.

Dedication to Quality

Each Frontiers article is a landmark of the highest quality, thanks to genuinely collaborative interactions between authors and review editors, who include some of the world's best academicians. Research must be certified by peers before entering a stream of knowledge that may eventually reach the public - and shape society; therefore, Frontiers only applies the most rigorous and unbiased reviews.
Frontiers revolutionizes research publishing by freely delivering the most outstanding research, evaluated with no bias from both the academic and social point of view. By applying the most advanced information technologies, Frontiers is catapulting scholarly publishing into a new generation.

What are Frontiers Research Topics?

Frontiers Research Topics are very popular trademarks of the Frontiers Journals Series: they are collections of at least ten articles, all centered on a particular subject. With their unique mix of varied contributions from Original Research to Review Articles, Frontiers Research Topics unify the most influential researchers, the latest key findings and historical advances in a hot research area! Find out more on how to host your own Frontiers Research Topic or contribute to one as an author by contacting the Frontiers Editorial Office: frontiersin.org/about/contact

THE SIGNIFICANCE OF MITOGENOMICS IN MYCOLOGY

Topic Editors:
Tomasz Kulik, University of Warmia and Mazury in Olsztyn, Poland
Anne D. Van Diepeningen, Wageningen University and Research, Netherlands
Georg Hausner, University of Manitoba, Canada

Citation: Kulik, T., Van Diepeningen, A. D., Hausner, G., eds. (2021).
The Significance of Mitogenomics in Mycology. Lausanne: Frontiers Media SA.
doi: 10.3389/978-2-88966-479-5

Table of Contents

04 ***Editorial: The Significance of Mitogenomics in Mycology***
Tomasz Kulik, Anne D. Van Diepeningen and Georg Hausner

08 ***Comparative Analyses of Mitochondrial Genomes Provide Evolutionary Insights Into Nematode-Trapping Fungi***
Ying Zhang, Guangzhu Yang, Meiling Fang, Chu Deng, Ke-Qin Zhang, Zefen Yu and Jianping Xu

21 ***Mitochondrial Genome Polymorphisms in the Human Pathogenic Fungus* Cryptococcus neoformans**
Yue Wang and Jianping Xu

37 ***Exploring the Relationship Among Divergence Time and Coding and Non-coding Elements in the Shaping of Fungal Mitochondrial Genomes***
Paula L. C. Fonseca, Fernanda Badotti, Ruth B. De-Paula, Daniel S. Araújo, Dener E. Bortolini, Luiz-Eduardo Del-Bem, Vasco A. Azevedo, Bertram Brenig, Eric R. G. R. Aguiar and Aristóteles Góes-Neto

54 ***Population Genomic Analysis Reveals a Highly Conserved Mitochondrial Genome in* Fusarium asiaticum**
Meixin Yang, Hao Zhang, Theo A. J. van der Lee, Cees Waalwijk, Anne D. van Diepeningen, Jie Feng, Balázs Brankovics and Wanquan Chen

67 ***The Mitochondrial Genome of the Phytopathogenic Fungus* Bipolaris sorokiniana *and the Utility of Mitochondrial Genome to Infer Phylogeny of Dothideomycetes***
Nan Song, Yuehua Geng and Xinghao Li

83 ***Diversity of Mobile Genetic Elements in the Mitogenomes of Closely Related* Fusarium culmorum *and* F. graminearum *sensu stricto Strains and Its Implication for Diagnostic Purposes***
Tomasz Kulik, Balazs Brankovics, Anne D. van Diepeningen, Katarzyna Bilska, Maciej Żelechowski, Kamil Myszczyński, Tomasz Molcan, Alexander Stakheev, Sebastian Stenglein, Marco Beyer, Matias Pasquali, Jakub Sawicki, Joanna Wyrębek and Anna Baturo-Cieśniewska

97 ***Fungal Mitogenomes: Relevant Features to Planning Plant Disease Management***
Rocio Medina, Mario Emilio Ernesto Franco, Laura Cecilia Bartel, Virginia Martinez Alcántara, Mario Carlos Nazareno Saparrat and Pedro Alberto Balatti

112 ***Detecting Introgression Between Members of the* Fusarium fujikuroi *and* F. oxysporum *Species Complexes by Comparative Mitogenomics***
Balázs Brankovics, Anne D. van Diepeningen, G. Sybren de Hoog, Theo A. J. van der Lee and Cees Waalwijk

frontiers in Microbiology

EDITORIAL
published: 07 January 2021
doi: 10.3389/fmicb.2020.628579

Editorial: The Significance of Mitogenomics in Mycology

Tomasz Kulik[1]*, *Anne D. Van Diepeningen*[2] and *Georg Hausner*[3]

[1] Department of Botany and Nature Protection, University of Warmia and Mazury in Olsztyn, Olsztyn, Poland, [2] B.U. Biointeractions and Plant Health, Wageningen Plant Research, Wageningen University & Research, Wageningen, Netherlands, [3] Department of Microbiology, University of Manitoba, Winnipeg, MB, Canada

Keywords: fungi, mitochondrion, mitochondrial DNA, homing endonuclease, evolution

Editorial on the Research Topic

The Significance of Mitogenomics in Mycology

Fungi are a diverse group of eukaryotic organisms, ranging from unicellular yeasts to multicellular filamentous microorganisms and mushrooms, with beneficial and harmful effects to human health and the environment (Wu et al., 2019). Fungal diversity encompasses a broad range of taxa and associated differences in morphology, ecology, and life history strategies (Hyde et al., 2019; Naranjo-Ortiz and Gabaldón, 2020).

Like other eukaryotes, fungi contain mitochondria that are responsible for ATP synthesis and perform many biological tasks in fungal cells ranging from the production of chemical energy to synthesis of protein co-factors, and fatty acid, heme, and iron-sulfur cluster biosynthesis. To date, however, most of our knowledge on mitochondrial function/dysfunction comes from studies on *Saccharomyces cerevisiae*, which shows a high tolerance to mutations inactivating oxidative phosphorylation and the loss of mtDNA (Malina et al., 2018). This is in contrast to filamentous fungi that are obligate aerobes and the presence of functional mtDNA is essential.

The mitochondrial respiration chain has been linked to adaptation of fungi to oxygen-limited conditions or oxidative stress during certain phases of their life cycle, which explains the ability of fungi to survive in different environments and their potential to shift to different modes of living (Marcet-Houben et al., 2009; Grahl et al., 2012). Besides coping with oxidative stress, fungal pathogenicity, virulence, and mycotoxin production have been linked to mitochondrial morphology, integrity (Tang et al., 2018) and dynamics (Neubauer et al., 2015), and fission and fusion of mitochondria (Verma et al., 2018) and their overall implication in a range of vital cellular functions appear to be the common denominators underlying these processes (Medina et al.).

Mitochondria have been found to confer drug tolerance in both human and plant fungal pathogens. The mechanisms of resistance are complex and can occur at many different levels, however lipid homeostasis in mitochondria (Shingu-Vazquez and Traven, 2011) and mutations in genes encoding proteins that are involved in mitochondrial processes (Mosbach et al., 2017) appear to play the most important role in drug resistance of fungi. On the other hand, considering the importance of mitochondria in numerous cellular tasks, it is not surprising that mitochondrial pathways have been considered important targets for developing fungicides (Hahn, 2014; Mosbach et al., 2017; Young et al., 2018; Carmona et al., 2020; Medina et al.).

Fungal mitochondria harbor their own genome (mitogenome), with genetic codes different from the nuclear genome. The mitogenome is responsible for the proper functioning of the cells and stability of nuclear genome. On the other hand, to sustain their functions and integrity, mitochondria require communication with the nuclear genome (Kaniak-Golik and Skoneczna, 2015). In fungi, the majority of mitochondrial proteins are encoded in the nuclear genome, produced in the cytosol as precursors, and imported into the mitochondria (Bolender et al., 2008).

OPEN ACCESS

Edited by:
Levente Kiss, University of Southern Queensland, Australia

Reviewed by:
Eric Roberto Guimarães Rocha Aguiar, Universidade Estadual de Santa Cruz, Brazil

***Correspondence:**
Tomasz Kulik
tomaszkulik76@gmail.com

Specialty section:
This article was submitted to Fungi and Their Interactions, a section of the journal Frontiers in Microbiology

Received: *12 November 2020*
Accepted: *10 December 2020*
Published: *07 January 2021*

Citation:
Kulik T, Van Diepeningen AD and Hausner G (2021) Editorial: The Significance of Mitogenomics in Mycology. Front. Microbiol. 11:628579. doi: 10.3389/fmicb.2020.628579

The *S. cerevisiae* mitochondrial proteome includes around 1,000 proteins, while 438 have been identified in *N. crassa* using proteomic studies (Ambrosio et al., 2013).

The typical fungal mitogenome of Ascomycota and Basidiomycota (dikarya fungi) contains 14 protein-coding genes (atp6, 8, and 9; cob; cox1– 3; and nad1– 6, 4L), the rnL and rnS genes, and usually from 20 to 31 of trn genes. The *R*ps3 gene encoding the ribosomal protein S3 can be also be found in many fungal mitogenomes. Fungi show variation in gene content. For example, mitogenomes of yeasts (family Saccharomycetaceae) lack and genes (Freel et al., 2015). In addition, a patchy distribution of the rnpB gene encoding the RNA subunit of the mitochondrial RNAse P is also frequently observed. In Ascomycota, mitochondrial genes are generally encoded in one strand, but in both strands in Basidiomycota (Zardoya, 2020).

Nearly all mechanisms responsible for maintaining the nuclear genome integrity, such as mismatch repair, base excision repair, and double-strand break repair via homologous recombination or the non-homologous end-joining pathway, also occur to maintain mtDNA stability (Kaniak-Golik and Skoneczna, 2015). In fungi, the mutation rate in mtDNA is usually lower than in nuclear genomes (De Chiara et al., 2020). However, it is worth noting that the mutation rate in mtDNA appears to be dependent upon the fungal group studied. For example, in plant pathogenic *Rhynchosporium* species the mutation rate in mtDNA was proved to be higher than in nuclear genomes (Torriani et al., 2014), however, the mechanisms underlying this variation remain unclear. It has been suggested that the higher mutation rate of mtDNA could be due to poor effectiveness of the mtDNA repair system due to the nearby production of reactive oxygen species (Mendoza et al., 2020). Mitogenomes can display increased variation due to gene rearrangements caused by mitogenome recombination (Aguileta et al., 2014). Fungal mitogenomes may also differ in gene order and composition, pseudogene content and tandem repeats in intergenic regions (Aguileta et al., 2014; Fonseca et al.). Among the other explanations of mitogenome variability in fungi are double-stranded RNA elements and the frequent mobility of present self-splicing introns (Wu and Hao, 2019; Mendoza et al., 2020).

The most frequently encountered introns in fungal mitogenomes are group I introns that can encode homing endonucleases (HEGs) with either LAGLIDADG or GIY-YIG motifs. Intron encoded proteins catalyze intron mobility and have been shown in some instances to act as maturases enhancing the splicing of introns (Hausner, 2003). Distribution of these introns is irregular among different lineages and their irregular distribution has also been observed at the strain level. On the other hand, the same introns and associated HEGs may also be present in mitogenomes of evolutionarily distant lineages (Hausner, 2003). Their irregular distribution in fungi is often explained with "early intron" or "late intron" evolutionary contradicting hypotheses. The first one supports that introns were introduced to eukaryotes at an early stage of their evolution, and a general evolutionary process dominated toward the loss of introns (Goddard and Burt, 1999). The second hypothesis suggests more recent intron expansion even between diverse species through horizontal transfer (Gonzalez et al., 1998). Both hypotheses could be proven based on the most recent pan genomic approach, which indicated an intron-rich ancestor of fungi as well as the existence of intron-late events through a range of recombinational events that resulted from both vertical and horizontal gene transmissions (Megarioti and Kouvelis, 2020). Although mitochondrial introns have been viewed by many as neutral elements (Goddard and Burt, 1999) recent studies are suggesting some introns may impact mitochondrial gene expression (Rudan et al., 2018), virulence in some fungal pathogens (Baidyaroy et al., 2011; Medina et al.), and resistance to certain fungicides (Cinget and Bélanger, 2020). With regards to fungi pathogenic toward humans, as group I introns are not found in mammalian genomes, they are starting to be explored as fungal specific druggable RNA targets (Gomes et al., 2018).

Fungal mitogenomes are usually represented as circular molecules, although linear versions with defined telomeric ends, and versions existing as linear concatemers have been reported (Bullerwell and Lang, 2005; Valach et al., 2011), and they can range in size from 12.055 bp to 500 kbp (James et al., 2013; Liu et al., 2020). The size variation is in part due to introns, intergenic spacers, plasmid insertions, partial duplications, and in some instances the proliferation of repeats (Hausner, 2003; Liu et al., 2020). Patterns of variation in mtDNA provide genetic information that is often sufficiently variable for comparative genomics as well as for evolutionary studies of fungi. The use of genomic data has greatly promoted the development of taxonomy and phylogenetic relationships of fungi, leading to the taxonomic revisions and the identification of new species. However, it is worth to note that despite molecular dating, some of fungal lineages still hold an uncertain phylogenetic position (Naranjo-Ortiz and Gabaldón, 2020). Characterization of mitogenome patterns may help to resolve these questions. Some recent examples of new phylogenetic insights were derived from studies in nematode-trapping fungi (Zhang et al.), the commercialized edible mushroom *Hypsizygus marmoreus* (Wang et al., 2019), and ectomycorrhizal fungi from the genus Rhizopogon (Li et al., 2019). It is worth noting however, that estimating phylogenetic relationships of fungi based on both mitogenome and nuclear phylogenies can be difficult due to their highly discordant evolutionary trajectories (De Chiara et al., 2020).

In population genetic studies on fungi, mitogenomic analyses may give different results from nuclear genome analyses, indicating nucleus and organelle may evolve via different trajectories. Wolters et al. (2015) revealed that the distribution of mitochondrial introns in *S. cerevisiae* had population-specific profiles. However, further work by De Chiara et al. (2020) showed that despite high mtDNA polymorphism, mitochondrial population structure poorly reflects the clustering based on nuclear data, which indicated that in yeasts both nuclear and mitochondrial genomes are affected by outbreeding. The limitations of mitogenomics in population surveys have been recently underlined in studies on plant pathogenic Fusaria. Comparative analysis of strains from worldwide field populations did not reveal a link between mitogenome variation and the

geographic origin of the populations mostly due to high sequence conservation and ancestral origin of introns and associated HEGs (Kulik et al.).

Mitogenomics shows promise in the field of fungal diagnostics. Efficient detection of fungi is difficult due to the inefficient recovery of genomic DNA for PCR, mostly due to the very low and uneven distribution of fungal biomass in tested samples and difficult to disrupt chitinous cell wall (Bilska et al., 2018). Markers developed on the basis of mitochondrial sequences provide a highly sensitive detection of fungi due to the multi-copy nature of mitogenomes. It has been also noted that mitochondrial DNA may be useful in deciphering cryptic species diversity (Kulik et al., 2020). However, development of novel diagnostic assays requires their evaluation in terms of uniformity and specificity against a test panel of different target and non-target fungi. This requires a continuously updating of knowledge on both fungal taxonomy and mitogenome variation. Continued investment in sequencing of both nuclear and mitochondrial genomes is necessary to open up dimensions for improved diagnostics, which should be consistent with the actual taxonomic/natural classification of fungi.

Mitogenomics can also bring new insights into the mechanisms on mitochondrial functioning, fungal pathogenicity, virulence and drug resistance. Fungi, still belong to a group of largely unexplored microorganisms in terms of integrative proteomic and genomic approaches for understanding mitochondrial processes (Ambrosio et al., 2013; Medina et al.). Today, there are a lot of open questions regarding the mitochondrial proteome and its role in the dynamic modulation of these organelle (Ambrosio et al., 2013; Mendoza et al., 2020). Mitochondrial inheritance has been explored in only a few fungal species (*S. cerevisiae*, *Cryptococcus neoformans, Microbotryum violaceum,* and *Ustilago maydis*) and these studies provided evidence for a large variation in inheritance mechanisms (Mendoza et al., 2020). We believe that the outlined knowledge gaps that exists in the field of fungal mitogenomics will stimulate the posting of additional questions that will promote research on the diverse cellular functions and roles of mitochondria in various fungal systems. Deciphering molecular mechanisms underlying these processes requires an integrative approach (mitogenomics, transcriptomics, and proteomics) combined with the knowledge on mitogenome structure and organization.

We are very proud of this special issue on the "Significance of Mitogenomics in Mycology" and would like to thank all contributors for submitting their cutting-edge research to it. All readers we wish a pleasant update on the possibilities and impossibilities of fungal mitogenomics in a varied range of fungal species.

AUTHOR CONTRIBUTIONS

All authors listed have made a substantial, direct and intellectual contribution to the work, and approved it for publication.

REFERENCES

Aguileta, G., De Vienne, D. M., Ross, O. N., Hood, M. E., Giraud, T., Petit, E., et al. (2014). High variability of mitochondrial gene order among fungi. *Genome Biol. Evol.* 6, 451–465. doi: 10.1093/gbe/evu028

Ambrosio, A. B., do Nascimento, L. C., Oliveira, B. V., L., Teixeira, P. J. P., Tiburcio, R. A., Toledo Thomazella, D. P., et al. (2013). Global analyses of Ceratocystis cacaofunesta mitochondria: from genome to proteome. *BMC Genomics* 14:913. doi: 10.1186/1471-2164-14-91

Baidyaroy, D., Hausner, G., Hafez, M., Michel, F., Fulbright, D. W., and Bertrand, H. (2011). A 971-bp insertion in the rns gene is associated with mitochondrial hypovirulence in a strain of Cryphonectria parasitica isolated from nature. *Fungal Genet. Biol.* 48, 775–783. doi: 10.1016/j.fgb.2011.05.006

Bilska, K., Kulik, T., Ostrowska-Kołodziejczak, A., Buśko, M., Pasquali, M., Beyer, M., et al. (2018). Development of a highly sensitive FcMito qPCR assay for the quantification of the toxigenic fungal plant pathogen Fusarium culmorum. *Toxins*10:211. doi: 10.3390/toxins10050211

Bolender, N., Sickmann, A., Wagner, R., Meisinger, C., and Pfanner, N. (2008). Multiple pathways for sorting mitochondrial precursor proteins. *EMBO Rep.* 9, 42–49. doi: 10.1038/sj.embor.7401126

Bullerwell, C. E., and Lang, B. F. (2005). Fungal evolution: the case of the vanishing mitochondrion. *Curr. Opin. Microbiol.* 8, 362–369. doi: 10.1016/j.mib.2005.06.009

Carmona, M., Sautua, F., Pérez-Hérnandez, O., and Reis, E. M. (2020). Role of fungicide applications on the integrated management of wheat stripe rust. *Front. Plant Sci.* 11:733. doi: 10.3389/fpls.2020.00733

Cinget, B., and Bélanger, R. R. (2020). Discovery of new group I-D introns leads to creation of subtypes and link to an adaptive response of the mitochondrial genome in fungi. *RNA Biol.* 17, 1252–1260. doi: 10.1080/15476286.2020.1763024

De Chiara, M., Friedrich, A., Barré, B., Breitenbach, M., Schacherer, J., and Liti, G. (2020). Discordant evolution of mitochondrial and nuclear yeast genomes at population level. *BMC Biol.* 18:49. doi: 10.1186/s12915-020-00786-4

Freel, K. C., Friedrich, A., and Schacherer, J. (2015). Mitochondrial genome evolution in yeasts: an all-encompassing view. *FEMS Yeast Res.* 15:fov023. doi: 10.1093/femsyr/fov023

Goddard, M. R., and Burt, A. (1999). Recurrent invasion and extinction of a selfish gene. *Proc. Natl. Acad. Sci. U.S.A.* 96, 13880–13885. doi: 10.1073/pnas.96.24.13880

Gomes, F. E. E. S., Arantes, T. D., Fernandes, J. A. L., Ferreira, L. C., Romero, H., Bosco, S. M. G., et al. (2018). Polymorphism in mitochondrial group I introns among *Cryptococcus neoformans* and *Cryptococcus gattii* genotypes and its association with drug susceptibility. *Front. Microbiol.* 9:86. doi: 10.3389/fmicb.2018.00086

Gonzalez, P., Barroso, G., and Labarère, J. (1998). Molecular analysis of the split cox1 gene from the Basidiomycota Agrocybe aegerita: relationship of its introns with homologous Ascomycota introns and divergence levels from common ancestral copies. *Gene* 220, 45–53. doi: 10.1016/S0378-1119(98)00421-1

Grahl, N., Dinamarco, T. M., Willger, S. D., Goldman, G. H., and Cramer, R. A. (2012). *Aspergillus fumigatus* mitochondrial electron transport chain mediates oxidative stress homeostasis, hypoxia responses and fungal pathogenesis. *Mol. Microbiol.* 84, 383–399. doi: 10.1111/j.1365-2958.2012.08034.x

Hahn, M. (2014). The rising threat of fungicide resistance in plant pathogenic fungi: Botrytis as a case study. *J. Chem. Biol.* 7, 133–141. doi: 10.1007/s12154-014-0113-1

Hausner, G. (2003). "Fungal mitochondrial genomes, plasmids and introns," in *Applied Mycology and Biotechnology Volume III: Fungal Genomics*. eds D. K. Arora and G. G. Khachatourians, (Amsterdam: Elsevier Science), 101–131. doi: 10.1016/S1874-5334(03)80009-6

Hyde, K. D., Xu, J., Rapior, S., Jeewon, R., Lumyong, S., Niego, A. G. T., et al. (2019). The amazing potential of fungi: 50 ways we can exploit fungi industrially. *Fungal Divers.* 97, 1–136. doi: 10.1007/s13225-019-00430-9

James, T. Y., Pelin, A., Bonen, L., Ahrendt, S., Sain, D., Corradi, N., et al. (2013). Shared signatures of parasitism and phylogenomics unite cryptomycota and microsporidia. *Curr. Biol.* 23, 1548–1553. doi: 10.1016/j.cub.2013.06.057

Kaniak-Golik, A., and Skoneczna, A. (2015). Mitochondria-nucleus network for genome stability. *Free Radic. Biol. Med.* 82, 73–104. doi: 10.1016/j.freeradbiomed.2015.01.013

Kulik, T., Bilska, K., and Zelechowski, M. (2020). Promising perspectives for detection, identification, and quantification of plant pathogenic fungi and oomycetes through targeting mitochondrial DNA. *Int. J. Mol. Sci.* 21:2645. doi: 10.3390/ijms21072645

Li, Q., Ren, Y., Shi, X., Peng, L., Zhao, J., Song, Y., et al. (2019). Comparative mitochondrial genome analysis of two ectomycorrhizal fungi (Rhizopogon) reveals dynamic changes of intron and phylogenetic relationships of the subphylum agaricomycotina. *Int. J. Mol. Sci.* 20:5167. doi: 10.3390/ijms20205167

Liu, W., Cai, Y., Zhang, Q., Shu, F., Chen, L., Ma, X., et al. (2020). Subchromosome-scale nuclear and complete mitochondrial genome characteristics of Morchella crassipes. *Int. J. Mol. Sci.* 21:483. doi: 10.3390/ijms21020483

Malina, C., Larsson, C., and Nielsen, J. (2018). Yeast mitochondria: an overview of mitochondrial biology and the potential of mitochondrial systems biology. *FEMS Yeast Res.* 18:40. doi: 10.1093/femsyr/foy040

Marcet-Houben, M., Marceddu, G., and Gabaldán, T. (2009). Phylogenomics of the oxidative phosphorylation in fungi reveals extensive gene duplication followed by functional divergence. *BMC Evol. Biol.* 9:295. doi: 10.1186/1471-2148-9-295

Megarioti, A. H., and Kouvelis, V. N. (2020). The coevolution of fungal mitochondrial introns and their homing endonucleases (GIY-YIG and LAGLIDADG). *Genome Biol. Evol.* 12, 1337–1354. doi: 10.1093/gbe/evaa126

Mendoza, H., Perlin, M. H., and Schirawski, J. (2020). Mitochondrial inheritance in phytopathogenic fungi—everything is known, or is it? *Int. J. Mol. Sci.* 21, 1–21. doi: 10.3390/ijms21113883

Mosbach, A., Edel, D., Farmer, A. D., Widdison, S., Barchietto, T., Dietrich, R. A., et al. (2017). Anilinopyrimidine resistance in *Botrytis cinerea* is linked to mitochondrial function. *Front. Microbiol.* 8:2361. doi: 10.3389/fmicb.2017.02361

Naranjo-Ortiz, M. A., and Gabaldón, T. (2020). Fungal evolution: cellular, genomic and metabolic complexity. *Biol. Rev.* 95:brv.12605. doi: 10.1111/brv.12605

Neubauer, M., Zhu, Z., Penka, M., Helmschrott, C., Wagener, N., and Wagener, J. (2015). Mitochondrial dynamics in the pathogenic mold *Aspergillus fumigatus*: therapeutic and evolutionary implications. *Mol. Microbiol.* 98, 930–945. doi: 10.1111/mmi.13167

Rudan, M., Dib, P. B., Musa, M., Kanunnikau, M., Sobočanec, S., Rueda, D., et al. (2018). Normal mitochondrial function in *Saccharomyces cerevisiae* has become dependent on inefficient splicing. *Elife* 7:e35330. doi: 10.7554/eLife.35330

Shingu-Vazquez, M., and Traven, A. (2011). Mitochondria and fungal pathogenesis: drug tolerance, virulence, and potential for antifungal therapy. *Eukaryot. Cell* 10, 1376–1383. doi: 10.1128/EC.05184-11

Tang, G., Zhang, C., Ju, Z., Zheng, S., Wen, Z., Xu, S., et al. (2018). The mitochondrial membrane protein FgLetm1 regulates mitochondrial integrity, production of endogenous reactive oxygen species and mycotoxin biosynthesis in Fusarium graminearum. *Mol. Plant Pathol.* 19, 1595–1611. doi: 10.1111/mpp.12633

Torriani, S. F. F., Penselin, D., Knogge, W., Felder, M., Taudien, S., Platzer, M., et al. (2014). Comparative analysis of mitochondrial genomes from closely related Rhynchosporium species reveals extensive intron invasion. *Fungal Genet. Biol.* 62, 34–42. doi: 10.1016/j.fgb.2013.11.001

Valach, M., Farkas, Z., Fricova, D., Kovac, J., Brejova, B., Vinar, T., et al. (2011). Evolution of linear chromosomes and multipartite genomes in yeast mitochondria. *Nucleic Acids Res.* 39, 4202–4219. doi: 10.1093/nar/gkq1345

Verma, S., Shakya, V. P. S., and Idnurm, A. (2018). Exploring and exploiting the connection between mitochondria and the virulence of human pathogenic fungi. *Virulence* 9, 426–446. doi: 10.1080/21505594.2017.1414133

Wang, G., Lin, J., Shi, Y., Chang, X., Wang, Y., Guo, L., et al. (2019). Mitochondrial genome in *Hypsizygus marmoreus* and its evolution in Dikarya. *BMC Genomics* 20, 765. doi: 10.1186/s12864-019-6133-z

Wolters, J. F., Chiu, K., and Fiumera, H. L. (2015). Population structure of mitochondrial genomes in *Saccharomyces cerevisiae*. *BMC Genomics* 16:451. doi: 10.1186/s12864-015-1664-4

Wu, B., and Hao, W. (2019). Mitochondrial-encoded endonucleases drive recombination of protein-coding genes in yeast. *Environ. Microbiol.* 21, 4233–4240. doi: 10.1111/1462-2920.14783

Wu, B., Hussain, M., Zhang, W., Stadler, M., Liu, X., and Xiang, M. (2019). Current insights into fungal species diversity and perspective on naming the environmental DNA sequences of fungi. *Mycology* 10, 127–140. doi: 10.1080/21501203.2019.1614106

Young, D. H., Wang, N. X., Meyer, S. T., and Avila-Adame, C. (2018). Characterization of the mechanism of action of the fungicide fenpicoxamid and its metabolite UK-2A. *Pest Manag. Sci.* 74, 489–498. doi: 10.1002/ps.4743

Zardoya, R. (2020). Recent advances in understanding mitochondrial genome diversity. *F1000Res.* 9:270. doi: 10.12688/f1000research.21490.1

Conflict of Interest: The authors declare that the research was conducted in the absence of any commercial or financial relationships that could be construed as a potential conflict of interest.

frontiers in Microbiology

ORIGINAL RESEARCH
published: 15 April 2020
doi: 10.3389/fmicb.2020.00617

Comparative Analyses of Mitochondrial Genomes Provide Evolutionary Insights Into Nematode-Trapping Fungi

Ying Zhang[1], Guangzhu Yang[1,2], Meiling Fang[1,2], Chu Deng[1,2], Ke-Qin Zhang[1], Zefen Yu[1] and Jianping Xu[1,3]**

[1] State Key Laboratory for Conservation and Utilization of Bio-Resources in Yunnan, and Key Laboratory for Southwest Microbial Diversity of the Ministry of Education, Yunnan University, Kunming, China, [2] School of Life Sciences, Yunnan University, Kunming, China, [3] Department of Biology, McMaster University, Hamilton, ON, Canada

Predatory fungi in Orbiliaceae (Ascomycota) have evolved a diversity of trapping devices that enable them to trap and kill nematodes, other small animals, and protozoans. These trapping devices include adhesive hyphae, adhesive knobs, adhesive networks, constricting rings, and non-constricting rings. Their diversity and practical importance have attracted significant attention from biologists, making them excellent model organisms for studying adaptative evolution and as biological control agents against parasitic nematodes. The putative origins and evolutionary relationships among these carnivorous fungi have been investigated using nuclear protein-encoding genes, but their patterns of mitogenome relationships and divergences remain unknown. Here we analyze and compare the mitogenomes of 12 fungal strains belonging to eight species, including six species representing all four types of nematode trapping devices and two from related but non-predatory fungi. All 12 analyzed mitogenomes were of circular DNA molecules, with lengths ranging from 146,101 bp to 280,699 bp. Gene synteny analysis revealed several gene rearrangements and intron transfers among the mitogenomes. In addition, the number of protein coding genes (PCGs), GC content, AT skew, and GC skew varied among these mitogenomes. The increased number and total size of introns were the main contributors to the length differences among the mitogenomes. Phylogenetic analyses of the protein-coding genes indicated that mitochondrial and nuclear genomes evolved at different rates, and signals of positive selection were found in several genes involved in energy metabolism. Our study provides novel insights into the evolution of nematode-trapping fungi and shall facilitate further investigations of this ecologically and agriculturally important group of fungi.

Keywords: entomopathogenic fungi, anamorphic Orbiliaceae, mitochondrial phylogeny, adaptive evolution, rps3

OPEN ACCESS

Edited by:
Tomasz Kulik,
University of Warmia and Mazury in Olsztyn, Poland

Reviewed by:
Yongjie Zhang,
Shanxi University, China
Cloe Pogoda,
University of Colorado Boulder, United States

****Correspondence:***
Zefen Yu
zfyuqm@hotmail.com
Jianping Xu
jpxu@mcmaster.ca;
jpxumcmaster@gmail.com

Specialty section:
This article was submitted to Fungi and Their Interactions, a section of the journal Frontiers in Microbiology

Received: *25 January 2020*
Accepted: *19 March 2020*
Published: *15 April 2020*

Citation:
Zhang Y, Yang G, Fang M, Deng C, Zhang K-Q, Yu Z and Xu J (2020) Comparative Analyses of Mitochondrial Genomes Provide Evolutionary Insights Into Nematode-Trapping Fungi. Front. Microbiol. 11:617. doi: 10.3389/fmicb.2020.00617

INTRODUCTION

Nematode-trapping fungi (NTF) are a taxonomically heterogeneous group of asexual ascomycetes that can form special structures (traps) to capture free-living nematodes in soil (Barron, 1977). Members of the Orbiliaceae family represent the largest group of NTF, which include at least 96 species belonging to genera *Arthrobotrys* (53 species, producing adhesive three-dimensional

networks), *Dactylellina* (28 species, producing adhesive knobs, non-constricting rings, and adhesive column), and *Drechslerella* (14 species, producing constricting rings) (Zhang and Hyde, 2014). These NTF species were originally defined based primarily on conidial characteristics such as size, septation, and type of conidiogenous cells (Subramanian, 1963). Recent research showed that trapping devices are also phylogenetically informative for classifying NTF species (Rubner, 1996; Scholler et al., 1999; Li et al., 2005; Yang and Liu, 2006; Yang et al., 2007).

Because of their unique life style and potential as biocontrol agents against parasitic nematodes, NTF have been studied over several decades. Those studies cover a range of topics, including their substrate preference, the origin and development of trapping devices, and the molecular mechanisms of pathogenesis against nematodes. Previous studies based on multiple nuclear gene phylogeny indicated that the trapping mechanisms within the Orbiliales have evolved along two major lineages, one leading to species with constricting rings and the other to species with adhesive traps, including three-dimensional networks, adhesive knobs, and adhesive branches (Yang et al., 2007). Furthermore, molecular clock calibration based on two fossil records estimated that the two major lineages diverged from each other ∼246 million years ago (Mya) (Yang et al., 2012).

So far, the genome sequences of several NTF have been obtained, assembled, and annotated, including strains from *Arthrobotrys conoides, Arthrobotrys oligospora*, *Dactylellina appendiculata, Dactylellina drechsleri, Dactylellina haptotyla, Drechslerella stenobrocha,* and *Dactylellina cionopaga.* Such a rich dataset has made it possible for evolutionary studies at the genomic level (Zhang W. et al., 2016). Genome sequence comparisons have shown that NTF tend to have expanded gene families coding chitin-degrading enzymes and proteases, possess a well-developed cellulose-degrading metabolism, but have relatively few plant pathogenesis-related genes. Together, these features are consistent with their saprotrophic ancestry (Liu et al., 2014). However, nothing is known about the evolutionary patterns and divergences of NTF from the mitochondrial genomic perspective.

Mitochondria are energy-generating organelles that play a critical role in numerous cellular functions, including ATP production, cellular homeostasis, and apoptosis (Wallace, 2005). Due to their distinct genome structure, inheritance pattern, and rates of evolution, mitochondrial genomes (mitogenomes) have been frequently used in evolutionary biology and systematic studies (Pantou et al., 2006; Kouvelis et al., 2008; Basse, 2010). However, among the estimated 2.2–3.8 million fungal species (Hawksworth and Lücking, 2017), only 375 records of fungal mitogenomes are published by the end of 2019[1]. These mitogenomes show a large variation in genome size, ranging from 12,055 bp in *Rozella allomycis* to 19,431 bp in the fission yeast *Schizosaccharomyces pombe* (Chen and Butow, 2005) and 235,849 bp in the common filamentous plant pathogen *Rhizoctonia solani* (Losada et al., 2014). Despite the large genome size variation, the fungal mitogenomes usually contain 14 genes that encode oxidative phosphorylation system proteins, the large (rnl) and small (rns) ribosomal RNA subunits, and a fairly constant set of tRNA genes (Gray et al., 1999; Lavín et al., 2008). The major contributor to the large genome size variations among the fungal mitogenomes are the varying number of introns, as well as the genes within those introns such as the endonuclease genes containing either the GIY-YIG or the LAGLIDADG motifs (Wu et al., 2009; Mardanov et al., 2014; Sandor et al., 2018). So far, most of these mitogenomes have been reported separately and there have been very few comparative analyses of mitogenomes of a specific group of fungi, including NTF.

In this study, we analyzed the complete mitochondrial genomes of six NTF species representing all four types of nematode trapping devices and two other closely related species incapable of forming any nematode trapping devices. To provide a better understanding of the mitogenomic diversity among NTF, for two species *A. oligospora* and *Drechslerella brochopaga*, we also analyzed the mitogenomes from four and two natural isolates, respectively. The 12 mitogenomes were annotated, and their gene contents, structures, and gene orders were compared to assess variation and conservation among NTF strains and species. All the mitogenomes we analyzed are largely syntenic, but the size and the intron content differ greatly. The Ka/Ks ratios obtained clearly suggested that though purifying selection was the dominant force driving the evolution of most protein-coding genes, signals of positive selection were found for several genes across NTF species. Our comparative analyses of mitogenomes of NTF provide an important foundation for future studies on NTF population genetics, taxonomy, mechanisms of trap formation, and biocontrol application.

MATERIALS AND METHODS

Sampling, DNA Extraction, and Genome Sequencing

The published mitochondrial genomes of six NTF species representing all four types of nematode trapping devices were analyzed and compared with each other as well as with two closely related species but are incapable of producing any nematode trapping devices (Jiang et al., 2018; Zhou et al., 2018; Deng and Yu, 2019a,b; Fang et al., 2019; Li and Yu, 2019; Wang S. et al., 2019; Zhang and Yu, 2019). In addition to the nine published mitogenomes, we generated the mitogenome sequences of three more natural strains of *A. oligospora* and included them for both inter- and intra-species comparisons among NTFs (**Table 1**). All the strains and species were identified based on their morphological features and their sequences at the internal transcribed spacer (ITS) regions of the ribosomal RNA gene cluster (Zhang Y. et al., 2016). To obtain their mitogenome sequences, their total genomic DNA was extracted from the mycelia collected from single-spore cultures growing on cellophane membrane on PDA according to the method described by Zhang et al. (2011). Sequencing libraries and the whole genome sequencing were performed with an Illumina HiSeq 2500 Platform by Novegene Co., Ltd. (Beijing, China).

[1]https://www.ncbi.nlm.nih.gov/genomes/GenomesGroup.cgi?opt=organelle&taxid4751&sort=Genome

TABLE 1 | Mitogenome features in six nematode-trapping fungal species and two related non-predatory species.

Species	Trapping devices*	Strains	Gen Bank No.	Genome Size	GC content(%)	Intron size	Exon size	IntronNo.															Tot.	tRNA No.	ORF	Intron I	Intron II
								cob	cox1	cox2	cox3	nad1	nad2	nad3	nad4	nad4L	nad5	nad6	atp6	atp8	atp9	rps3	rnpB					
Arthrobotrys oligospora(AO83)	AN	YMF1.01883	MK571436	160613	24.97	71121	12249	3	12	7	3	2	4	0	2	0	1	0	1	0	0	1	0	35	24	41	20	0
Arthrobotrys oligospora(AO75)	AN	YMF1.02775	MN977365	155181	25.15	78430	12982	3	12	7	3	2	3	0	2	0	2	0	2	0	0	0	0	36	26	49	8	0
Arthrobotrys oligospora(AO65)	AN	YMF1.02765	MN977364	159392	25.14	80982	13157	4	15	7	3	2	2	1	2	0	3	0	2	0	0	0	0	41	25	63	14	0
Arthrobotrys oligospora(AO37)	AN	YMF1.03037	MN977366	165815	24.86	79479	12640	2	11	6	3	2	3	0	2	0	2	0	1	0	0	0	0	32	25	53	12	0
Arthrobotrys musiformis(AM)	AN	YMF1.03721	MK547645	179060	24.61	82220	14055	4	13	1	5	3	0	0	2	0	7	1	2	0	1	0	0	39	18	51	23	2
Drechslerella brochopaga(DB29)	CR	YMF1.01829	MK820635	280699	26	177801	12948	4	12	4	9	3	4	0	2	0	9	1	2	0	1	1	1	51	28	77	9	1
Drechslerella brochopaga(DB16)	CR	YMF1.03216	MK550698	193195	25.84	91902	12053	5	7	5	4	0	1	1	0	0	5	0	0	0	0	1	0	28	22	59	16	0
Dactylellina leptospora(DL)	AK&NCR	YMF1.00042	MK307795	201677	25.11	101927	12594	5	7	8	8	4	6	1	2	0	5	0	3	0	1	0	0	50	25	71	21	1
Dactylellina haptotyla(DH)	AK&NCR	CBS200.50	MK554671	146101	22.92	63920	12834	5	7	4	4	1	1	1	1	0	5	1	2	0	0	0	1	32	25	42	23	0
Dactylellina cionopagum(DC)	AC	YMF1.00569	MK307796	194125	26.6	96838	13675	7	11	2	7	4	4	1	2	0	4	0	3	0	1	0	1	46	25	56	25	2
Dactylella tenuis(DT)	NONE	YMF1.00469	MK820634	186056	26.21	89297	12660	6	8	3	8	0	5	1	1	0	7	0	1	0	1	1	1	41	24	51	20	1
Dactylella dorsalia(DD)	NONE	YMF1.01835	MK547647	191042	25.3	107237	12361	6	17	6	6	2	5	0	2	0	8	1	2	0	0	0	1	55	25	85	26	0

**AN, adhesive networks; AK & NCR, adhesive knobs and non-constricting rings; CR, constricting rings; AC, adhesive column; NONE, no trapping device produced.*

Assembly and Annotation of Mitochondrial Genomes

The sequencing, assembly, and annotation for nine of the 12 mitogenomes analyzed in this study have been described previously (Jiang et al., 2018; Zhou et al., 2018; Deng and Yu, 2019a,b; Fang et al., 2019; Li and Yu, 2019; Wang S. et al., 2019; Zhang and Yu, 2019). To assemble and annotate the three remaining mitogenomes of *A. oligospora* strains, their mitogenome sequence reads were first identified for homology with the published *A. oligospora* mitogenome (GenBank accession number MK571436) using the NCBI BLAST algorithm. For each strain, all mitogenome reads were extracted from the whole genome sequencing data according to our previously described methods (Deng and Yu, 2019a). We then used the SPAdes 3.9.0 software with a kmer size of 17 to *de novo* assemble the three *A. oligospora* strains' mitogenomes with the obtained clean reads (Bankevich et al., 2012). The gaps were filled by separate PCR and sequencing with primers on regions flanking the gaps, resulting in one circular mitochondrial genome for each strain. The mitogenomes were annotated using both MFannot[2] and GLIMMER[3]. The tRNAs were identified and annotated using tRNAscan-SE (Brooks and Lowe, 2005). All ORFs were searched and identified by ORFFinder[4]. Syntenic blocks in all 12 mitogenomes were identified using MAUVE 2.3.1 based on whole mitogenome sequence alignments (Darling et al., 2004). For each strain, we determined the relative synonymous codon usage (RSCU) in 14 mitochondrial protein coding genes (PCGs) using CodonW1.4.2[5] with the fungal mitochondrial genetic code 4. The following formulas were used to assess mitogenome strand asymmetry: AT skew = [A − T]/[A + T]; GC skew = [G − C]/[G + C].

The non-synonymous (Ka) and synonymous substitution rates (Ks) for all 14 mitochondrial PCGs of the NTF mitogenomes were calculated using KaKs_Calculator2.0 (Wang et al., 2010). The calculated Ka/Ks ratios were then analyzed to infer the potential selection pressure on each gene pair. Generally, a Ka/Ks ratio greater than, equal to, or less than 1 indicates positive (diversifying) selection, neutral evolution, or purifying (negative) selection, respectively.

Transition transversion biases were estimated for both the mitogenomic PCGs and the three single-copy nuclear protein-coding genes: the second largest subunit of RNA polymerase II gene (*rpb2*), the translation elongation factor 1-α gene (*tef1*-α), and the β tubulin gene (β-*tub*). These estimates were obtained by employing Maximum Composite Likelihood (MCL) statistical method with the Tamura-Nei model and gaps/missing data were excluded. In addition, we also obtained the Maximum Likelihood estimation of transition transversion biases by employing Kimura 2-parameter substitution model, where evolution rates were set as Gamma distributed with Invariant sites (G + I) and the number of discrete gamma categories was 5. The transition transversion bias estimates by MCL and ML were carried out in MEGA6 (Tamura and Nei, 1993; Tamura et al., 2013).

[2]https://megasun.bch.umontreal.ca/cgi-bin/dev_mfa/mfannotInterface.pl

[3]https://www.ncbi.nlm.nih.gov/genomes/MICROBES/glimmer_3.cgi

[4]https://www.ncbi.nlm.nih.gov/orffinder/

[5]http://codonw.sourceforge.net/index.html

Phylogenetic Analysis

To determine the evolutionary relationships of our selected NTF and other species from the phylum Ascomycota, amino acid sequences at each of the 14 PCGs (*atp6, 8–9, cob, cox1–3, nad1–6,* and *nad4L*) were individually analyzed for all selected taxa. The 14 gene trees were compared among themselves for their tree topology congruences. As there was no evidence of phylogenetic incongruence, the concatenated amino acid sequences of these 14 PCGs were used to construct a more robust phylogeny among the taxa. Here we included 94 species from other representative phyla and classes, including Pezizomycotina, Saccharomycotina, Taphrinomycotina, Zygomycota, Blastocladiomycota, and Basidiomycota. Our 14 individual gene trees showed no evidence of significant incongruence. Thus, the multiple protein sequences were concatenated and aligned using MUSCLE in software MEGA6.0 (Edgar, 2004; Tamura et al., 2013). MrBayes v3.2.6 (Huelsenbeck and Ronquist, 2001) was used to construct the phylogenetic tree using the Bayesian inference (BI) method based on the combined gene set. In this phylogenetic analysis, the first 25% trees were discarded as burn-in, and the remaining trees were used to calculate Bayesian posterior probabilities (BPP) in a 50% majority-rule consensus tree.

RESULTS

Genome Size and Intron Distribution

The mitogenomes of the 12 fungal strains investigated here were all composed of circular DNA molecules with genome sizes ranging from 146,101 bp to 280,699 bp (**Table 1**). The two species incapable of forming trapping devices have mitogenomes sized 186,056 bp and 191,042 bp, respectively, well within the range of the mitogenomic sizes of those with nematode trapping ability. However, despite their large mitogenome size difference (almost two-fold difference between the largest and the smallest mitogenomes), the concatenated lengths of all exons were very similar among the strains, from DB16's 12,053 bp to AM's 14,055 bp, a difference of about 2 kb. Indeed, strain DB29 has the largest mitogenome at 280,699 bp but an intermediate concatenated exon size of 12,948 bp. We note that the concatenated exons excluded those in the open reading frames (ORFs) of introns. Indeed, some of the introns contain ORFs coding for potential endonucleases (group I) or reverse-transcriptases (group II). Most of the mitochondrial introns we annotated in these 12 strains belong to group I, only 1 or 2 introns distributed in strains AM21, DB29, DL42, DT, and DC are group II introns.

Among the 14 protein coding genes (*cox1, cox2, cox3*, *cob*, *atp6, atp8, atp9*, *nad1, nad2, nad3, nad4, nad4L, nad5, nad6*), 12 contained at least one intron in one of the 12 strains (**Table 1**). The gene containing the most introns was *cox1*. However, two genes, *nad4L* and *atp8*, have no intron in any of the 12 strains. The variations in intron numbers were found both among species as well as among strains within species, in this case *A. oligospora*

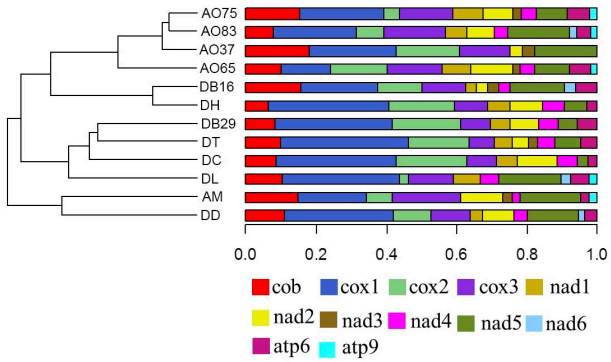

FIGURE 1 | Dendrograms showing the relationships among strains based on their relative intron numbers in each of the 14 mitochondrial core protein coding genes. The "plotTree.barplot" function from the *phytools* R package (Revell, 2011) was used to estimate the similarities between samples. A distance matrix was first calculated using the intron numbers distributed in the 14 protein coding genes within each strain.

and *Dr. brochopaga*. Overall, though there are differences in how introns are distributed among species, there is no clear pattern for association between the total number of introns and specific type of trapping devices (**Figure 1**). Our results are consistent with the dynamic nature of intron distribution in fungal mitogenomes.

Gene Arrangement Analysis

All the mitogenomes from the eight fungal species encode an essential set of conserved genes including three cytochrome c oxidase subunits (*cox1, cox2, cox3*), apocytochrome b (*cob*), three ATP synthase subunits (*atp6, atp8, atp9*), seven subunits of NADH dehydrogenase (*nad1, nad2, nad3, nad4, nad4L, nad5, nad6*), the small and large ribosomal RNA subunits (*rns, rnl*). The mitogenome-encoded ribosomal small subunit protein 3 (*rps3*) and the ORF coding for a putative *rnpB* were also found among our strains. The number of tRNA genes in the mitochondrial genomes of the NTF species ranges from 18 to 28. All the genes are located on the same DNA strand. The gene order of the 14 major PCGs was highly conserved across the mitogenomes of the six NTF species, with the exception of switched locations of *atp9* and *nad1* genes in DB16 (**Figure 2**). However, compared to the six NTF species, the two non-predatory fungal species DD and DT had a large rearranged mitogenome region, with *atp8* being from the upstream of the *nad4* gene changed to the downstream of *cox1* gene. Based on the gene orders, the 12 mitogenomes could be divided into three types as shown in **Figure 2**. The first type contains the four strains of *A. oligospora* and the representative of each of the following species AM, DL, DH, DC, as well as DB29. The second type is represented by DB16, and the third type by DD and DT. The high gene synteny among these mitogenomes is also reflected by the Mauve alignment (**Figure 3**). All 12 mitogenomes could be divided into four homologous regions. The red, light green and blue regions are all similar in their sizes, except for the large light green region in DD that is also inverted compared to all other strains. In contrast, the sizes of the largest syntenic regions (in dark green) differed substantially among these species according to their mitochondrial genome sizes (**Figure 3**).

AT and GC Skews

The lengths and GC contents of the 15 core PCGs varied among the 12 mitogenomes (**Figure 4**). The low GC content of all 12 strains (ranging from 22.92% to 26.6%) is similar to other fungal mitogenomes in Pezizomycotina (Lin et al., 2015). Here, the mitogenome from DC contained the highest GC content (**Supplementary Table S1**). Our analyses identified that the AT skews of most genes in most of our samples were negative. The only exceptions were the *rps3* gene in most strains (**Supplementary Table S2**), the *atp9* gene in three samples (DC, AM, and DD), and the *nad4L* gene in five samples (all AO samples and AM). Conversely, GC skew was positive in most PCGs except at *atp8* gene in all strains, and the *cob, cox2-3,* and *nad3* genes for some of the strains. Our results suggested that the nucleotide compositions varied among NTF species and PCGs. Interestingly, in contrast to the skews calculated for other species of NTF, all adhesive network- producing strains have more Ts than As in their protein coding genes, indicating that their mitogenomes were likely subjected to different selection pressures than other NTF species and the two non-predatory species.

Codon Usage Analysis

Codon usage analysis indicated that the most frequently used codons were UUU (for Phenylalanine; Phe), UUA (for Leucine; Leu), AUU (for Isoleucine; Ile), AUG (for Methionine; Met), GUU (for Valine; Val), and AGA (for Serine; Ser), CCU (for Proline; Pro), ACU (for Threonine; Thr), GCU (for Alanine; Ala), UAU (for Tyrosine; Tyr), CAU (for Histidine; His), GGU (for Arginine; Arg), AAU (for Asparagine; Asp), UGU (for Cysteine; Cys), CAA (for Glutamine; Gln), GAA (for Glutamic acid; Glu), GGA (for Glycine; Gly), AAA (for Lysine; Lys) (**Supplementary Table S3**). Our analyses showed that the codon usage patterns were highly similar among the 12 mitogenomes, with the most commonly used codon for each amino acid all being the same across all 12 strains (**Figure 5**). The bias in high A + T ratios in these mitogenomes have likely contributed to the preference of codons with high A + T content.

Evolutionary Rates of PCGs and Nuclear Genes

The mean nucleotide frequencies of the three analyzed nuclear genes are A = 24.66%, T/U = 24.70%, C = 26.38%, and G = 24.27%, and those of mitogenomic PCGs are 29.31, 41.12, 14.03, and 15.54%, respectively. The rates of transitional and transversional substitutions among mitochondrial and nuclear genes vary, with the rates of transitional substitutions from T to C and from A to G at much higher frequencies in nuclear genes than in mitochondrial genes. Similarly, much higher rates of transversional substitutions from A to C, T to G, C to G and G to C were found in nuclear genes than mitochondrial genes. In contrast, rates for remaining types of transitional and transversional substitutions were found much higher in

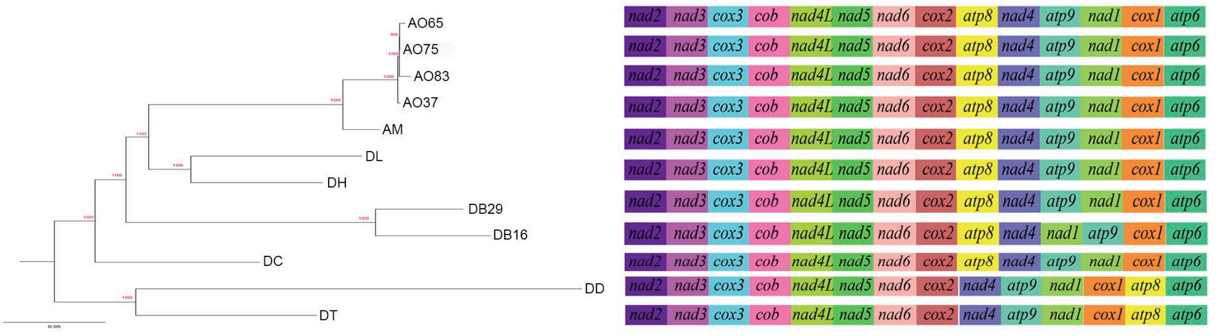

FIGURE 2 | Phylogeny of nematode trapping fungi and their close relatives based on their concatenated nucleotide sequences of the 14 mitochondrial core protein coding genes. The gene order in each mitogenome is indicated.

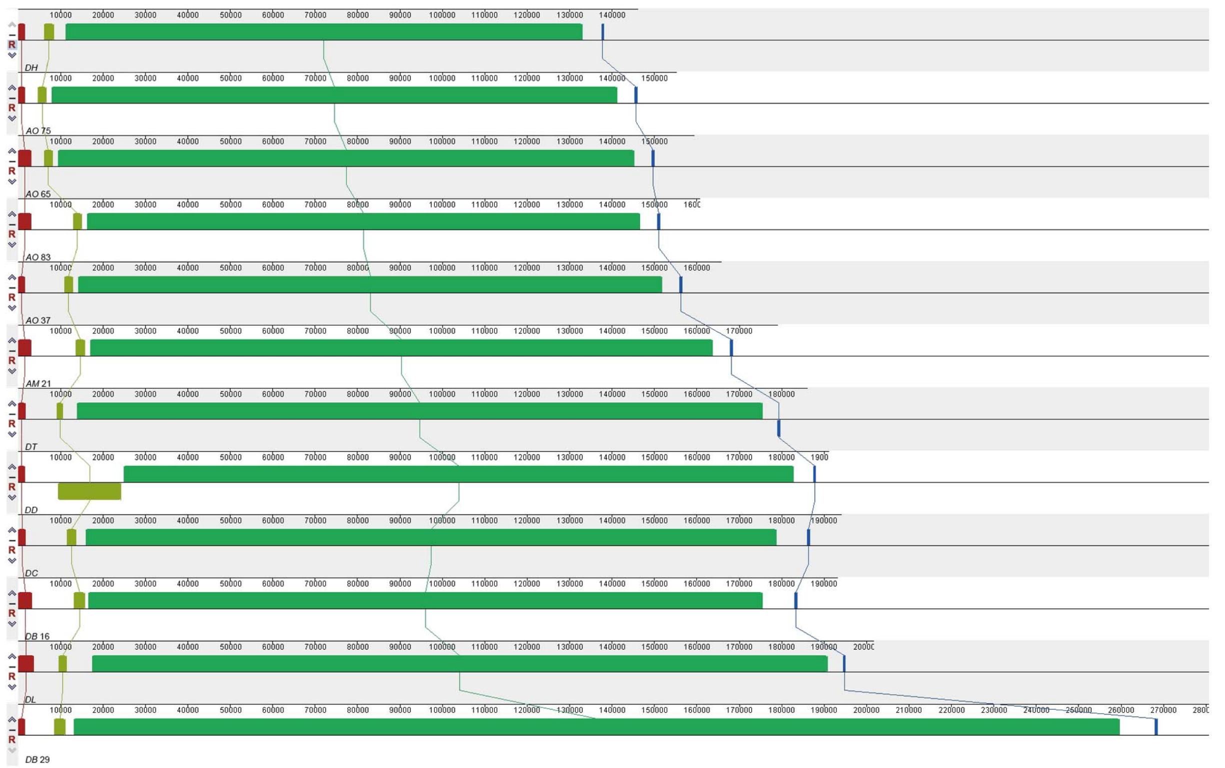

FIGURE 3 | Co-linearity analysis of 12 fungal mitogenomes analyzed in this study, generated with Mauve 2.3.1.

mitogenomes than in nuclear genomes of the same group of species (**Table 2**).

Among the 15 mitochondrial PCGs, seven (*rps3, cox1-2, nad2-3,* and *nad5-6*) had a higher non-synonymous substitution rate (Ka) than synonymous substitution rate (Ks) between several species pairs. Our results indicate that besides purifying selection, NTF species were subject to positive selection at specific gene loci (**Figure 6**).

Phylogenetic Analysis

Our single gene based phylogenetic analyses revealed no evidence for statistically significant incongruences among the 14 protein-coding gene trees. Thus, here we focus on analyzing the concatenated mitochondrial protein sequences. Our results revealed many well-support backbone nodes in Ascomycota, similar to those revealed by nuclear genes (Schoch et al., 2009; **Figure 7**). For example, high statistical supports were found for subclasses Saccharomycotina and Pezizomycotina. Interestingly, Saccharomycotina was found to be more closely related to Taphrinomycotina than to Pezizomycotina. Data presented here suggested that the common ancestor of Orbiliomycetes and Pezizomycetes likely represented an early diverging lineage of the Pezizomycotina (James et al., 2006), with the remaining four classes sampled here forming a well-supported clade. Moreover,

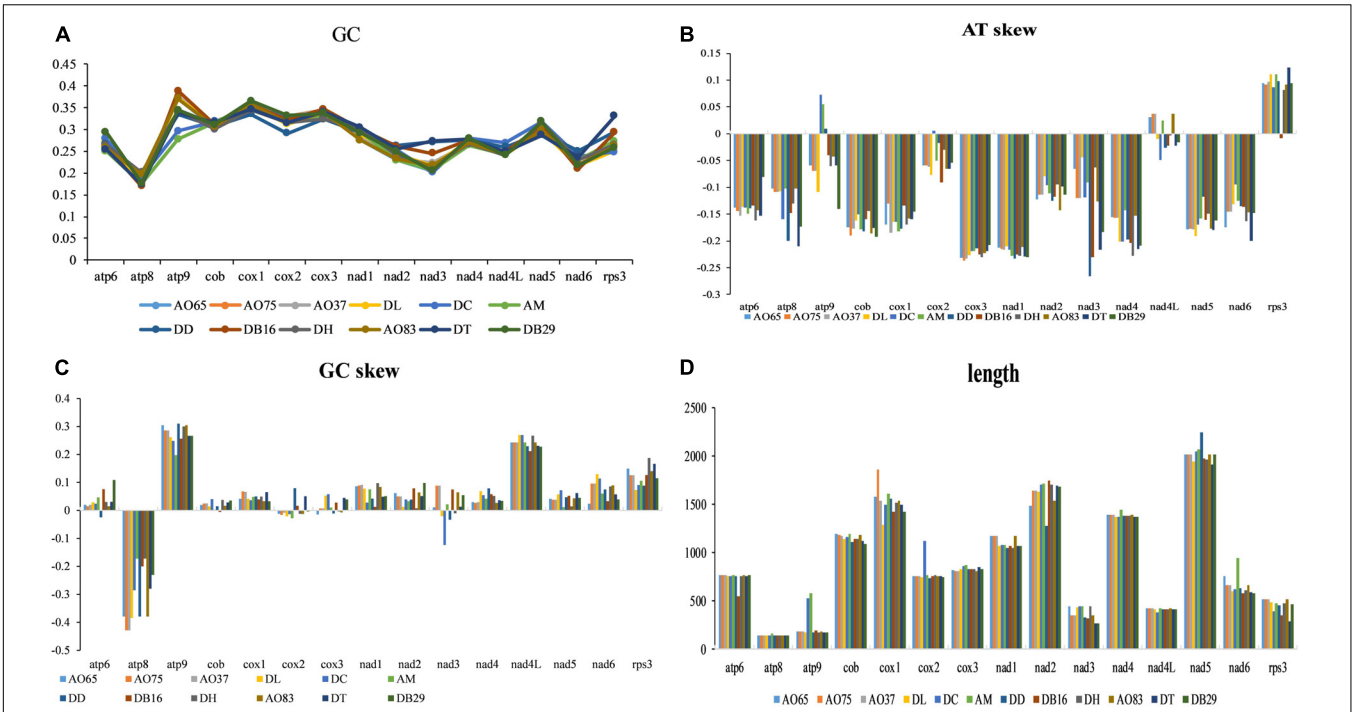

FIGURE 4 | Variation in the length and base composition of each of the 15 protein-coding genes among 12 fungal mitochondrial genomes. **(A)** GC content across the 15 genes; **(B)** AT skew; **(C)** GC skew; **(D)** gene length variation.

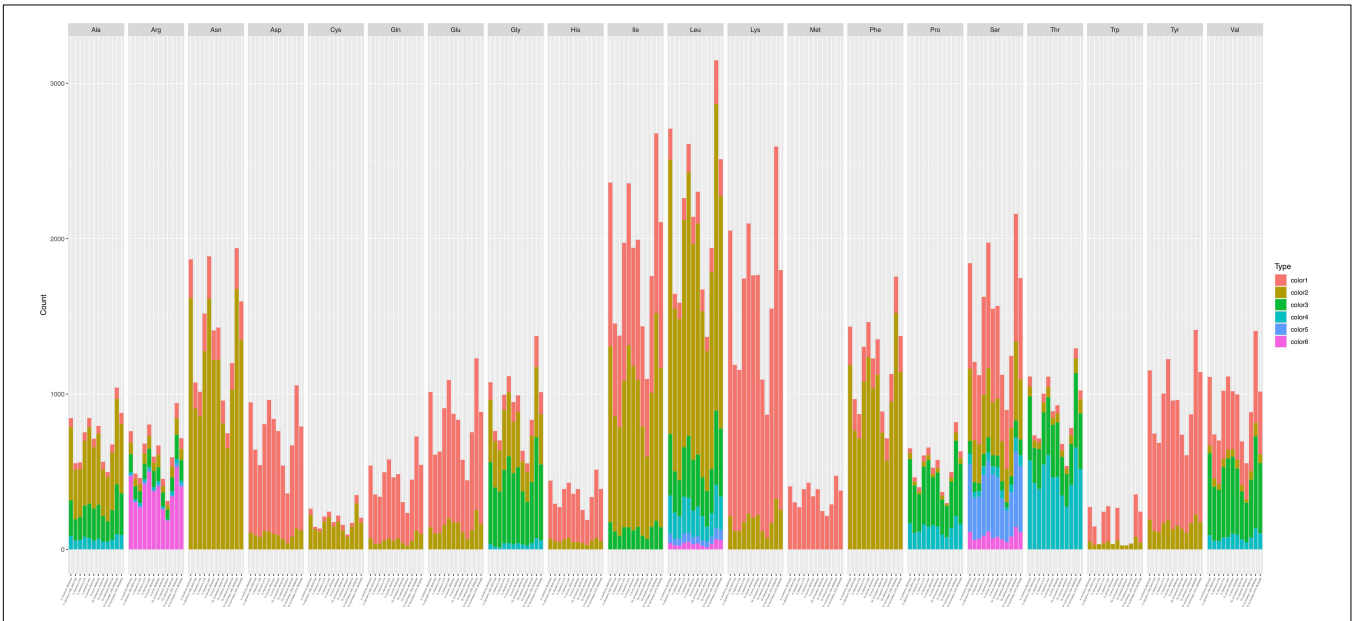

FIGURE 5 | Codon usage in the 12 fungal mitochondrial genomes. Frequency of codon usage is plotted on the *y*-axis.

in both the mitochondrial and nuclear phylogenies, these NTFs were found to be within a well-supported monophyletic group (Li et al., 2005; Yang et al., 2007). Our results suggest that non-predatory species with similar morphological characters (except the traps) to these NTFs (such as our DT and DD), may have differentiated from other Orbiliomycetes at an early stage during evolution. In our phylogeny based on concatenated mitochondrial protein sequences, the species producing adhesive column (DC) was found to be the first one diverging from the non-predatory species DT and DD. Therefore, DC likely represents one of the early branching members of NTFs. Other predators producing constricting rings and adhesive

TABLE 2 | Probability of substitution (*r*) from one base (row) to another base (column).

a. Mitochondrial genes				
From\To	**A**	**T**	**C**	**G**
A	–	*8.2627*	*2.8185*	**8.6270**
T	*5.8906*	–	**8.8802**	*3.1237*
C	*5.8906*	**26.0330**	–	*3.1237*
G	**16.2688**	*8.2627*	*2.8185*	–
b. Nuclear genes				
From\To	**A**	**T**	**C**	**G**
A	–	*3.8228*	*4.084*	**10.74**
T	*3.8172*	–	**24.48**	*3.756*
C	*3.8172*	**22.915**	–	*3.756*
G	**10.911**	*3.8228*	*4.084*	–

For simplicity, the sum of r-values is made equal to 100. Rates of different transitional substitutions are shown in bold and those of transversional substitutions are shown in italics.

knobs and networks seemed to form a well-support clade that emerged later.

DISCUSSION

In this study, we obtained the mitogenome sequences of three strains of *A. oligospora*. These three mitogenome sequences were analyzed together with nine previously published mitochondrial genomes. Together, these 12 mitogenomes represent six species of NTF and two related species of non-predatory fungi. Our analyses indicated that these 12 fungal mitogenomes are among the largest and most variable in length of the known eukaryotic mitogenomes (Paquin et al., 1997; Salavirta et al., 2014). The size of published fungal mitogenomes varies from 12.06 kb to 235.85 kb, which represents a 19.6-fold difference in size. Likewise, great mitogenome size variations (146–280 kb) were revealed among NTF species, largely due to differences in the number and size of introns (28–55 introns per species).

Interestingly, the NTFs and their closely related two non-predatory fungal species are among the species with large mitogenomes, with strain DB29 having the largest mitogenome of all known fungi sequenced to date. Furthermore, two strains of the same species, DB29 and DB16, showed a large difference in their genome sizes, 280,699 and 193,195 bp, respectively. Based on mitogenome sequence comparisons, almost all the size differences among the 12 mitogenomes could be attributed to mitochondrial introns. However, it's currently not known why certain strains and species accumulate more introns than other strains and species. Here, the two strains of *Dr. brochopaga* with different mitogenome sizes came from different sources: DB29 was isolated from the ascospore germination culture of its teleomorphic form *Orbilia orientalis* (Raitv.) Baral (Yu et al., 2006), whereas DB16 was directly obtained from a single conidium in a soil sample (Guo et al., 2009). In the lab, strain DB29 is capable of sexual reproduction while strain DB16 is incapable of sexual reproduction. It's tempting to speculate that the ability of strain DB29 to reproduce sexually through mating may have contributed to the spread of introns to its mitogenome and consequently to its large mitogenome size.

Similarly, the mitogenome size differences among strains of *A. oligospora* were primarily due to the size and distribution of introns. In *A. oligospora*, strains belong to one of two mating types. The mating type genes regulate mating (hyphal fusion) and meiosis. Recent research has shown increasing evidence for mitochondrial DNA recombination under both laboratory and field conditions, though it is widely believed that the inheritance of mitochondrial DNA in fungi is uniparental and non-recombining (Wilson and Xu, 2012; Breton and Stewart, 2015; Xu and Wang, 2015; Wang et al., 2017). Indeed, mutation of a specific gene involved in sex-determination caused the rapid spread of multiple introns in the human pathogenic yeast *Cryptococcus neoformans* (Yan et al., 2018). In the case of NTF and their close relatives, further studies are needed to investigate the mobility of introns in genetic crosses. In addition, mitochondrial- and nuclear-associated plasmids and double-stranded RNA (dsRNA) elements are common in fungi and they can spread during hyphal fusion, potentially contributing to the diversity and size expansion in the mitogenomes observed in this study.

Because all mitogenomes are believed to have originated from a common ancestor, the mitochondrial gene order can also reflect the evolutionary relationships among organisms (Zheng et al., 2018). A comparative alignment of 12 mitogenomes with the Mauve program clearly showed a largely syntenic relationship among all samples we investigated, but the sizes and relative positions of homologous fragments showed slight variation among some of the species. Here, the two non-predatory species had a distinct location for *atp8* that's different from that in other species. Closely related plants often contain mitochondrial genomes with different gene orders, which have been attributed to homologous recombination within individual mitochondrial genomes mediated by their high proportions of repeat sequences (Maréchal and Brisson, 2010). However, despite their potential importance, the mitochondrial gene order variations among fungi have rarely been evaluated (Aguileta et al., 2014). It is possible that the DD and DT gene arrangement represents the ancestral condition and those of the NTF are an evolutionarily derived condition. As indicated in the phylogeny, DD is located on the basal branch in the Orbiliomycetes clade, this change in gene order could be caused by an intra-molecular recombination within the mitochondrial genome of the common ancestor of the analyzed NTF.

The GC content of mitochondrial genomes varies among organisms, and can be affected by mutation bias, selection, and biases of reconstitution-related DNA repair (Chen et al., 2014). Interestingly, in almost all fungal mitogenomes sequenced so far, codon usage is biased strongly toward codons ending in A or T (Li et al., 2018a,b). Indeed, over 94% of the optimal codons in the 10 NTF mitogenomes end in A or T (**Supplementary Table S2**). This was likely due to the high AT content found in fungal mitogenomes, where the rates of transitional and transversional

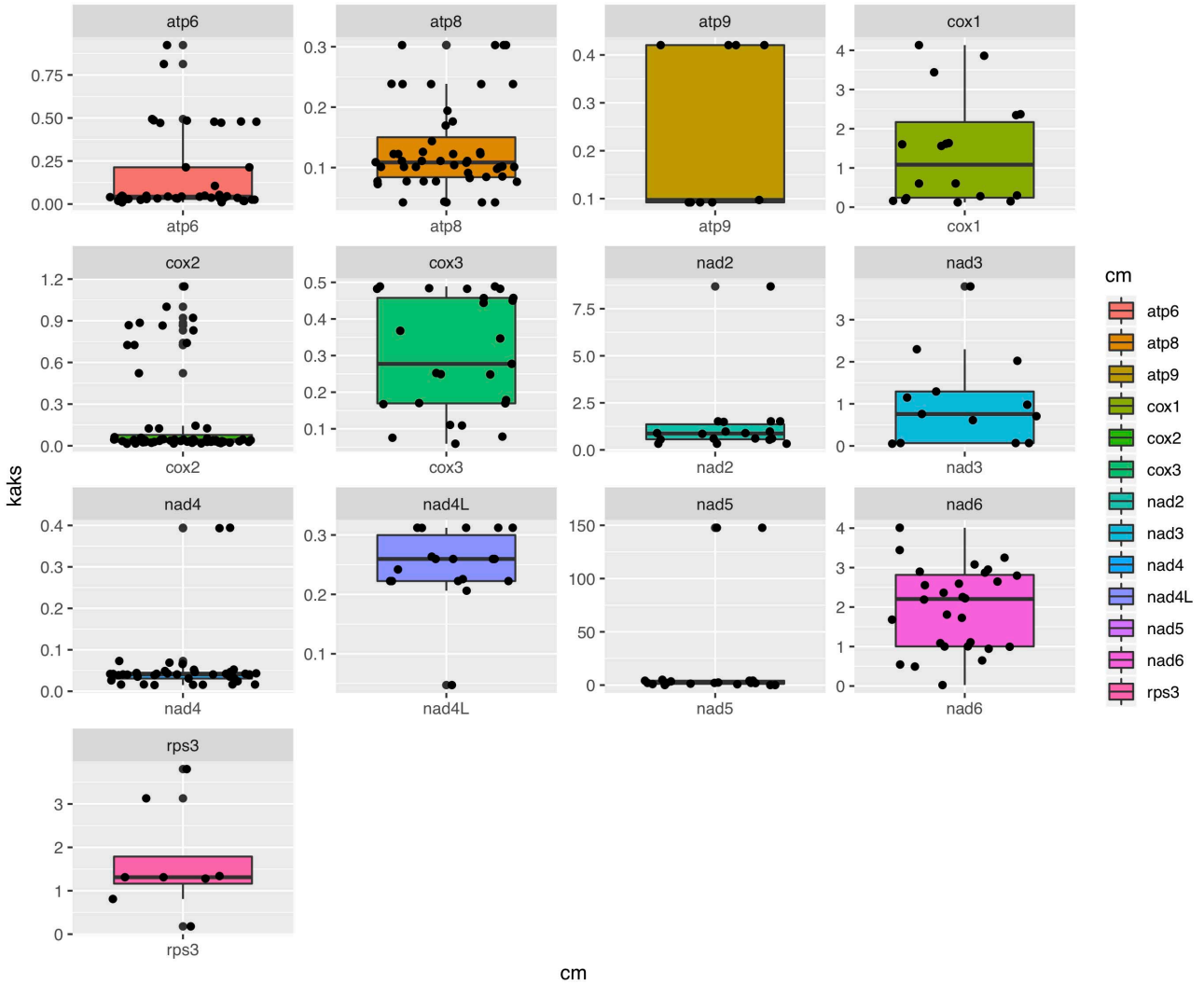

FIGURE 6 | Box-plot comparisons of the Ka/Ks ratios estimated in the various mitochondrial genes. The estimates were based on pairwise alignments of samples.

substitution from C, G to T, A are much higher than those of the reverse direction and those of nuclear genes.

As one of the most important organelles, mitochondrion generates the universal energy currency ATP and plays an important role in almost all biological activities. Even though mitochondria were originated from a common ancestral alpha-proteobacterium, they may have evolved together with different nuclear genomes and adapted to different environments (Yan et al., 2007; Einer et al., 2017; Zhang B. et al., 2017). Previous studies have shown that different groups of eukaryotes seem to have different mitogenome mutation rates, and the rates of mutation in fungal mitochondrial genomes are generally considered intermediate between those in animals (highest mutation rate) and plants (lowest mutation rate) (Aguileta et al., 2014). However, there are significant differences among fungal groups in their relative nuclear-mitochondrial genome mutation rates (Sandor et al., 2018). Regardless, mitochondrial genes have been used for evolutionary studies in a variety of fungi, such as the endophytic fungus *Phialocephala scopiformis* (Robicheau et al., 2016), the entomopathogens *Hirsutella vermicola* (Zhang Y.-J. et al., 2017), *Pochonia chlamydosporia* (Lin et al., 2015), and *H. thompsonii* (Wang et al., 2018). For example, a mitogenomic phylogeny showed that all of the invertebrate-pathogenic fungi cluster together to form a monophyletic group in Hypocreales, which is noticeably distinguished from a cluster comprising of plant fungal pathogens (Lin et al., 2015). Based on mitochondrial gene sequences, our NTFs were also found to be in a well-supported monophyletic group different from the two non-predatory species, consistent with these invertebrate-pathogenic fungi sharing a common ancestor.

At present, there are several hypotheses on the origin and evolution of nematode-trapping lifestyles in the Ascomycota, and these hypotheses differ in the order of emergence of individual trap types, including what the ancestral trap type might be (Rubner, 1996; Ahren et al., 1998; Li et al., 2005; Yang et al., 2007). Based on the phylogenetic relationship revealed in our

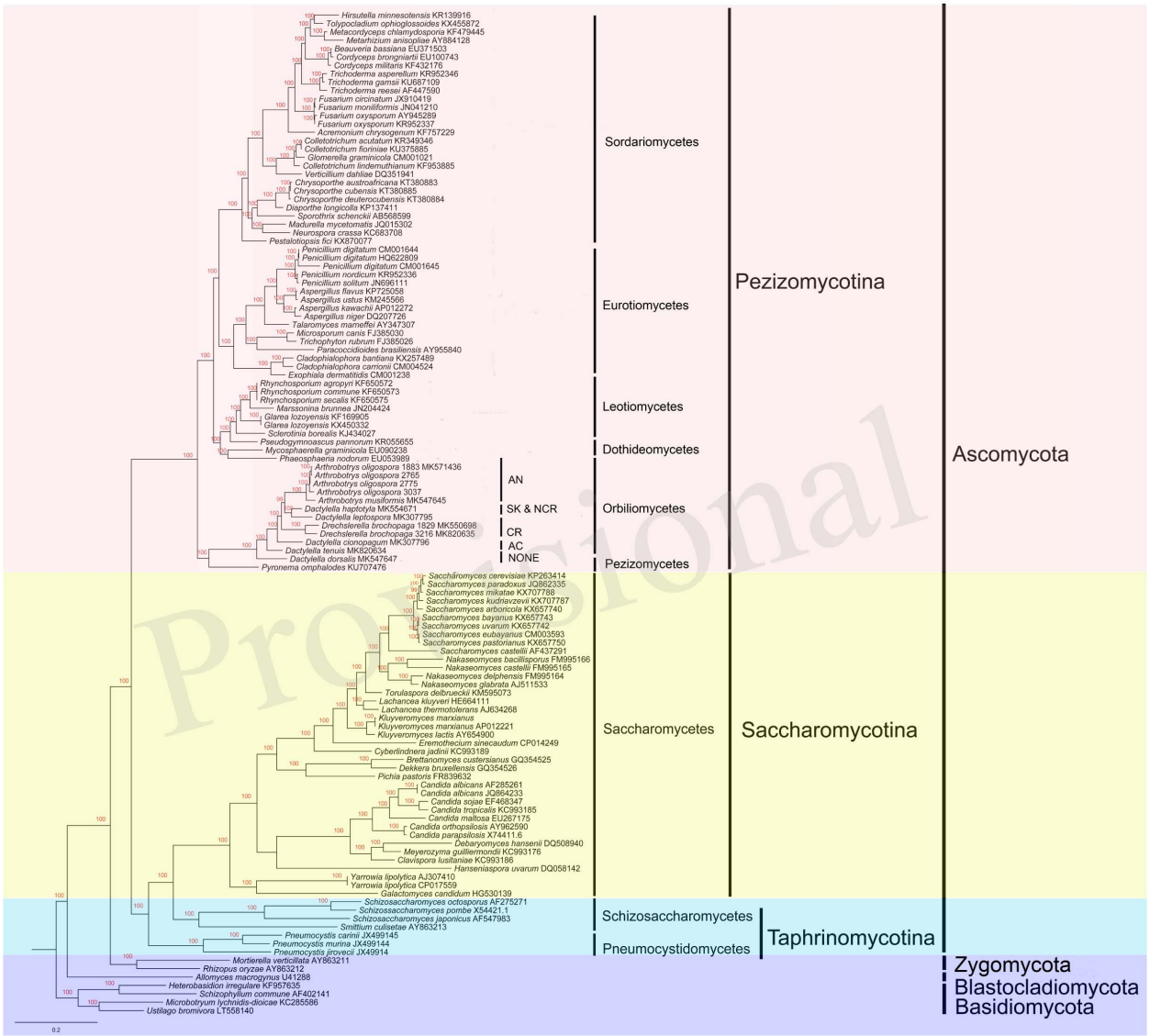

FIGURE 7 | Bayesian tree of 104 species from the five main classes of Pezizomycotina, as well as representative species from other fungal phyla. The tree was constructed based on concatenated amino acid sequences of 14 conserved protein coding genes in fungi *atp6, 8–9, cob, cox1–3, nad1–6,* and *nad4L*. The resulting Bayesian posterior probabilities (BPP) ≥ 70% are shown above internal branches. GenBank accession numbers of all sequences are given. AN, adhesive networks; AK & NCR, Adhesive knobs and non-constricting rings; CR, constricting rings; AC, adhesive column; NONE, no trapping device produced.

study, predatory fungi evolved from non-predatory ancestors and we propose that adhesive column was likely the first type to emerge. This was then followed by the emergence of constricting rings (CR). Our results are consistent with the hypothesis of Yang et al. (2007) that the trapping mechanisms within the Orbiliales have evolved along two major lineages, one leading to species with constricting rings and the other to species with adhesive traps, including three-dimensional networks, knobs, and branches. Indeed, physiological and microscopic observations indicate that CR and various adhesive devices have distinctly different materials. For example, microscopically within trap cells, CR contains unique, oblong-shaped, electron-dense inclusions, which are absent in the ring cells after nematodes are captured, whereas cells of adhesive devices exhibit multiple globose electron-dense bodies that persist (Tzean and Estey, 1981; Nordbring-Hertz, 1988). Our analyses demonstrated that, though with similar morphology, non-constricting rings (NCR) were phylogenetically distant from the CR, which is consistent with the phylogeny reconstructed based on multiple nuclear gene sequences. Although the rates of transitional and transversional substitutions between mitochondrial and nuclear genes varied among our study organisms, the framework established by the mitogenome sequences showed that the origins and divergence patterns of various predatory fungi in Ascomycota were similar to those inferred based on nuclear gene sequences. Overall, our results indicate that mitochondrial genes

can be useful molecular markers for NTF taxonomy, systematics, population genetics, and evolutionary studies.

Due to their functional constraints, mitochondrially encoded protein sequences typically evolve slower than predicted by the high nucleotide substitution rate in the mitochondrial genome (Giorgi et al., 1999). Thus, we expected to observe prevalent evidence for purifying selection on non-synonymous mutations during mitochondrial evolution (Meiklejohn et al., 2007). However, our analyses showed a mixed pattern. Interestingly, a recent analysis of diverse animal taxa showed that 26% of non-synonymous mitochondrial substitutions may have been fixed by adaptive evolution (James et al., 2015). Furthermore, frequent non-synonymous polymorphisms in both *atp6* and *VAR1* genes were observed in yeast, consistent with relaxed purifying selection on either protein-coding genes or the intergenic regions (Jung et al., 2012), resulting in fast evolution of yeast mitochondrial genomes. Similar to most yeasts, NTF can grow as saprophytes in soils. However, different from yeasts, NTF can enter the parasitic stage by developing specific traps. During the switch between different lifestyles, multiple fungal signal transduction pathways are activated by its nematode prey to further regulate downstream genes associated with diverse cellular processes such as energy metabolism, biosynthesis of the cell wall and adhesive proteins, cell division, glycerol accumulation, and peroxisome biogenesis (Yang et al., 2011; Meerupati et al., 2013). Therefore, genes involved in energy metabolism (e.g., cytochrome c oxidase, ATP synthase and NADH dehydrogenase subunits) might be targets of natural selection and adaptation to meet the huge change in energy demand, facilitating genetic changes in these genes.

Other than these energy metabolism-related genes with high Ka/Ks ratios, our analyses also showed a high Ka/Ks ratio in the *rps3* gene among the 12 mitogenomes. Interestingly, the mushroom species *Hypsizygus marmoreus* also has a high Ka/Ks ratio (1.4) in *rps*3 gene, consistent with positive selection of this gene and its functional importance (Wang G. et al., 2019). Similarly, the *rps3* gene in the entomopathogenic fungus *P. chlamydosporia* has also likely experienced positive selection, leading to a unique evolutionary pattern in Hypocreales (Lin et al., 2015). The RPS3 protein plays a critical role in ribosome biogenesis and DNA repair in eukaryotes (Kim et al., 2013). This is the only mitochondrial ribosomal protein encoded by mitogenomes in NTFs. It's currently unknown why this protein underwent diversifying selection among several distinct groups of fungi. This and other issues such as the relevance of our findings on NTF mitogenomes to other functionally important groups of fungi (e.g., those parasitizing insects, plants, and other animals) remain to be investigated.

DATA AVAILABILITY STATEMENT

The datasets generated in this study can be found in GenBank (Accession number MK571436).

AUTHOR CONTRIBUTIONS

JX, ZY, K-QZ, and YZ conceived and designed the study. YZ and JX wrote the manuscript. GY, CD, and MF conducted the experiments. YZ, GY, CD and MF analyzed the data. YZ and JX revised the manuscript. All authors read and approved the final manuscript.

FUNDING

This research is jointly supported by the National Natural Science Foundation of China (31760010 and 31770026) to YZ and ZY, the Top Young Talents Program of the Ten Thousand Talents Plan in Yunnan Province to YZ, and the "Double First Class" Research Project in Yunnan University (C176280107) to JX.

SUPPLEMENTARY MATERIAL

The Supplementary Material for this article can be found online at: https://www.frontiersin.org/articles/10.3389/fmicb.2020.00617/full#supplementary-material

TABLE S1 | Dataset of AT skew, GC skew, GC content and length of the 15 protein coding genes in the 12 analyzed mitogenomes.

TABLE S2 | Locations of the rps3 gene in each of the 12 analyzed mitogenomes.

TABLE S3 | Dataset of the relative synonymous codon usage (RSCU) in the 14 mitochondrial protein-coding genes.

REFERENCES

Aguileta, G., de Vienne, D., Ross, O., Hood, M., Giraud, T., Petit, E., et al. (2014). High variability of mitochondrial gene order among fungi. *Genome Biol. Evol.* 6, 451–465. doi: 10.1093/gbe/evu028

Ahren, D., Ursing, B. M., and Tunlid, A. (1998). Phylogeny of nematode-trapping fungi based on 18S rDNA sequences. *FEMS Microbiol. Lett.* 158, 179–184. doi: 10.1016/S0378-1097(97)00519-3

Bankevich, A., Nurk, S., Antipov, D., Gurevich, A., Dvorkin, M., Kulikov, A., et al. (2012). SPAdes: a new genome assembly algorithm and its applications to single-cell sequencing. *J. Comput. Biol.* 19, 455–477. doi: 10.1089/cmb.2012.0021

Barron, G. L. (ed.) (1977). *The Nematode-Destroying Fungi. [Topics in Mycology No. 1.]*. Guelph: Canadian Biological Publications.

Basse, C. W. (2010). Mitochondrial inheritance in fungi. *Curr. Opin. Microbiol.* 13, 712–719. doi: 10.1016/j.mib.2010.09.003

Breton, S., and Stewart, D. (2015). Atypical mitochondrial inheritance patterns in eukaryotes. *Genome* 58, 423–431. doi: 10.1139/gen-2015-0090

Brooks, A., and Lowe, T. (2005). The tRNAscan-SE, snoscan and snoGPS web servers for the detection of tRNAs and snoRNAs. *Nucleic Acids Res.* 33, W686–W689. doi: 10.1093/nar/gki366

Chen, H., Sun, S.-C., Norenburg, J., and Sundberg, P. (2014). Mutation and selection cause codon usage and bias in mitochondrial genomes of ribbon worms (Nemertea). *PLoS One* 9:e85631. doi: 10.1371/journal.pone.0085631

Chen, X. J., and Butow, R. A. (2005). The organization and inheritance of the mitochondrial genome. *Nat. Rev. Genet.* 6, 815–825. doi: 10.1038/nrg1708

Darling, A., Mau, B., Blattner, F., and Perna, N. (2004). Mauve: multiple alignment of conserved genomic sequence with rearrangements. *Genome Res.* 14, 1394–1403. doi: 10.1101/gr.2289704

Deng, C., and Yu, Z. (2019a). The complete mitochondrial genomes of *Dactylellina leptospora* (Orbiliales, Orbiliaceae). *Mitochondrial DNA B* 4, 1615–1616. doi: 10.1080/23802359.2019.1604098

Deng, C., and Yu, Z. (2019b). The complete mitochondrial genomes of the nematode-trapping fungus *Dactylellina cionopaga*. *Mitochondrial DNA B* 4, 866–867. doi: 10.1080/23802359.2019.1573115

Edgar, R. (2004). MUSCLE: a multiple sequence alignment method with reduced time and space complexity. *BMC Bioinformatics* 5:113. doi: 10.1186/1471-2105-5-113

Einer, C., Hohenester, S., Wimmer, R., Wottke, L., Artmann, R., Schulz, S., et al. (2017). Mitochondrial adaptation in steatotic mice. *Mitochondrion* 40, 1–12. doi: 10.1016/j.mito.2017.08.015

Fang, M., Wang, S., Xu, J., Jiang, L., Zhou, D., Zhang, K.-Q., et al. (2019). Characterization of the complete mitochondrial genome of *Drechslerella brochopaga*, a fungal species trapping nematodes with constricting rings. *Mitochondrial DNA B* 4, 858–859. doi: 10.1080/23802359.2019.1572466

Giorgi, C., Gissi, C., Pesole, G., and Reyes, A. (1999). Evolutionary genomics in Metazoa: the mitochondrial DNA as a model system. *Gene* 238, 195–209. doi: 10.1016/s0378-1119(99)00270-x

Gray, M., Burger, G., and Lang, B. (1999). Mitochondrial evolution. *Science* 283, 1476–1481. doi: 10.1126/science.283.5407.1476

Guo, J.-W., Yu, Z. F., Li, C., and Zhang, K.-Q. (2009). The evaluation of sexual reproduction capacity of orbiliaceous anamorphs. *Mycosystema* 28, 692–697.

Hawksworth, D. L., and Lücking, R. (2017). Fungal diversity revisited: 2.2 to 3.8 million species. *Microbiol. Spectr.* 5:FUNK-0052-2016. doi: 10.1128/microbiolspec.FUNK-0052-2016

Huelsenbeck, J. P., and Ronquist, F. (2001). MRBAYES: bayesian inference of phylogenetic trees. *Bioinformatics* 17, 754–755. doi: 10.1093/bioinformatics/17.8.754

James, J., Piganeau, G., and Eyre-Walker, A. (2015). The rate of adaptive evolution in animal mitochondria. *Mol. Ecol.* 25, 67–78. doi: 10.1111/mec.13475

James, T., Kauff, F., Schoch, C., Matheny, P., Valerie, H., Cox, C., et al. (2006). Reconstructing the early evolution of Fungi using a six-gene phylogeny. *Nature* 443, 818–822. doi: 10.1038/nature05110

Jiang, L., Zhang, Y., Xu, J., Zhang, K.-Q., and Zhang, Y. (2018). The complete mitochondrial genomes of the nematode-trapping fungus *Arthrobotrys oligospora*. *Mitochondrial DNA B* 3, 968–969. doi: 10.1080/23802359.2018.1507651

Jung, P., Friedrich, A., Reisser, C., Hou, J., and Schacherer, J. (2012). Mitochondrial genome evolution in a single protoploid yeast species. *G3* 2, 1103–1111. doi: 10.1534/g3.112.003152

Kim, Y., Kim, H., and Kim, J. (2013). Cytoplasmic ribosomal protein S3 (rpS3) plays a pivotal role in mitochondrial DNA damage surveillance. *BBA Bioenergetics* 1833, 2943–2952. doi: 10.1016/j.bbamcr.2013.07.015

Kouvelis, V. N., Sialakouma, A., and Typas, M. A. (2008). Mitochondrial gene sequences alone or combined with ITS region sequences provide firm molecular criteria for the classification of *Lecanicillium* species. *Mycol. Res.* 112, 829–844. doi: 10.1016/j.mycres.2008.01.016

Lavín, J. L., Oguiza, J. A., Ramírez, L., and Pisabarro, A. G. (2008). Comparative genomics of the oxidative phosphorylation system in fungi. *Fungal Genet. Biol.* 45, 1248–1256. doi: 10.1016/j.fgb.2008.06.005

Li, Q., Liao, M., Yang, M., Xiong, C., Jin, X., Chen, Z., et al. (2018a). Characterization of the mitochondrial genomes of three species in the ectomycorrhizal genus *Cantharellus* and phylogeny of agaricomycetes. *Int. J Biol. Macromol.* 118, 756–769. doi: 10.1016/j.ijbiomac.2018.06.129

Li, Q., Wang, Q., Cheng, C., Jin, X., Chen, Z., Xiong, C., et al. (2018b). Characterization and comparative mitogenomic analysis of six newly sequenced mitochondrial genomes from ectomycorrhizal fungi (Russula) and phylogenetic analysis of the Agaricomycetes. *Int. J Biol. Macromol.* 119, 792–802. doi: 10.1016/j.ijbiomac.2018.07.197

Li, W.-J., and Yu, Z.-F. (2019). The complete mitochondrial genomes of *Dactylella tenuis*, a fungus phylogenetically close to nematode-trapping fungus. *Mitochondrial DNA B* 4, 2704–2705. doi: 10.1080/23802359.2019.1644229

Li, Y., Hyde, K. D., Jeewon, R., Cai, L., Vijaykrishna, D., and Zhang, K. (2005). Phylogenetics and evolution of nematode-trapping fungi (Orbiliales) estimated from nuclear and protein coding genes. *Mycologia* 97, 1034–1046. doi: 10.3852/mycologia.97.5.1034

Lin, R., Liu, C., Shen, B., Bai, M., Ling, J., Chen, G., et al. (2015). Analysis of the complete mitochondrial genome of *Pochonia chlamydosporia* suggests a close relationship to the invertebrate-pathogenic fungi in Hypocreales. *BMC Microbiol.* 15:5. doi: 10.1186/s12866-015-0341-8

Liu, K., Zhang, W., Lai, Y., Xiang, M., Wang, X., Zhang, X., et al. (2014). *Drechslerella stenobrocha* genome illustrates the mechanism of constricting rings and the origin of nematode predation in fungi. *BMC Genomics* 15:114. doi: 10.1186/1471-2164-15-114

Losada, L., Pakala, S. B., Fedorova, N. D., Joardar, V., Shabalina, S. A., Hostetler, J., et al. (2014). Mobile elements and mitochondrial genome expansion in the soil fungus and potato pathogen *Rhizoctonia solani* AG-3. *FEMS Microbiol. Lett.* 352, 165–173. doi: 10.1111/1574-6968.12387

Mardanov, A. V., Beletsky, A. V., Kadnikov, V. V., Ignatov, A. N., and Ravin, N. V. (2014). The 203 kbp mitochondrial genome of the phytopathogenic fungus sclerotinia borealis reveals multiple invasions of introns and genomic duplications. *PLoS One* 9:e107536. doi: 10.1371/journal.pone.0107536

Maréchal, A., and Brisson, N. (2010). Recombination and the maintenance of plant organelle genome stability. *New Phytol.* 186, 299–317. doi: 10.1111/j.1469-8137.2010.03195.x

Meerupati, T., Andersson, K.-M., Friman, E., Kumar, D., Tunlid, A., and Ahrén, D. (2013). Genomic mechanisms accounting for the adaptation to parasitism in nematode-trapping fungi. *PLoS Genet.* 9:e1003909. doi: 10.1371/journal.pgen.1003909

Meiklejohn, C., Montooth, K., and Rand, D. (2007). Positive and negative selection on the mitochondrial genome. *Trends genet.* 23, 259–263. doi: 10.1016/j.tig.2007.03.008

Nordbring-Hertz, B. (1988). Nematophagous fungi: strategies for nematode exploitation and for survival. *Microbiol. Sci.* 5, 108–116.

Pantou, M. P., Kouvelis, V. N., and Typas, M. A. (2006). The complete mitochondrial genome of the vascular wilt fungus *Verticillium dahliae*: a novel gene order for *Verticillium* and a diagnostic tool for species identification. *Curr. Genet.* 50, 125–136. doi: 10.1007/s00294-006-0079-9

Paquin, B., Laforest, M., Forget, L., Roewer, I., Wang, Z., Longcore, J., et al. (1997). The fungal mitochondrial genome project: evolution of fungal mitochondrial genomes and their gene expression. *Curr. Genet.* 31, 380–395. doi: 10.1007/s002940050220

Revell, L. (2011). Phytools: an R package for phylogenetic comparative biology (and other things). *Methods Ecol. Evol.* 3, 217–223. doi: 10.1111/j.2041-210X.2011.00169.x

Robicheau, B., Young, A., Labutti, K., Grigoriev, I., and Walker, A. (2016). The complete mitochondrial genome of the conifer needle endophyte, Phialocephala scopiformis DAOMC 229536 confirms evolutionary division within the fungal Phialocephala fortinii s.l. – Acephala appalanata species complex. *Fungal Biol.* 121, 212–221. doi: 10.1016/j.funbio.2016.11.007

Rubner, A. (1996). Revision of predacious hyphomycetes in the *Dactylella-Monacrosporium* complex. *Stud. Mycol.* 39, 1–134.

Salavirta, H., Oksanen, I., Kuuskeri, J., Mäkelä, M., Laine, P., Paulin, L., et al. (2014). Mitochondrial genome of *Phlebia radiata* is the second largest (156 kbp) among fungi and features signs of genome flexibility and recent recombination events. *PLoS One* 9:e97141. doi: 10.1371/journal.pone.0097141

Sandor, S., Zhang, Y., and Xu, J. (2018). Fungal mitochondrial genomes and genetic polymorphisms. *Appl. Microbiol. Biotechnol.* 102, 9433–9448. doi: 10.1007/s00253-018-9350-5

Schoch, C., Sung, G.-H., Lopez-Giraldez, F., Townsend, J., Miadlikowska, J., Valerie, H., et al. (2009). The ascomycota tree of life: a phylum-wide phylogeny clarifies the origin and evolution of fundamental reproductive and ecological traits. *Syst. Biol.* 58, 224–239. doi: 10.1093/sysbio/syp020

Scholler, M., Hagedorn, G., and Rubner, A. (1999). A reevaluation of predatory orbiliaceous fungi. II. A new generic concept. *Sydowia* 51, 89–113.

Subramanian, C. V. (1963). Dactylella, *Monacrosporium* and *Dactyllina*. *J. Ind. Bot. Soc.* 42, 291–300.

Tamura, K., and Nei, M. (1993). Estimation of the number of nucleotide substituions in the control region of mitochondrial DNA in humans and chimpanzees. *Mol. Biol. Evol.* 10, 512–526. doi: 10.1093/oxfordjournals.molbev.a040023

Tamura, K., Stecher, G., Peterson, D., Filipski, A., and Kumar, S. (2013). MEGA6: molecular evolutionary genetics analysis version 6.0. *Mol. Biol. Evol.* 30, 2725–2729. doi: 10.1093/molbev/mst197

Tzean, S. S., and Estey, R. H. (1981). Species of *Phytophthora* and Pythium as Nematode-destroying Fungi. *J. Nematol.* 13, 160–163.

Wallace, D. (2005). A mitochondrial paradigm of metabolic and degenerative diseases, aging, and cancer: a dawn for evolutionary medicine. *Ann. Rev. Genet.* 39, 359–407. doi: 10.1146/annurev.genet.39.110304.095751

Wang, D., Zhang, Y., Zhang, Z., Zhu, J., and Yu, J. (2010). KaKs_calculator 2.0: a toolkit incorporating gamma-series methods and sliding window strategies. *Genom. Proteom. Bioinform.* 8, 77–80. doi: 10.1016/s1672-0229(10)60008-3

Wang, G., Lin, J., Shi, Y., Chang, X., Wang, Y., Guo, L., et al. (2019). Mitochondrial genome in Hypsizygus marmoreus and its evolution in *Dikarya*. *BMC Genomics* 20:765. doi: 10.1186/s12864-019-6133-z

Wang, S., Fang, M., Xu, J., Jiang, L., Zhou, D., Zhang, K.-Q., et al. (2019). Complete mitochondrial genome and phylogenetic analysis of *Orbilia dorsalia*, a species producing mature sexual structures on culture. *Mitochondrial DNA B* 4, 573–574. doi: 10.1080/23802359.2018.1558121

Wang, L., Zhang, S., Li, J.-H., and Zhang, Y.-J. (2018). Mitochondrial genome, comparative analysis and evolutionary insights into the entomopathogenic fungus *Hirsutella thompsonii*: mitogenome and intron evolution in *H. thompsonii*. *Environmen. Microbiol.* 20, 3393–3405. doi: 10.1111/1462-2920.14379

Wang, P., Sha, T., Zhang, Y., Cao, Y., Mi, F., Liu, C., et al. (2017). Frequent heteroplasmy and recombination in the mitochondrial genomes of the basidiomycete mushroom *Thelephora ganbajun*. *Sci. Rep.* 7:1626. doi: 10.1038/s41598-017-01823-z

Wilson, A., and Xu, J. (2012). Mitochondrial inheritance: diverse patterns and mechanisms with an emphasis on fungi. *Mycology* 3, 158–166. doi: 10.1080/21501203.2012.684361

Wu, Y., Yang, J., Yang, F., Liu, T., Leng, W., Chu, Y., et al. (2009). Recent dermatophyte divergence revealed by comparative and phylogenetic analysis of mitochondrial genomes. *BMC Genomics* 10:238. doi: 10.1186/1471-2164-10-238

Xu, J., and Wang, P. (2015). Mitochondrial inheritance in basidiomycete fungi. *Fungal Biol. Rev.* 29, 209–219. doi: 10.1016/j.fbr.2015.02.001

Yan, Z., Li, Z., Yan, L., Yu, Y.-T., Yi, C., Chen, J., et al. (2018). Deletion of the sex-determining gene SXI1α enhances the spread of mitochondrial introns in *Cryptococcus neoformans*. *Mobile DNA* 9:24. doi: 10.1186/s13100-018-0129-0

Yan, Z., Sun, S., Shahid, M., and Xu, J. (2007). Environment factors can influence mitochondrial inheritance in the fungus *Cryptococcus neoformans*. *Fungal Genet. Biol.* 44, 315–322. doi: 10.1016/j.fgb.2006.10.002

Yang, E., Xu, L., Yang, Y., Zhang, X., Xiang, M., Wang, C., et al. (2012). Origin and evolution of carnivorism in the Ascomycota (fungi). *Proc. Natl. Acad. Sci. U.S.A.* 109, 10960–10965. doi: 10.1073/pnas.1120915109

Yang, J., Wang, L., Ji, X., Feng, Y., Li, X., Zou, C.-G., et al. (2011). Genomic and proteomic analyses of the fungus *Arthrobotrys oligospora* provide insights into nematode-trap formation. *PLoS Pathog.* 7:e1002179. doi: 10.1371/journal.ppat.1002179

Yang, Y., and Liu, X. (2006). New generic approach to the taxonomy of predatory anamorphic *Orbiliaceae* (Ascomycotina). *Mycotaxon* 97, 153–161.

Yang, Y., Yang, E. C., An, Z. Q., and Liu, X. Z. (2007). Evolution of nematode-trapping cells of predatory fungi of the Orbiliaceae based on evidence from rRNA-encoding DNA and multiprotein sequences. *Proc. Natl. Acad. Sci. U.S.A.* 104, 8379–8384. doi: 10.1073/pnas.0702770104

Yu, Z. F., Zhang, Y., Qiao, M., Baral, H. O., Weber, E., and Zhang, K. Q. (2006). *Drechslerella brochopaga*, the anamorph of Orbilia (Hyalinia) orientalis. *Mycotaxon* 96, 163–168.

Zhang, B., Zhang, Y.-H., Wang, X., Zhang, H., and Lin, Q. (2017). The mitochondrial genome of a sea anemone *Bolocera* sp. exhibits novel genetic structures potentially involved in adaptation to the deep-sea environment. *Ecol. Evol.* 7, 4951–4962. doi: 10.1002/ece3.3067

Zhang, Y.-J., Zhang, H.-Y., Liu, X., and Zhang, S. (2017). Mitochondrial genome of the nematode endoparasitic fungus *Hirsutella vermicola* reveals a high level of synteny in the family Ophiocordycipitaceae. *Appl. Microb. .Biotechnol.* 101, 3295–3304. doi: 10.1007/s00253-017-8257-x

Zhang, K. Q., and Hyde, K. D. (2014). *Nematode-Trapping Fungi*. Cham: Springer Science & Business.

Zhang, W., Chen, X., Liu, X., and Xiang, M. (2016). Genome studies on nematophagous and entomogenous fungi in China. *J. Fungi* 2:9. doi: 10.3390/jof2010009

Zhang, Y., Zhang, Y. R., Dong, J. Y., He, X. X., Qiao, M., Baral, H. O., et al. (2016). *Orbilia tianmushanensis* sp nov., a new member of the *O. luteorubella* group with an unusual asexual morph. *J. Microb.* 54, 9–13. doi: 10.1007/s12275-016-5369-4

Zhang, Y., Yu, Z.-F., Xu, J., and Zhang, K.-Q. (2011). Divergence and dispersal of the nematode-trapping fungus *Arthrobotrys oligospora* from China. *Environ. Microb. Rep.* 3, 763–773. doi: 10.1111/j.1758-2229.2011.00297.x

Zhang, Y.-Q., and Yu, Z. (2019). The complete mitochondrial genomes of the nematode-trapping fungus *Arthrobotrys musiformis*. *Mitochondrial DNA B* 4, 979–980. doi: 10.1080/23802359.2019.1581106

Zheng, B.-Y., Cao, L.-J., Tang, P., van Achterberg, C., Hoffmann, A., Chen, H., et al. (2018). Gene arrangement and sequence of mitochondrial genomes yield insights into the phylogeny and evolution of bees and sphecid wasps (Hymenoptera: Apoidea). *Mol. Phylogenet. Evol.* 124, 1–9. doi: 10.1016/j.ympev.2018.02.028

Zhou, D., Zhang, Y., Xu, J., Jiang, L., Zhang, K.-Q., and Zhang, Y. (2018). The complete mitochondrial genome of the nematode-trapping fungus *Dactylellina haptotyla*. *Mitochondrial DNA B* 3, 964–965. doi: 10.1080/23802359.2018.1507650

Conflict of Interest: The authors declare that the research was conducted in the absence of any commercial or financial relationships that could be construed as a potential conflict of interest.

frontiers in Microbiology

ORIGINAL RESEARCH
published: 21 April 2020
doi: 10.3389/fmicb.2020.00706

Mitochondrial Genome Polymorphisms in the Human Pathogenic Fungus *Cryptococcus neoformans*

Yue Wang[1] *and Jianping Xu*[1,2]*

[1] *Department of Biology, McMaster University, Hamilton, ON, Canada,* [2] *Institute of Bast Fiber Crops and Center of Southern Economic Crops, Chinese Academy of Agricultural Sciences, Changsha, China*

The *Cryptococcus* complex consists of at least seven evolutionary divergent lineages and causes ∼200,000 fatal human infections each year worldwide. The dominant lineage is *Cryptococcus neoformans* which consists of three haploid clades VNI, VNII, and VNB, their haploid hybrids, and various diploids derived from intra- and inter-clade mating events. In this study, we analyzed the mitogenomes of 184 strains of *C. neoformans*. Our analyses revealed that all 184 mitogenomes contained the same 15 protein-coding genes in the same gene order. However, their mitogenome sizes varied between 24,740 and 31,327 bp, primarily due to differences in the number and size of mitochondrial introns. Twelve nucleotide sites within five mitochondrial genes were found to contain introns in at least one of the 184 strains, ranging from 2 to 7 introns within each mitogenome. The concatenated mitochondrial exon sequences of the 15 protein-coding genes and two rRNA genes showed that VNI, VNII, and VNB strains were separated into distinct clades or sub-clades, largely consistent with results based on nuclear genome SNPs. However, several novel findings were observed. First, one strain of the VNB clade contained mitogenome exon sequences identical to the main VNI mitogenome type but was distant to other VNB mitogenomes. Second, hybrids among clades VNI, VNII, and VNB identified based on their nuclear genome SNPs contained mitogenomes from different clades, with evidence of their mitogenomes inherited from either the *MAT***a** or the *MAT*α parents. Third, the eight diploid VNB (*C. neoformans*) × VNIV (*C. deneoformans*) hybrids contained recombinant mitogenomes. Fourth, analyses of intron distribution and the paired exon–intron phylogenies for each of the 12 exon–intron pairs suggested frequent gains and losses of mitochondrial introns during the evolution of *C. neoformans*. The combined mitogenome exon-based phylogeny and intron distributions suggested that clades VNI, VNII and VNB could be further divided into sub-clades. Together, our results revealed a dynamic evolution of mitochondrial genomes in this important human fungal pathogen.

Keywords: *Cryptococcus*, mtDNA inheritance, intron distribution, phylogeny, mating type, recombination

OPEN ACCESS

Edited by:
Tomasz Kulik,
University of Warmia and Mazury in Olsztyn, Poland

Reviewed by:
Xingzhong Liu,
Institute of Microbiology (CAS), China
Kin-Ming (Clement) Tsui,
Weill Cornell Medicine - Qatar, Qatar
Xiaofei Liang,
Northwest A&F University, China

***Correspondence:**
Jianping Xu
jpxu@mcmaster.ca;
jpxumcmaster@gmail.com

Specialty section:
This article was submitted to Fungi and Their Interactions, a section of the journal Frontiers in Microbiology

Received: *30 January 2020*
Accepted: *26 March 2020*
Published: *21 April 2020*

Citation:
Wang Y and Xu J (2020) Mitochondrial Genome Polymorphisms in the Human Pathogenic Fungus Cryptococcus neoformans. Front. Microbiol. 11:706. doi: 10.3389/fmicb.2020.00706

INTRODUCTION

The human pathogenic *Cryptococcus* species complex contains at least seven evolutionary divergent lineages and their hybrids (Hagen et al., 2015, Hagen et al., 2017; Kwon-Chung et al., 2017; Samarasinghe and Xu, 2018). Together, they are responsible for over 200,000 deaths per year globally (Rajasingham et al., 2017). Cryptococcal infections can occur in multiple forms and at multiple body sites, including respiratory infections, skin lesions, and meningoencephalitis. The most common and most deadly form of cryptococcal infection is Cryptococcal meningitis, a leading cause of death among HIV/AIDS patients worldwide (Rajasingham et al., 2017). These yeasts are commonly found in soils, bird droppings, and tree barks (Litvintseva et al., 2011; Samarasinghe and Xu, 2018). Currently, based on one school of thought, the seven evolutionarily divergent lineages within the species complex should each be recognized as a distinct *Cryptococcus* species (Hagen et al., 2017). The most common of these seven species is *Cryptococcus neoformans,* which has also been variably called *Cryptococcus neoformans* serotype A, *C. neoformans* var. *grubii*, *C. neoformans* molecular types (clades) VNI, VNII, and VNB in the literature (Hagen et al., 2017; Kwon-Chung et al., 2017; Samarasinghe and Xu, 2018). The focus of this paper is on this group of yeasts and we will use the species name *C. neoformans* to represent this group.

As a medically important organism, a large body of research has been conducted on *C. neoformans*, including establishing a diversity of animal models, identifying the genes associated with virulence, and investigating its molecular epidemiology and population genetics. Indeed, many types of molecular markers such as isozyme electrophoresis, PCR-fingerprinting, amplified fragment length polymorphisms (AFLP), PCR-restriction fragment length polymorphisms (RFLP), multilocus sequence typing (MLST), and whole-genome shotgun sequencing have been used to analyze the patterns of genetic variation from local to global scales for *C. neoformans* (Xu et al., 2000b; Cogliati, 2013; Rhodes et al., 2017). These studies have identified that *C. neoformans* is composed of three divergent haploid clades VNI, VNII, VNB, as well as hybrids among the three clades (Rhodes et al., 2017). In addition, sub-Sahara Africa has been shown to contain the highest genetic diversity and is most likely the center of origin for *C. neoformans* (Litvintseva et al., 2007). These studies have also revealed both ancient and recent migrations among regions within continents and between continents for strains in the different clades (Xu et al., 2000b; Cogliati, 2013; Rhodes et al., 2017). However, most of the analyses so far have focused on nuclear genes and genomes. There is very limited information on the variations of mitochondrial genes and genomes at the population level in *C. neoformans*.

The mitochondrion is an important organelle within eukaryotic cells, responsible for the production of ATP, the energy currency in living organisms. Aside from ATP generation, mitochondria are also involved in several other cellular processes, such as cell senescence and the maintenance of ion homeostasis (Burger et al., 2003; Chatre and Ricchetti, 2014). Within cells, mitochondria interact with multiple other membrane-bound structures including the nucleus, lysosomes, and the endoplasmic reticulum to impact cell survival and reproduction (Chatre and Ricchetti, 2014). In pathogenic fungi, mitochondria have been found to playing a role in virulence, regulating biofilm and hyphal growth, and activating drug resistance (Burger et al., 2003; Chatre and Ricchetti, 2014; Calderone et al., 2015). The mitochondrial genome in the type strain of *C. neoformans*, H99, has been sequenced and annotated (GenBank accession number NC004336). It has a genome size of 24,874 bp and contains 14 common fungal mitochondrial protein-coding genes associated with the electron transport chain and ATP synthesis (*ND1, ND2, ND3, ND4, ND4L, ND5, ND6, ATP6, ATP8, ATP9, COX1, COX2, COX3,* and *COB*). In addition, it contains the ribosomal protein S3 (*rps3*) and the small and large subunits of the mitochondrial ribosomal RNA (SsRNA and LsRNA) genes. Two other genes were also identified in the H99 mitogenome: ribonuclease P (*rnp*) and a hypothetical protein orf267. There are 20 tRNA genes in the H99 mitogenome, encoding 19 of the 20 amino acids (the tRNA-Cys is missing while there are two copies of the tRNA-Met gene). Two of the genes in the H99 mitogenome contain introns, a 1121 bp intron in the *ND1* gene and a 1142 bp intron in the *COB* gene. The two introns contain one open reading frame each coding for a protein with the LAGLIDADG motifs that are characteristic of homing endonuclease genes. The H99 mitogenome is over 20% smaller than that of JEC21 (33,194 bp), a model strain of a closely related species *Cryptococcus deneoformans* (Litter et al., 2005). The major contributor to the mitogenome size difference between H99 and JEC21 is the large number of introns in the JEC21 mitogenome.

Cryptococcus neoformans is predominantly a haploid. However, diploid and aneuploid strains can also be found in both clinical and environmental sources. It can reproduce both asexually via budding and sexually via mating (Zhao et al., 2019). During asexual reproduction, both the nuclear and mitochondrial genomes are faithfully transmitted from the parental cells to offspring. However, new mutations could emerge during asexual reproduction, including nucleotide substitutions and changes in chromosome structure and chromosome number, especially under certain selection pressure such as exposure to antifungal drugs (e.g., Hua et al., 2019; Dong et al., 2020). If asexual reproduction were the only mode of reproduction for *C. neoformans* in nature, we should observe strain relationships inferred based on their nuclear genome sequences to be similar to those based on their mitochondrial genome sequences. On the other hand, if sexual mating were common, due to their different inheritance patterns in sexual crosses (Xu et al., 2000a), strains relationships inferred based on their nuclear and mitochondrial genome sequences could be different.

Sexual mating in *C. neoformans* is controlled by one locus with two alternative alleles, *MAT***a** and *MAT*α. In laboratory crosses involving *MAT***a** and *MAT*α strains, the progeny primarily inherits mitochondria from the *MAT***a** parent (Yan and Xu, 2003). If sexual reproduction were common, most strains would show mixed ancestries in their nuclear genomes while their mitogenomes would follow those of their *MAT***a** parent. Consequently, at the population level, we would see linkage equilibrium among alleles at different nuclear loci but mitogenome markers may be different. Population genetic

and genomic studies based on nuclear genome markers have revealed evidence for both sexual and asexual reproductions in natural populations of *C. neoformans* (Hiremath et al., 2008; Rhodes et al., 2017). However, same-sex mating between strains of *MAT*α is also possible and in such a cross, as shown in laboratory crosses, biparental mitochondrial inheritance, including recombinant mitogenomes, may be observed among progeny (Yan et al., 2004).

The objectives of this study are to analyze the patterns of variation of mitochondrial genes and genomes in natural populations of *C. neoformans*. We focus on analyzing the mitochondrial genome data obtained and released in Rhodes et al. (2017). In the Rhodes et al. (2017) study, they sequenced the genomes of 188 *C. neoformans* strains and analyzed single nucleotide polymorphisms and copy number variations for nuclear genes in these strains. However, their mitochondrial genomes were not analyzed. Thus, the significance of the mitogenome in the evolution of *C. neoformans* remains unknown. The 188 strains that they sequenced were selected to represent *C. neoformans* from different geographic regions, different ecological niches, and/or different MLSTs at seven nuclear loci. However, the sample sizes representing different geographic regions, ecological niches, and MLST were not balanced (Rhodes et al., 2017; **Supplementary Tables S1, S2**). In this study, we extracted the mitochondrial DNA sequences from each of those strains, assembled their mitochondrial genomes, and analyzed the patterns of genome size variation, intron distribution variation, and single nucleotide polymorphisms. Our analyses identified several novel insights in the evolution of this important human fungal pathogen.

MATERIALS AND METHODS

Strains and Nuclear Genotype Information

The strains analyzed here were from the study by Rhodes et al. (2017, see their **Supplementary Table S1** for details). Briefly, these strains came from 14 different countries representing all major regions of the world where *C. neoformans* have been found (Africa, Asia, Australia, Caribbean, Europe, and North and South America). These strains were isolated from different ecological niches (bird guano, soil, trees, animals, and humans). In addition, they were selected for genome sequencing based on their MLST results at seven nuclear gene fragments so as to be representative of the genetic diversity in their respective geographic regions. Thus, even though this collection of strains may not represent the true global population structure of *C. neoformans*, they likely capture most of the global genetic diversity of this species. As a result, we believe that the mitogenomes from these strains should similarly represent the mitogenome diversity of the global *C. neoformans*.

Analyses of the nuclear genomes from the 188 strains revealed that 157 of the 188 isolates were haploid and belonged to one of three major clades (VNI, VNII, and VNB), consistent with results from previous MLST studies of these strains. However, seven haploid isolates showed hybrid ancestry, including five VNI/VNB hybrids and two VNII/VNB hybrids. The remaining 24 isolates displayed evidence of heterozygosity within individual strains, consistent with diploidy or aneuploidy. Genomic analyses revealed that these 24 diploid isolates were likely the mating products of: (i) between strains from within the same lineage (VNI × VNI, 4 strains; VNII × VNII, 4 strains; and VNB × VNB, 3 strains); (ii) between different lineages within *C. neoformans* (VNI × VNB, 2 strains; VNII × VNB, 2 strains); (iii) between two species *C. neoformans* × *C. deneoformans* (8 strains); and (iv) between *C. neoformans* × *Cryptococcus gattii* (1 strain) (Rhodes et al., 2017). The distributions of these 188 strains based on their geographic, ecological, mating type, and nuclear genotypes are summarized in **Supplementary Tables S1, S2**. **Figure 1** shows a simplified representation of sample distributions in a 3D bubble plot generated using the R package 'plotly 4.9.1'[1]. Among the 188 strains analyzed in this study, 112 were the VNI molecular type (60%), 158 were *MAT*α (84%), and 141 were from human patients (75%) (**Supplementary Tables S1, S2**). Thus, other molecular types (VNII, VNB, and their hybrids), *MAT***a** strains, and non-clinical samples such as those from the environment were under-represented.

Mitogenome Sequence Data Retrieval and Assembly

For all 188 strains, their whole-genome sequence data were retrieved from NCBI database according to the Sequence Read Archive (SRA) accession numbers provided by Rhodes et al. (2017, **Supplementary Table S1** in their study). Since all the sequences were generated by paired-end sequencing, fastq-dump from sratoolkit (Leinonen et al., 2010) was used to extract fastq files from the run files and separated them into forward and reverse files.

The program NOVOPlasty3.7 (Dierckxsens et al., 2017) was used to assemble the mitochondrial genome for each of the strains. For each configuration file, the project name, forward read path, and reverse read path were specified. The initial genome size range was set as 19000–35000 bp which covers the known mitogenome size range for all varieties of the human pathogenic *Cryptococcus* species complex (Litter et al., 2005). The *ND5* gene sequence from isolate H99 was used as the seed sequence to retrieve the overlapping reads from the fastq files and then initiate the assembly, using NOVOPlasty3.7. The whole mitogenome sequence of H99 was given as a reference to help resolve duplicated regions in each mitogenome when necessary. Assembly parameters used those in the default setting as recommended.

Mitogenome Annotation

The fungal mitogenomes vary significantly in their genome size and gene content (Sandor et al., 2018). At present, there is no analytical pipeline developed specifically for annotating fungal mitogenomes. We tried two programs for our annotation: MitoS (Bernt et al., 2013) and MitoZ (Meng et al., 2019). MitoS is a popular webserver that requires assembled mitogenomes as input files for annotation and it annotates one mitogenome at

[1]https://rdrr.io/cran/plotly/

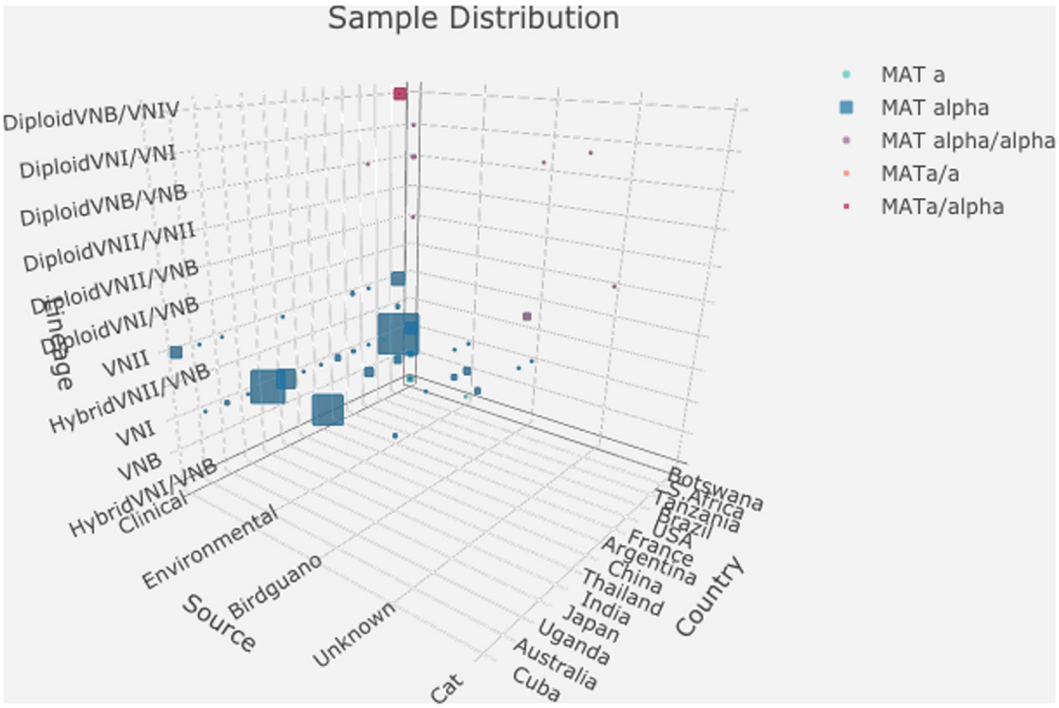

FIGURE 1 | Distributions of 188 strains based on their geographic origin, ecological niche, mating type, and nuclear ploidy, and clade. The detailed data used to generate this graph is presented in **Supplementary Table S2**.

a time. In contrast, MitoZ is a pipeline consisting of several independent modules of *de novo* assembly, findMitoScaf (find Mitochondrial Scaffolds), annotation and visualization. MitoZ was originally developed to assemble and annotate animal mitogenomes (which are generally conserved in their size and genome content) (Meng et al., 2019). However, it can generate mitogenome assembly together with annotation and visualization results from high throughput raw sequence reads. For protein coding gene annotation, MitoZ allows user-defined Perl script to combine with BLAST and user-defined python script to precisely locate the start and stop codons through batch processing. In this study, we modified the protocols of the program MitoZ_v2.44 to annotate the 188 *C. neoformans* mitogenomes. Because the published Cryptococcal mitogenomes are known to be larger and contain more genes than animal mitogenomes, we replaced the list of animal mitochondrial genes with known Cryptococcal mitochondrial genes already published and deposited in GenBank, including building new HMM profiles for all the Cryptococcal genes. To build the HMM profiles, we first downloaded all the known mitochondrial gene sequences of the *Cryptococcus* species complex from the NCBI database. We then aligned the multiple sequences for each gene using MAFFT v7.429 (Katoh et al., 2002). The alignment for each *Cryptococcus* mitochondrial gene was then imported into HMMER_v3.2.1[2] to build the HMM profiles. Since most animal mitochondrial genomes do not contain introns, the program MitoZ does not implement the HMM model to identify introns. Thus, after assembly and annotation through MitoZ, we used a greedy BLAST to separate exons and intron(s) within each gene (Zhang et al., 2000).

Analyses of Mitogenome Size Distributions

The distributions of mitogenome sizes among the assembled mitogenomes were analyzed using Boxplot to compare strains belonging to different categories such as geographic origins, ecological niches, mating types, and genetic lineages. The statistical significance of the differences in mitogenome sizes and intron numbers among groups within each category was determined based on one-way ANOVA. The distributions of mitogenome size and intron number with different sample characteristics were drawn with R package 'ggplot2' (Wickham, 2016). In these graphs, to help visualization of the number of data points around each intron number category and each mitogenome size category, we artificially introduced 0.2 intron as the standard deviation around each intron number category and 200 bp as the standard variation around each mitogenome size category.

Phylogenetic Analyses

Phylogenetic analyses were conducted with package phangorn 2.5.5 (Schliep, 2011) in R. Two types of phylogenetic analyses were performed. In the first, we concatenated the exon sequences of all 17 known and shared coding genes (*ND1, ND2, ND3,*

[2]http://hmmer.org/

ND4, ND4L, ND5, ND6, ATP6, ATP8, ATP9, COX1, COX2, COX3, COB, RPS3, LsRNA, and SsRNA) in the mitogenomes and aligned them with msa:msaMuscle (Bodenhofer et al., 2015). A Neighbor-Joining (Saitou and Nei, 1987) tree based on the mean nucleotide sequence differences between strains was built. Statistical supports for individual branches were assessed based on 1000 bootstraps. The relevant strain features such as geographic origins, ecological niches, mating type, lineage/genotype group, and intron distributions were plotted along the concatenated exon phylogenetic tree using the program ggtree 1.14.6 (Yu et al., 2017).

The second type of phylogenetic analyses was an individualized exon–intron phylogeny comparison for each intron and its corresponding exon sequences. In our *C. neoformans* mitogenome assemblies, each of 12 nucleotide sites within five genes contained an intron from multiple strains (see section "Results" below). These five genes were (i) the large subunit of the ribosomal RNA (*LsRNA*) gene (four positions within this gene contained introns); (ii) *COB* (two positions within this gene contained introns); (iii) *COX1* (four positions within this gene contained introns); (iv) *COX2* (one position within this gene contained intron); and (v) *ND1* (one position within this gene contained intron). For introns at each of these 12 positions, we first aligned the intron sequences and obtained a phylogeny using the NJ method in MEGA X (Kumar et al., 2018). Similarly, the exon phylogeny for each of the five genes was also constructed. These paired exon and intron phylogenies were then compared with each other. The exon–intron co-phylogenies were constructed using R 'phytools 0.7-02' (Revell, 2012).

RESULTS

We successfully extracted and assembled the mitochondrial genome sequences of 183 strains, each into a single circularized molecule. Of the remaining five strains, we were unable to assemble a circularized mitogenome. These five strains were not included into the subsequent analyses. However, we included the already assembled H99 mitogenome into our analyses as a reference, giving a total of 184 assembled *C. neoformans* mitogenomes for our comparative analyses. Among the 184 assembled mitogenomes, their genome sizes varied between 24,740 and 31,327 bp long (**Supplementary Table S1**). All assembled mitogenomes contained the same set of 17 genes in the same following order: *ND2, ND3, COX2, ND1, COB, SRP3, LsRNA, COX3, ND4, ND4L, ND5, ND6, SsRNA, ATP6, ATP9, COX1*, and *ATP8*. This gene order is also identical to those of the mitogenomes in strain B3501A of the closely related species *C. deneoformans* and in strain R265 of *Cryptococcus gattii* (Litter et al., 2005; Ma and May, 2010). All 184 mitogenomes contained introns and their intron numbers varied between 2 and 7. These introns were distributed across 12 different nucleotide sites located within five genes *LsRNA, COB, COX1, COX2,* and *ND1*. Below we first describe the main results with regard to mitogenome size and intron distributions among clades/genotype groups, geographic populations, ecological niches, and mating types. This is then followed by results from the analyses of nucleotide polymorphisms in either the exons and/or introns in these mitogenomes.

Mitogenome Size and Intron Number Distributions

Distributions Based on Clades/Nuclear Genotypes

The summary mitogenome size and intron number distributions within and among clades/genotype groups are presented in **Figures 2A,B**. Among the three haploid clades VNI, VNII, and VNB, the mean mitogenome size of VNII is significantly bigger than those of VNI and VNB ($p < 0.0001$ in both cases), but those of VNI and VNB not significantly different from each other ($p = 0.49$). Of the remaining genotype groups, the two VNII/VNB haploid hybrids had the biggest mitogenome sizes while those of the diploid VNI/VNB hybrids, haploid VNI/VNB hybrids, and diploid VNI/VNI strains had among the smallest mitogenomes (**Figure 2A**). However, due to the limited sample sizes in these genotype categories, statistical tests in the significance of their mitogenome size differences were not determined. The intron numbers showed an overall distribution parallel to that of the mitogenome size distributions (**Figures 2A,B**). We note, however, that there are some subtle differences between the two. For example, the eight diploid VNB/VNIV hybrids all had seven introns in each of its mitogenome, the highest intron number in a given mitogenome among the 184 strains but their mitogenome sizes were not the biggest (**Figures 2A,B** and **Supplementary Table S1**).

Distribution Based on Geographic Origins

The summary mitogenome size and intron number distributions within and among geographic regions (countries) are presented in **Figures 2C,D**. Most countries with sample sizes relatively large showed a range of mitogenome sizes (**Figure 2C** and **Supplementary Table S1**). The only exception seemed to be the seven strains from Cuba that all had an identical mitogenome size of 29,951 bp. We conducted one-way pairwise ANOVA for the three geographic populations with large sample sizes: Botswana, India, and South Africa. Our analyses showed that overall, the South African population had an average mitogenome size significantly larger than those from Botswana and India ($p < 0.0001$ in both cases) while no significant size difference was found between those from Botswana and India ($p = 0.82$). Again, the intron number distributions within and between the different countries were similar to those of mitogenome size distribution (**Figures 2C,D**).

Distribution Based on Ecological Niches

The summary mitogenome size and intron number distributions within and among ecological niches are presented in **Figures 2E,F**. Most of the 184 strains were from clinical sources, with relatively few from other sources. Of the four types of ecological niches as classified in the Rhodes et al. (2017) study, three showed a range of mitogenome size and intron number variations among strains (**Figures 2E,F**). One-way ANOVA results show that the clinical population of *C. neoformans* from humans had an average mitogenome size significantly larger than that from environmental sources

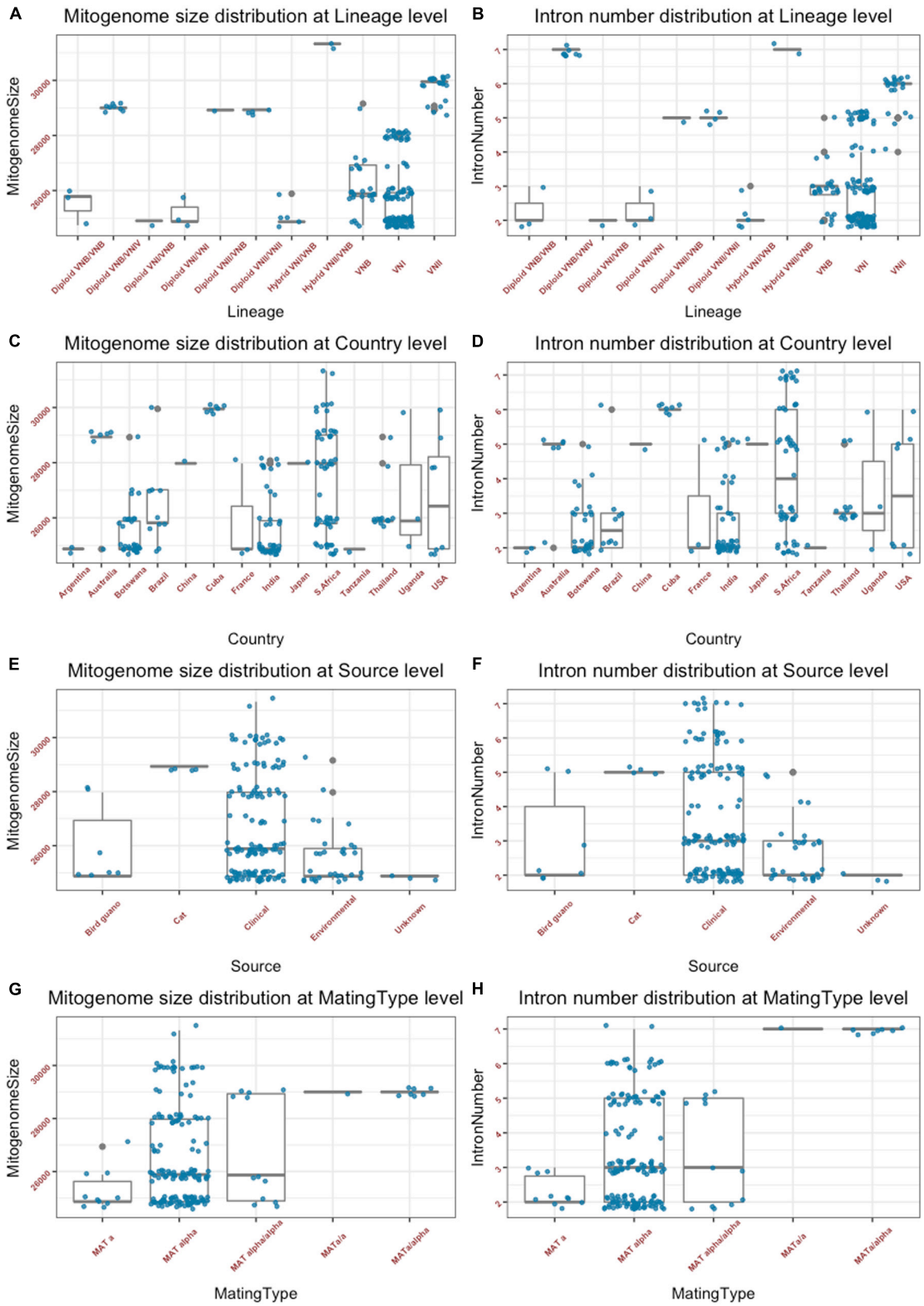

FIGURE 2 | Mitogenome sizes and intron numbers distribution among strain features as defined based on various characteristics. **(A,B)** Variations within and among clades and genotype groups as defined based on nuclear genome SNPs. **(C,D)** variations within and among their geographic (country) origins. **(E,F)** Variations within and among ecological niches. **(G,H)** Variations within and among different mating types or mating type combinations. Random noise was added to plots using a uniform distribution with 0.38 horizontal jitter. The vertical jitter was set as 200 bp for genome size and 0.2 for intron number.

[p = 0.002; for this analysis, due to small sample size for the bird-guano population, we combined the bird-guano strains with the "environmental strains" in Rhodes et al. (2017) into one "environmental sample."]. Interestingly, all four strains from cats were diploid VNII/VNII isolates from Australia and they had the same mitogenome size (28,932 bp), contained the same number of mitochondrial introns (5) at exactly the same mitogenome locations (**Supplementary Table S2**), and had identical mitogenome exon sequences (see section "Results" below).

Distributions Based on Mating Types

The summary mitogenome size and intron number distributions among mating type groups are presented in **Figures 2G,H**. For both mitogenome size and intron number, *MAT*α strains showed greater ranges of variation than those of *MAT***a** strains. However, there was no statistically significant difference between the *MAT***a** and *MAT*α populations in their mean mitogenome sizes. Interestingly, of the three remaining mating type combinations (*MAT***a/a**, *MAT*α**/a**, and *MAT*α/α), two (the *MAT***a/a** and *MAT***a/**α) of them showed similar mitogenome sizes and intron numbers to each other while the *MAT*α/α combination showed a broader range for both mitogenome size and intron number than those of *MAT***a/a** and *MAT***a/**α. The eight strains of the *MAT***a/a** and *MAT***a/**α mating types were of the diploid VNB/VNIV hybrids from South Africa. Based on their nuclear genotypes, these eight strains were likely descendants of the same recent hybridization event. Indeed, they all shared the same mitogenome size and intron number (**Supplementary Table S1**).

The close association between mitogenome size and intron number as demonstrated in **Figure 2** is further confirmed in the direct correlational analyses between them using the 184 strain. As shown in **Figure 3**, a statistically highly significant correlation, with a high correlation coefficient, was found between mitogenome size and intron number in the global population of *C. neoformans*. As expected, the length of summed intron sequences was significantly correlated with mitogenome size (r = 0.980, p = 4.41E-131) (**Supplementary Table S2**). Interestingly, the summed lengths of intergenic regions and the summed lengths of exon sequences were also positively correlated with mitogenome sizes, with correlation coefficients of 0.707 (p = 2.20E-29) and 0.241 (p = 9.61E-3) respectively (**Supplementary Table S2**).

Concatenated Exon Sequence Phylogeny

We used the concatenated exon sequences from all 17 *C. neoformans* mitochondrial coding genes to construct a phylogeny (**Figure 4**). This phylogenetic tree was then used as a reference to show the phylogenetic distributions of all 184 strains based on their clade affiliations (as determined based on nuclear genome SNPs), ecological and geographic origins, and mating types (Rhodes et al., 2017). In addition, the distributions of individual introns were also mapped onto the mitochondrial exon phylogenetic tree (**Figure 4**). Below we provide brief descriptions of the mitogenome phylogeny and the distributions of various strain features.

Mitogenome Clades and Subclades

Our phylogenetic analysis separated the 184 mitogenomes into several large clades as well as a few intermediate types (**Figure 4**). Among the 184 strains, the most distantly related mitogenomes were from the eight diploid VNB/VNIV hybrids. This was then followed by one group of VNB strains (sub-clade VNB1, containing both haploid VNB and diploid VNB/VNB strains), strains of VNI (both haploid VNI and diploid VNI strains, in two distinct groups, sub-clades VNI1 and VNI2), the second group of VNB strains (sub-clade VNB2, containing both haploid VNB and diploid VNB/VNB strains), and finally the two sub-clades of VNII strains (sub-clade VNII1 contains both haploid VNII and diploid VNII strains while sub-clade VNII2 contains only haploid VNII strains) (**Figure 4**). The mitogenomes of hybrids (VNI/VNB, VNII/VNB hybrids) are dispersed within or between these groups and these will be described in detail in a latter section.

Main Differences Between Mitogenome Exon Phylogeny and Nuclear Genome SNP Phylogeny

Aside from the phylogenetic distinctions of mitogenomes within and among the main clades described above, we also note three major differences between the phylogeny based on the mitogenome exon sequences and that based on nuclear genome SNPs as shown in Rhodes et al. (2017). In the first, the mitogenomes of haploid VNB strains were clustered into two distinct sub-clades separated by a large cluster mostly composed of VNI strains (**Figure 4**). In addition, the mitogenome clustering patterns of the VNB strains were different from those based on nuclear genome SNPs. For example, strains V2, V31, V87, CCTP15, SA8961, V17, WM1408 were clustered together on the mitogenome exon phylogeny (in the VNB2 sub-clade). However, based on nuclear genome SNPs, while strains V2, V31 and V87 were clustered together, the other four strains were dispersed into a different cluster (Rhodes et al., 2017). Second, the VNI strains were separated into two phylogenetically distinct sub-clades VNI1 and VNI2, with each subclade having overall more similar mitogenome exon sequences to the VNB1 and VNB2 sub-clades respectively (**Figure 4**). Importantly, sub-clade VNI2 consists of 21 strains from diverse geographic areas including China (CHC193), India (6 strains such as INCr132), Thailand (CM30), the US (A5-35-17 and C8), South Africa (9 strains such as CCTP3), France (AD1-7a), and Japan (Jp1088). These 21 strains also formed a genotypic cluster based on nuclear genome SNPs as shown by Rhodes et al. (2017). Third, several VNB clade strains identified based on their nuclear genome SNPs showed very similar (e.g., strain Bt85 from Botswana) or identical (strain RCT21 from South Africa) mitogenome exon sequences to those of VNI1 and VNI2 sub-clades respectively (**Figure 4**). This result suggested that these strains were likely hybrids, with their mitochondrial and nuclear genomes within each strain belonging to different lineages.

Mitogenomes of Diploid Strains

The diploid VNI/VNI, VNB/VNB, VNII/VNII strains all have mitogenome exon sequences within the predicted main VNI, VNB, and VNII clades respectively. For example, all four VNII/VNII diploid strains have identical mitochondrial exon

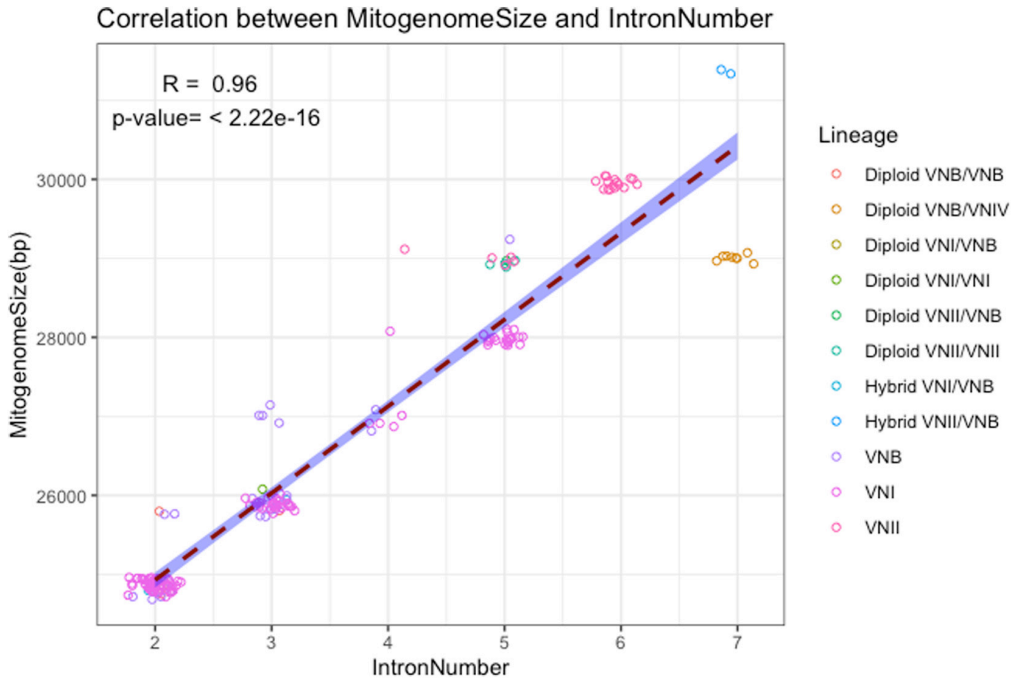

FIGURE 3 | Correlation between mitogenome size and intron number. The regression line and the 95% confidence interval are shown. Random noise was added to points using normal distribution to show the number of data points around each value. The standard deviations given to the X axis (intron number) and the Y axis (mitogenome size) are 0.1 intron and 60 bp respectively.

sequences to each other and clustered within the haploid VNII2 sub-clade. Similarly, of the three VNB/VNB diploid strains, one (MMRL2445) was clustered within the haploid VNB2 sub-clade while the other two (Bt50 and Bt158) were clustered within the VNB1 sub-clade. The three VNI/VNI diploid strains were all clustered within the main VNI1 sub-clade. However, the inter-clade diploid hybrids showed inconsistent mitogenome exon phylogenetic distributions. For example, the diploid VNI/VNB strain Bt66 has a mitogenome exon genotype clustered within one of the VNB sub-clades (**Figure 4**). In contrast, two diploid VNII/VNB hybrids (MW-RSA852 and CCTP51) had intermediate mitochondrial exon genotypes between VNB and VNII. For the eight diploid VNB/VNIV hybrids, they all showed mitogenomes very different from the known VNB mitogenomes as well as distinct from the reference mitogenome of VNIV (*C. deneoformans*) (**Figure 4**). These results suggest the potential biparental mitochondrial inheritance and/or mitogenome recombination during hybridization in nature.

Mitogenomes of Haploid Hybrids

Of the seven haploid hybrids among clades within *C. neoformans*, their mitogenome exon sequences also showed different phylogenetic distribution patterns. For example, of the five VNI/VNB haploid hybrids as identified based on their nuclear genome SNPs, four (Bt125, Bt131, Bt162, and Bt163) had mitogenomes more similar to those of the main VNI1 sub-clade while one strain (Ftc260-1) was clustered into the VNB1 sub-clade (**Figure 4**).

Geographic Distributions on Mitogenome Tree

With regard to geographic distributions along the mitogenome exon phylogenetic tree, South Africa has the broadest distribution, with strains represented in all major clades and sub-clades of the phylogeny (**Figure 4**). Other countries with broad phylogenetic representations include Botswana and Brazil. The Asian samples are primarily clustered into the VNI sub-clades (**Figure 4**). Overall, the geographic distributions on the phylogeny are largely consistent with those identified based on nuclear genome SNPs. We would like to note that due to strain representation bias among geographic regions, the geographic distribution identified here may not be truly representative of those in natural populations of this species.

Ecological and Mating Type Distributions on Mitogenome Tree

Of the remaining two characters associated with these strains, mating type and ecological niches, their distributions on the mitogenome exon phylogeny are overall similarly consistent with their nuclear genome SNP-based phylogenetic distributions. Specifically, strains of *MAT*α are broadly distributed on the phylogenetic tree. The relatively few strains with mating types *MAT***a** and *MAT*α/α are not clustered but are broadly distributed onto the phylogeny, often with identical mitogenome exon sequences to those of *MAT*α strains, consistent with the lack of mitogenome sequence differentiation between *MAT***a** and *MAT*α strains in nature. However, the seven diploid strains of

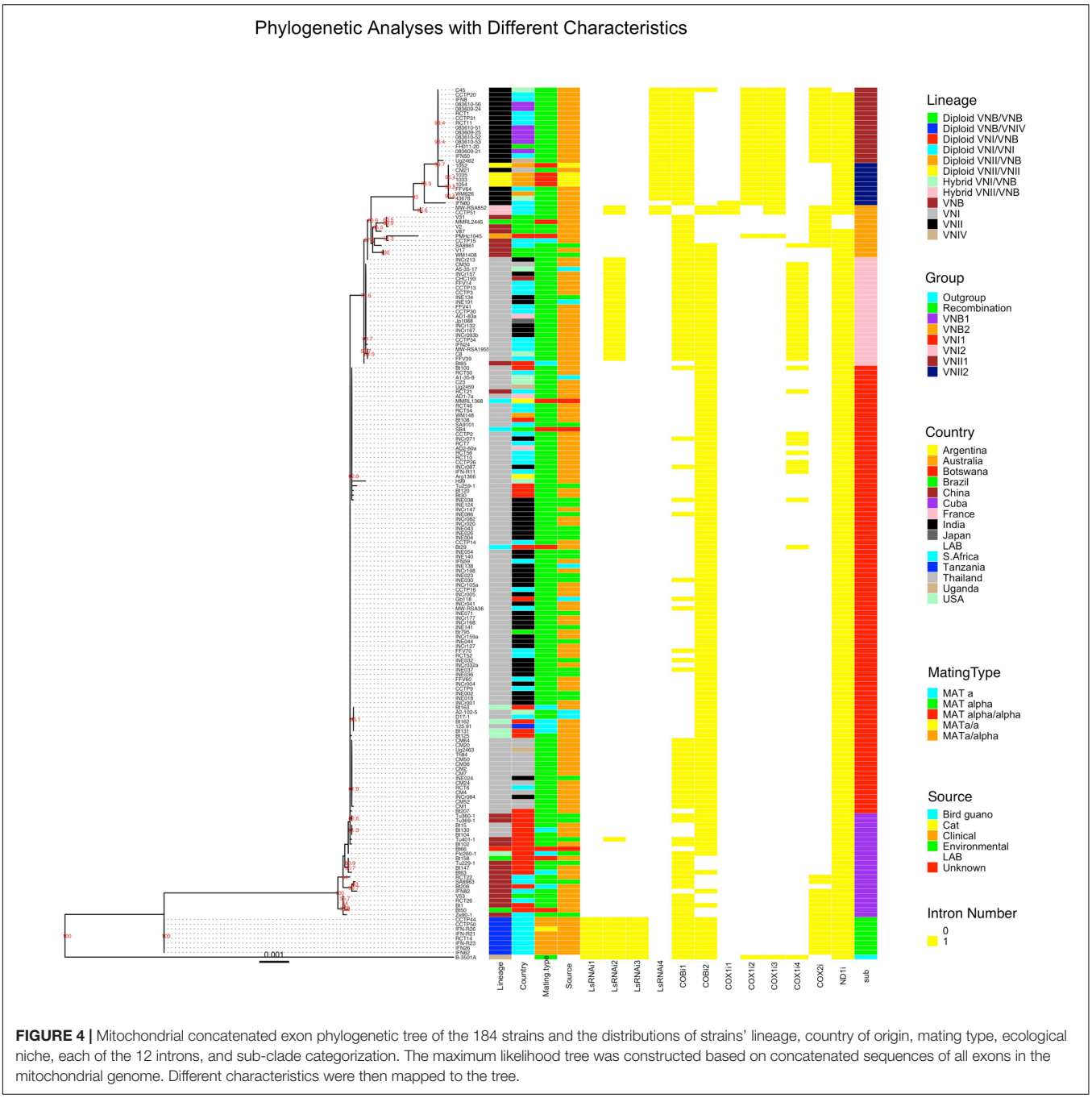

FIGURE 4 | Mitochondrial concatenated exon phylogenetic tree of the 184 strains and the distributions of strains' lineage, country of origin, mating type, ecological niche, each of the 12 introns, and sub-clade categorization. The maximum likelihood tree was constructed based on concatenated sequences of all exons in the mitochondrial genome. Different characteristics were then mapped to the tree.

*MAT***a**/α and one diploid strain of *MAT***a/a** of the VNB/VNIV hybrid origins all had identical mitogenomes to each other. As mentioned above, these 8 strains were likely derived from the same recent hybridization event between strains of VNB and VNIV. Ecologically, the clinical and non-clinical samples within both the VNI and VNB clades are interspersed with each other on the mitogenome exon phylogeny, with strains from different ecological niches often share identical mitogenome exon sequences (**Figure 4**). The exceptions are the diploid VNB/VNIV hybrids and the VNII isolates where only strains from humans and in the case of VNII, four strains from diseased cats, were included for analyses. Thus, in these two clades, there was no environmental strain for mitogenome comparison.

Comparisons of Intron Phylogeny With Their Corresponding Exon Phylogeny

In this sample of 184 strains *C. neoformans*, a total of 12 nucleotide sites located within five mitochondrial genes were found to contain introns. The detailed intron distribution for each strain is shown in **Supplementary Table S2** and **Figure 4**. Some introns were found in only a few isolates while others were found in most of the isolates. For example, the first intron located

in *COX1* gene (i.e., the intron closest to the 5′ end of the *COX1* gene), COX1i1, was found in only three strains with one from the VNII2 sub-clade and two representing VNII/VNB hybrids. On the other hand, the ND1i intron was found in all but four strains (three of them in the VNB2 sub-clade and one in the VNII1 sub-clade). Similar to the ND1i intron, intron COBi1 was broadly distributed along the phylogenetic tree, found in representative strains of all major clades (**Figure 4**). Most of the remaining introns showed some biases in distribution on the mitogenome exon phylogeny (**Figure 4**). The details of which will be briefly described below.

At each of the 12 intron-containing nucleotide sites, the introns from all the strains were highly similar to each other. In contrast, DNA sequences from introns at different positions were generally highly divergent from each other (data not shown). Among introns at these 12 positions, 11 contained open reading frames coding for either the GIY-YIG endonuclease (in introns ND1i and LsRNAi4) or the LAGLIDADG endonuclease (in introns COBi1, COBi2, COX1i1, COX1i2, COX1i3, COX1i4, COX2i, LsRNAi2, and LsRNAi3). The only intron without an open reading frame was LsRNAi1. Blast analyses of these intronic sequences revealed that their closest matches in GenBank were all from fungi, with different introns in the *C. neoformans* mitogenomes having the highest E scores to introns from different fungal species (details not shown). Below we describe the phylogenetic comparisons between the introns at each of 12 intron positions and their corresponding exons among the 184 strains.

Exon–Introns Phylogenetic Relationships Within the *LsRNA* Gene

As shown in **Figure 4** and described above, a total of four nucleotide sites within the mitochondrial *LsRNA* gene contained introns in the analyzed population. The phylogenies based on the *LrRNA* exon sequences and sequences at each of the four introns are shown in **Supplementary Figures S1–S4**. Two of the four introns, LsRNAi1 and LsRNAi3, were found only in the eight VNB/VNIV diploid strains. Furthermore, all eight strains showed identical exon and intron sequences for both introns LsRNAi1 and LsRNAi3 (**Supplementary Figures S1, S3**). In addition to the eight VNB/VNIV hybrids, intron LsRNAi2 was also found in all the 21 strains of the VNI2 sub-clade, as well as one strain of VNB1 (Tu401-1) and two VNII/VNB hybrids (MW-RSA852 and CCTP51) (**Figure 4** and **Supplementary Figure S2**). DNA sequence variations among strains within the LsRNAi2 intron separated the strains into three unique alleles, with the VNB1 strain and all the 21 VNI strains belonging to one allele while the other two alleles were represented separately by the VNII/VNB and the VNB/VNIV hybrids respectively, consistent with their phylogenetic separation based on *LsRNA* exon sequence (**Figure 4** and **Supplementary Figure S2**). The fourth intron in *LsRNA*, LsRNAi4, was found only in VNII strains and the two VNII/VNB hybrids (MW-RSA852 and CCTP51) (**Figure 4** and **Supplementary Figure S4**). Indeed, all VNII strains has intron LsRNAi4 except one, IFN80, from South Africa. DNA sequence variations among strains within the LsRNAi4 intron separated the strains into two unique alleles, with all the VNII strains sharing one allele and the two VNII/VNB hybrids sharing a different allele (**Figure 4** and **Supplementary Figure S4**).

Exon–Intron Phylogenetic Relationship Within the *COB* Gene

As shown in **Supplementary Table S2** and **Figure 4**, there are two introns in the *COB* gene, with both introns broadly distributed along the mitochondrial exon phylogenetic tree. The phylogenies based on the *COB* exon sequences and sequences at each of the two introns are shown in **Supplementary Figures S5, S6**. Each of the 184 strains analyzed here has at least one intron in the *COB* gene, with several groups of strains containing both introns (**Figure 4**). For the COBi1 intron, all strains of VNII clade, all strains in VNI2 sub-clade, some strains in VNI1 subclade, most strains in the VNB clade, and all the VNB/VNIV diploid hybrids contained this intron. Aside from the patchy distributions within the VNI and VNB clades (**Figure 4**), there was no obvious phylogenetic incongruence between the *COB* exon phylogeny and the COBi1 intron phylogeny, with both the exon and intron sequences highly similar to each other with few nucleotide differences separating them (**Supplementary Figure S5**).

For the COBi2 intron, all strains of VNI contained it while VNII and VNB strains showed patchy distributions. Indeed, only one strain in the VNII clade has this intron. The hybrids also showed patchy distributions, with most of them containing the intron. Similar to the comparison between *COB* exon phylogeny and COBi1 intron phylogeny, we found no obvious phylogenetic incongruence between the *COB* exon phylogeny and COBi2 phylogeny (**Supplementary Figure S6**).

Exon–Intron Phylogenetic Relationships Within the *COX1* Gene

As shown in **Figure 4** and **Supplementary Table S2**, a total of four nucleotide sites within the *C. neoformans* mitochondrial *COX1* gene contained introns in our sample. The phylogenies based on the *COX1* exon sequences and sequences at each of the four introns are shown in **Supplementary Figures S7–S10**. One intron COX1i1 was only found in three phylogenetically closely related strains and the intron sequences from two of them, MW-RSA852 and CCTP51, were identical to each other, consistent with their *COX1* exon sequence identity (**Supplementary Figure S7**). The third strain IFN80 had different COX1 exon and COX1i1 intron sequences from the above two strains (**Supplementary Figure S7**). Compared to intron COX1i1, introns COX1i2 and COX1i3 have broader and very similar distributions to each other (**Figure 4** and **Supplementary Figures S8, S9**). Both the COX1i2 and COX1i3 introns were found in all the analyzed VNII strains but were absent in all the analyzed VNI and VNB strains. In addition, one diploid VNII/VNB hybrid strain PMHc1045.ENR.STOR contained both COX1i2 and COX1i3 introns. Interestingly, two other hybrids of VNII/VNB, MW-RSA852 and CCTP51, contained only the COX1i3 intron but not the COX1i2 intron. No sequence variation was observed among the COX1i2 alleles (**Supplementary Figure S8**) and for the COX1i3 intron, all VNII strains shared identical DNA sequences (**Supplementary**

Figure S9). However, the two hybrids had slightly different intron COX1i3 sequences from those of VNII strains (**Supplementary Figure S9**). Different from those of the other three introns within the *COX1* gene, only one strain of VNB (SA8961) and a subset of the VNI strains contained the COX1i4 intron. Furthermore, the COX1i4 introns in all the VNI strains had identical nucleotide sequences (**Supplementary Figure S10**). Overall, we observed very limited sequence variations among alleles for any of the four *COX1* introns, especially for those in the same clade and/or sub-clade as identified based on their nuclear genome SNPs and mitogenome exon sequences (**Supplementary Figures S7–S10**).

Exon–Intron Phylogenetic Relationship Within the *COX2* Gene

As shown in **Figure 4** and **Supplementary Table S2**, one intron was found within *COX2*. No strain within VNI was found to contain this intron. Within the VNII clade, all strains of the VNII1 sub-clade contained the intron while none of the strains within the VNII2 sub-clade contained the intron (**Figure 4**). However, the pattern is different for strains in the VNB clade with a portion of strains in both VNB1 and VNB2 sub-clades having the intron while other don't. Phylogenetic analyses between the *COX2* exon phylogeny and the COX2i intron phylogeny revealed very limited exon sequence variations but a large number of intron sequence types (**Supplementary Figure S11**). Interestingly, the COX2i intron phylogeny matched well the concatenated mitogenome exon phylogeny, with introns in VNII strains, VNB strains, and the diploid VNB/VNIV hybrids all clustered separately from each other (Figure S11). This result is consistent with the early acquisition of the COX2i intron during *C. neoformans* evolution, followed by specific losses in individual clades and sub-clades.

Exon–Intron Phylogenetic Relationship Within the *ND1* Gene

All analyzed *C. neoformans* strains in this study except four contained the ND1i intron. Of the four strains without the intron, one belonged to the VNII1 sub-clade (strain C48), two belonged to the VNB2 sub-clade (V2 and V31), and one was a VNB/VNB diploid (MMRL2445) (**Figure 4** and **Supplementary Table S2**). Comparisons between the *ND1* exon phylogeny and the ND1i intron phylogeny revealed no exon sequence variation among the strains within *ND1* but a large number of intron sequence types (**Supplementary Figure S12**). However, the ND1i intron phylogeny matched well with the concatenated mitogenome exon phylogeny, with introns in VNII strains, VNB strains, and the diploid VNB/VNIV hybrids all clustered separately from each other. This result is consistent with the early acquisition of the ND1i intron during *C. neoformans* evolution, followed by specific loss(es) in the four strains or their ancestor(s).

Evidence for Mitogenome Recombination

Our phylogenetic analysis based on the concatenated mitochondrial exon sequences demonstrated that the eight diploid VNB/VNIV hybrids from South Africa contained mitogenomes distinctly different from both the reference VNIV (*C. deneoformans*) strain B-3501A and all the remaining *C. neoformans* samples (including all VNB strains; **Figure 4**). To investigate the potential origins of the mitogenomes of these eight strains, we compared each of their 17 protein- and rRNA-coding gene sequences individually with each other and with those from the B-3501A and all the other 176 *C. neoformans* strains. Our analyses revealed that all eight VNB/VNIV hybrids had identical concatenated exon sequences to each other. However, depending on the specific gene, their exon sequences may be identical or closely related to either the known VNB strain(s) or the B-3501A strain. Specifically, three (*RPS3, LsRNA,* and *COX3*) of the 17 coding genes in these eight strains had identical or highly similar sequences (>99% sequence identity) to the B-3501A alleles but were distinctly different from all the other 176 *C. neoformans* strains (<93% sequence identity). In contrast, 13 of the 17 coding genes (genes *ATP6, ATP8, ATP9, COB, COX1, COX2, ND1, ND2, ND3, ND4L, ND5, ND6,* and *SsRNA*) in these eight strains had allelic sequences identical or highly similar to the alleles in the 176 *C. neoformans* strains (>99% sequence identity at each locus). Interestingly, in the *ND4* gene, the first 373 nucleotides of the eight hybrids were identical to the B-3501A allele while nucleotides from 465 to 1452 bp (the remaining part of the gene) were identical or highly similar (>99%) to most alleles of the other 176 *C. neoformans* strains. The intermediate nucleotides between those two regions, from 374 to 464 bp of the *ND4* gene, corresponding to 4599–4691 nt of the published H99 mitogenome (GenBank accession number NC004336), were identical among all the strains we analyzed, including B-3501A, H99, the eight VNB/VNIV hybrids, and all the remaining 176 *C. neoformans* isolates. This region contained one recombination breakpoint.

Since the three genes (*RPS3, LsRNA,* and *COX3*) showing identical or high sequence similarity to B-3501A were located next to each together in the mitogenome, flanked by *ND4* from one side and *COB* from the other, the intergenic sequence between RPS3 and COB must contain the other recombination breakpoint. Indeed, whole genome sequence comparisons of the assembled mitogenomes of B-3501, H99, and the VNB/VNIV hybrids revealed the other recombination breakpoint to be between 23,058 and 23,059 nt (positions refer to that in the H99 genome), at the end of *COB* gene. [Due to the large number of files and large file sizes in the phylogenetic analyses of the 17 coding genes, the detailed graphs and data of the analyses are not presented but they are available from the authors.] **Figure 5** is a schematic diagram showing the composition of the eight VNB/VNIV hybrid mitogenomes.

DISCUSSION

In this study, we analyzed the mitogenome variations among 184 strains of *C. neoformans*, the most prevalent human pathogen of the *Cryptococcus* species complex. Our analyses identified large genome size and intron number variations among the analyzed strains. In addition, the

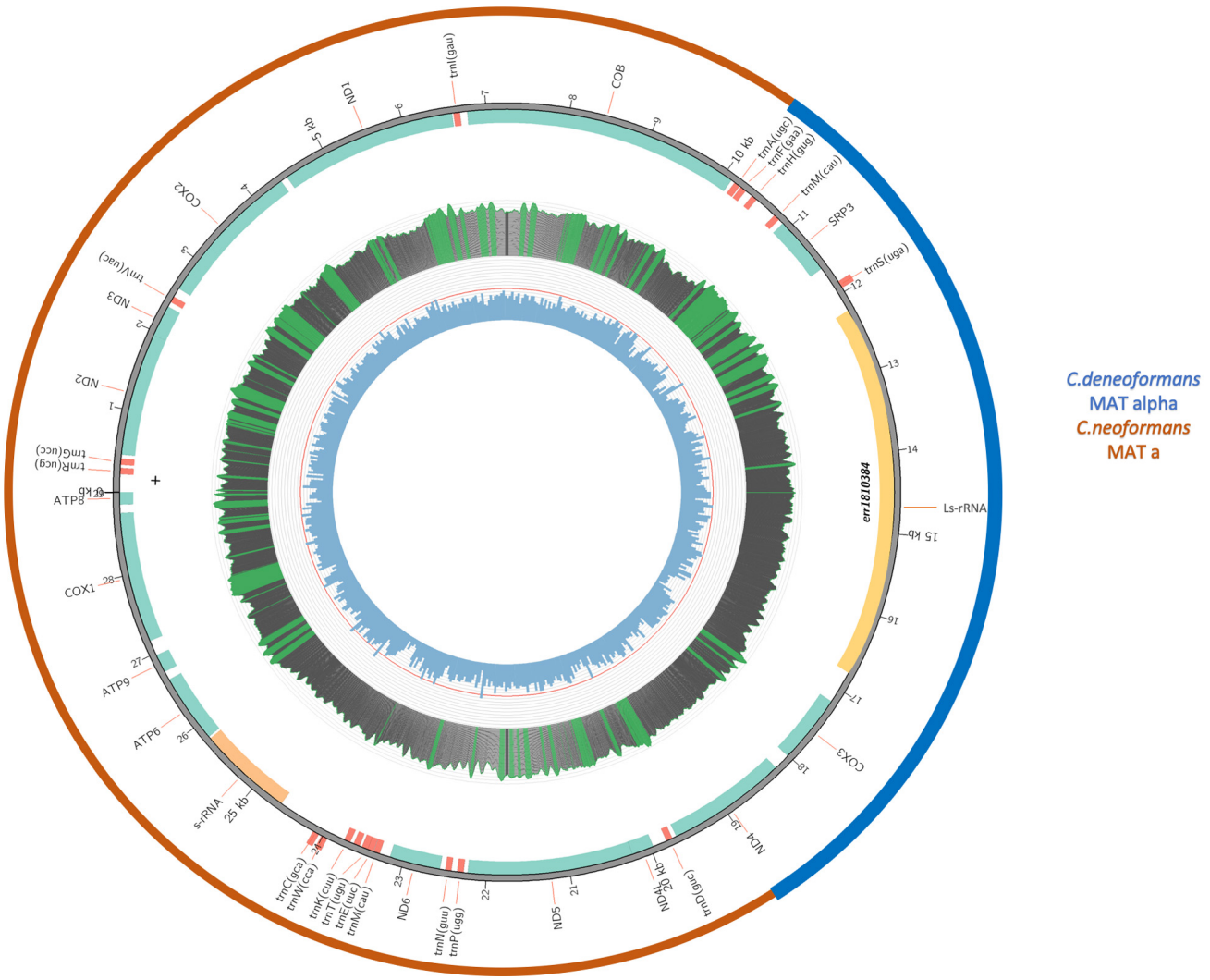

FIGURE 5 | A schematic diagram showing the composition of the eight VNB/VNIV hybrid mitogenomes. The inner circle indicates GC content, with the red line indicating 50% GC content. Middle circle indicates nucleotide coverage in sequence reads. For this sample, the coverage ranges from 5000 to 8000x. Green means the coverage is over top quartile; red means lower than 20x. The second circle from the outside indicates the locations of individual genes. The outermost circle indicates the likely origins of the mitogenome from either *C. neoformans* (Red) or *C. deneoformans* (blue).

concatenated mitogenome exon sequences revealed strain relationships largely consistent with those derived from nuclear genome SNPs. However, inconsistencies were also observed, especially among hybrids from between different lineages. Overall, there was little evidence for mitogenome-based strain relationships according to geographic origin or ecological niches. Interestingly, unambiguous evidence for mitogenome recombination was found for several strains. Below we discuss the relevance and potential implications of our results.

Mitogenome Size and Intron Number Variation

Previous studies have shown that fungal mitogenomes can vary in size from ∼12 to over 200 kb, a difference of over 20 folds (Sandor et al., 2018[3]; Zhang et al., 2020). The mitogenome sizes for strains of *C. neoformans* analyzed here are within the range of published fungal mitogenome sizes, but toward the small end. However, most of previous studies had relatively few, or in some cases only one, strain from each species. To our knowledge, the 184 mitogenomes analyzed here represented the largest number of fungal mitogenomes from within the same species in a single study. Our results demonstrated that within *C. neoformans*, the mitogenome sizes among strains can vary by over 20%.

Despite the relatively large mitogenome size variation among strains, all the mitogenomes of the 184 strains contained the same number of protein-coding genes, ribosomal RNA genes, and tRNA genes; and in the same order. The mitochondrial

[3]https://www.ncbi.nlm.nih.gov/genomes/GenomesGroup.cgi?opt=organelle&taxid=4751&sort=Genome

genes found in these *C. neoformans* strains were also commonly found in most of the published fungal mitochondrial genomes. The main contributor to the mitogenome size differences among *C. neoformans* strains was introns (both intron number and summed intron lengths), also similar to previous comparisons among fungal species (Sandor et al., 2018; Zhang et al., 2020). These comparisons suggest that the main mechanisms driving mitogenome size variation among strains within fungal species are likely similar to those driving mitogenome size variation among fungal species. In both cases, intron gains and losses are primarily responsible for the variations in fungal mitogenome sizes. The open reading frames in 11 of the 12 introns encoding endonucleases are consistent with the mobility of these introns (Yan et al., 2018). However, our study also found that intergenic regions and exon sequences contributed significantly to mitogenome size variations in *C. neoformans*.

In this study, *C. neoformans* strains from most geographic regions and ecological niches showed a range of mitogenome sizes and a diversity of intron distributions. The lack of a clear geographic and ecological pattern for the *C. neoformans* mitogenomes is consistent with the organism's ubiquitous distributions in a variety of ecological niches and with its long-distance dispersal ability. As suggested in other studies (e.g., Xu et al., 2000b; Rhodes et al., 2017; Samarasinghe et al., 2019), both natural factors such as wind and bird migrations and anthropogenic factors such as human travel and commercial trade could have contributed to the gene flow of *C. neoformans* and the observed lack of geographic pattern for mitogenome size and intron distributions.

However, due to the biased/limited samples from certain geographic regions and ecological niches, we would like to note that more extensive sampling might reveal certain region-specific differences in mitogenome size and intron number distributions. For example, the Far East Asian population of *C. neoformans* is dominated by ST5 and its clonal derivatives based on MLST at seven nuclear loci (Chen et al., 2018). The two strains analyzed here, CCH193 from China and Jp1088 from Japan, have identical mitogenome sequences and very similar nuclear genome sequences. It's likely that most, if not all, ST5 strains from Far East Asia have the same mitogenome size and intron number. Genome sequences from additional strains are needed in order to confirm this hypothesis.

Mitogenome Exon Phylogeny

Aside from genome size and intron number variations among strains, single nucleotide polymorphisms were also found among the 184 mitogenomes. The strain relationships and their clade affiliations as revealed by mitogenome SNPs were largely consistent with those inferred based on nuclear genome SNPs (**Figure 4**). Overall, the results indicate that through most of the evolutionary history of this species, these clades and sub-clades have been evolving independently. However, phylogenetic analyses of mitogenome exon SNPs revealed several novel features that are different from those based on nuclear genome SNPs. For example, *C. neoformans* strains were clustered into additional mitogenome sub-clades (VNI1, VNI2, VNII1, VNII2, VNB1, and VNB2), some of which were different in their clustering patterns from those inferred based on their nuclear genome SNPs (**Figure 4**).

One strain showing different clustering pattern between the mitochondrial and nuclear genomes is strain RCT21 from South Africa. This strain showed a nuclear genome of the VNB type, almost identical to the nuclear genome sequence of another strain of VNB, RCT26 (Rhodes et al., 2017). However, RCT21 has a mitogenome of the VNI1 type, with identical mitogenome exon sequences to a large number of VNI1 strains, but very different from that of RCT26 which were clustered into VNB1, as expected (**Figure 4**). At present, the detailed process for generating RCT21 is not known. One possibility for the inconsistent grouping between the nuclear and mitochondrial genomes of RCT21 was that it might have been derived from a mating event between a VNI and a VNB strain, with the mating product, a dikaryotic hypha, containing two haploid parental nuclei but inheriting the mitogenome of the VNI parent. However, during hyphal extension of the dikaryon and before sexual reproduction, asexual spores such as conidia or chlamydospores containing one of the two haploid nuclei may form. If the nucleus in the haploid asexual spore was that of the original VNB parent, a recombinant like RCT21 could be formed. Indeed, this process was used to generate a laboratory strain containing the nuclear genome from one parent but mitochondrial genome from another in an early study (Yan and Xu, 2003). However, as revealed by the combined results of the Rhodes et al. (2017) study and this study, most inter-clade hybrids contained nuclear genes from both parental clades but mitochondrial genome from one parent.

Mitogenome Recombination

Our sequence analyses revealed that the eight VNB/VNIV hybrids from South Africa contained mitogenomes with signature sequences from both the VNB and the VNIV clades. In addition, we were able to identify the regions where recombination breakpoints were most likely located (**Figure 5**). Laboratory investigations of *C. neoformans* (serotype A) and *C. deneoformans* (serotype D) crosses revealed that their mitogenomes were uniparentally inherited from the *MAT***a** parent (Xu et al., 2000a). In addition, analyses of natural serotype AD hybrids were found to contain mitochondrial DNA also from the *MAT***a** parent (Yan and Xu, 2003). Specifically, a serotype AD strain having its *MAT***a** locus from a serotype A parent and its *MAT***a** locus from a serotype D parent, i.e., an **a**AD**a** hybrid, would have a mitochondrial genotype of the serotype A parent. Conversely, a serotype AD strain having its *MAT***a** locus from a serotype D parent and its *MAT***a** locus from a serotype A parent, i.e., an **a**AD**a** hybrid, would have a mitochondrial genotype of the serotype D parent. The recombinant mitogenomes here of the eight VNB/VNIV hybrids seemed different from those earlier studies where uniparental mitogenome inheritance was shown.

At present, the mechanisms for the difference between these eight hybrids and earlier investigated hybrids are not known. However, there are a couple of possibilities. In the first, the mating condition(s) under which the eight VNB/VNIV hybrids were generated might have been different from the laboratory conditions used to generate laboratory serotype AD hybrids and different from those of the other natural serotype

AD hybrids analyzed earlier. Previous studies have shown that under stressful conditions, such as UV irradiation and high temperature, during *C. neoformans* mating, biparental mitochondrial inheritance could be common and that progeny could have recombinant mitochondrial genotypes (Yan et al., 2007). The second possibility might be due to the differences in the markers analyzed between this study and earlier studies. Earlier studies of mitochondrial inheritance in *C. neoformans* were primarily based on 1–2 PCR-RFLP markers, targeting one or two single nucleotide polymorphisms (Xu et al., 2000a; Yan and Xu, 2003). Analyzing additional markers in those crosses might have revealed mitogenome recombination events.

Mitogenome Intron Distributions

We observed variations in the number of strains containing each of the 12 introns among the 184 strains. None of the 12 introns were distributed in all the 184 strains and none of the 184 strains were found to have all 12 introns. However, some of the introns (e.g., ND1i and COBi2) were more frequently found than others (e.g., COX1i1) among the 184 strains. Despite the overall broad distributions for most of the introns, some introns showed biased distributions at the clade or sub-clade levels as defined based on the concatenated mitochondrial exon sequences. If we use strain B-3501A of the closely related species *C. deneoformans* B-3501A as the mitogenome phylogeny outgroup for *C. neoformans*, the ancestral intron state of the *C. neoformans* would be containing nine of the introns (LsRNAi1, LsRNAi2, LsRNAi3, COBi1, COBi2, COX1i2, COX1i3, COX1i4, and ND1i). Based on this assumption, as none of the 176 strains of *C. neoformans* contained introns LsRNAi1 and LsRNAi3, these two must have been lost in the ancestor of *C. neoformans*. Similarly, intron LsRNAi2 was lost in the ancestor of *C. neoformans* but was regained by the ancestor of the VNI2 sub-clade. As for intron LrRNAi4, it was likely newly gained by the VNII clade. In contrast to the single gain and lost events for the four *LsRNA* introns, the two introns in *COB*, COBi1 and COBi2, were likely gained and/or lost multiple times. The COX1i1 intron was similar to that of LsRNAi4, likely gained recently once by an ancestor of VNII but was lost again in some of the descendants. Introns COX1i2, COX1i3, COX1i4, and COX2i were likely lost once and/or re-gained once or twice during the evolution of *C. neoformans*. Finally, the simplest explanation for the ND1i distribution is that it lost twice, one in the VNB2 sub-clade and the other for strain C45 of the VNII1 sub-clade. Based on the high sequence similarity among alleles within each of the low-frequency introns, most of the intron gains (or regains) seemed recent (**Supplementary Figures S1–S12**).

We note that the above inferred intron gains and losses were based on a single strain of a closely related species *C. deneoformans* as the outgroup. If other strains with different intron distributions were used as the outgroup and for ancestral state inference, the number of gain/loss events would differ. At present, the ecological, evolutionary and molecular mechanisms driving the mitogenome intron distributions are largely unknown. A recent study revealed that mutation in the sex-determining gene *SXI1*a could lead to the rapid spread of mitochondrial introns in *C. deneoformans* (Yan et al., 2018). However, regardless of the potential mechanisms, the highly skewed distributions of intron(s) toward certain clade and sub-clade suggest a potentially fast and efficient method for their identification, based on 1–3 PCR reactions. For example, the presence of both intron LsRNAi4 and COX1i2 would be indicative of strains in the VNII clade, and a further assay based on intron COX2i would allow the separation of VNII1 (the presence of this intron) from VNII2 (the absence of this intron). Similarly, the presence of both LsRNAi2 and COX1i4 would be indicative of their VNI2 subclade affiliation. The usefulness of the suggested tests needs experimental validation, including more samples, especially those from under-represented clades, geographic regions, and ecological niches, for analyses.

CONCLUSION

In this study, we assembled and analyzed the mitogenomes of a large number of strains of the human fungal pathogen *C. neoformans*. Our analyses identified variations among strains in both genome size and intron number. In addition, the mitogenome phylogeny based on concatenated exon sequences revealed the potential evolutionary relationships among the 184 strains with regard to their other features such as their nuclear genome affiliations, and their geographic and ecological origins. Our analyses identified several novel insights into the evolution of this organism. Furthermore, our results opened up new avenues of future research. For example, where did the introns in *C. neoformans* originate? How did they invade the mitogenomes of *C. neoformans*? How did *C. neoformans* maintain their mitogenome structure and gene order, despite the seemingly frequent intron gain and loss events? What are the effects of these introns on the adaptation and pathogenicity of *C. neoformans* clades and sub-clades? Will continued anthropogenic activities increase the spread of mitochondrial introns? Answers to these and other related questions could provide additional insights into the evolution and diversification of *C. neoformans* as well as their potential effects on its pathogenicity.

DATA AVAILABILITY STATEMENT

All datasets generated for this study are included in the article/**Supplementary Material**.

AUTHOR CONTRIBUTIONS

YW retrieved and analyzed the data. JX conceived and guided the study. Both authors contributed to writing the manuscript.

FUNDING

This research was supported by the Natural Sciences and Engineering Research Council of Canada (CRDPJ 474638-14).

ACKNOWLEDGMENTS

We thank the international consortium for sequencing the 188 strains of *Cryptococcus neoformans* and for making their raw sequence data freely available for analyses.

SUPPLEMENTARY MATERIAL

The Supplementary Material for this article can be found online at: https://www.frontiersin.org/articles/10.3389/fmicb.2020.00706/full#supplementary-material

FIGURE S1 | Co-phylogenetic tree of *LsRNA* concatenated exons and LsRNAi1.

FIGURE S2 | Co-phylogenetic tree of *LsRNA* concatenated exons and LsRNAi2.

FIGURE S3 | Co-phylogenetic tree of *LsRNA* concatenated exons and LsRNAi3.

FIGURE S4 | Co-phylogenetic tree of *LsRNA* concatenated exons and LsRNAi4.

FIGURE S5 | Co-phylogenetic tree of *COB* concatenated exons and COBi1.

FIGURE S6 | Co-phylogenetic tree of *COB* concatenated exons and COBi2.

FIGURE S7 | Co-phylogenetic tree of *COX1* concatenated exon and COX1i1.

FIGURE S8 | Co-phylogenetic tree of *COX1* concatenated exon and COX1i2.

FIGURE S9 | Co-phylogenetic tree of *COX1* concatenated exon and COX1i3.

FIGURE S10 | Co-phylogenetic tree of *COX1* concatenated exon and COX1i4.

FIGURE S11 | Co-phylogenetic tree of *COX2* concatenated exon and COX2i.

FIGURE S12 | Co-phylogenetic tree of *ND1* concatenated exon and ND1i.

TABLE S1 | Mitogenome size and intron number distributions among nuclear genome-based clades, geographic regions, ecological niches, and mating types.

TABLE S2 | Details of all strains analyzed in this study. Included in this table for each strain are strain name, geographic origin, ecological niche, mating type, GenBank accession numbers, mitogenome size, intron number and distributions, summed intron length, summed exon length, and summed intergenic spacer length.

REFERENCES

Bernt, M., Donath, A., Jühling, F., Externbrink, F., Florentz, C., Fritzsch, G., et al. (2013). MITOS: improved de novo metazoan mitochondrial genome annotation. *Mol. Phylogen. Evol.* 69, 313–319. doi: 10.1016/j.ympev.2012.08.023

Bodenhofer, U., Bonatesta, E., Horejš-Kainrath, C., and Hochreiter, S. (2015). msa: an R package for multiple sequence alignment. *Bioinformatics* 31, 3997–3999. doi: 10.1093/bioinformatics/btv494

Burger, G., Gray, M. W., and Lang, B. F. (2003). Mitochondrial genomes: anything goes. *Trends Genet.* 19, 709–716. doi: 10.1016/j.tig.2003.10.012

Calderone, R., Li, D. M., and Traven, A. (2015). System-level impact of mitochondria on fungal virulence: to metabolism and beyond. *FEMS Yeast Res.* 15:fov027. doi: 10.1093/femsyr/fov027

Chatre, L., and Ricchetti, M. (2014). Are mitochondria the Achilles' heel of the Kingdom Fungi? *Curr. Opin. Microbiol.* 20, 49–54. doi: 10.1016/j.mib.2014.05.001

Chen, Y. H., Yu, F., Bian, Z. Y., Hong, J. M., Zhang, N., Zhong, Q. S., et al. (2018). Multilocus sequence typing reveals both shared and unique genotypes of *Cryptococcus neoformans* in Jiangxi Province. *China. Sci Rep.* 8:1495. doi: 10.1038/s41598-018-20054-4

Cogliati, M. (2013). Global molecular epidemiology of *Cryptococcus neoformans* and *Cryptococcus gattii*: an atlas of the molecular types. *Scientifica* 2013:675213. doi: 10.1155/2013/675213

Dierckxsens, N., Mardulyn, P., and Smits, G. (2017). NOVOPlasty: de novo assembly of organelle genomes from whole genome data. *Nucleic Acids Res.* 45:e18. doi: 10.1093/nar/gkw955

Dong, K., You, M., and Xu, J. (2020). Genetic changes in experimental populations of a hybrid in thel *Cryptococcus neoformans* species complex. *Pathogens* 9:3. doi: 10.3390/pathogens9010003

Hagen, F., Khayhan, K., Theelen, B., Kolecka, A., Polacheck, I., Sionov, E., et al. (2015). Recognition of seven species in the *Cryptococcus gattii/Cryptococcus neoformans* species complex. *Fungal Genet Biol.* 78, 16–48. doi: 10.1016/j.fgb.2015.02.009

Hagen, F., Lumbsch, H. T., Arsic Arsenijevic, V., Badali, H., Bertout, S., Billmyre, R. B., et al. (2017*).). Importance of resolving fungal nomenclature: the case of multiple pathogenic species in the *Cryptococcus* Genus. *mSphere* 2, e238–e217. doi: 10.1128/mSphere.00238-17

Hiremath, S. S., Chowdhary, A., Kowshik, T., Randhawa, H. S., Sun, S., and Xu, J. (2008). Long-distance dispersal and recombination in environmental populations of *Cryptococcus neoformans* var. grubii from India. *Microbiology* 154, 1513–1524. doi: 10.1099/mic.0.2007/015594-0

Hua, W. J., Vogan, A. A., and Xu, J. (2019). Genotypic and phenotypic analyses of two "isogenic" strains of the human fungal pathogen *Cryptococcus neoformans* var. *neoformans*. *Mycopathologia* 184, 195–212 doi: 10.1007/s11046-019-00328-9

Katoh, K., Misawa, K., Kuma, K., and Miyata, T. (2002). MAFFT: a novel method for rapid multiple sequence alignment based on fast fourier transform. *Nucleic Acids Res.* 30, 3059–3066. doi: 10.1093/nar/gkf436

Kumar, S., Stecher, G., Li, M., Knyaz, C., and Tamura, K. (2018). MEGA X: molecular evolutionary genetics analysis across computing platforms. *Mol Biol Evol.* 35, 1547–1549. doi: 10.1093/molbev/msy096

Kwon-Chung, K. J., Bennett, J. E., Wickes, B. L., Meyer, W., Cuomo, C. A., Wollenburg, K. R., et al. (2017*). The case for adopting the "Species Complex" nomenclature for the etiologic agents of Cryptococcosis. *mSphere* 2, e357–e316. doi: 10.1128/mSphere.00357-16

Leinonen, R., Akhtar, R., Birney, E., Bonfield, J., Bower, L., Corbett, M., et al. (2010). Improvements to services at the European nucleotide archive. *Nucleic Acids Res.* 38, D39–D45. doi: 10.1093/nar/gkp998

Litter, J., Keszthelyi, A., Hamari, Z., Pfeiffer, I., and Kucsera, J. (2005). Differences in mitochondrial genome organization of *Cryptococcus neoformans* strains. *Antonie Van Leeuwenhoek* 88, 249–255. doi: 10.1007/s10482-005-8544-x

Litvintseva, A. P., Lin, X., Templeton, I., Heitman, J., and Mitchell, T. G. (2007). Many globally isolated AD hybrid strains of *Cryptococcus neoformans* originated in Africa. *PLoS Pathog.* 3:e114. doi: 10.1371/journal.ppat.0030114

Litvintseva, A. P., Xu, J., and Mitchell, T. G. (2011*). "ASM press: *Population Structure* and Ecology of *Cryptococcus*," in *Cryptococcus: From Human Pathogen to Model Organism*, eds J. Heitman, J. Kwon-Chung, J. Perfect, and A. Casadevall.

Ma, H.-S., and May, R. C. (2010). Mitochondria and the regulation of hypervirulence in the fatal fungal outbreak on Vancouver Island. *Virulence* 1, 197–201. doi: 10.4161/viru.1.3.11053

Meng, G. L., Li, Y. Y., Yang, C. T., and Liu, S. L. (2019). MitoZ: a toolkit for animal mitochondrial genome assembly, annotation and visualization. *Nucleic Acids Res.* 47:e63 doi: 10.1093/nar/gkz173

Rajasingham, R., Smith, R. M., Park, B. J., Jarvis, J. N., Govender, N. P., Chiller, T. M., et al. (2017). Global burden of disease of HIV-associated cryptococcal meningitis: an updated analysis. *Lancet Infect Dis.* 17, 873–881. doi: 10.1016/S1473-3099(17)30243-8

Revell, L. J. (2012). Phytools: an R package for phylogenetic comparative biology (and other things). *Methods Ecol. Evol.* 3, 217–223. doi: 10.1111/j.2041-210x.2011.00169.x

Rhodes, J., Desjardins, C. A., Sykes, S. M., Beale, M. A., Vanhove, M., Sakthikumar, S., et al. (2017). Tracing genetic exchange and biogeography of *Cryptococcus neoformans* var. grubii at the global population level. *Genetics* 207, 327–346. doi: 10.1534/genetics.117.203836

Saitou, N., and Nei, M. (1987). The neighbor-joining method: a new method for reconstructing phylogenetic trees. *Mol Biol Evol.* 4, 406–425.

Samarasinghe, H., Aljohani, R., Jimenez, C., and Xu, J. (2019). Fantastic yeasts and where to find them: the discovery of a predominantly clonal *Cryptococcus deneoformans* population in Saudi Arabian soils. *FEMS Microbiol Ecol.* 95:fiz122. doi: 10.1093/femsec/fiz122

Samarasinghe, H., and Xu, J. (2018). Hybrids and hybridization in the *Cryptococcus neoformans* and *Cryptococcus gattii* species complexes. *Infect.Genet. Evol.* 66, 245–255. doi: 10.1016/j.meegid.2018.10.011

Sandor, S., Zhang, Y., and Xu, J. (2018). Fungal mitochondrial genomes and genetic polymorphisms. *Appl. Microbiol. Biot.* 102, 9433–9448. doi: 10.1007/s00253-018-9350-5

Schliep, K. P. (2011). Phangorn: phylogenetic analysis in R. *Bioinformatics* 27, 592–593. doi: 10.1093/bioinformatics/btq706

Wickham, H. (2016). *ggplot2: Elegant Graphics for Data Analysis*. New York, NY: Springer-Verlag New York.

Xu, J., Ali, R., Gregory, D., Amick, D., Lambert, S., Yoell, H., et al. (2000a). Uniparental mitochondrial transmission in sexual crosses in *Cryptococcus neoformans*. *Curr. Microbiol.* 40, 269–273. doi: 10.1007/s002849910053

Xu, J., Vilgalys, R., and Mitchell, T. G. (2000b). Multiple gene genealogies reveal recent dispersion and hybridization in the human pathogenic fungus *Cryptococcus neoformans*. *Mol. Ecol.* 9, 1471–1481. doi: 10.1046/j.1365-294x.2000.01021.x

Yan, Z., Hull, C. M., Heitman, J., Sun, S., and Xu, J. (2004). SXI1alpha controls uniparental mitochondrial inheritance in *Cryptococcus neoformans*. *Curr Biol.* 14, R743–R744.

Yan, Z., and Xu, J. (2003). Mitochondria are inherited from the MATa parent in crosses of the basidiomycete fungus *Cryptococcus neoformans*. *Cryptococcus neoformans*. *Genetics* 163, 1315–1325.

Yan, Z., Li, Z., Yan, L., Yu, Y., Cheng, Y., Chen, J., et al. (2018). Deletion of the sex-determining gene SXI1alpha enhances the spread of mitochondrial introns in *Cryptococcus neoformans*. *Mobile DNA*. 9:24. doi: 10.1186/s13100-018-0129-0

Yan, Z., Sun, S., Shahid, M., and Xu, J. (2007). Environment factors can influence mitochondrial inheritance in the fungus *Cryptococcus neoformans*. *Fungal Genet Biol.* 44, 315–322. doi: 10.1016/j.fgb.2006.10.002

Yan, Z., and Xu, J. (2003). Mitochondria are inherited from the MATa parent in crosses of the basidiomycete fungus *Cryptococcus neoformans*. *Genetics* 163, 1315–1325.

Yu, G., Smith, D., Zhu, H., Guan, Y., and Lam, T. (2017). ggtree: an R package for visualization and annotation of phylogenetic trees with their covariates and other associated data. *Methods Ecol. Evol.* 8, 28–36. doi: 10.1111/2041-210x.12628

Zhang, Y., Yang, G., Fang, M., Deng, C., Zhang, K.-Q., Yu, Z., et al. (2020). Comparative analyses of mitochondrial genomes provide evolutionary insights into nematode-trapping fungi. *Front. Microbiol.* doi: 10.3389/fmicb.2020.00617

Zhang, Z., Schwartz, S., Wagner, L., and Miller, W. (2000). A greedy algorithm for aligning DNA sequences. *J. Comput. Biol.* 7, 203–214.

Zhao, Y., Lin, J., Fan, Y., and Lin, X. (2019). Life cycle of *Cryptococcus neoformans*. *Annu Rev Microbiol.* 73, 17–42. doi: 10.1146/annurev-micro-020518-120210

Conflict of Interest: The authors declare that the research was conducted in the absence of any commercial or financial relationships that could be construed as a potential conflict of interest.

frontiers in Microbiology

ORIGINAL RESEARCH
published: 29 April 2020
doi: 10.3389/fmicb.2020.00765

Exploring the Relationship Among Divergence Time and Coding and Non-coding Elements in the Shaping of Fungal Mitochondrial Genomes

Paula L. C. Fonseca[1], Fernanda Badotti[2], Ruth B. De-Paula[3], Daniel S. Araújo[1], Dener E. Bortolini[4], Luiz-Eduardo Del-Bem[4,5], Vasco A. Azevedo[4], Bertram Brenig[6], Eric R. G. R. Aguiar[4†] and Aristóteles Góes-Neto[1,4*]*

[1] Molecular and Computational Biology of Fungi Laboratory, Department of Microbiology, Instituto de Ciências Biológicas, Universidade Federal de Minas Gerais, Belo Horizonte, Brazil, [2] Department of Chemistry, Centro Federal de Educação Tecnológica de Minas Gerais, Belo Horizonte, Brazil, [3] Department of Molecular and Cellular Oncology, The University of Texas MD Anderson Cancer Center, Houston, TX, United States, [4] Program of Bioinformatics, Instituto de Ciências Biológicas, Universidade Federal de Minas Gerais, Belo Horizonte, Brazil, [5] Department of Botany, Instituto de Ciências Biológicas, Universidade Federal de Minas Gerais, Belo Horizonte, Brazil, [6] Institute of Veterinary Medicine, Burckhardtweg, University of Göttingen, Göttingen, Germany

The order Hypocreales (Ascomycota) is composed of ubiquitous and ecologically diverse fungi such as saprobes, biotrophs, and pathogens. Despite their phylogenetic relationship, these species exhibit high variability in biomolecules production, lifestyle, and fitness. The mitochondria play an important role in the fungal biology, providing energy to the cells and regulating diverse processes, such as immune response. In spite of its importance, the mechanisms that shape fungal mitogenomes are still poorly understood. Herein, we investigated the variability and evolution of mitogenomes and its relationship with the divergence time using the order Hypocreales as a study model. We sequenced and annotated for the first time *Trichoderma harzianum* mitochondrial genome (mtDNA), which was compared to other 34 mtDNAs species that were publicly available. Comparative analysis revealed a substantial structural and size variation on non-coding mtDNA regions, despite the conservation of copy number, length, and structure of protein-coding elements. Interestingly, we observed a highly significant correlation between mitogenome length, and the number and size of non-coding sequences in mitochondrial genome. Among the non-coding elements, group I and II introns and homing endonucleases genes (HEGs) were the main contributors to discrepancies in mitogenomes structure and length. Several intronic sequences displayed sequence similarity among species, and some of them are conserved even at gene position, and were present in the majority of mitogenomes, indicating its origin in a common ancestor. On the other hand, we also identified species-specific introns that advocate for the origin by different mechanisms. Investigation of mitochondrial gene transfer to the nuclear genome revealed that nuclear copies of the *nad5* are the most frequent while *atp8*, *atp9*, and *cox3* could not be identified in any of the nuclear genomes analyzed. Moreover, we also estimated the divergence time of each species

OPEN ACCESS

Edited by:
Tomasz Kulik, University of Warmia and Mazury in Olsztyn, Poland

Reviewed by:
Yongjie Zhang, Shanxi University, China
Bård Ove Karlsen, Nordland Hospital, Norway

***Correspondence:**
Eric R. G. R. Aguiar
ericgdp@gmail.com
Aristóteles Góes-Neto
arigoesneto@icb.ufmg.br; arigoesneto@gmail.com

†Present address:
Eric R. G. R. Aguiar, Department of Biological Science, Center of Biotechnology and Genetics, Universidade Estadual de Santa Cruz, Ilhéus, Brazil

Specialty section:
This article was submitted to Fungi and Their Interactions, a section of the journal Frontiers in Microbiology

Received: *30 January 2020*
Accepted: *30 March 2020*
Published: *29 April 2020*

Citation:
Fonseca PLC, Badotti F, De-Paula RB, Araújo DS, Bortolini DE, Del-Bem L-E, Azevedo VA, Brenig B, Aguiar ERGR and Góes-Neto A (2020) Exploring the Relationship Among Divergence Time and Coding and Non-coding Elements in the Shaping of Fungal Mitochondrial Genomes. Front. Microbiol. 11:765. doi: 10.3389/fmicb.2020.00765

and investigated its relationship with coding and non-coding elements as well as with the length of mitogenomes. Altogether, our results demonstrated that introns and HEGs are key elements on mitogenome shaping and its presence on fast-evolving mtDNAs could be mostly explained by its divergence time, although the intron sharing profile suggests the involvement of other mechanisms on the mitochondrial genome evolution, such as horizontal transference.

Keywords: mitogenomes, Ascomycota, non-coding elements, structural variation, gene transfer, divergence time

INTRODUCTION

The mitochondrion is an important organelle of eukaryotic cells, involved in multiple processes that are necessary for cell survival and reproduction. It is responsible for the ATP production, the universal energy-transfer biomolecule in living organisms, through the oxidative phosphorylation pathway. In addition to respiratory metabolism and energy production function, mitochondria is also involved in other processes such as senescence during the cell cycle and the maintenance of ion homeostasis (Burger et al., 2003; Basse, 2010; Chatre and Ricchetti, 2013).

Conversely to the majority of other intracellular membrane structures, mitochondria contain their own genome that is capable of independent replication and inheritance. Nonetheless, over evolutionary time, most of the genes in the initial endosymbiont have been transferred to the nuclear genome and only a few genes are retained in mitochondrial genomes (mitogenomes). Indeed, most of the mitochondrial proteins are encoded by the nuclear genome and transported to the mitochondria (Burger et al., 2003). Within each mitochondrion, there are typically multiple copies of the genome, which replicate independently of the nuclear genome and cell cycle (Chatre and Ricchetti, 2013). Furthermore, most of the mitochondrial genomes are composed of a single circular chromosome, although some organisms contain linear mitochondrial genomes made up of multiple subunits (Burger et al., 2003).

Fungal mitogenomes are generally characterized by the presence of 14 conserved protein-coding genes involved in electron transport (*cytochrome oxidase subunits 1*, *2*, and *3*, *NADH dehydrogenase subunits 1*, *2*, *3*, *4*, *4L*, *5*, and *6*) and ATP synthesis (*ATP synthase subunits 6*, *8*, and *9*, and *apocytochrome b*). In addition, mitochondrial genome typically has one of the small (SSU rRNA) and large subunits ribosomal RNAs (LSU rRNA), and a set of transfer RNA (tRNA) genes (Bullerwell and Lang, 2005; Al-Reedy et al., 2012; Ferandon et al., 2013; Brankovics et al., 2018). Despite the relatively conserved gene content, genome structural changes caused by insertion of repetitive elements, gain or loss of introns, and/or gene transfers to the nucleus often lead to mitogenome size variations (Burger et al., 2003).

Introns are present in many fungal mitogenomes. These sequences can be divided into two groups: group I and group II. Introns Group I (IGI) presents six subclasses and are more abundant in mitogenomes than the group II. IGI can encode cellular proteins, such as *rps3* ribosomal protein or maturases like homing endonucleases (HEGs), which are likely involved in the splicing process (Hausner, 2003). IGI are located within genes and are associated with shaping of mitogenomes, gene rearrangements and also in the host fitness (Hausner, 2003; Belfort, 2017). Introns type II are self-splicing and consist in a sequence of approximately 600 nucleotides. Usually, they are similar to IGI and can be classified into four groups (Michel et al., 1989; Hausner, 2003).

A recent study (Sandor et al., 2018) based on 20 species/groups of fungi revealed, for most of them, higher genetic diversity of nuclear genes and genomes than for the mitochondrial ones. This pattern is more similar to the observed in plants but different from most of the animals. The mechanisms responsible for the structural variations in fungal mitochondrial genomes and its relationship with fungi divergence time are still poorly understood. Nevertheless, the increasing availability of fungal mitogenome sequences in public databases can help us to understand the factors that drive fungi mitogenome variations of fungi.

The order Hypocreales (Ascomycota) is a monophyletic group with more than 2700 species of fungi, distributed in 240 genera divided in sexual (teleomorph) and asexual (anamorph) morphs (Varshney et al., 2016; Wijayawardene et al., 2018). Organisms of this order show a great variability of ecological functions and may display roles ranging from saprobes to pathogens. Special interest has been given to economically important species in the fields of pharmacology and medicine, biological control and biotechnology (Rehner and Samuels, 1995; Varshney et al., 2016), such as *Trichoderma harzianum*. This species is widely distributed in soil and plants due to its diversity of ecological niches (Druzhinina et al., 2011; Contreras-Cornejo et al., 2016). Furthermore, *T. harzianum* acts as a biofertilizer, promoting plant growth, and as a biocontrol agent during plant infections (Druzhinina et al., 2011; Harman, 2011), and has been considered an attractive alternative to the usage of chemical fungicides (Schmoll et al., 2016). Despite its economic relevance and wide distribution, the nuclear genome of *T. harzianum* is not yet fully assembled, and the mitochondrial genome is still not available in public databases.

Herein, we performed the deep sequencing of *T. harzianum* HB324 mitochondrial genome and compared it with 34 other reference species from the Hypocreales order that were available in public databases. We performed *de novo* structural and functional annotation of all species analyzed. The standardized annotation allowed us to perform comparative analyses revealing high variation among the mitogenomes, even within individuals

from the same family. Mitochondrial genome length varied from 24,565 to 103,844 bp. Despite the size variation, the copy number, size, and structure of protein-coding genes were highly conserved, suggesting that differences in the genome length are likely related to non-coding regions, such as introns, HEGs and unidentified ORF (uORF). Introns were the most widespread non-coding element found in mitogenomes. Analyses based on sequence similarity have revealed greater sharing of intronic sequences within families. In some cases, we observed conservation even in the position of intron insertion, such as the intron within gene *rrnL,* present in almost all species. In contrast, species with higher divergence time showed smaller similarity among intronic sequences. We also investigated whether the genetic divergence between fungal species would be positively correlated with the size of the mitogenome and the prevalence of protein-coding and non-coding mitochondrial elements. Fungi species that evolve faster presented a higher frequency of non-coding elements on their mitogenomes. Therefore, our data suggests that the difference in the size of the mitogenomes is due to the presence of non-coding components. Besides, species that evolve faster have a greater proportion of non-coding elements, corroborating their role in the shaping of fungi mitochondrial genomes.

MATERIALS AND METHODS

Sequencing, Assembly and Annotation of the Mitochondrial Genome of *Trichoderma harzianum* HB324

Pure culture of *T. harzianum* HB324 isolate was grown on 2% malt extract agar (MEA) for 5 days. The mycelium was collected from the agar surface and transferred to a 2 mL tube containing lysis buffer. DNA extraction was performed according to the instructions of FastDNA kit (MP Biomedicals, CA, United States). The quality and quantity of genomic DNA were assessed by electrophoresis and fluorometric analyses using Qubit dsDNA BR Assay Kit (Thermo Fisher Scientific, Waltham, MA, United States). The sequencing library was prepared using the NEBNext Fast DNA Fragmentation and Library Preparation Kit (New England Biolabs, Ipswich, NE, United States) according to the manufacturer's instructions. The library was sequenced on a HiSeq 2500 sequencer (Illumina, San Diego, CA, United States).

Quality of reads was assessed using FastQC v0.11.5 program[1]. Adapter sequences and bases with Phred score < 20 were removed using BBduk software from BBtools package[2]. After trimming, sequences were assembled using the software SPAdes v 3.11.1 software (Bankevich et al., 2012). The identification of mitochondrial sequences was performed using similarity searches against reference mitochondrial genomes deposited in NCBI RefSeq database using BLASTn (Altschul et al., 1990). The contigs with the highest coverage scores were selected for subsequent annotation. The raw data were deposited on NCBI SRA database under the accession number PRJNA604815.

Annotation of mtDNA was performed using MITOS2 software[3], with the NCBI fungi RefSeq 81 database as reference and using the genetic code 4 (Mold, Protozoan, Coelenterate Mitochondrial Code) for CDS translation. The softwares MFannot and RNAweasel[4] were used for annotation of intronic regions and uORF sequences. The introns identified in the *T. harzianum* mitogenome have been named according to the nomenclature proposed by Johansen and Haugen (2001) and Zhang and Zhang (2019). Repetitive DNA sequences were identified using uGene (Okonechnikov et al., 2012), and a circular mitogenome map of *T. harzianum* HB324 was generated using the output annotation file of Geneious v9.1.6[5]. Since mitogenomes from Hypocreales order are circular, we verified the completeness of *T. harzianum* mitogenome by amplifying the *rrnl* ribosomal gene that presented three exons, one at the beginning (position 1591 – 2191) and other at the end (position 30158-30370) of the assembled genome. The oligonucleotides used to perform the amplification were: rrnl_F 5′ TTGTTGCACTAATCTCCGAA 3′ and rrnl_R 5′ ATTGCATCTTGTGATCCTGT 3′. PCR products were purified and sequenced[6] (Belo Horizonte, Brazil) on an ABI 3130 automated sequencer (Applied Biosystems, Life Technologies Q7, CA, United States).

Comparative Analysis of the Mitogenomes of Hypocreales Order

Comparative analyses were performed using the assembled mitogenome of *T. harzianum* HB324 plus 34 reference mitogenomes of species of the order Hypocreales publicly available on NCBI Organelle Genome Resources database[7]. Identification of fungal species and accession numbers for their mitochondrial and nuclear genomes are provided on **Supplementary Table S1**.

The 34 mitogenomes retrieved from public databases were reannotated using the software MITOS2[3], RNAWeasel and MFannot[4] to standardize the annotation and thus, allowing the comparative analysis. The resultant annotation file of each mitogenomes was submitted to manual curation taking into account number and presence of core genes and tRNAs. Gene duplication was confirmed by comparative analysis using sequence similarity among putative duplicated sequences. Duplication was considered when target sequences presented both identity and coverage of at least 50%. The mitogenome characterization included analyses of fungal mitogenome length, gene copy numbers and integrity, presence of introns, homing endonucleases, coding and non-coding regions, *tandem* repeats, unidentified ORFs (uORFs), as well as GC content. We developed in-house scripts to parse software outputs and calculate genome stats (**Supplementary Text S1**). In case of

[1]http://www.bioinformatics.babraham.ac.uk/projects/fastqc/

[2]https://sourceforge.net/projects/bbmap/

[3]http://mitos2.bioinf.uni-leipzig.de/index.py

[4]http://megasun.bch.umontreal.ca/RNAweasel/

[5]https://www.geneious.com

[6]www.myleus.com

[7]https://www.ncbi.nlm.nih.gov/genome/organelle/

duplicated genes, it was estimated whether the two copies have coding potential using CPC2 software (Kang et al., 2017). Coding regions were considered as those regions composed by protein-coding genes, ribosomal and tRNA sequences. The non-coding regions were defined as the regions composed by intergenic, intronic, uORFs and HEGs sequences. Correlation analyses were performed using *Pearson* correlation in order to verify whether mitogenome length and number of annotated genomic elements were responsible for a positive association, such as number of protein-coding genes, introns and HEGs. All the analyses were performed using R software (R Core Team, 2013) and the packages hmisc (Harrell, 2019), gplots (Warnes et al., 2019), ggplot (Wickham, 2016), and reshape (Wickham, 2018). The mitochondrial gene ordering was determined using an in-house script and considering the ribosomal gene *rrnL* as the first element.

Sequence Similarity and Conservation of Intronic Sequences

Sequence similarity analyses were performed for all the introns identified in the 35 species investigated in this study according to the methodology proposed by Pogoda et al. (2019) with minor modifications. Similarity searches were performed using BLASTn from Blast package (Altschul et al., 1990) and sequences with coverage and identity higher than 60 and 50%, respectively, were considered similar. It was also established if there was sequence similarity between introns of the same species, which could be indicative of intron duplication. Intron similarity was based on sequence identity and was visualized using R software with circlize package (Gu et al., 2014) and correlation plots, which were performed in R software with ggplot and corrplot packages (Wickham, 2016; Wei and Simko, 2017). Intron conservation was evaluated based on the intronic sequence insertion positions on the target gene. In this case, the introns located within genes were aligned into its respective gene and it was verified if the position of the insertion was conserved among the same gene in different species, as demonstrated by Deng et al. (2016) and Zubaer et al. (2018). In our analysis, we considered the position of insertion as a region composed of 11 nucleotides that precede the intron, allowing only one nucleotide of mismatch. The data were plotted using the R software.

Transfer of Mitochondrial Genes to the Nuclear Genome

The presence of fungal mitochondrial genes in the nuclear genome was assessed by sequence similarity searches using Blast software according to Li et al. (2019) with some modifications. For this analysis, 18 nuclear fungal genomes publicly available to date (out of the 35 evaluated in this study) were used (**Supplementary Table S1**). For each of the species evaluated, the protein-coding genes were translated into amino acid sequences and ribosomal gene (nucleotide sequences) were compared with the nuclear genome. Transference of mitochondrial genes to the nuclear genome (NUMT) was considered when the two sequences presented at least 50% of similarity and coverage with *E*-value < 1e-10.

Evolutionary Analyses

Genes exclusively found in the mitogenomes were used for molecular clock analyses. For each species, we concatenated the gene sequences of *atp8*, *atp9,* and *cox3*. Since these genes were not present in any nuclear genome evaluated, they were used to calculate the synonymous substitution rate (dS) for each species. Sequences were aligned by MAFFT (Katoh et al., 2017) and submitted to the web platform SNAP[8]. The results of dS were compiled and for each species was estimated the $\overline{dS}$ based on the formula: $\sum \frac{dS}{n-1}$ was estimated. We calculated *Pearson* correlations between the $\overline{dS}$ from the last common ancestor for each pair of species with the size of protein-coding genes, introns, HEGs, uORFs, and the genome size. These analyses were carried out with the ggplot package on R. From the alignment of *atp8*, *atp9,* and *cox3* genes, a time tree scaled analysis was also performed. The selection of the best nucleotide substitution model was made using MEGA X based on AIC criteria (Akaike, 1974). The Maximum Likelihood tree with 1000 replicates using the model GTR G+I was built in the same software. RealTime-ML analyses were carried out using the GTR G+I model to create the evolutionary time-based tree. Three ancestral nodes were used for time calibration: the common ancestor node between the order Hypocreales and *Neurospora crassa* (outgroup) ranging from 314 to 414 Mya (Van der Nest et al., 2015), the common ancestor of the family Nectriaceae with *Acremonium chrysogenum* (*incertae sedis* - Hypocreales) ranging from 246 to 294 Mya (Sung et al., 2008), and the common ancestor of the families Hypocreaceae, Ophiocordycipitaceae, and Clavicipitaceae ranging from 162 to 168 Mya (Yang et al., 2012).

RESULTS

Deep Sequencing of *T. harzianum* mtDNA Reveals Variance Within *Trichoderma* Genus

The mitogenome of *T. harzianum* isolate HB324 is a circular DNA molecule of 32,277 bp (**Supplementary Text S2**), GC content of 27.74%, composed of 14 genes related to the oxidative phosphorylation (*atp6, atp8, atp9, cox1, cox2, cox3, cob, nad1 – nad4, nad4L, nad5, nad6*), 28 genes encoding for transfer RNAs, two ribosomal RNAs [one encoding to the small subunit (*rrns*) and other for the large subunit (*rrnl*)] and the ribosomal gene encoding to *rps3* protein. The protein-encoding region represented 52,23% of the genome, while non-coding elements cover up 22,37% including four uORFs (or hypothetical genes), five introns IGI and six homing endonucleases (HEGs). All the features were encoded in the same DNA strand (**Figure 1**). The *rnl* gene amplification confirmed that the mitogenome was complete and is a circular molecule (see primer positions represented by double black arrows in **Figure 1**). Detailed information of features annotation is available in **Supplementary Table S2**.

[8]https://www.hiv.lanl.gov/content/sequence/SNAP/SNAP.html

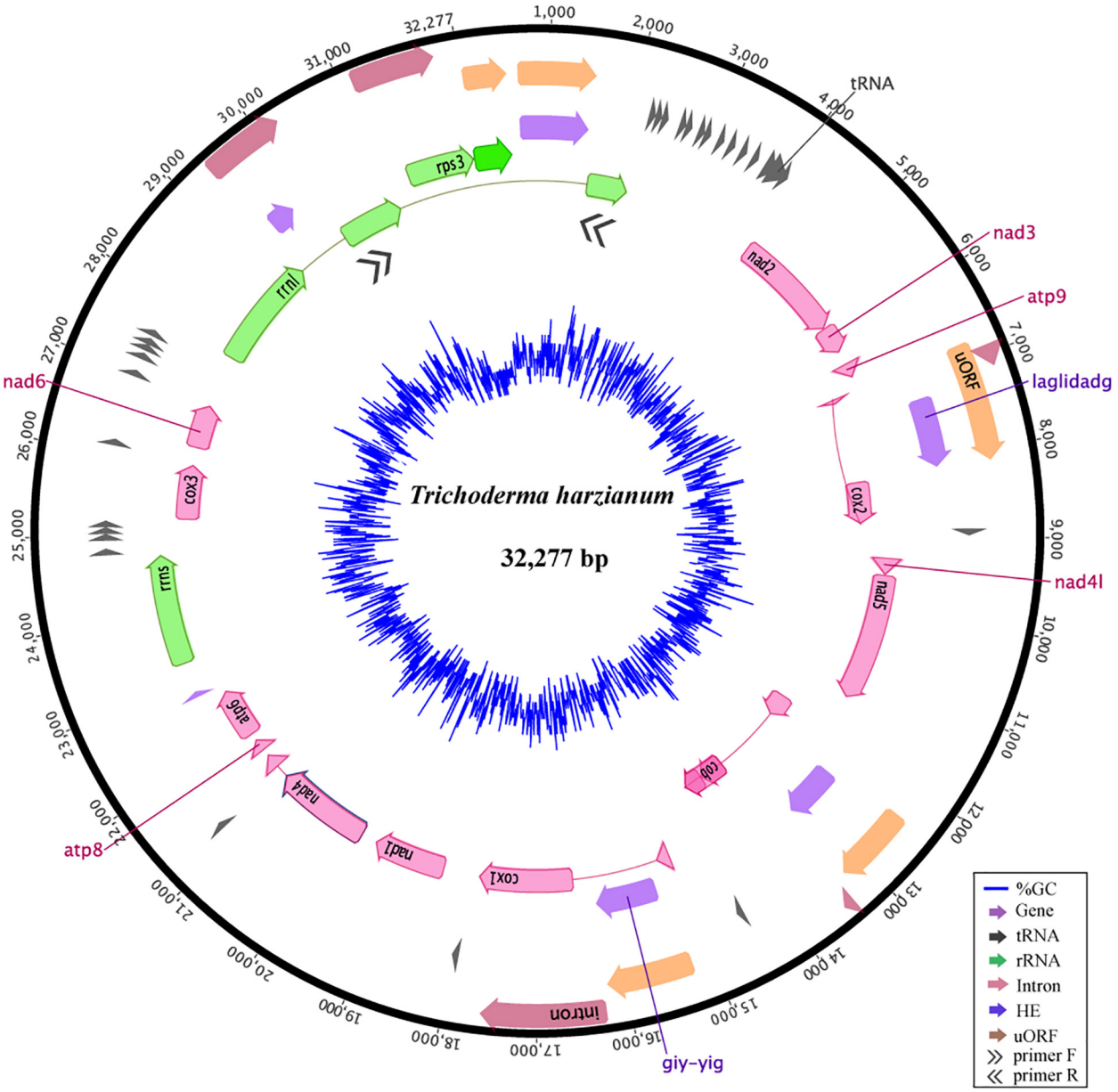

FIGURE 1 | Mitochondrial genome of the *Trichoderma harzianum* isolate HB324. Homing endonucleases and introns are represented in purple and red, respectively. Ribosomal genes are shown in green, tRNA encoding genes are represented in gray, ORFs without defined function (uORF) are colored in orange and core genes are highlighted in pink. Elements connected by thin lines represent fragments from the same gene. The blue ring represents the GC content. Double arrows represents the primers and region amplified in the gene *rnl*.

Compared to other *Trichoderma* mitochondrial genomes, *T. harzianum* has the second largest genome and the highest number of IGI sequences within genes (5) (**Figure 2A**). The species *T. reesei* has the largest mtDNA, even with a smaller number of fragmented genes when compared to *T. harzianum* (4); however, the IGI size accounts for almost 25% of its genome size. In contrast, *T. gamsii* and *T. asperellum* have the smallest mitochondrial genomes (**Figure 2A**). The number and size of IGIs in both species represented only 5 and 10% of their mtDNA, respectively. Since it was observed a considerable variation in the structure and size of mitogenomes even within the same genera, such as *Trichoderma*, we decided to extrapolate our investigation to all the families from Hypocreales order (**Figure 2A**).

Comparative Analyses Reinforce Discrepancies Among Mitogenomes of Hypocreales Order

The comparative analyses of the 34 mitogenomes from species of Hypocreales order and the mitochondrial genome of

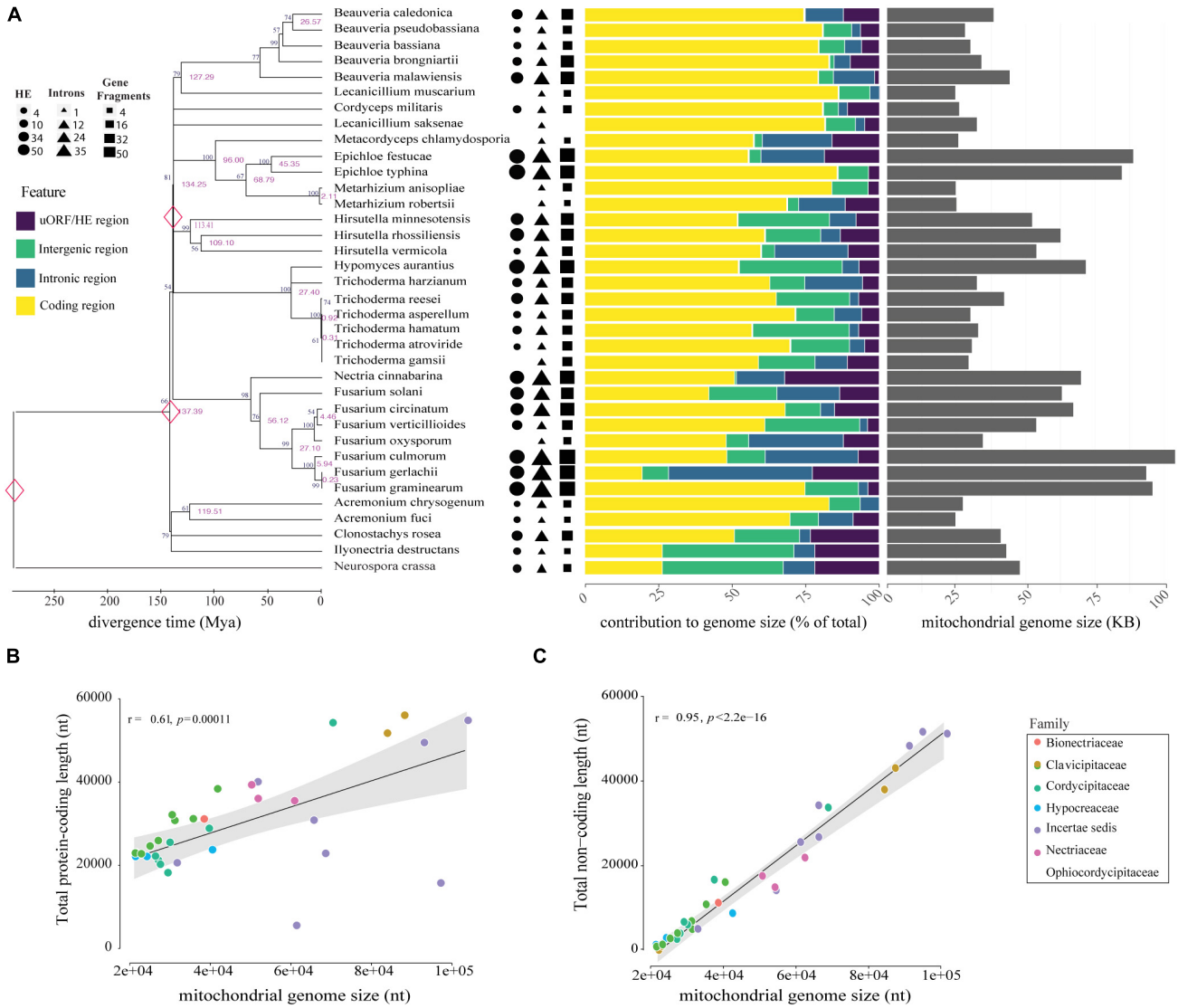

FIGURE 2 | Genomic and phylogenetic characterization of the 35 mitogenomes analyzed in this study. **(A)** Timetree analysis, mitogenome composition (%) and genome size (nt) of species evaluated are shown on the left, middle and right panels, respectively. In the analysis of genomic content, yellow represents protein-coding regions, purple represents uORF and HEGs, introns are showed in blue and intergenic region in green. Genomic data was normalized according to the mitogenome size of each species. Correlations between mitogenome size and protein-coding **(B)** or non-coding content **(C)**. Correlation was computed using Pearson test.

T. harzianum sequenced in this study revealed high variation in mitogenome length and content. The mitogenome sizes ranged from 24,565 (*Acremonium fuci)* to 103,844 bp (*Fusarium culmorum*), with a mean value of 47,492 bp (**Figure 2A**). The largest genomes exhibited the largest intronic regions (for instance, *Fusarium gerlachii, F, culmorum* and *F. graminearum*) and the smallest encoding regions (remarkable to *F. solani* and *F. graminearum*). Small genomes are less occupied by introns, or they are absent, such as in *Metacordyceps chlamydosporia*, *Metarhizium anisopliae,* and *M. robertsii.* The absence of uORFs was also observed in genomes of reduced size, for example, *Beauveria pseudobassiana, B. bassiana, Lecanicillium muscarium, F. oxysporum* and *Acremonium fuci* (**Figure 2A**).

The correlation analyses indicated that genome size is somehow correlated with the total length of protein-coding region (**Figure 2B**). Nonetheless, length of non-coding regions showed a higher and more significant correlation with the size of mitogenomes (**Figure 2C**). Other non-coding elements, such as uORFs and tandem repeats, also showed a positive and significant correlation with the mitogenome size (**Supplementary Figure S1**). Nevertheless, mitogenome length did not correlate with evolutionary history of the species, suggesting that the structure and content are prone to recent and fast evolutionary changes (**Figure 2A**). **Supplementary Table S3** provides the size, number of mitochondrial genes, uORFs, introns, GC content, and repetitive elements for each of the mitogenomes analyzed.

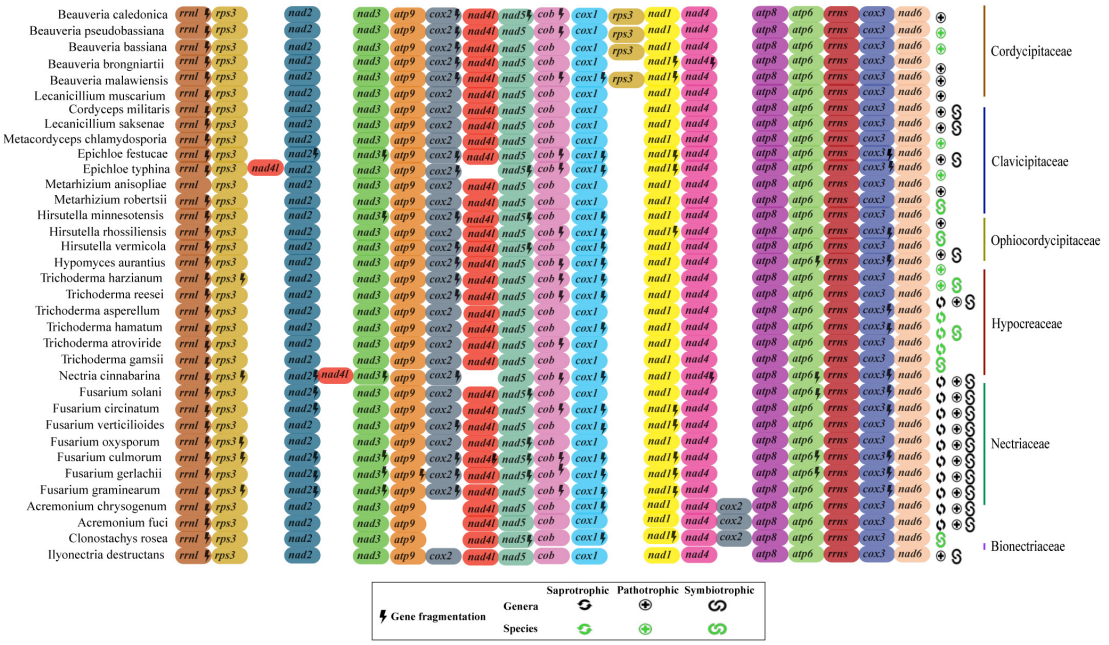

FIGURE 3 | Genomic ordering of the 17 core elements present on mitochondrial genomes. Were analyzed 14 protein-coding genes, two ribosomal genes and the *rps3* protein from the 35 fungal species investigated in this study. Each gene is indicated by a different color. Genes that showed more than one fragment are marked with a lightning (fragmented genes). Classification of the species at family level is shown in the right. The ecological function (saprobic, pathogen, and symbiotic) of each species is also shown. In green it is represented the ecological function at species level and in black at genera level.

Although we observed correlation between the coding region and mtDNA length, the structural analysis of the 17 mitochondrial genes (14 protein-coding genes, two rRNA and one *rps3*) of the 35 fungal mitogenomes revealed that Hypocreales mitogenomes display high conservation. Nonetheless, variations were found in the genomes of the species *Acremonium chrysogenum, A. fuci*, and *Clonostachys rosea,* in which the position of the *cox2* gene is displaced. The species *Epichloe typhina* and *Nectria cinnabarina* presented a change in the position of the gene *nad4L*. Additionally, the four species of the genus *Beauveria* showed two copies of the gene *rps3* (**Figure 3**). This was the only gene for which two copies of a quite similar size were detected. One copy was located within the *rrnl* gene and the other is freestanding, situated between *cox1* and *nad1* genes. The freestanding gene copies are presumably able to encode to proteins (active), whereas those located within the *rrnl* seems to be disrupted, with exception for the genes of *Beauveria caledonica*, as no coding potential was detected for both copies. Still, although we noticed differences in the ordering and copy numbers of protein-coding genes among Hypocreales mitogenomes, our analyses revealed low variation regarding the structure and genic content representativeness, pointing out that the differences observed among mitogenomes mainly accumulate on non-coding regions (**Figure 3** and **Supplementary Figure S2**).

Diversity of Non-coding Elements

Non-coding elements were found in all mitogenomes evaluated. The representativeness of these elements oscillated from 3% in *Lecanicillium muscarium* to 48% *in Fusarium graminearum*. The content of these elements varied among and within families, suggesting that it is not only related to phylogenetic relationships (**Figure 2A**). Among the non-coding elements, we identified IGIs containing uORFs and HEGs. Six types of introns were found in the analyzed mitogenomes, five types classified as elements of group I and one type belonging to group II. In the total, 349 introns were identified, out of which 210 had a putative uORF. Besides, 450 HEGs were identified and classified according to their genomic origin as freestanding or located within intronic sequences. The most frequent type of HEG was LAGLIDADG (63.78%), followed by GIY-YIG, that was identified in 36.2% of the HEG occurrences. The species with the highest number of HEGs was *Fusarium graminearum*, with 32 occurrences. *Epichloe festucae* exhibited the highest number of uORFs (46), while the highest number of introns was identified in *Fusarium culmorum,* totalizing 39 elements (**Figure 2A**).

Distribution and Evolutionary Conservation of Intronic Sequences in the Mitochondrial Genes

The number of IGIs detected in the mitochondrial genes varied significantly. Considering all the introns identified in the mitogenomes, the genes that showed the highest number of IGIs were *cox1* (109 IGIs), followed by *rrnl* (43), *cob* (50), *cox2* (27), *cox3* (20) and *nad2* (20). In contrast, we did not find any occurrence of IGIs within *rrns* ribosomal gene. The introns located within genes *cox1* (57%), *cob* (45%), and *cox3* (31%)

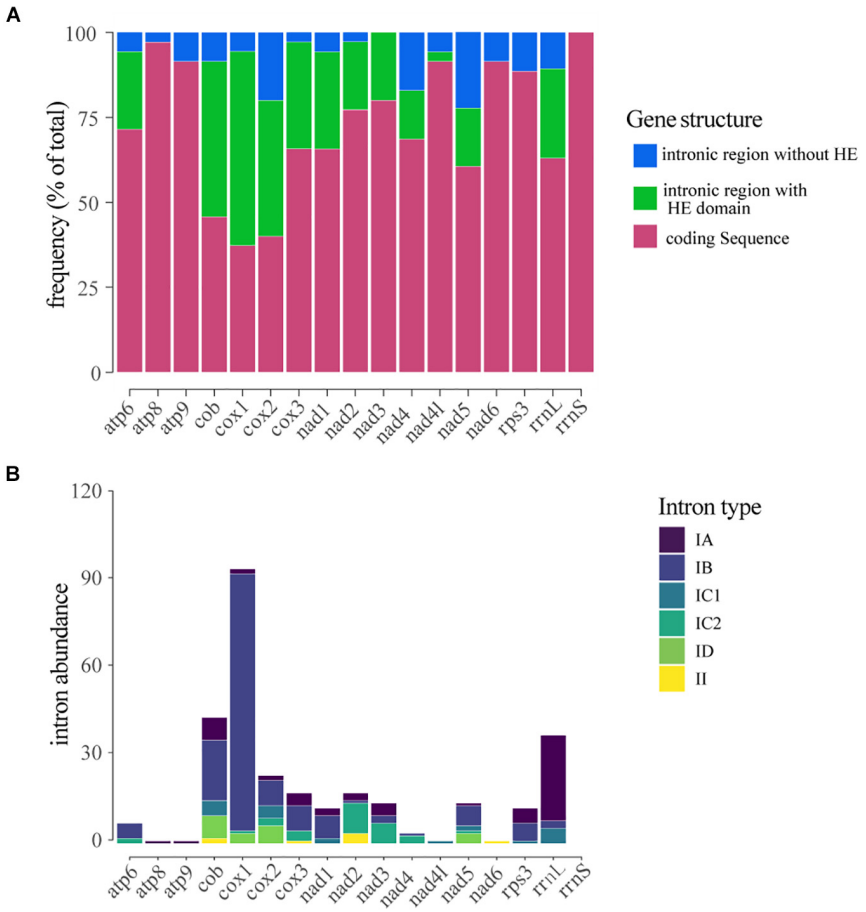

FIGURE 4 | Distribution and classification of introns located within mitochondrial genes. **(A)** Frequency of introns and/or homing endonucleases located within the gene. **(B)** Classification of the introns detected in each gene.

exhibited the highest frequency of sequences containing HEGs (**Figure 4A**). The number and size of IGIs correlated positively to the number and size of HEGs, suggesting the HE could have a role in IGIs spread, and consequently, in the length and structure of the mitogenomes (**Supplementary Figure S3**).

Most of the introns found in this study were classified as group I, mainly type IB (208 – 59,6%) while only eight were classified as group II introns. The type IA intron showed the largest abundance and stood out for its average size of 1,000 bp, while the other introns presented a mean size of ∼250 bp. Group I introns were detected in all genes analyzed; however, in the genes *atp6*, *cob*, *cox1*, *cox2*, *cox3,* and *nad1* the type IB intron was the most common; in the genes *rrnl*, *rps3* and *atp9* type IA introns were prevalent; in the genes *nad2*, *nad3*, and *nad4* the type IC1 intron showed higher frequency, and in *nad4l* gene only the type IC2 intron was detected. Group II introns were only detected in the genes *cox1*, *cox2*, *cox3,* and *nad2* (**Figure 4B**).

Interestingly, we noticed sequence similarity among intronic sequences from different species. High similarity among IGI sequences was observed among species of the same family as, for example, *F. graminearum*, *F. culmorum,* and *F. gerlachii* which shared 27 introns sequences (**Figure 5**). We also noticed similarity among IGIs sequences from different families, such as for Hypocreaceae, Cordycipitaceae, Clavicipitaceae, and Nectriaceae (**Figure 5**). The IGI sequence identified in the *rrnl* gene was the most widespread element within mitogenomes from Hypocreales order, displaying high similarity with introns located within the same gene and other different genes, such as *atp6*, *cob*, *cox1*, *cox2*, *cox3*, *nad1*, *nad2*, *nad3*, *nad5*, and *rps3*. This profile suggests that the conservation of IGI sequences among genes could have originated from a common ancestor (**Supplementary Figure S4**). Other examples of IGI sequence sharing are notable, such as for *cox1* and *cob*; *cob* and *cox2*; *nad2* and *nad3*; *nad3* and *nad5*; *nad4l* and *nad6; atp6* and *cox3* (**Figure 6**). Despite conservation of many IGIs, such as those located within the genes *rrnl*, *cox1,* and *cob*, we identified IGIs that are not shared and figure as specific to some species, suggesting that these sequences could be acquired by different mechanisms, such as horizontal transference (**Supplementary Figure S4**).

We also investigated the conservation of intronic sequences taking into account the insertion site and gene which it is located. In this context, we were also able to detect IGI sequences that were conserved among species, although the conservation was always restricted to the maximum of 50% of the analyzed

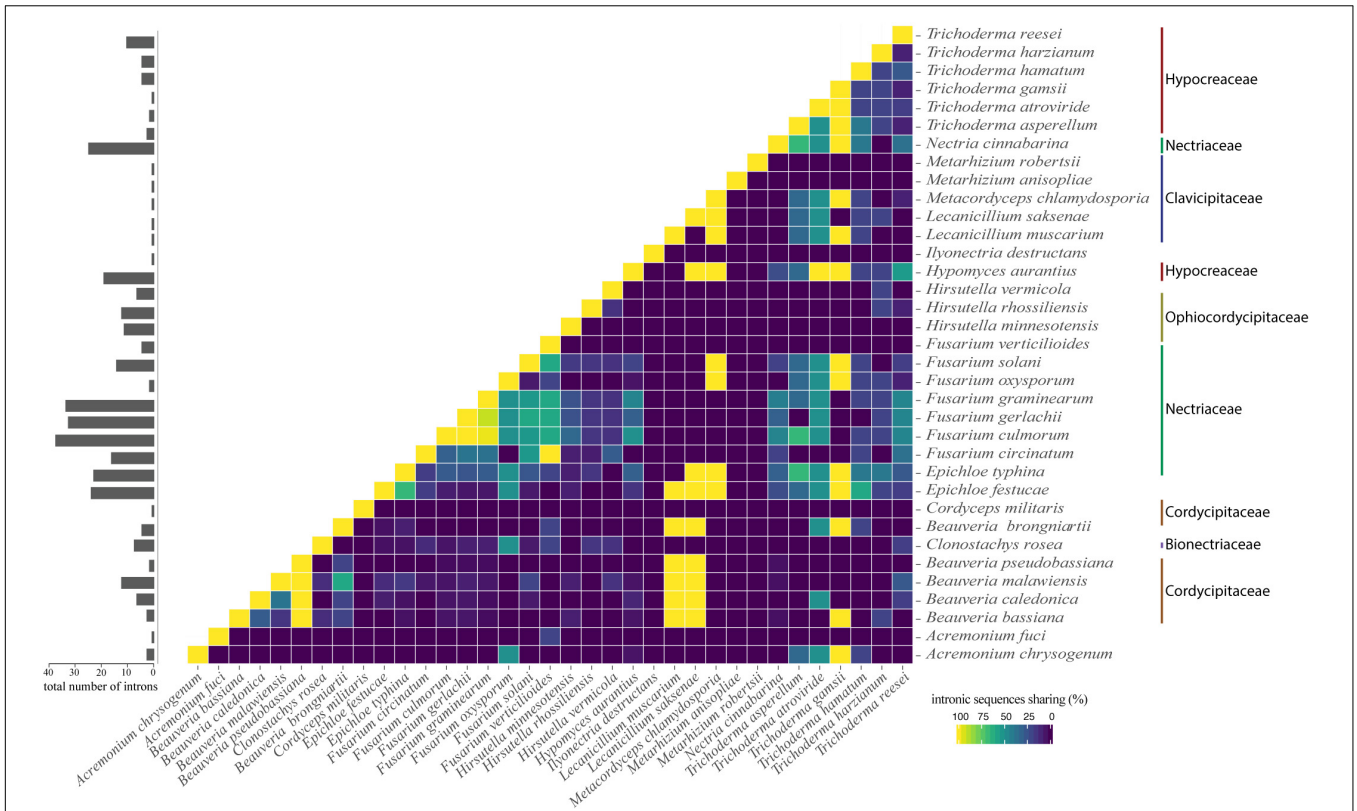

FIGURE 5 | Correlation plot showing profile of intron similarity among species. The number of introns for each species is shown in the bar chart on the left panel. The value was normalized by comparison with the species that showed the largest number of introns.

species (**Figure 7**). Nevertheless, closely related species showed higher rates of IGI sharing based on position. For instance, some species of the genus *Fusarium* shared, with at least one other species, IGIs in almost all the mitochondrial genes evaluated. The gene *cox1* presented the highest number of shared IGIs per position, with 21 events. Besides, the *nad3* and *nad5* genes were the genes with the lowest numbers of conservation events (2 introns in each gene) (**Figure 7** and **Supplementary Table S4**).

Transfer of Mitochondrial Genes to Nuclear Genomes

Our results showed that mitochondrial genomes have numerous HEG elements, which are capable of self-mobilization (Hausner, 2003). Since HEGs can interrupt or structurally modify mitochondrial genes impacting on mitogenome evolution, we evaluated the duplication of mitochondrial genes to the nuclear genome. We investigated the presence of the 14 mitochondrial protein-encoding genes and the ribosomal genes in nuclear genomes of 18 fungal species belonging to Hypocreales order available in public databases. Except for *atp8*, *atp9,* and *cox3*, all the other mitochondrial genes were found duplicated, in at least one species, in the nuclear genomes. The genes *nad5* and *cob* showed the highest frequencies of duplication in the nuclear genomes (three events each), followed by *cox1*, *rrnl, nad1, and nad2* (two copies each) and *rrns*, *rps3*, *nad3*, *nad4L*, *nad4*, *atp6,* and *cox2* with only one event of transference to the nuclear genome.

Regarding the number of events in the same species, *Fusarium graminearum* had four genes (*nad6*, *atp6*, *cob,* and *nad5*) with copies in both nuclear and mitochondrial genomes, while the species *Trichoderma harzianum* (*nad2*, *cob,* and *cox1*) and *T. gamsii* (*nad1*, *nad3,* and *nad5*) had three genes that were possibly transferred to the nuclear genomes. The species *Metacordyceps chlamydosporia*, *Cordyceps militaris*, *Fusarium circinatum*, *F. verticillioides*, *F. oxysporum*, *Trichoderma asperellum*, *Epichloe typhina* and *Clonostachys rosea* did not show any event of duplication of mitochondrial genes to the nuclear genome (**Supplementary Figure S5**).

Relationship Among Divergence Time and Coding and Non-coding Elements on Mitogenomes

The timed phylogenetic analyses based on the sequences of the genes *atp8*, *atp9*, and *cox3* showed that the order Hypocreales evolved over a period of 137.39 Mya. The species *Ilyonectria destructans* and *Clonostachys rosea* diverged ∼120 Mya, while the species *Fusarium graminearum* and *F. gerlachii* diverged recently, ∼0.23 Mya. Assessment of the estimated time-tree suggested that the presence of introns may not be

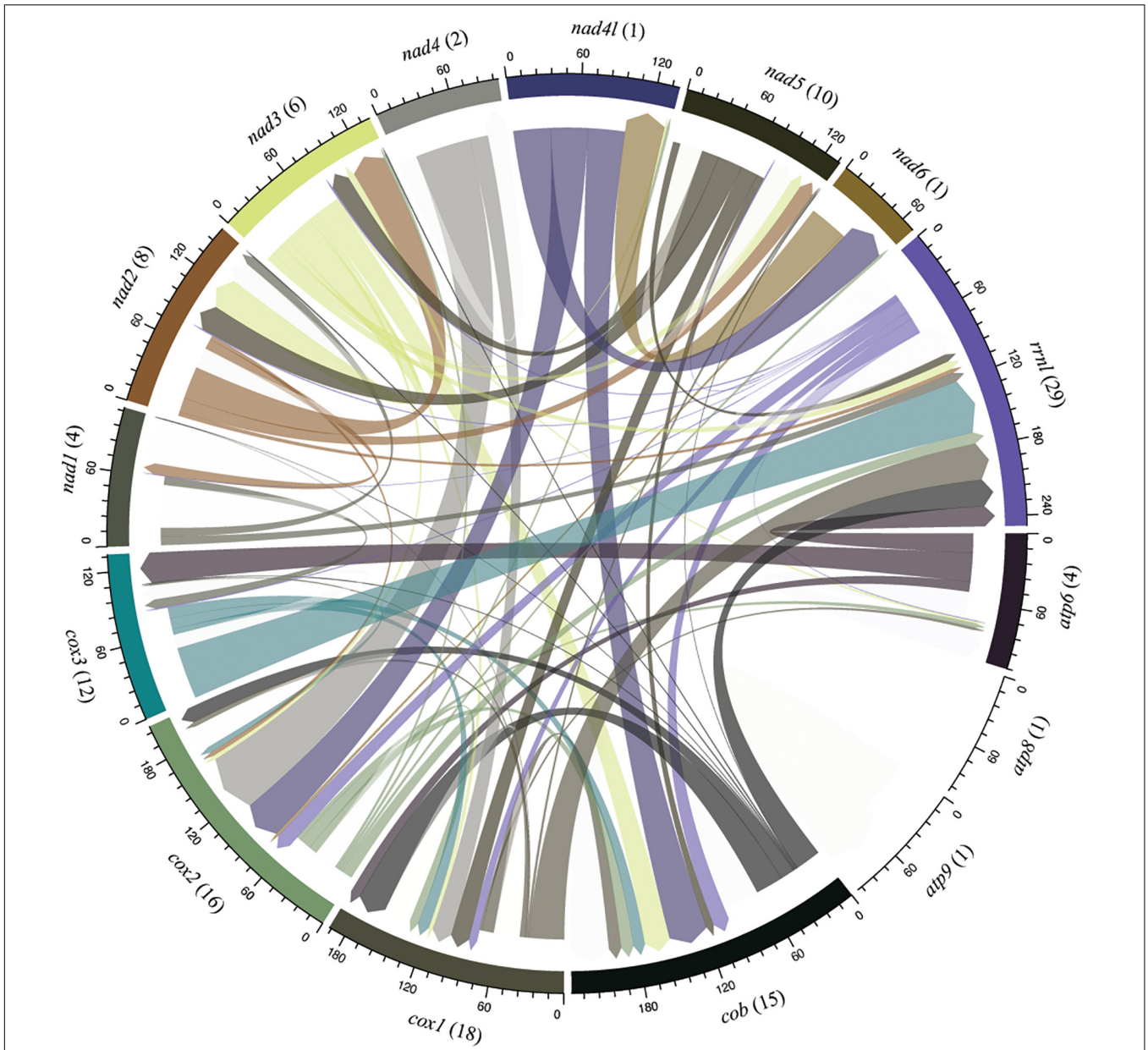

FIGURE 6 | Sharing profile of group I introns according to the mitochondrial gene origin. Circular plot indicates intron sharing pattern based on sequence similarity among core elements of the mitochondrial genomes. Each gene is represented by a colored segment. Introns that are shared with more than one gene (translocation) are shown in different color. Introns shared among species located within the same gene are not shown in the figure and were investigated in the **Figure 7**. The number of introns shared in each gene are indicated in parenthesis. Introns from the genes *atp8* and *atp9* present sequence similarity only with introns identified in its respective gene.

related to phylogenetic relationships (**Figure 2A**). Nonetheless, there was a significant correlation among the average rate of substitutions at silent sites of each species $\overline{dS}$ and the mtDNA size, indicating that evolutionary time have a role on mitogenome shaping (**Figure 8A**). Moreover, there was a significant correlation between $\overline{dS}$ and total length of introns (**Figure 8B**), total length of HEGs (**Figure 8C**) and total length of uORFs (**Figure 8D**). On the other hand, we did not observe correlation among $\overline{dS}$ and the total length of protein-coding regions (**Figure 8E**), indicating that fast-evolving mitogenomes tend to accumulate evolutionary changes in non-coding regions.

DISCUSSION

Comparative genomics has been used to elucidate the population structure and to understand the functions of each species

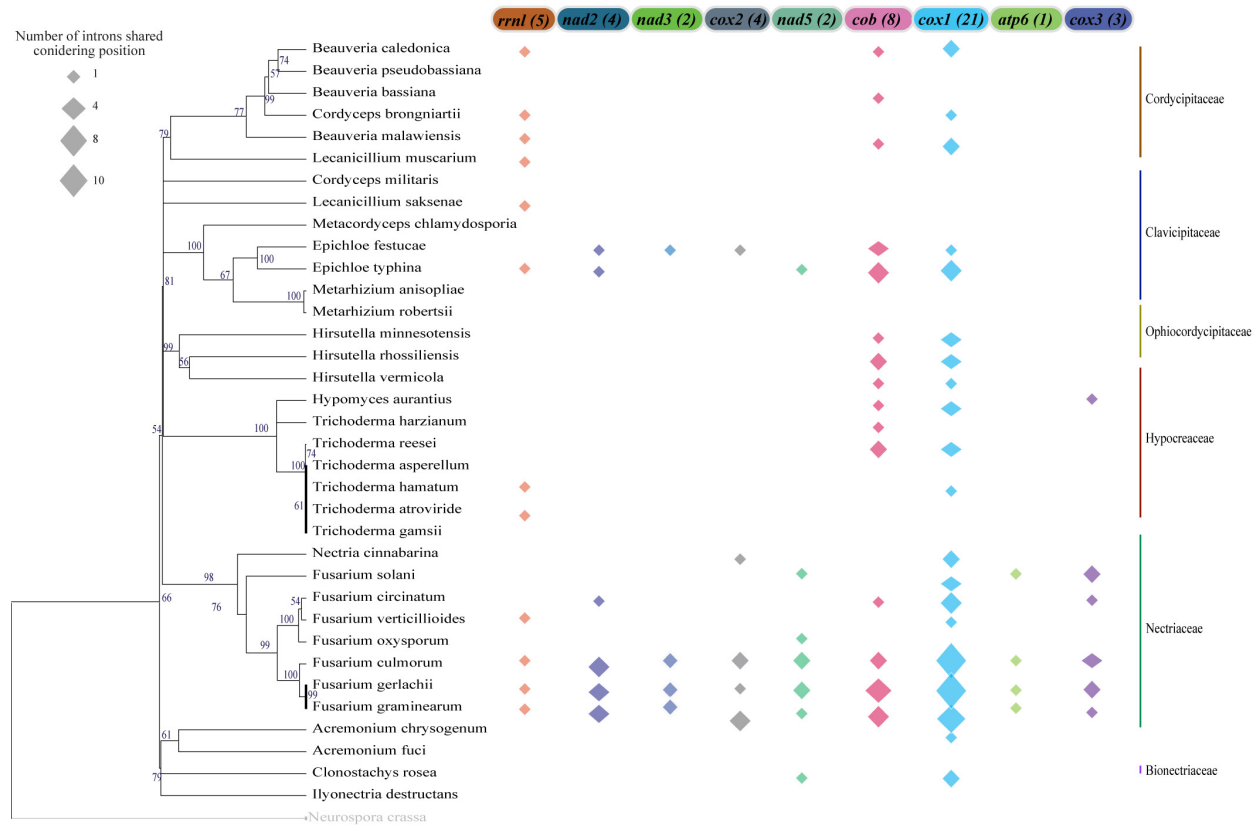

FIGURE 7 | Group I Intron sharing pattern considering insertion sites on the mitochondrial genes. For the insertion point that is common in more than one species, the position was considered conserved and it was shown in the figure. The total number of sharing events are indicated in parentheses next to each gene name. The size of the polygon represents the number of sharing events in each gene and species. The mitochondrial genes that are not represented in the figure do not present any sharing position event or do not present intron sequences.

in an environment (Nadimi et al., 2016). In the last years, this methodology has revealed the main genomic organization of fungal species, factors related to fungal pathogenicity, production of substances and enzymes of commercial interest, and other aspects of fungal evolution and biology (Stajich, 2017). Mitogenomes are studied for phylogenetic relationships, phylogeography and structure dynamics in the population since their genomes present conserved gene content, rapid evolutionary rate and many copies in the host's cell (Moore, 1997). Herein, we present a new mitochondrial genome of *Trichoderma harzianum* and performed comparative analysis including 34 species from Hypocreales order to investigate variations in the mitochondrial genome size and structure, intron sharing, presence of NUMTs, and the relationship among divergence time and coding and non-coding elements that compose these mitogenomes.

Trichoderma species are found in almost every environment, mainly in soil and plant root ecosystems (Harman et al., 2004) and are widely applied in agriculture as biocontrol agents, inhibiting the growth of other fungi and nematodes (Lorito et al., 2010). Furthermore, some species can stimulate plant growth and development by stablishing mutualistic beneficial interactions (Bonfante and Requena, 2011). The species *T. harzianum* is widely used in agricultural industries due to its mycoparasitic activity, which inhibits many plant pathogens (Lorito et al., 2010). *T. harzianum* HB324 was isolated by our research group from *Hevea brasiliensis* (rubber tree) leaves and our data have shown that this isolate can act as biocontrol agent against the phytopathogen *Colletotrichum* sp. (Fonseca et al., 2018). Despite the economic and ecological importance of this fungus, its mitochondrial genome has not been yet available. In the current work, the complete sequencing of mitochondrial genome of *T. harzianum* HB324 isolate is presented, and its mitogenome has 32,277 bp, being the second largest of the genus and contain four uORFs, five introns and six domains of HEGs.

The remarkable variation in the mitogenomes sizes of the 35 fungal species evaluated in this study (from 24 to 103 Kb) was observed at both genus and species levels: within strains of *Trichoderma*, *Beauveria,* and *Fusarium,* for example, it reached up to 70 Kb. These results reinforce those previously reported. There are studies describing genomes of around 18 Kb in *Hanseniaspora uvarum* (Pramateftaki et al., 2006) and up to 235 Kb in *Rhizoctonia solani* (Losada et al., 2014). Variations in mitogenome sizes at genus and species level have also been reported within species of the genera *Schizosaccharomyces* (Bullerwell et al., 2003) and *Fusarium* (Al-Reedy et al., 2012),

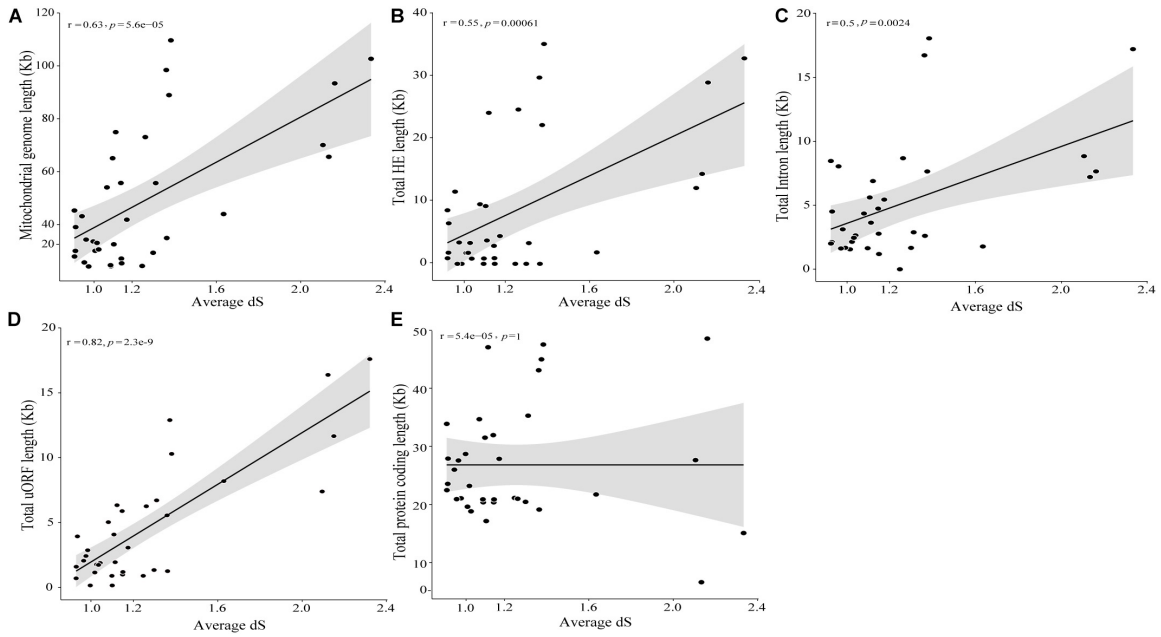

FIGURE 8 | Correlation among divergence time and mitochondrial genome characteristics. Correlation analyses among divergence time and mitochondrial genome **(A)**, intron **(B),** HEGs **(C),** uORF **(D)** and protein coding **(E)** length.

as well as within the species of *Saccharomyces cerevisiae* (Wolters et al., 2015), *Cordyceps militaris* (Zhang et al., 2015), and *Rhizophagus irregularis* (Formey et al., 2012).

The wide size range of the mitogenomes evaluated in our study may be explained in part by variations in length of intergenic regions, and differences in number and length of introns. The presence or absence of introns have been widely described as the major contributing factor for such variation among fungi (Jung et al., 2010; Joardar et al., 2012; Zhang et al., 2015). Among the fungal strains evaluated in our study, *F. graminearum* had the highest number of introns (35), accounting for 54% of the entire mitochondrial genome. Our results are similar to those reported to *Podospora anserina* (Ascomycota), for which 33 mitochondrial introns were detected (Cummings et al., 1990), as well as to the Basidiomycota mushroom *Agaricus bisporus,* for which 45.3% of the mitochondrial genome was composed of introns (Ferandon et al., 2013). Our analysis also revealed fungal species with no intron sequences, such as *Metarhizium anisopliae* and as previously described for *Mycosphaerella graminicola* (Torriani et al., 2008).

In fungal mitogenomes two classes of introns are found, group I and/or group II. They can be distinguished from each other by their sequence, structure and splicing mechanisms. Group I has been reported as the most widespread in fungal mitogenomes and can be subdivided into IA, IB, IC1, IC2, IC3, and ID (Saldanha et al., 1993; Hausner, 2003; Lang et al., 2007). Mitochondrial introns can self-disperse in mtDNA, acting as mobile elements due to the presence of enzymes that are able to cleave double-stranded DNA to insert introns into new genomic locations (Lazowska et al., 1980; Pellenz et al., 2002). HEGs are encoded by group I and II introns or can be found freestanding. They are classified into six families, but only two are detected in fungal mitogenomes, LAGLIDADG and GIY-YIG (Stoddard, 2014).

In our study, we identified all group I subgroups of introns, except IC3, and a few sequences of the group II. The most common intron type was IB (59.6%) and IA (17.2%), while group II introns were the least frequent, and accounted for only 2.3% of the intron sequences identified. Furthermore, 450 HE sequences, 275 LAGLIDADG and 175 GIY-YIG, were detected. Our data are corroborated by many studies, such as that published by Zubaer et al. (2018), who described the presence of 81 introns, 72 of which containing HE, in the fungus *Endoconidiophora resinifera*. Most of the introns detected (32) were classified as group IB, while only three introns group II were encountered. Moreover, the HEG of the LAGLIDADG family was the most frequent. In *Ophiocordyceps sinensis*, 52 introns were found, of which only six were classified as group II, and subgroup I was recovered as the most frequent (Li et al., 2015).

Group I introns (IGI) are considered the largest class of introns. Introns from this group are mostly self-splicing or are spliced by protein factors that stabilize the intronic RNA that undergoes conformational changes, such circularization. This type of intron can also have repetitive sequences or protein coding sequences at the ends of the intron, as seen in the case of the *rps3* ribosomal protein gene (Nielsen and Johansen, 2009). In addition, some introns have been described to be involved in rRNA and tRNA folding (Cao and Woodson, 2000; Rangan et al., 2004), suggesting that introns are important regulators of the expression of genes encoding proteins and ribosomes in mitogenomes (Nielsen and Johansen, 2009). IGIs may also be important for the fitness of the fungal host. Intron group I colonized by HEGs can promote RNA splicing, due to the

presence of maturase which acts as a cofactor promoting the splicing between the intron and the precursor RNA (Lambowitz and Perlman, 1990; Belfort, 2003). IGIs may have their splicing rate altered due to exposure to certain environmental factors (Lambowitz et al., 1998). For example, in chloroplasts, it has been reported that type IGI splicing was activated by light (Deshpande et al., 1997). Splicing inhibitory factors have also been described, such as the molecular Flavin mononucleotide (FMN), which directly interferes with the affinity of the intron with molecules involved in the catalysis of the intron itself (Kim and Park, 2000). Since growth conditions such as temperature, luminosity, pH and salinity have already been described influencing the rate of splicing in other organisms, it was suggested by Belfort (2017) suggested that some IGIs can work as biosensors when exposed to certain environmental factors, promoting a selective advantage over the intronless fungi. Fungal species such as budding yeast and *Neurospora crassa*, which do not present introns have been described presenting respiratory defects (Lambowitz and Perlman, 1990; Hausner, 2003). Additionally, type I introns have been studied to be used as ribozymes that have the ability to inactivate specific regions of the host itself or viral sequences based on the messenger RNA (mRNA) cleavage (Johansen et al., 1997; Lambowitz et al., 1998).

Our data also revealed a positive correlation between the number and length of IGIs and HE. This has also been reported for the fungus *Agaricus bisporus* (Ferandon et al., 2013) and *E. resinifera*, for which most of the introns contained HE domain, and 50% of intron size was due to the presence of HEGs (Zubaer et al., 2018).

Introns were distributed all over the mitochondrial genes evaluated, and *cox1* was the main introns reservoir, followed by *rrnl*, *cox2*, *cob*, *cox3,* and *nad2*. According to Ferandon et al. (2013) and Zubaer et al. (2018), *cox1* is the main intron reservoir in fungal mitogenomes. The authors reported the presence of 19 introns in *A. bisporus* and 23 introns in *E. resinifera*, which was considered the fungal species with the largest number of introns in this gene. Introns have also been identified in other genes, such as *cox2*, *cob,* and *rrnl* in two species of *Rhizopogon* (Agaricomycotina) (Li et al., 2019). In the fungus *O. sinensis* (Hypocreales), the genes *cox1* and *rrnl* were reported as the main reservoir of introns (Li et al., 2015). Moreover, in the fungus *Stemphillium lycopersici* the putative *cox1* and *cox2* gene fusion accounted for nearly half of the number of introns encountered in the mitochondrial genome (Franco et al., 2017).

It is well known that groups I and II introns can propagate as moving elements through different mechanisms: group I by HE activity and group II by reverse protein transcription (Bonen and Vogel, 2001; Hausner, 2003; Lang et al., 2007). Since introns have the ability to disperse throughout the genome, we investigated intron sharing among genes and species. According to our data, there is a high intron sharing rate among fungal species of the order Hypocreales (267 out of 349 introns were shared among species). These findings may be an indicative of horizontal intron transfer. Horizontal intron transfer mechanisms in fungal mitochondrial DNA have already been described in many species, such as *Chrysoporthe* (Kanzi et al., 2016), *Aspergillus* and *Penicillium* (Joardar et al., 2012) and *Armillaria* (Kolesnikova et al., 2019). Moreover, besides the introns sharing in species of the order Hypocreales being more frequent among those taxonomically related, it was also observed for species belonging to different families. Mardanov et al. (2014) identified nine introns in rRNA genes from *Sclerotinia borealis*, but only three introns sequences presented similarity with rRNA introns in the Helotiales order. Other four sequences exhibited similarity with mitochondrial genes from species that are not related to this order. In the same study, it was described that species from this order had the same intron insertion position in the *cox1* gene. In our study, we also checked for the presence of intron sharing by position in mitochondrial genes. We found that the *cox1* gene, followed by the *cob* and *rrnl* genes, had the highest sharing rate among species, displaying respectively 21, 8, and 5 different insertions events. Nevertheless, we also found conserved insertion positions in the species evaluated. Joardar et al. (2012) showed that the *cox1* gene for Aspergillus species presented variable insertions sites. Furthermore, Guha et al. (2018) analyzed 129 fungal species from Ascomycota phylum and found 21 different sites of intron insertion in the gene *cob*. These authors also described that some positions are more common for insertion sites and suggested that these locations may be preferred by HEGs activity. In addition, it was shown that introns insertion site preservation could be related to the host fitness. In *Saccharomyces cervisiae,* for instance, the presence of introns in nuclear and mitochondrial genes helps to resist starvation conditions (Parenteau et al., 2019).

Two IGI sequences classified as type IA located in the *rrnl* gene were the most shared among the fungal species in our analyses and were also detected in the genes *cox1* and *cob*. According to Zubaer et al. (2018), some introns occurring in the *rrnl* gene are well conserved and widespread in many fungal species of the phylum Ascomycota. In Saccharomycetales, the presence of an IGI in the gene *rrnl*, called *omega* intron, has been studied in detail (Goddard and Burt, 1999). The authors observed a cycle of invasion and degeneration for this intron, which, in order to be maintained in mitogenome continue transposing into other genes or genomes (horizontal transfer). This invasion cycle occurs through the presence of HEGs that promote intron insertion into a mitochondrial DNA region. This mechanism of invasion cycle is mainly responsible for intron diversity in mtDNAs, as well as sequence sharing among different fungal species (Goddard and Burt, 1999; Wu and Hao, 2014). IGIs may also transpose via reverse splicing of RNA. This mechanism is based on the recombination of the intron-containing rRNA molecule that is reverse transcribed into DNA and inserted by recombination processes in other sites of the mitochondrial genome (Roman and Woodson, 1995; Hausner, 2003). This mechanism can corroborate that both introns IA detected in the gene *rrnl* are the most shared among species and present in other genes other than *rrnl*. Furthermore, some introns were found exclusively in one species (such as for *Metarhizium anisopliae*) or in a unique gene (*atp8* and *atp9*), not being shared with no other species or gene.

Mitochondrial genes have numerous sequences of HEGs, which are capable of self-mobilization. Since HEGs can interrupt or structurally modify mitochondrial genes (Joardar et al., 2012;

Kolesnikova et al., 2019), we evaluated the duplication of mitochondrial genes to the nuclear genome. Duplication was found a common phenomenon among the mitochondrial genes of species belonging to the order Hypocreales, since among the 17 core genes, only *atp8*, *atp9,* and *cox3* were not detected in the nuclear genome. Duplication of NUMTs is a common phenomenon in other kingdoms, such as in mammals (Metazoa) (Tsuji et al., 2012). In Fungi, few studies that have verified duplications of mitochondrial genes in the nuclear genome have been described (Wright and Cummings, 1983; Specht et al., 1992; Brankovics et al., 2018; Wang et al., 2018). The species *Schizopphillum commune* has a duplication of the *atp9* gene (Specht et al., 1992), and in *Podospora anserina* there are mitochondrial plasmids containing *cox1* and *cox3* genes during its senescence (Wright and Cummings, 1983). Furthermore, in *Fusarium gramineraum,* a mitochondrial pangenomic analysis revealed a 3,174 bp NUMT fragment (Brankovics et al., 2018). In our gene ordering analyses, some species, such as *Metacordyceps chlamydosporia*, *Cordyceps militaris* and *Fusarium circinatum* did not show any duplication of mitochondrial genes, as found and described in *Hirsutella thompsonii* (Wang et al., 2018).

Based on the NUMT data, we also evaluated the divergence time by molecular clock analyses using mitochondrial genes that are exclusively from the mitochondrial genome. Molecular clock is used to investigate the timing of phylogenetic events, such as dating the origin of taxonomic groups or events of gene duplication, diversification or gene loss (Weir and Schluter, 2008). Herein, we estimated that the order Hypocreales probably originated around 137.39 Mya. Compared to an estimation based on 638 protein sequences in the nuclear genome, which indicates that Hypocreales originated approximately at 193 Mya (Kubicek et al., 2019). It is well known that the evolutionary rate of fungal mtDNA is close to that of plants, which have the lowest nucleotide substitution rates (Aguileta et al., 2014; Sandor et al., 2018). The evolution rate is based on the percentage of base substitutions in conserved genetic regions. Clark-Walker (1991) demonstrated that the percentage of substitution in mitochondrial genes was lower than that of nuclear genes, suggesting that fungal mitogenomes evolve slower than their respective nuclear genomes. Therefore, the time found in our analyses is expected, since mitochondrial genomes evolve slower than nuclear genomes.

Also, based in the value of $\overline{dS}$ of each species, it was possible to estimate the relationship among the genome size and the neutral substitution rates. The more fast evolving a mitogenome is, the larger its size and more abundant in non-coding regions, such as introns, HEGs and uORFs, while the protein coding-region are mostly unchanged. This indicates that the protein-coding genes of mitogenomes are under the influence of negative selection, since the coding regions remains stable independently of the neutral substitutions rates.

Fungal mitochondrial genomes usually contain 14 core protein-coding genes involved in the electron transport chain ATP synthase complex (Kang X. et al., 2017). In addition to these genes, they also have two ribosomal genes and *rps3* protein that are also conserved. In our analysis, most of the species presented the 14 core genes widely described for fungal mitogenomes, the two ribosomal genes and *rps3* protein.

The ordering of the mitochondrial genes of the evaluated species of the order Hypocreales is remarkably conserved. Nonetheless, the species *Acremonium fuci*, *A. chrysogenum* and *Clonostachys rosea* presented the gene *cox2* displaced, while *Nectria cinnabarina* and *Epichloe typhina* displayed a rearrangement for the *nad4l* gene. Differences in genome ordering can be attributed due to non-homologous recombination processes, plasmid sequence integration or presence of transposable elements, such as IGI sequences and HEGs (Gordenin et al., 1993; Lavrov et al., 2002; Rocha, 2003; Repar and Warnecke, 2017).

Species of the *Beauveria* genera exhibited an additional copy of the gene *rps3* as a freestanding gene. The *rps3* gene is the only ribosomal protein encoded by fungal mtDNA and may be located as a freestanding gene or inserted within an intron of the *rrnl* gene (Sethuraman et al., 2009). Gene duplication may occur due to truncated sequences or loss of function. In the mitogenomes of *Beauveria* evaluated, *rps3* copies were almost the same size. Nevertheless, only freestanding copies had coding potential, suggesting that the *rps3* copy located in the *rrnl* gene could be a pseudogene.

In the current study we provided the complete sequencing of the mitogenome of the fungus *Trichoderma harzianum,* a commercially important fungal strain. Comparative analyses of 35 species of the order Hypocreales revealed a structural dynamic in the mitochondrial genome of this well-studied and diverse order of the Fungi kingdom. The genome size variability found was mainly correlated with the presence of non-coding elements, such as introns and HEGs, which could be considered the determinant elements for the shape of mitochondrial genomes, as described in other Orders. Some studies, such as the one described by Mardanov et al. (2014) verified the difference in mitogenomes size and presence of introns in the orders Peltigetales and Helotiales and showed a dynamic of acquisition and loss of introns during evolution. In our work, we estimated that mitogenomes that evolve faster, have longer length of mitogenome and non-coding region.

DATA AVAILABILITY STATEMENT

The in-house scripts generated for this study can be found in the **Supplementary Text S1** and are available in GitHub repository (https://github.com/paulaluize/mitogenomes). The original contributions presented in the study are publicly available. This data can be found here: https://www.ncbi.nlm.nih.gov/nucleotide/; accession number MT263519.

AUTHOR CONTRIBUTIONS

PF, BB, VA, EA, and AG-N conceived and designed experiments. PF, RD-P, DA, DB, EA, FB, L-ED-B, and AG-N analyzed the data. PF, FB, L-ED-B, EA, and AG-N wrote the manuscript. All authors read and approved the final manuscript.

FUNDING

This work was funded by Coordenação de Aperfeiçoamento de Pessoal de Nível Superior (CAPES), and Conselho Nacional de Desenvolvimento Científico e Tecnológico (CNPq). The funders had no role in study design. Data collection and analysis, decision to publish or preparation of the manuscript. AG-N receives a research grant for scientific productivity from the Conselho Nacional de Desenvolvimento Científico e Tecnológico (CNPq), Brazil (no. 310764/2016-5).

ACKNOWLEDGMENTS

We would like to thank the Graduate Programs of Microbiology (http://www.microbiologia.icb.ufmg.br/pos/) and Bioinformatics (http://www.pgbioinfo.icb.ufmg.br/) and Pró Reitoria de Pesquisa (PRPq) of the Universidade Federal de Minas Gerais (UFMG) and the Department of Chemistry of Centro Federal de Educação Tecnológica de Minas Gerais (CEFET-MG). We would also like to thank Gabriel Peixoto Quintanilha for helping with mtDNA assembly.

SUPPLEMENTARY MATERIAL

The Supplementary Material for this article can be found online at: https://www.frontiersin.org/articles/10.3389/fmicb.2020.00765/full#supplementary-material

FIGURE S1 | Pearson's correlation of genomic features and size of mitochondrial genome. The presence and size of homing endonucleases, introns, genome size, uORFs, coding region, repeats, tRNAs and rRNAs were evaluated. The correlation ranges from −1 (red) to 1 (blue). Asterisks indicate the significance of the correlation, where * indicate $p < 0.05$, ** indicate $p < 0.005$, and *** indicate $p < 0.0005$.

FIGURE S2 | Analysis of size variation of the mitochondrial genes. Green represents the size of the exon that presents the conserved domain that characterizes the gene. Yellow represents the sum of all exons of the gene (aa).

FIGURE S3 | Pearson's correlation between the sizes of introns and homing endonucleases.

FIGURE S4 | Phylogenetic analyses of introns classified as subgroup IA. The tree was constructed using Maximum Likelihood with 1000 replicates of bootstrap. The species and gene which the intron was originated are shown for each sequence.

FIGURE S5 | Identification of events of mitochondrial gene transfer to the nuclear genomes (NUMT). In this analyses, 18 species with nuclear genome available in public databases were evaluated.

TABLE S1 | Accession numbers of mitochondrial and nuclear genomes analyzed in this study.

TABLE S2 | Features annotated in the mitogenome of *Trichoderma harzianum* isolate HB324.

TABLE S3 | Genomic characteristics of the mitochondrial genomes from Hypocreales order. The table contains information about genome length, features, GC content and repeats.

TABLE S4 | Overview of intron sharing analysis based on gene position for the species evaluated in this study.

TEXT S1 | Scripts used in this work.

TEXT S2 | Mitochondrial genome sequence of *Trichoderma harzianum* HB324.

REFERENCES

Aguileta, G., de Vienne, D., Ross, O., Hood, M., Giraud, T., Petit, E., et al. (2014). High variability of mitochondrial gene order among Fungi. *Genome Biol. Evol.* 6, 451465. doi: 10.1093/gbe/evu028

Akaike, H. (1974). *A New Look at the Statistical Model Identification*. Berlin: Springer, 215–222. doi: 10.1007/978-1-4612-1694-0_16

Al-Reedy, R. M., Malireddy, R., Dillman, C. B., and Kennell, J. C. (2012). Comparative analysis of Fusarium mitochondrial genomes reveals a highly variable region that encodes an exceptionally large open reading frame. *Fungal Genet. Biol.* 49, 2–14. doi: 10.1016/j.fgb.2011.11.008

Altschul, S. F., Gish, W., Miller, W., Myers, E. W., and Lipman, D. J. (1990). Basic local alignment search tool. *J. Mol. Biol.* 215, 403–410.

Bankevich, A., Nurk, S., Antipov, D., Gurevich, A. A., Dvorkin, M., Kulikov, A. S., et al. (2012). SPAdes: a new genome assembly algorithm and its applications to single-cell sequencing. *J. Comput. Biol.* 19, 455–477. doi: 10.1089/cmb.2012.0021

Basse, C. (2010). Mitochondrial inheritance in fungi. *Curr. Opin. Microbiol.* 13, 712–719. doi: 10.1016/j.mib.2010.09.003

Belfort, M. (2003). Two for the price of one: a bifunctional intron-encoded DNA endonuclease-RNA maturase. *Genes Dev.* 17, 2860–2863. doi: 10.1101/gad.1162503

Belfort, M. (2017). Mobile self-splicing introns and inteins as environmental sensors. *Curr. Opin. Microbiol.* 38, 51–58. doi: 10.1016/j.mib.2017.04.003

Bonen, L., and Vogel, J. (2001). The ins and outs of group II introns. *Trends Genet.* 17, 322–331. doi: 10.1016/s0168-9525(01)02324-1

Bonfante, P., and Requena, N. (2011). Dating in the dark: how roots respond to fungal signals to establish arbuscular mycorrhizal symbiosis. *Curr. Opin. Plant. Biol.* 14, 451–457. doi: 10.1016/j.pbi.2011.03.014

Brankovics, B., Kulik, T., Sawicki, J., Bilska, K., Zhang, H., de Hoog, G., et al. (2018). First steps towards mitochondrial pan-genomics: detailed analysis of *Fusarium graminearum* mitogenomes. *Peerj* 6:e5963. doi: 10.7717/peerj.5963

Bullerwell, C., and Lang, B. (2005). Fungal evolution: the case of the vanishing mitochondrion. *Curr. Opin. Microbiol.* 8, 362–369. doi: 10.1016/j.mib.2005.06.009

Bullerwell, C. E., Leigh, J., Forget, L., and Lang, B. F. (2003). A comparison of three fission yeast mitochondrial genomes. *Nucleic Acids Res.* 31, 759–768. doi: 10.1093/nar/gkg134

Burger, G., Gray, M., and Franz Lang, B. (2003). Mitochondrial genomes: anything goes. *Trends Genet.* 19, 709–716. doi: 10.1016/j.tig.2003.10.012

Cao, Y., and Woodson, S. A. (2000). Refolding of rRNA exons enhances dissociation of the *Tetrahymena intron*. *RNA* 6, 1248–1256. doi: 10.1017/s1355838200000893

Chatre, L., and Ricchetti, M. (2013). Prevalent coordination of mitochondrial DNA transcription and initiation of replication with the cell cycle. *Nucleic Acids Res.* 41, 3068–3078. doi: 10.1093/nar/gkt015

Clark-Walker, G. (1991). Contrasting mutation rates in mitochondrial and nuclear genes of yeasts versus mammals. *Curr. Genet.* 20, 195–198. doi: 10.1007/bf00326232

Contreras-Cornejo, H., Macías-Rodríguez, L., del-Val, E., and Larsen, J. (2016). Ecological functions of *Trichoderma* spp. and their secondary metabolites in the rhizosphere: interactions with plants. *FEMS Microbiol. Ecol.* 92:fiw036. doi: 10.1093/femsec/fiw036

Cummings, D., McNally, K., Domenico, J., and Matsuura, E. (1990). The complete DNA sequence of the mitochondrial genome of Podospora anserina. *Curr. Genet.* 17, 375–402. doi: 10.1007/bf00334517

Deng, Y., Zhang, Q., Ming, R., Lin, L., Lin, X., Lin, Y., et al. (2016). Analysis of the mitochondrial genome in *Hypomyces aurantius* reveals a novel twintron complex in fungi. *Int. J. Mol. Sci.* 17:1049. doi: 10.3390/ijms17071049

Deshpande, N. N., Bao, Y., and Herrin, D. L. (1997). Evidence for light/redox-regulated splicing of psbA pre-RNAs in *Chlamydomonas chloroplasts*. *RNA* 3, 37–48.

Druzhinina, I., Seidl-Seiboth, V., Herrera-Estrella, A., Horwitz, B., Kenerley, C., Monte, E., et al. (2011). Trichoderma: the genomics of opportunistic success. *Nat. Rev. Microbiol.* 9, 749–759. doi: 10.1038/nrmicro2637

Ferandon, C., Xu, J., and Barroso, G. (2013). The 135 kbp mitochondrial genome of *Agaricus bisporusis* the largest known eukaryotic reservoir of group I introns and plasmid-related sequences. *Fungal Genet. Biol.* 2013, 85–91. doi: 10.1016/j.fgb.2013.01.009

Fonseca, P., Vaz, A., Badotti, F., Skaltsas, D., Tomé, L., Silva, A., et al. (2018). A multiscale study of fungal endophyte communities of the foliar endosphere of native rubber trees in Eastern Amazon. *Sci. Rep*. 8:16151. doi: 10.1038/s41598-018-34619-w

Formey, D., Molès, M., Haouy, A., Savelli, B., Bouchez, O., Bécard, G., et al. (2012). Comparative analysis of mitochondrial genomes of *Rhizophagus irregularis*–syn. Glomus irregulare–reveals a polymorphism induced by variability generating elements. *New Phytol.* 196, 1217–1227. doi: 10.1111/j.1469-8137.2012.04283.x

Franco, M., López, S., Medina, R., Lucentini, C., Troncozo, M., Pastorino, G., et al. (2017). The mitochondrial genome of the plant-pathogenic fungus *Stemphylium lycopersici* uncovers a dynamic structure due to repetitive and mobile elements. *PLoS One* 12:e0185545. doi: 10.1371/journal.pone.0185545

Goddard, M., and Burt, A. (1999). Recurrent invasion and extinction of a selfish gene. *Proc. Natl. Acad. Sci.* 96, 13880–13885. doi: 10.1073/pnas.96.24.13880

Gordenin, D., Lobachev, K., Degtyareva, N., Malkova, A., Perkins, E., and Resnick, M. (1993). Inverted DNA repeats: a source of eukaryotic genomic instability. *Mol. Cell. Biol.* 13, 5315–5322. doi: 10.1128/mcb.13.9.5315

Gu, Z., Gu, L., Eils, R., Schlesner, M., and Brors, B. (2014). circlize implements and enhances circular visualization in R. *Bioinformatics* 30, 2811–2812. doi: 10.1093/bioinformatics/btu393

Guha, T. K., Wai, A., Mullineux, S. T., and Hausner, G. (2018). The intron landscape of the mtDNA cytb gene among the Ascomycota: introns and intron-encoded open reading frames. *Mitochondrial DNA Part A* 29, 1015–1024. doi: 10.1080/24701394.2017.1404042

Harman, G. (2011). Trichoderma—not just for biocontrol anymore. *Phytoparasitica* 39, 103–108. doi: 10.1007/s12600-011-0151-y

Harman, G. E., Howell, C. R., Viterbo, A., Chet, I., and Lorito, M. (2004). *Trichoderma* species–opportunistic, avirulent plant symbionts. *Nat. Rev. Microbiol.* 2, 43–56. doi: 10.1038/nrmicro797

Harrell, F. E. J. (2019). *Package 'Hmisc'. R Package Version 4.3-0*. Available online at: https://cran.rstudio.com/web/packages/Hmisc/Hmisc.pdf (accessed October 27, 2019).

Hausner, G. (2003). Fungal Mitochondrial Genomes, plasmids and introns. *Appl. Mycol. Biotechnol.* 3, 101–131. doi: 10.1016/s1874-5334(03)80009-6

Joardar, V., Abrams, N., Hostetler, J., Paukstelis, P., Pakala, S., Pakala, S., et al. (2012). Sequencing of mitochondrial genomes of nine *Aspergillus* and *Penicillium* species identifies mobile introns and accessory genes as main sources of genome size variability. *BMC Genomics* 13:698. doi: 10.1186/1471-2164-13-698

Johansen, S., Einvik, C., Elde, M., Haugen, P., Vader, A., and Haugli, F. (1997). "Group I introns in biotechnology: prospects of application of ribozymes and rare-cutting homing endonucleases," in *Biotechnology Annual Review*, Ed. M. R. El-Gewely Vol. 3, (Amsterdem: Elsevier), 111–150. doi: 10.1016/s1387-2656(08)70031-0

Johansen, S., and Haugen, P. (2001). A new nomenclature of group I introns in ribosomal DNA. *RNA* 7, 935–936. doi: 10.1017/s1355838201010500

Jung, P., Friedrich, A., Souciet, J., Louis, V., Potier, S., de Montigny, J., et al. (2010). Complete mitochondrial genome sequence of the yeast *Pichia farinosa* and comparative analysis of closely related species. *Curr. Genet.* 56, 507–515. doi: 10.1007/s00294-010-0318-y

Kang, Y., Yang, D., Kong, L., Hou, M., Meng, Y., Wei, L., et al. (2017). CPC2: a fast and accurate coding potential calculator based on sequence intrinsic features. *Nucleic Acids Res.* 45, W12–W16. doi: 10.1093/nar/gkx428

Kang, X., Hu, L., Shen, P., Li, R., and Liu, D. (2017). SMRT sequencing revealed mitogenome characteristics and mitogenome-wide DNA modification pattern in *Ophiocordyceps sinensis*. *Front. Microbiol.* 8:1422. doi: 10.3389/fmicb.2017.01422

Kanzi, A., Wingfield, B., Steenkamp, E., Naidoo, S., and van der Merwe, N. (2016). Intron derived size polymorphism in the mitochondrial genomes of closely related *Chrysoporthe* species. *PLoS One* 11:e0156104. doi: 10.1371/journal.pone.0156104

Katoh, K., Rozewicki, J., and Yamada, K. (2017). MAFFT online service: multiple sequence alignment, interactive sequence choice and visualization. *Briefings Bioinform.* 20, 1160–1166. doi: 10.1093/bib/bbx108

Kim, J. Y., and Park, I. K. (2000). The flavin coenzymes: a new class of group I intron inhibitors. *Biochim. Biophys. Acta* 1475, 61–66. doi: 10.1016/s0304-4165(00)00044-1

Kolesnikova, A., Putintseva, Y., Simonov, E., Biriukov, V., Oreshkova, N., Pavlov, I., et al. (2019). Mobile genetic elements explain size variation in the mitochondrial genomes of four closely-related *Armillaria* species. *BMC Genomics* 20:351. doi: 10.1186/s12864-019-5732-z

Kubicek, C., Steindorff, A., Chenthamara, K., Manganiello, G., Henrissat, B., Zhang, J., et al. (2019). Evolution and comparative genomics of the most common *Trichoderma* species. *BMC Genomics* 20:485. doi: 10.1186/s12864-019-5680-7

Lambowitz, A. M., Caprara, M. G., Zimmerly, S., and Perlman, P. S. (1998). Group I and group II ribozymes as RNPs: clues to the past and guides to the future. *RNA World* 2, 451–485.

Lambowitz, A. M., and Perlman, P. S. (1990). Involvement of aminoacyl-tRNA synthetases and other proteins in group I and group II intron splicing. *Trends Biochem. Sci.* 15, 440–444. doi: 10.1016/0968-0004(90)90283-h

Lang, B., Laforest, M., and Burger, G. (2007). Mitochondrial introns: a critical view. *Trends Genet.* 23, 119–125. doi: 10.1016/j.tig.2007.01.006

Lavrov, D., Boore, J., and Brown, W. (2002). Complete mtDNA sequences of two millipedes suggest a new model for mitochondrial gene rearrangements: duplication and nonrandom loss. *Mol. Biol. Evol.* 19, 163–169. doi: 10.1093/oxfordjournals.molbev.a004068

Lazowska, J., Jacq, C., and Slonimski, P. (1980). Sequence of introns and flanking exons in wild-type and box3 mutants of cytochrome b reveals an interlaced splicing protein coded by an intron. *Cell* 22, 333–348. doi: 10.1016/0092-8674(80)90344-x

Li, Q., Ren, Y., Shi, X., Peng, L., Zhao, J., Song, Y., et al. (2019). Comparative mitochondrial genome analysis of two *Ectomycorrhizal* fungi (Rhizopogon) reveals dynamic changes of intron and phylogenetic relationships of the Subphylum Agaricomycotina. *Int. J. Mol. Sci.* 20:5167. doi: 10.3390/ijms20205167

Li, Y., Hu, X., Yang, R., Hsiang, T., Wang, K., Liang, D., et al. (2015). Complete mitochondrial genome of the medicinal fungus *Ophiocordyceps sinensis*. *Sci. Rep.* 5:13892. doi: 10.1038/srep13892

Lorito, M., Woo, S. L., Harman, G. E., and Monte, E. (2010). Translational research on Trichoderma: from'omics to the field. *Ann. Rev. Phytopathol.* 48, 395–417. doi: 10.1146/annurev-phyto-073009-114314

Losada, L., Pakala, S., Fedorova, N., Joardar, V., Shabalina, S., Hostetler, J., et al. (2014). Mobile elements and mitochondrial genome expansion in the soil fungus and potato pathogenRhizoctonia solaniAG-3. *FEMS Microbiol. Lett.* 352, 165–173. doi: 10.1111/1574-6968.12387

Mardanov, A. V., Beletsky, A. V., Kadnikov, V. V., Ignatov, A. N., and Ravin, N. V. (2014). The 203 kbp mitochondrial genome of the phytopathogenic fungus *Sclerotinia borealis* reveals multiple invasions of introns and genomic duplications. *PLoS One* 9:e107536. doi: 10.1371/journal.pone.0107536

Michel, F., Kazuhiko, U., and Haruo, O. (1989). Comparative and functional anatomy of group II catalytic introns—a review. *Gene* 82, 5–30. doi: 10.1016/0378-1119(89)90026-7

Moore, W. S. (1997). Mitochondrial-gene trees versus nuclear-gene trees, a reply to Hoelzer. *Evolution* 51, 627–629. doi: 10.1111/j.1558-5646.1997.tb02452.x

Nadimi, M., Daubois, L., and Hijri, M. (2016). Mitochondrial comparative genomics and phylogenetic signal assessment of mtDNA among arbuscular mycorrhizal fungi. *Mol. Phylogenet. Evol.* 98, 74–83. doi: 10.1016/j.ympev.2016.01.009

Nielsen, H., and Johansen, S. D. (2009). Group I introns: moving in new directions. *RNA Biol.* 6, 375–383. doi: 10.4161/rna.6.4.9334

Okonechnikov, K., Golosova, O., and Fursov, M. (2012). Unipro UGENE: a unified bioinformatics toolkit. *Bioinformatics* 28, 1166–1167. doi: 10.1093/bioinformatics/bts091

Parenteau, J., Maignon, L., Berthoumieux, M., Catala, M., Gagnon, V., and Elela, S. A. (2019). Introns are mediators of cell response to starvation. *Nature* 565, 612–617. doi: 10.1038/s41586-018-0859-7

Pellenz, S., Harington, A., Dujon, B., Wolf, K., and Schäfer, B. (2002). Characterization of the I-Spom I endonuclease from fission yeast: insights into the evolution of a group I intron-encoded homing endonuclease. *J. Mol. Evol.* 55, 302–313. doi: 10.1007/s00239-001-2327-2324

Pogoda, C. S., Keepers, K. G., Nadiadi, A. Y., Bailey, D. W., Lendemer, J. C., Tripp, E. A., et al. (2019). Genome streamlining via complete loss of introns has occurred multiple times in lichenized fungal mitochondria. *Ecol. Evol.* 9, 4245–4263. doi: 10.1002/ece3.5056

Pramateftaki, P., Kouvelis, V., Lanaridis, P., and Typas, M. (2006). The mitochondrial genome of the wine yeastHanseniaspora uvarum: a unique genome organization among yeast/fungal counterparts. *FEMS Yeast Res.* 6, 77–90. doi: 10.1111/j.1567-1364.2005.00018.x

R Core Team (2013). *R: A Language and Environment for Statistical Computing*. Vienna: R Foundation for Statistical Computing.

Rangan, P., Masquida, B., Westhof, E., and Woodson, S. A. (2004). Architecture and folding mechanism of the Azoarcus group I pre-tRNA. *J. Mol. Biol.* 339, 41–51. doi: 10.1016/j.jmb.2004.03.059

Rehner, S. A., and Samuels, G. J. (1995). Molecular systematics of the Hypocreales: a teleomorph gene phylogeny and the status of their anamorphs. *Can. J. Bot.* 73, 816–823.

Repar, J., and Warnecke, T. (2017). Mobile introns shape the genetic diversity of their host genes. *Genetics* 205, 1641–1648. doi: 10.1534/genetics.116.199059

Rocha, E. (2003). DNA repeats lead to the accelerated loss of gene order in bacteria. *Trends Genet.* 19, 600–603. doi: 10.1016/j.tig.2003.09.011

Roman, J., and Woodson, S. A. (1995). Reverse splicing of the Tetrahymena IVS: evidence for multiple reaction sites in the 23S rRNA. *RNA* 1, 478–490.

Saldanha, R., Mohr, G., Belfort, M., and Lambowitz, A. M. (1993). Group I and group II introns. *FASEB J.* 7, 15–24. doi: 10.1096/fasebj.7.1.8422962

Sandor, S., Zhang, Y., and Xu, J. (2018). Fungal mitochondrial genomes and genetic polymorphisms. *Appl. Microbiol. Biotechnol.* 102, 9433–9448. doi: 10.1007/s00253-018-9350-5

Schmoll, M., Dattenböck, C., Carreras-Villaseñor, N., Mendoza-Mendoza, A., Tisch, D., Alemán, M. I., et al. (2016). The genomes of three uneven siblings: footprints of the lifestyles of three *Trichoderma* species. *Microbiol. Mol. Biol. Rev.* 80, 205–327. doi: 10.1128/mmbr.00040-15

Sethuraman, J., Majer, A., Iranpour, M., and Hausner, G. (2009). Molecular evolution of the mtDNA Encoded rps3 gene among Filamentous Ascomycetes fungi with an emphasis on the Ophiostomatoid Fungi. *J. Mol. Evol.* 69, 372–385. doi: 10.1007/s00239-009-9291-9

Specht, C., Novotny, C., and Ullrich, R. (1992). Mitochondrial DNA of *Schizophyllum commune*: restriction map, genetic map, and mode of inheritance. *Curr. Genet.* 22, 129–134. doi: 10.1007/bf00351472

Stajich, J. E. (2017). Fungal genomes and insights into the evolution of the kingdom. *Fungal Kingdom* 54, 619–633. doi: 10.1128/9781555819583.ch29

Stoddard, B. (2014). Homing endonucleases from mobile group I introns: discovery to genome engineering. *Mobile DNA* 5:7. doi: 10.1186/1759-8753-5-7

Sung, G., Poinar, G., and Spatafora, J. (2008). The oldest fossil evidence of animal parasitism by fungi supports a Cretaceous diversification of fungal–arthropod symbioses. *Mol. Phylogenet. Evol.* 49, 495–502. doi: 10.1016/j.ympev.2008.08.028

Torriani, S., Goodwin, S., Kema, G., Pangilinan, J., and McDonald, B. (2008). Intraspecific comparison and annotation of two complete mitochondrial genome sequences from the plant pathogenic fungus *Mycosphaerella graminicola*. *Fungal Genet. Biol.* 45, 628–637. doi: 10.1016/j.fgb.2007.12.005

Tsuji, J., Frith, M., Tomii, K., and Horton, P. (2012). Mammalian NUMT insertion is non-random. *Nucleic Acids Res.* 40, 9073–9088. doi: 10.1093/nar/gks424

Van der Nest, M., Steenkamp, E., McTaggart, A., Trollip, C., Godlonton, T., Sauerman, E., et al. (2015). Saprophytic and pathogenic fungi in the *Ceratocystidaceae* differ in their ability to metabolize plant-derived sucrose. *BMC Evol. Biol.* 15:273. doi: 10.1186/s12862-015-0550-7

Varshney, D., Jaiswar, A., Adholeya, A., and Prasad, P. (2016). Phylogenetic analyses reveal molecular signatures associated with functional divergence among Subtilisin like Serine Proteases are linked to lifestyle transitions in Hypocreales. *BMC Evol. Biol.* 16:793. doi: 10.1186/s12862-016-0793-y

Wang, L., Zhang, S., Li, J., and Zhang, Y. (2018). Mitochondrial genome, comparative analysis and evolutionary insights into the entomopathogenic fungus Hirsutella thompsonii. *Environ. Microbiol.* 20, 3393–3405. doi: 10.1111/1462-2920.14379

Warnes, G. R., Bolker, B., Bonebakker, L., Gentleman, R., Liaw, W. H. A., Lumley, T., et al. (2019). *gplots: Various R Programming Tools for Plotting Data. R package version 3.0.1.1*. Available online at: https://cran.r-project.org/web/packages/gplots/index.html (accessed May 15, 2019).

Wei, T., and Simko, V. (2017). *R package "corrplot": Visualization of a Correlation Matrix (version 0.84)*. Available online at: https://github.com/taiyun/corrplot (accessed November 17, 2019).

Weir, J., and Schluter, D. (2008). Calibrating the avian molecular clock. *Mol. Ecol.* 17, 2321–2328. doi: 10.1111/j.1365-294x.2008.03742.x

Wickham, H. (2016). *ggplot2: Elegant Graphics for Data Analysis*. New York, NY: Springer-Verlac.

Wickham, H. (2018). *reshape: Flexibly Reshape Data. R package version 0.8.8*. Available online at: https://cran.r-project.org/web/packages/reshape/index.html (accessed November 17, 2018).

Wijayawardene, N., Hyde, K., Lumbsch, H., Liu, J., Maharachchikumbura, S., Ekanayaka, A., et al. (2018). Outline of Ascomycota: 2017. *Fungal Divers.* 88, 167–263. doi: 10.1007/s13225-018-0394-8

Wolters, J., Chiu, K., and Fiumera, H. (2015). Population structure of mitochondrial genomes in *Saccharomyces cerevisiae*. *BMC Genomics* 16:451. doi: 10.1186/s12864-015-1664-4

Wright, R., and Cummings, D. (1983). Integration of mitochondrial gene sequences within the nuclear genome during senescence in a fungus. *Nature* 302, 86–88. doi: 10.1038/302086a0

Wu, B., and Hao, W. (2014). Horizontal transfer and gene conversion as an important driving force in shaping the landscape of mitochondrial introns. *G3* 4, 605–612. doi: 10.1534/g3.113.009910

Yang, E., Xu, L., Yang, Y., Zhang, X., Xiang, M., Wang, C., et al. (2012). Origin and evolution of carnivorism in the Ascomycota (fungi). *Proc. Natl. Acad. Sci. U.S.A.* 109, 10960–10965. doi: 10.1073/pnas.1120915109

Zhang, S., and Zhang, Y. J. (2019). Proposal of a new nomenclature for introns in protein-coding genes in fungal mitogenomes. *IMA Fungus* 10:15.

Zhang, Y., Zhang, S., Zhang, G., Liu, X., Wang, C., and Xu, J. (2015). Comparison of mitochondrial genomes provides insights into intron dynamics and evolution in the caterpillar fungus *Cordyceps militaris*. *Fungal Genet. Biol.* 77, 95–107. doi: 10.1016/j.fgb.2015.04.009

Zubaer, A., Wai, A., and Hausner, G. (2018). The mitochondrial genome of *Endoconidiophora resinifera* is intron rich. *Sci. Rep.* 8:17591. doi: 10.1038/s41598-018-35926-y

Conflict of Interest: The authors declare that the research was conducted in the absence of any commercial or financial relationships that could be construed as a potential conflict of interest.

frontiers in Microbiology

ORIGINAL RESEARCH
published: 05 May 2020
doi: 10.3389/fmicb.2020.00839

Population Genomic Analysis Reveals a Highly Conserved Mitochondrial Genome in *Fusarium asiaticum*

Meixin Yang[1,2†], Hao Zhang[1†], Theo A. J. van der Lee[2], Cees Waalwijk[2], Anne D. van Diepeningen[2], Jie Feng[1], Balázs Brankovics[2] and Wanquan Chen[1*]*

[1] State Key Laboratory for Biology of Plant Diseases and Insect Pests, Institute of Plant Protection, Chinese Academy of Agriculture Sciences, Beijing, China, [2] Biointeractions and Plant Health, Wageningen Plant Research, Wageningen, Netherlands

OPEN ACCESS

Edited by:
László Galgóczy,
Hungarian Academy of Sciences (MTA), Hungary

Reviewed by:
Todd Ward,
United States Department of Agriculture (USDA), United States
Firas Talas,
ETH Zürich, Switzerland

***Correspondence:**
Balázs Brankovics
balazs.brankovics@wur.nl
Wanquan Chen
wqchen@ippcaas.cn

[†] These authors have contributed equally to this work

Specialty section:
This article was submitted to Fungi and Their Interactions, a section of the journal Frontiers in Microbiology

Received: 29 January 2020
Accepted: 07 April 2020
Published: 05 May 2020

Citation:
Yang M, Zhang H, van der Lee TAJ, Waalwijk C, van Diepeningen AD, Feng J, Brankovics B and Chen W (2020) Population Genomic Analysis Reveals a Highly Conserved Mitochondrial Genome in Fusarium asiaticum. Front. Microbiol. 11:839. doi: 10.3389/fmicb.2020.00839

Fusarium asiaticum is one of the pivotal members of the *Fusarium graminearum* species complex (FGSC) causing Fusarium head blight (FHB) on wheat, barley and rice in large parts of Asia. Besides resulting in yield losses, FHB also causes the accumulation of mycotoxins such as nivalenol (NIV) and deoxynivalenol (DON). The aim of this study was to conduct population studies on *F. asiaticum* from Southern China through mitochondrial genome analyses. All strains were isolated from wheat or rice from several geographic areas in seven provinces in Southern China. Based on geographic location and host, 210 isolates were selected for next generation sequencing, and their mitogenomes were assembled by GRAbB and annotated to explore the mitochondrial genome variability of *F. asiaticum*. The *F. asiaticum* mitogenome proves extremely conserved and variation is mainly caused by absence/presence of introns harboring homing endonuclease genes. These variations could be utilized to develop molecular markers for track and trace of migrations within and between populations. This study illustrates how mitochondrial introns can be used as markers for population genetic analysis. SNP analysis demonstrate the occurrence of mitochondrial recombination in *F. asiaticum* as was previously found for *F. oxysporum* and implied for *F. graminearum*. Furthermore, varying degrees of genetic diversity and recombination showed a high association with different geographic regions as well as with cropping systems. The mitogenome of *F. graminearum* showed a much higher SNP diversity while the interspecies intron variation showed no evidence of gene flow between the two closely related and sexual compatible species.

Keywords: *Fusarium asiaticum*, mitogenome, introns, migrations, population genomics

INTRODUCTION

Members of the *Fusarium graminearum* species complex (FGSC) are the main causal agents of *Fusarium* head blight (FHB) and infect wheat (*Triticum aestivum* L.), maize (*Zea mays* L.) and other small grain cereals, causing significant losses in grain quality and yield around the world (Goswami and Kistler, 2004). In addition, infected crops often accumulate mycotoxins, such as

deoxynivalenol, zearalenone and nivalenol, which pose a serious health risk to animals and humans (D'Mello et al., 1999). FGSC comprises at least 16 distinct species (Sarver et al., 2011). The most important member is the globally occurring species *F. graminearum*. The second most important species is *F. asiaticum,* the main causal agent of FHB in Asia including China, Korea, Nepal, and Japan (van der Lee et al., 2015). *F. asiaticum* is particularly dominant in the Middle-Lower Reaches of the Yangtze River (MLRYR) and southwest of China, where FHB is the most prevalent (Zhang et al., 2012). In a previous study, we have found that the specific crop rotations correlate with the occurrence of FGSC species, where wheat/rice rotations were found to be highly conducive for *F. asiaticum* (Zhang et al., 2016a).

Crop debris (wheat and rice straw, corn stalks, and debris from other crops) is a crucial element for *Fusarium* to complete its life cycle, since infested crop residues form the overwintering niches for FHB pathogens. In the next cropping season ascospores, the primary inoculum of FHB, are released from perithecia forming on the surface of crop debris (Schmale and Bergstrom, 2003). In Brazil and United States, *F. graminearum* was determined as the predominant species on wheat (Gale et al., 2011; Del Ponte et al., 2015), whereas *F. asiaticum* was exclusively associated with rice growing areas (Kuhnem et al., 2016). In southern China where rice is the predominant crop grown, *F. asiaticum* is widespread, while *F. graminearum* is mainly found in Northern China, where wheat and maize are cultivated in monoculture or in rotation (Zhang et al., 2012).

Several population studies have shown shifts and high dynamics in *Fusarium* populations (Waalwijk et al., 2003; Gale et al., 2007; Ward et al., 2008). In Canada, a rapid displacement of 15ADON producing *F. graminearum* by a newly introduced 3ADON-producing *F. graminearum* population was observed (Ward et al., 2008). While in the South of the United States an influx of NIV producers, both *F. asiaticum* and *F. graminearum*, was reported (Gale et al., 2011). In our previous studies, NIV-producing *F. asiaticum* were shown to be replaced by 3ADON-producing *F. asiaticum* from east to west in China (Zhang et al., 2012). Besides, changes in chemotype (or mycotoxin profile), fungicide resistance (Talas and McDonald, 2015; Zhang et al., 2016b) and virulence might be distinct between populations. Hence, it is important to monitor shift of different *Fusarium* populations (Gale et al., 2007; Zhang et al., 2012). This will aid the understanding of population dynamics and the evolutionary principles underlying the FHB outbreaks.

The "second genome" of eukaryotes, the mitochondrial genome, is a highly informative phylogenetic marker generally used for inferring evolutionary and phylogenetic relationships at diverse taxonomic levels (Basse, 2010). The high copy numbers of mitochondrial genomes (mitogenomes) within individual cells facilitate accessing their genomes (Gillett et al., 2014). Besides, homologous regions are easy to identify, as the mitogenome has a relatively simple composition (Avise et al., 1983). Mobile mitochondrial introns prove common in many fungi (Haugen et al., 2005) and though they may interfere with polymerase chain reaction amplification methods, in next-generation sequencing (NGS) they provide additional markers.

Significant differences exist in fungal mitogenomes related to genome structure, gene arrangement, repeat content and size (Li et al., 2018a,b, 2019). In previous studies of the genus *Fusarium*, mitogenomes show many common features: in most *Fusarium* spp., including *F. verticillioides*, *F. oxysporum*, *F. graminearum* and *F. solani*, mitogenomes harbor 14 protein coding genes, a wide range of tRNA coding genes and two rRNA coding genes, rns (mtSSU) and rnl (mtLSU). All of these genes are encoded on the same strand and genes are organized in the same order (Pantou et al., 2008; Al-Reedy et al., 2012). In our previous study of *Fusarium* mitogenomes, we have found that intraspecific differences in mitogenomes sizes are mainly due to the absence/presence of introns. Mitochondrial recombination has been described in *F. oxysporum* and *F. graminearum*. The spread of introns can take place by three different mechanisms: horizontal transfer, vertical inheritance and recombination (Al-Reedy et al., 2012; Brankovics et al., 2018). Therefore, mitogenomes of *Fusarium* are potential markers to track and trace the spread of populations.

To date, the mitogenome of *F. asiaticum* has not been assembled and hence the species' variation and diversity of this mitogenome is unknown. In this study, we sequenced, *de novo* assembled and annotated mitogenomes of 210 *F. asiaticum* isolates collected from four ecological regions of China. Subsequently, variation analysis was conducted and a pan-mitogenome of *F. asiaticum* was created. The efficacy of using mitochondrial introns as markers for population genetic analysis was investigated, and combined with other mitochondrial variations the population diversity of *F. asiaticum* in Southern China was assessed. Finally, interspecies comparative mitochondrial genomic analyses were performed on 24 previously published mitogenomes of *F. graminearum* and the 210 mitogenomes of *F. asiaticum* generated in this study.

MATERIALS AND METHODS

Isolates

Two hundred and ten *F. asiaticum* strains and twenty-four *F. graminearum* strains were analyzed in this study (**Supplementary Table S1**). The *F. asiaticum* strains were collected from six provinces in Southern China, which can be divided into four ecological regions: Hubei, Jiangsu, and Anhui Province are located in the Middle-Lower reaches of the Yangtze River (MLRYR) and regarded as one ecological region. The Hunan Province is a transition region between plains and mountains, its northern part is adjacent to MLRYR. The Sichuan and Fujian Provinces are both mountainous regions. The cropping system is also different among these regions. In the MLRYR, which is the main wheat producing area in Southern China, wheat-rice rotation is predominant. In Sichuan Province, crop diversity is much higher and

the acreage of wheat is significantly smaller compared to MLRYR (Zeng et al., 2011). In Sichuan Province, wheat is rotated with rice, maize, soybean and several other crops, but wheat-rice rotation is the most common. In the MLRYR and Sichuan, *Fusarium* strains were isolated from diseased wheat heads and perithecia on rice stubble (debris of the previous crop) by a single-spore isolation procedure described previously (Yang et al., 2018). In Fujian and Hunan Provinces no wheat is grown, two harvests of rice/year is the prevalent cropping system and consequently all *Fusarium* strains isolated from this regions are from rice stubble. A detailed sampling information of these strains are shown in **Supplementary Table S1**.

Sequencing

Whole genome sequencing of *F. asiaticum* isolates were performed by Biomarker Technologies Corporation (Beijing, China). Random sheared shotgun library with specific index of each *F. asiaticum* strain was made using the Illumina TruSeq DNA Sample Prep Kit, according to manufacturer's protocols (Illumina). The concentration of independent genomic library was quantitated by QUBIT 3.0 fluorometer. The 210 independent libraries were pooled with equal amount by adjusting the solution volume and then were sequenced using the Illumina HiSeq X Ten platform which supported the acquisition of 2 × 150 bp paired-end reads at ∼50X coverage per sample. Subsequently, Casava 1.8 software was used to de-multiplex reads which were filtered for quality using *fastp* with forced polyG tail trimming (*-g*) and minimum quality Phred score ≥ 20 (*-q 20*). The *F. graminearum* strains were sequenced by other research groups, and their mitochondrial genome sequences were downloaded and analyzed in this study (Yuen and Mila, 2015; Wang et al., 2017; Brankovics et al., 2018).

Mitochondrial Genome Assembly

The mitogenomes of the sequenced strains were assembled by GRAbB (Genomic Region Assembly by Baiting) with the SPAdes assembler (Bankevich et al., 2012; Nurk et al., 2013; Brankovics et al., 2016), which had also been used for mitogenome assembly of *F. graminearum* strains (Brankovics et al., 2018). Isolate PH-1 (HG970331) was used as the reference sequence to bait the mitogenome sequences. The assembled contigs were joined based on overlap to form a single contig using the helper scripts from the GRAbB package[1]. The final overlapping sequence was clipped during the process, which confirmed that all sequences were derived from a circular configuration.

Mitochondrial Genome Annotation

Mitochondrial genome annotation was performed as described by Brankovics et al., 2018. Briefly, MFannot[2], NCBI's ORF Finder[3], CD-Search (Marchler-Bauer and Bryant, 2004), InterPro (Mitchell et al., 2015), tRNAscan-SE (Pavesi et al., 1994) were combined to annotate the mitogenome sequence. The annotation information of the mitogenomes has been deposited at GenBank: MN935220-MN935429. GenBank accession numbers are also listed in **Supplementary Table S1**.

Variation Analysis of Mitogenomes

The mitogenomes of *F. asiaticum* and *F. graminearum* strains were aligned using MUSCL v3.8.31 (Edgar, 2004) and manually curated. The alignment was used to extract variations using the *msa2vcf* function of Jvarkit[4]. Subsequently, variant locations in exonic, intronic, or intergenic regions were identified. In the case of exonic variants, they were characterized as synonymous or non-synonymous variation and amino acid changes were noted. The structure and variant annotation were visualized using the *ggplot2* package in *R*.

Since intronic sequences behave as mobile genetic elements in fungal mitochondrial genomes we partitioned the analysis into two: one focusing on the intron sequences and the other on the non-intronic regions (intergenic and coding sequences).

Intron Analysis

The intron size information for each strain was extracted from the annotation file and used as markers to analyze genotypic differentiation of introns of strains among different populations (**Supplementary Table S3**). Multilocus genotype (MLG), rarefaction Multilocus genotype (eMLG), allele frequencies, and Nei genetic distance analyses of the population from different ecological regions were conducted with GENALEX version 6.5 (Peakall and Smouse, 2012). Simpson's index (Lambda), Nei's gene diversity index (Hexp), value of the standardized index of association for each population factor (rbarD), *P*-value for rbarD from the number of reshuffles indicated in sample (p.rD), and principal component analysis (PCA) were performed with *R* package *Poppr* (Kamvar et al., 2014). The correlation analysis between geographical distance and genetic distance of *F. asiaticum* from 50 sampling sites was conducted by Mantel test in *R* package *ade4* (Mantel, 1967).

Analysis of Non-intronic Regions

Intronic regions were clipped out from the mitogenome alignment and parsimony informative sites were extracted excluding gapped sites. The sites were checked manually, especially the SNP rich regions. A region where most of the SNPs could be traced to some strains containing longer poly tracts than other isolates was identified as poor quality region and removed from the downstream analysis. This region is also the common breakpoint in mitochondrial genome assemblies before circularization. Subsequently, the curated data was used for network construction using PopART (Population Analysis with Reticulate Trees) (Leigh et al., 2015). The geographic origin and the host information was used to color the network nodes.

Phylogenetic Analysis

A *F. culmorum* mitogenome (accession number NC_026993.1) was added to the non-intronic alignment of the *F. asiaticum* and *F. graminearum* strains. The alignment was generated by

[1]https://github.com/b-brankovics/grabb

[2]http://megasun.bch.umontreal.ca/cgi-bin/mfannot/mfannotInterface.pl

[3]https://www.ncbi.nlm.nih.gov/orffinder/

[4]http://lindenb.github.io/jvarkit/

MUSCLE v3.8.31. Phylogenetic analysis was conducted using the ML method which was run using IQ-Tree with model selection and 1000 bootstraps with the *F. culmorum* strain as outgroup. The best model selected was TPM2u + I + G4.

RESULTS

Mitogenomes of *F. asiaticum*

Features of the *F. asiaticum* Mitogenome

The complete mitogenomes of all 210 *F. asiaticum* strains were assembled into single circular DNA molecules, with the total size ranging from 89,966 to 98,925 bp. All mitogenomes encoded the same set of genes: 14 Protein coding genes (PCGs), 28 tRNA, two rRNA, and one large open reading frame with unknown function (LV-uORF), all with the same orientation and order. The intronic regions vary in length from 44, 676 to 53,583 bp, which accounts for almost half of the entire length of the mitogenome in each strain.

Variations Among *F. asiaticum* Mitogenomes

A total of 120 polymorphic sites were identified in the 210 *F. asiaticum* mitogenomes, including 76 SNPs and 44 indels (**Figure 1**). There were 40 SNPs detected in intergenic regions and 22 SNPs were located in introns. Only 11 SNPs were identified in the conserved protein coding regions, showing a low level of variation and all of them were synonymous mutations. The remaining 3 SNPs were identified in the large variable open reading frame with unknown function (LVuORF or orf1931 region, among which two caused non-synonymous substitutions: at position 1648 from proline (CCT) to serine (TCT) and at position 1840 from arginine (CGC) to leucine (CTC) residues in the predicted protein. Indels were only detected in intergenic and intronic regions with sizes varying from 1 to 1994 bp. The vast majority of indels in intergenic regions were short; 24/26 were shorter than 4 bp, one was 16 bp and the largest 163 bp long. In sharp contrast, all large indels (>900 bp) were found in intronic regions totaling 14704 bp in length.

Within the 210 *F. asiaticum* mitogenomes a total of 38 introns were identified, 31 of them were present in all genomes while seven were variable. The number of introns in each individual isolate ranged from 31 to 36. Thirty-six strains contained the minimum number of 31 introns while only one strain contained the maximum number of 36 introns. The length variation of mitochondrial genome in *F. asiaticum* is mainly caused by variation in the intron regions. Three large indels (cox2-i228, cob-i823, and cox1-i621) are putatively due to an additional intron insertion inside an already present intron, because the insert region coded for an additional HEG. Among the seven introns which showed presence/absence pattern, three were absent in most isolates: two (atp9-i181 and cob-i779) were just present in one strain and one (cox2-i552) was found in four strains. We investigated the size composition of the other four introns. As shown in **Figure 2**, Sichuan showed a significantly higher ratio of intron absence than the other three regions for cox1-i287, cox1-i1287, and cox2-i318. While for cob-i201, Sichuan had the highest presence ratio and it was the only province with multiple haplotypes.

Analysis of Non-intronic Regions of the Mitogenomes of *F. asiaticum*

Parsimony informative sites were extracted from the non-intronic regions of the *F. asiaticum* mitogenome alignment. Excluding gapped sites, this yielded 30 parsimony informative positions out of the 48376 bp-long alignment. Subsequently, the 30 sites were manually curated at which point 8 were removed, because they were due to length variations of neighboring poly tracts, resulting in 22 reliable parsimony informative sites. The curated alignment was used for analysis in PopArt, where 13 haplotypes were detected among the 210 *F. asiaticum* isolates. Composition of haplotypes in four regions was similar with one predominant haplotype found in all regions (180265) (**Figure 3**). The intronless sequences of *F. asiaticum* are extremely conserved, 156 of 210 strains had the same haplotype (**Figure 3**). There was no clear grouping between haplotypes and ecological regions nor between haplotypes and hosts (**Supplementary Figure S1**). However, we found the strains from Sichuan (6/13) and Hunan (7/13) contained more haplotypes than MLRYR (5/13) and Fujian (5/13), and they have more region-specific haplotypes. This revealed that Sichuan and Hunan population were more divergent than the other two. Furthermore, a closed loop was formed by five haplotypes in the network, indicative of recombination in the mitogenomes of *F. asiaticum* population (**Figure 4**). Detailed analysis of the SNPs involved revealed that the two "side" branches linking the two largest haplotypes differ each by single SNPs in coding sequences that represent synonymous mutations: 140005 and 171375 shared the *cox2*-A234G SNP (position refers to nucleotide position in the coding sequence), while 171156 and the 180197 haplotype group shared the *cob*-C163T SNP. The three additional SNPs involved were the same on all three branches. These three SNPs are adjacent to each other and are located in an intergenic region. Although only five sites are indicative of recombination, they represent 23.8% of the parsimony informative sites used for this analysis. Furthermore, considering the low level of variation observed it is highly unlikely that two SNPs located in coding sequences of highly conserved genes have independent origins or that same three adjacent SNPs mutated the same way in three different backgrounds.

Population Analysis of *F. asiaticum* by Intron Pattern

To understand the population structure and estimate the genetic variability of the intron regions of *F. asiaticum*, all 210 strains were genotyped based on their intron composition (**Supplementary Table S3**): a total of 41 MLGs were identified. The number of MLGs ranged from 16 in Hunan, 17 in MLRYR to 19 in Fujian and Sichuan. In order to eliminate the influence of population size, the normalized multilocus genotypes eMLGs were used to compare the genotypic diversity among the populations. Isolates from Fujian showed the highest genotypic diversity, followed by those from Sichuan, MLRYR and Hunan. The Simpson's index (lambda) and Nei's gene diversity index

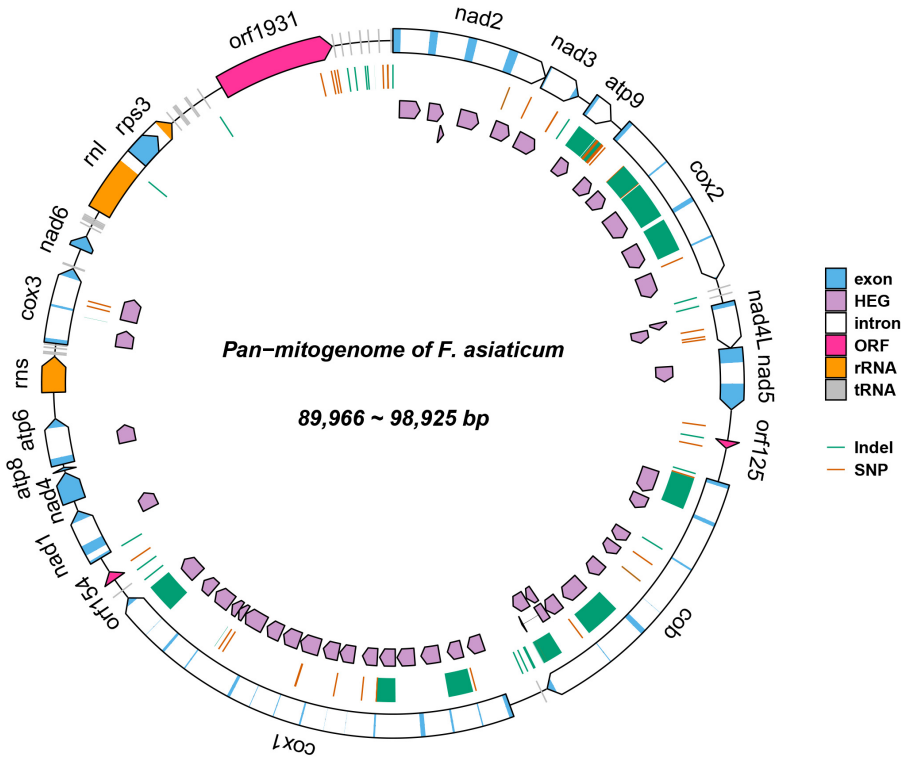

FIGURE 1 | Pan-mitogenome of 210 *Fusarium asiaticum* isolates. This figure summarizes all the genetic variability observed within the species. Regions affected by indels are highlighted in green and SNPs are indicated in red.

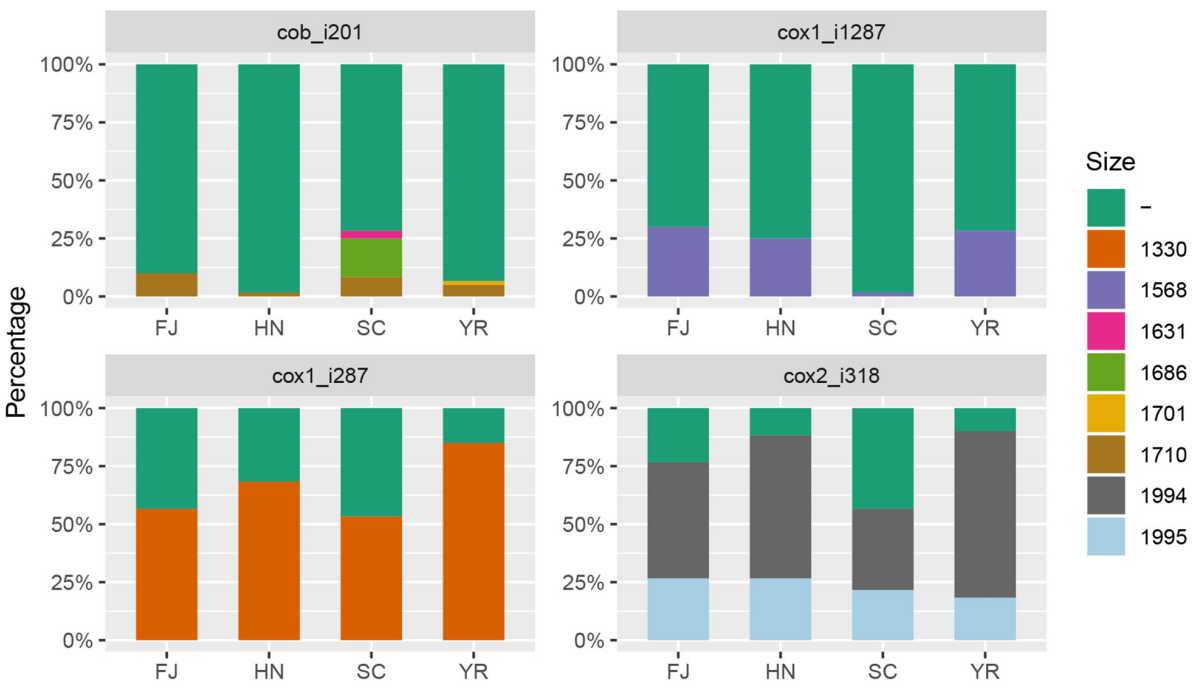

FIGURE 2 | The size composition of four introns: cox2_i318, cob_i201, cox1_i287, cox1_i1287. FJ, Fujian; HN, Hunan; SC, Sichuan; YR, Middle-Lower Reaches of Yangtze River. -: absence, and numbers indicate length of introns in base pairs.

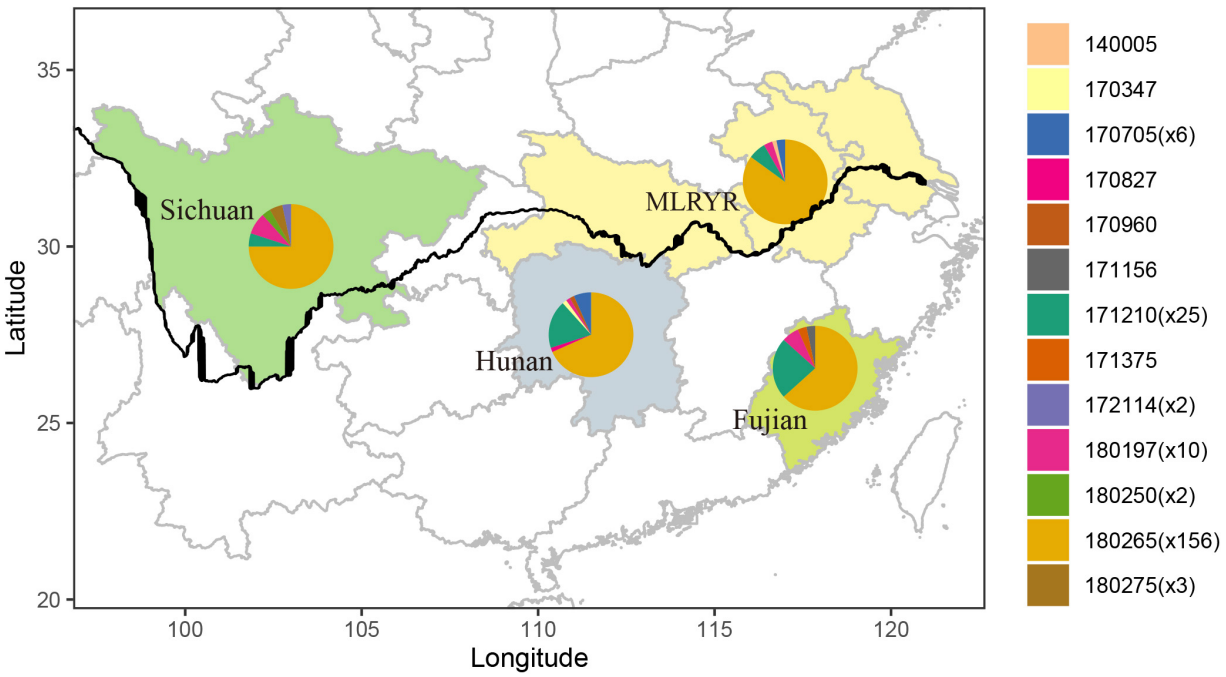

FIGURE 3 | Map of four ecological regions indicating the distribution of haplotypes composed by non-intronic regions from 210 *F. asiaticum* isolates. The figure in parenthesis means the number of specific haplotypes.

(Hexp) also showed similar pattern compared with the eMLG analysis. In both cases, Fujian and Sichuan showed a higher lambda and Hexp value (**Table 1**), indicating higher diversity in these populations compared to those from MLRYR and Hunan. All four populations had unique alleles, with the highest frequency of unique alleles found in Sichuan (0.143), followed by Hunan (0.095) and MLRYR (0.071), while particularly in Fujian a low value was observed (0.048) (**Table 2**). Association indices (rbarD) were used to estimate the recombination within populations. Significant ($P = 0.0099$) linkage disequilibrium with a high rbarD value (0.1758) was observed in Sichuan, indicating limited genetic exchange among strains from this province. Although linkage disequilibrium could be a result of gene flow from other populations, considering that Sichuan shows the highest haplotype diversity and it is a mountainous region limited genetic exchange is the most likely explanation. In the other three regions, the rbarD values were much lower and not significant at the 0.05 level, suggesting genetic exchange among these populations. Pairwise Nei's genetic distance of the four populations ranged from 0.001 to 0.01 (**Table 2**). The longest distance was observed between MLRYR and Sichuan, while MLRYR-Hunan and Hunan-Fujian showed the lowest distance.

Interspecies Comparative Mitochondrial Genomes Analyses

Variations Between Mitogenomes of *F. asiaticum* and *F. graminearum*

To compare the genetic variation in populations of *F. asiaticum* and *F. graminearum*, we aligned the above 210 *F. asiaticum* and 24 *F. graminearum* mitochondrial sequences and performed a variant calling analysis (**Figure 5**). A total of 442 variations were identified including 318 SNPs and 124 indels. Most SNPs are located in intergenic (173) and intron (72) regions, others were found in the LV-uORF (34), tRNA (18), rRNA (3), and protein coding sequences (18). Further analysis showed that all the SNPs found in exons were synonymous mutations, but 21 of 34 SNPs in the LV-uORF caused non-synonymous substitutions (**Supplementary Table S2**). Similarly, 96% of the indels were located in intergenic (82) and intronic (37) regions, while others were in tRNA (4), and rRNA (1), but no indel was found in exon and LV-uORF regions. The length of indels varied from 1 to 2923 bp, but indels with different length were unevenly distributed in different regions (**Figure 6**). All large indels (>1000 bp) and more than a half of the middle-length indels (100–1000 bp) were located in intron regions. Short indels (<100 bp) were mainly observed in intergenic regions. The length variation of *F. asiaticum* and *F. graminearum* mitogenomes is mainly derived from variation in the intronic regions (**Table 3**).

Intron Analysis

A total of 42 introns was identified in *F. asiaticum* and *F. graminearum* populations, 28 of them were core introns, present in all isolates of the two species, the other 12 showed presence/absence variation. We found two *F. graminearum* specific introns (cox2-i108 and cob-i278) and one *F. asiaticum* specific intron (cob-i823), which were fixed in one species and absent from the other species. Interestingly, some introns showed clear association with the two species. Atp9-i181 and cob-i779 were absent in most *F. asiaticum* strains (209/220),

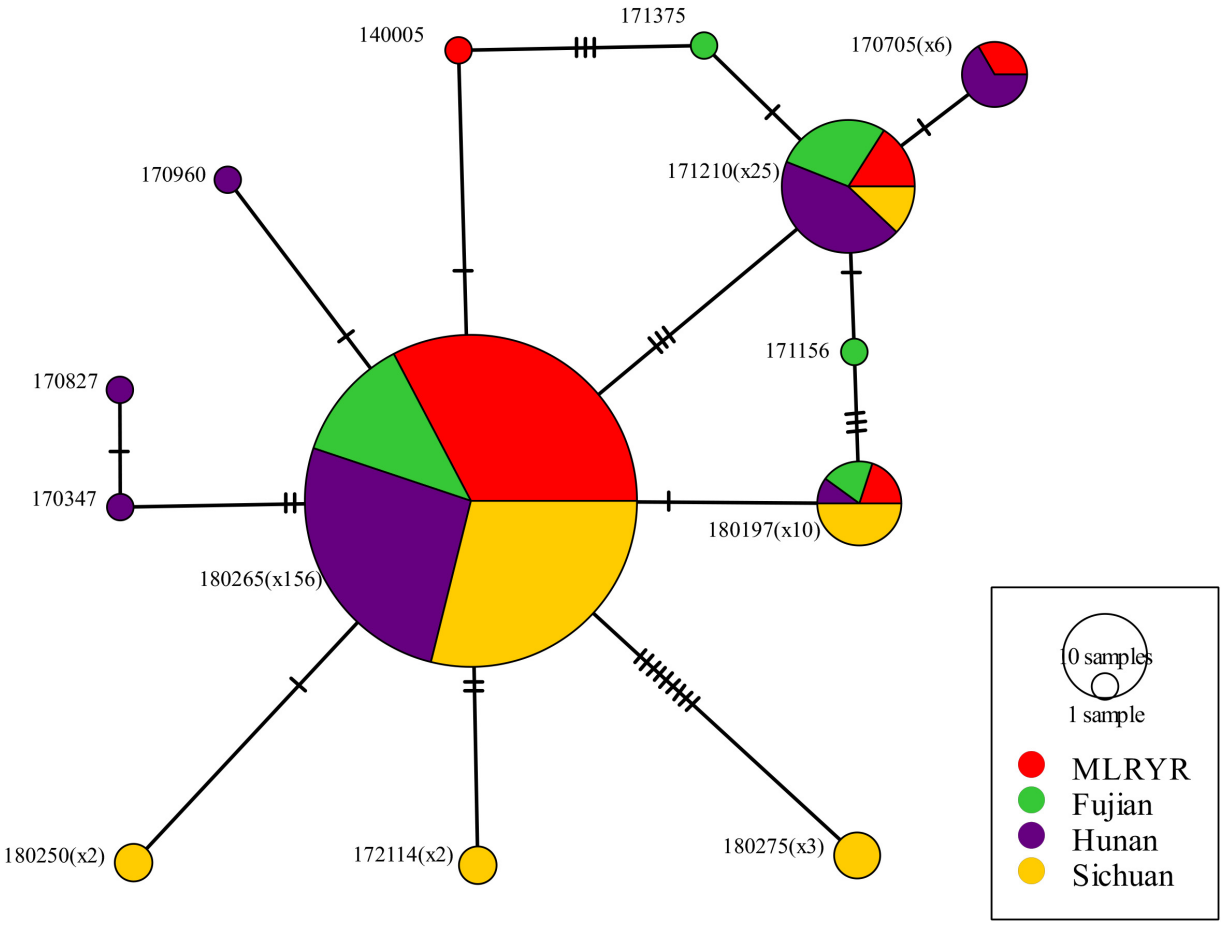

FIGURE 4 | Minimum spanning network inferred from non-intronic regions from 210 *F. asiaticum* isolates. Each perpendicular black line indicates an individual SNP. The number of each haplotype is reflected by size of each circle and by the exact number is given in parentheses following the haplotype codes, except for those haplotypes representing only single isolates.

TABLE 1 | Summary of population genetic structure of intron regions of 210 *F. asiaticum* mitogenomes in diverse geographical regions.

Pop	N[a]	MLG[b]	eMLG[c]	Private Alleles[d]	lambda[e]	Hexp[f]	rbarD[g]	p.rD[h]
MLRYR	60	17	12	0.071	0.836	0.0388	0.0168	0.1980
Hunan	60	16	11.9	0.095	0.872	0.0427	0.0104	0.2673
Fujian	30	19	19	0.048	0.927	0.0525	−0.0256	0.9505
Sichuan	60	19	13.5	0.143	0.983	0.0576	0.1758	0.0099*

[a]N = the number of samples from each region; [b]MLG = number of identified multilocus genotype; [c]eMLG = expected number of MLG at the lowest common sample size; [d]Private Alleles = number of private alleles; [e]lambda = Simpson's index; [f]Hexp = Nei's gene diversity index; [g]rbarD = value of the standardized index of association for each population factor; [h]p.rD = P-value for rbarD from the number of reshuffles indicated in sample; Asterisks represent significant linkage disequilibrium.

but fixed in the *F. graminearum* population. The size of nad2-i762 was different in the two species, 1475 bp in *F. asiaticum* and 1465 bp in *F. graminearum*. A similar situation was also found in cox2-i228, of which the size in most *F. asiaticum* strains (208/220) was 1146 bp, while a 1159 bp intron was mainly found in *F. graminearum* (16/24) as well as one strain with a 1146 bp intron, one with a 1147 intron bp and six strains with no intron at that location at all. Based on genotypes of intron size, 41 and 15 MLGs were identified in *F. asiaticum* and *F. graminearum* populations respectively. Taking into account the difference of population size, *F. graminearum* showed a higher eMLG value indicating higher genotypic diversity within the population. Simpson's index, haploid genetic diversity and Nei's gene diversity index also suggested a higher level of diversity of *F. graminearum* than of the *F. asiaticum* population (**Table 4**). In a PCA plot, *F. graminearum* isolates distributed in a larger area, whereas most *F. asiaticum* strains were quite close to each other indicating low level of variation. The two species are clearly separated by the PCA analysis (**Figure 7**). Applying the Mantel test revealed that the geographical and the genetic distances

between the populations did not have a linear relationship ($r = -0.028$, $P = 0.615$).

Phylogenetic Analysis

A maximum likelihood phylogenetic tree was constructed based on the non-intronic (exonic and intergenic regions) alignment of *F. asiaticum*, *F. graminearum* and *F. culmorum*, as outgroup (**Supplementary Figure S2**). The two species separate into two separate clades with high support.

DISCUSSION

Fusarium head blight is one of the most devastating diseases in wheat around the world. China has witnessed frequent outbreaks of this disease resulting in serious losses in recent decades, especially in Southern China where *F. asiaticum* was the predominant species on both wheat and barley (Yang et al., 2008, 2018). Our previous study demonstrated that pathogens on rice debris were the primary inoculum of FHB of wheat (Yang et al., 2018). In this study, a large *F. asiaticum* population isolated from wheat kernels or from rice stubble in different ecological regions was sequenced and the mitogenomes of 210 isolates were assembled individually. The size of mitogenomes of *F. asiaticum* was between 89,966 and 98,925 bp, which was similar to the mitogenome size of isolate PH-1 (95,638 bp) of the closely related species *F. graminearum* (Brankovics et al., 2018) and *F. culmorum* (103,844 bp) (Kulik et al., 2016). The sizes and genomic content of mitogenomes among the large number of *F. asiaticum* strains showed a high level of conservation.

In a previous study, we identified 723 variations in 24 *F. graminearum* mitogenomes (Brankovics et al., 2018). In contrast, a significantly lower number of variations (442) was found in a larger set of *F. asiaticum* isolates ($N = 210$) in this study. The genetic variation in the mitochondrial genome is the result of two types of events: (i) small sequence variations (SNPs and short indels) and (ii) intron gain or loss. In our previous study, length variation across *F. graminearum* mitogenomes was found to be largely due to variation of intronic regions (Brankovics et al., 2018). A similar result was observed among the 210 *F. asiaticum* mitogenomes analyzed in this study. In the current research, we found the majority of indels in intergenic regions were very short, whereas all large indels were due to complete or partial gain and loss of introns. The average length of indels in intronic regions was more than seven times longer than those in intergenic regions.

All SNPs detected in the 14 protein-encoding genes of *F. asiaticum* mitogenomes were synonymous. This

TABLE 2 | Matrix of Nei's Genetic Distance for intron regions of 210 *F. asiaticum* mitogenomes between populations from diverse geographical regions.

	MLRYR	Hunan	Fujian	Sichuan
MLRYR	0.000			
Hunan	0.001	0.000		
Fujian	0.004	0.001	0.000	
Sichuan	0.010	0.006	0.004	0.000

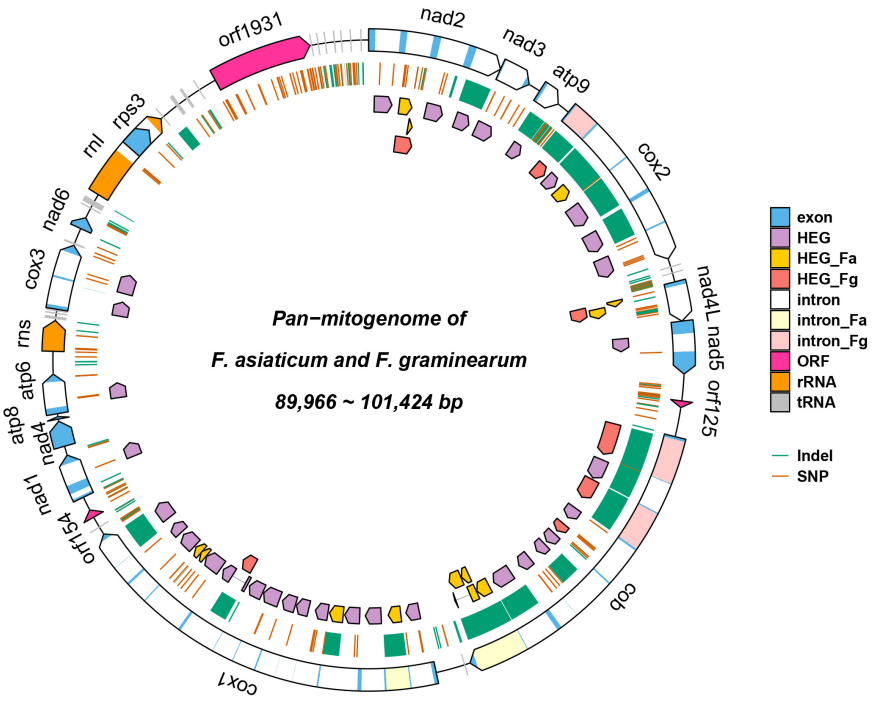

FIGURE 5 | Pan-mitogenome of 210 *F. asiaticum* and 24 *Fusarium graminearum* strains. HEG_Fa and HEG_Fg represent *F. asiaticum* and *F. graminearum* specific HEGs, respectively; intron_Fa and intron_Fg represent *F. asiaticum* and *F. graminearum* specific introns.

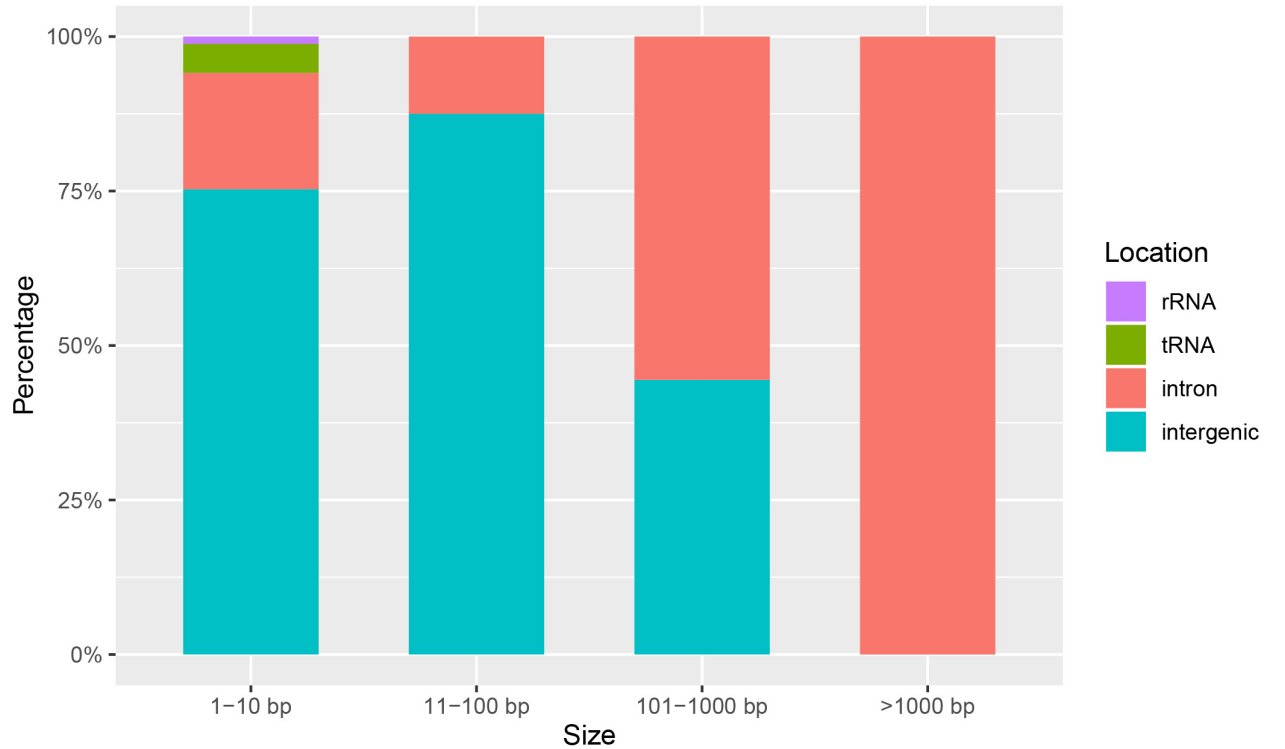

FIGURE 6 | Length distribution of indels in intergenetic, intron, rRNA, and tRNA between different length of intervals in the mitogenome of *F. asiaticum* and *F. graminearum*.

contrasts to the LV-uORF, a large open reading frame with unknown function that will be discussed in more detail below. High level of conservation was also detected in the analysis of the parsimony informative sites of the non-intronic sequences of *F. asiaticum*, only 13 haplotypes were identified and 74% isolates had the same haplotype. Heterologous recombination in the mitochondrial genome was demonstrated in the asexual species *F. oxysporum* (Brankovics et al., 2017) and also in the sexual reproducing homothallic species *F. graminearum* comparative analyses pinpointed toward recombination events (Brankovics et al., 2017, 2018). The population genomic approach used in the current study allowed a more detailed analyses of the existence of recombination events. The analysis of the non-intronic regions showed a closed network of six haplotypes (**Figure 4**) demonstrating the occurrence of mitochondrial recombination in *F. asiaticum*.

Several previous studies have reported *F. asiaticum* as the predominant species in the wheat producing areas along the Yangtze River (Zhang et al., 2007; Yang et al., 2018). In a previous study based on variable number of tandem repeats (VNTR) markers, we have shown a high level of genetic diversity and insufficient recombination in the *F. asiaticum* population from the Southwest of China (Sichuan province) which was suggested to be due to geographical barriers observed in this mountainous region and a recent migration of population inferred by unbiased gene flow. In contrast, in middle and lower reaches of Yangtze River Region the pathogen behaved as a random mating population with frequent outcrossing (Zhang et al., 2010, 2012).

Because variation in intronic regions was most prominent, variations in specific introns was used as molecular markers for further population analyses. In agreement with previous population studies performed by VNTR markers (Zhang et al., 2010, 2012), higher genetic diversity and limited genetic exchange were observed in Sichuan, whereas in the MLRYR region a high level of recombination was detected. Hence, we propose that also intron markers can be used for population analyses of *F. asiaticum*. Sichuan province is a mountainous region and the significant linkage disequilibrium there may be due to the geographic isolation of local populations. We did not find strong evidences of a newly introduced population in this study, but the contribution of a recent migration to the high association index should also be considered in respect to previously published data (Zhang et al., 2012). In this study, the Mantel test revealed that no clear geographical patterning of *F. asiaticum* was observed in population differentiation (P = 0.615), which is in contrast to our previous study (Zhang et al., 2010). Nevertheless, there are major different factors in two studies, such as different markers, hosts, selection pressure and cropping system, might causing inconsistent consequence.

Two non-wheat growing regions were included in this analysis, this is of interest as we previously reported that the cropping system has a dominant effect on the population structure (Yang et al., 2018), we included two non-wheat growing regions, Fujian and Hunan. Similar as Sichuan, Fujian is also a mountainous region, where higher genetic diversity was observed than the plain region, MLRYR, and the transition region, Hunan. Although a high level of diversity was identified in both Sichuan and Fujian, the type of diversity found was rather distinct. The frequency of specific alleles in both populations varied substantially and recurrent recombination may increase the genetic diversity on a population level even further. Our results revealed that the highest frequency of private alleles contributed most for the high diversity in Sichuan, while the Fujian population showed the lowest value of private alleles, whereas the lowest association index (in Fujian) revealed that diversity was mainly due to more frequent genetic exchange. In addition, linkage equilibrium was also observed in Hunan and MLRYR indicating frequent recombination in the plain and transition regions. Notably, among the three populations with linkage equilibrium, the genetic diversity of rice growing areas in Hunan and Fujian were higher than wheat-rice rotation areas in MLRYR. Wheat has a strong selective effect on different *Fusarium* pathogens in FGSC (Zhang et al., 2016a), and we hypothesize that wheat growing may result in a decrease of the genetic diversity. In contrast, in Hunan and Fujian, *F. asiaticum* can grow saprophytically on rice debris and lack of selective pressure by the host may preserve the high diversity (Yang et al., 2018).

It has been reported that mitochondrial introns can spread through horizontal transfer during sexual and clonal reproduction (Brankovics et al., 2018). The presence/absence frequency of introns could be used to evaluate the spread of these introns. We identified seven introns which showed presence/absence pattern in *F. asiaticum* population. Three of them were at very low frequency, which indicated they have not (yet) dispersed in the population. The absence frequency of the

TABLE 3 | The distribution of the length of indels in intergenetic, intron, rRNA and tRNA between different length of intervals in the mitogenome of *F. asiaticum* and *F. graminearum*.

Location	1–10 bp	11–100 bp	101–1000 bp	>1000 bp	Total
Intergenic	64	14	4	0	82
Intron	16	2	5	14	37
rRNA	1	0	0	0	1
tRNA	4	0	0	0	4
Total	85	16	9	14	124

TABLE 4 | Genotypic diversity of *F. asiaticum* and *F. graminearum* mitogenomes basing intron regions.

Population	N[a]	MLG[b]	eMLG[c]	h[d]	lambda[e]	Hexp[f]
F. asiaticum	210	41	12.6	0.051	0.901	0.0511
F. graminearum	24	15	15	0.098	0.913	0.1022

[a]*N = the number of samples from each region;* [b]*MLG = number of identified multilocus genotype;* [c]*eMLG = expected number of MLG at the lowest common sample size;* [d]*h = Haploid genetic diversity;* [e]*lambda = Simpson's index;* [f]*Hexp = Nei's gene diversity index.*

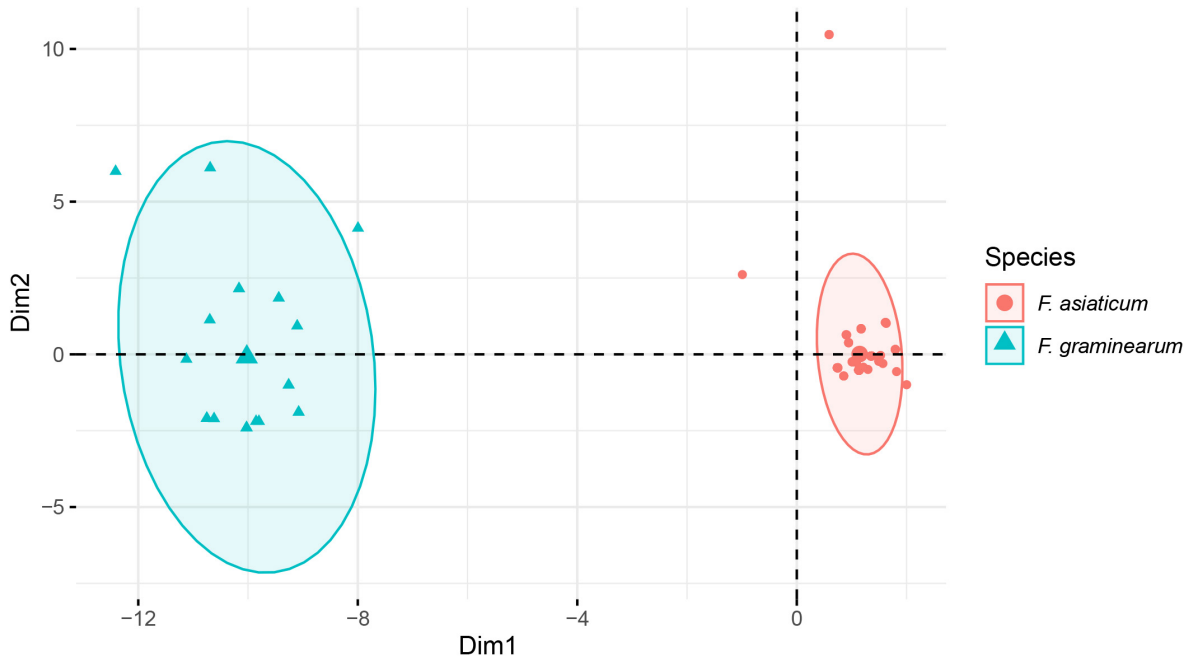

FIGURE 7 | Principal component analysis of intron regions of *F. asiaticum* and *F. graminearum* mitogenomes.

other four introns in each ecological region showed significant relation with population genetic structure. Limited genetic exchange in the Sichuan population may restrict the spread of introns, which resulted in a higher absence frequency of three introns (cox1-i287, cox1-i1287, and cox2-i318) in this region. In the other three regions random mating may have promoted the spread of each of these introns. The specific alleles in the Sichuan population also reflect the low recombination with other regions.

Comparative mitogenomic analyses between *F. asiaticum* and *F. graminearum* revealed more variations than intraspecies of *F. asiaticum*. The LV-uORF is a high variable region in some *Fusarium* species. However, the variations in LV-uORF between *F. asiaticum* and *F. graminearum* were relatively small. Nevertheless, significant more SNPs were found in the LV-uORF region of interspecies than intraspecies comparisons and 20 of 32 SNPs caused non-synonymous substitutions, while no nonsense mutations were obserced. This fuels the debate whether or not the ORF is actually coding for a protein or not. Based on the relatively high number of non-synonymous substitutions it at least seems under a different selection pressure compared to other mitochondrial genes.

As expected, the main variations observed among the *F. asiaticum* mitogenomes were in intronic regions and size differences are primarily related to the presence/absence of introns. All population genetic parameters (eMLG, haploid genetic diversity, Simpson's index as well as Nei's gene diversity index) revealed a higher level of diversity in *F. graminearum* compared to *F. asiaticum*. Therefore, we can conclude that the mitogenome of *F. asiaticum* was more conserved than *F. graminearum*. This is also in agreement with the global distribution of the two species. *F. graminearum* is widely distributed all over the world with high genetic diversity. In contrast, *F. asiaticum* seems to be a regional species mainly encountered in East Asia and some confined regions elsewhere, where it coincides with rice production (Suga et al., 2008; Lee et al., 2009; Gale et al., 2011; Zhang et al., 2012; Del Ponte et al., 2015). The smaller geographic distribution and similar environment conditions may lead to a stricter and directional selection, leading to a reduced diversity in the population. However, time and space as well as the scale of sampling can also influence this conclusion. The 24 *F. graminearum* isolates studied by Brankovics et al. (2018) were sampled across ∼100 years, from multiple hosts and originated from all six continents, while all the 210 *F. asiaticum* isolates from the present study originated from Southern China within 4 years. Therefore, additional *F. asiaticum* strains from locations outside China as well as historical collections should be involved in the future to further confirm the conservation of mitogenome of this species. Hybrids between *F. graminearum* and *F. asiaticum* can be generated by *in vitro* crosses (Jurgenson et al., 2002). However, the frequency of occurrence of several species-specific introns as well as PCA analyses revealed a clear species boundary between *F. graminearum* and *F. asiaticum* on a large evolutionary time scale. Moreover, comprehensive surveys were performed in New Zealand (Monds et al., 2005), Japan (Suga et al., 2008), and China (Zhang et al., 2012) but the only natural hybrid encountered so far in the *F. graminearum* species complex was between *F. meridionale* and *F. asiaticum* reported from Nepal (O'Donnell et al., 2000). Our detailed studies on the mitogenome also provide no indication of gene flow between these closely related species.

CONCLUSION

Based on the mitochondrial genomic analysis of a large population, we constructed a pan-mitogenome of *F. asiaticum*, which is highly conserved within the species. The length variation was mainly due to presence/absence of intron which harbored homing endonuclease genes. Intron patterns can be used as genetic markers for monitoring population dynamics. Recombination in mitogenomes was identified in *F. asiaticum* as was previously reported for the asexual species *F. oxysporum* and the homothallic species *F. graminearum*. Different levels of genetic diversity and recombination were observed in different ecological regions, which coincided with geographic characteristics and cropping conditions. The interspecies analysis revealed a higher diversity of the global species *F. graminearum* than *F. asiaticum* and clear interspecies differences. The results of this research extend our knowledge on the variability and recombination of mitochondrial genome of *F. asiaticum* and improve our understanding of the evolution and dispersal of this species. It also demonstrates the power of population genomics and the application to track and trace migration using the mitogenome.

DATA AVAILABILITY STATEMENT

The datasets generated for this study can be found in the GenBank, the accession numbers are listed in **Supplementary Table S1**.

AUTHOR CONTRIBUTIONS

HZ, WC and JF conceived and designed the experiments. MY performed the experiments. MY, HZ, and BB analyzed the data. MY, HZ, BB, TL, CW, and AD wrote the manuscript.

FUNDING

This work was supported by the National Key R&D Program of China (2018YFD0200500 and 2017YFE0126700) and the European Union's Horizon 2020 Research and Innovation Programme under Grant Agreement No. 678781 (MycoKey).

SUPPLEMENTARY MATERIAL

The Supplementary Material for this article can be found online at: https://www.frontiersin.org/articles/10.3389/fmicb.2020.00839/full#supplementary-material

FIGURE S1 | Minimum spanning network inferred from non-intronic regions from 210 *F. asiaticum* isolates. Each black line on lineage indicates one SNP. The number of each haplotype is reflected by area of each circle.

FIGURE S2 | A maximum likelihood phylogenetic tree constructed based on the non-intronic (exonic and intergenic regions) alignment of 210 *F. asiaticum*, 24 *F. graminearum,* and one *F. culmorum*.

TABLE S1 | Strains information in this study.

TABLE S2 | Positions and types of non-synonymous substitutions occurred in the LV-uORF caused by SNPs.

TABLE S3 | Intron locations and lengths within standard mitochondrial genes of *Fusarium asiaticum* and *F. graminearum* strains.

REFERENCES

Al-Reedy, R. M., Malireddy, R., Dillman, C. B., and Kennell, J. C. (2012). Comparative analysis of *Fusarium* mitochondrial genomes reveals a highly variable region that encodes an exceptionally large open reading frame. *Fungal Genet. Biol.* 49, 2–14. doi: 10.1016/j.fgb.2011.11.008

Avise, J. C., Shapira, J. F., Daniel, S. W., Aquadro, C. F., and Lansman, R. A. (1983). Mitochondrial DNA differentiation during the speciation process in *Peromyscus*. *Mol. Biol. Evol.* 1, 38–56. doi: 10.1093/oxfordjournals.molbev.a040301

Bankevich, A., Nurk, S., Antipov, D., Gurevich, A. A., Dvorkin, M., Kulikov, A. S., et al. (2012). SPAdes: a new genome assembly algorithm and its applications to single-cell sequencing. *J. Comput. Biol.* 19, 455–477. doi: 10.1089/cmb.2012.0021

Basse, C. W. (2010). Mitochondrial inheritance in fungi. *Curr. Opin. Microbiol.* 13, 712–719. doi: 10.1016/j.mib.2010.09.003

Brankovics, B., Kulik, T., Sawicki, J., Bilska, K., Zhang, H., de Hoog, G. S., et al. (2018). First steps towards mitochondrial pan-genomics: detailed analysis of *Fusarium graminearum* mitogenomes. *PeerJ* 6:e5963. doi: 10.7717/peerj.5963

Brankovics, B., van Dam, P., Rep, M., de Hoog, G. S., van der Lee, T. A. J., Waalwijk, C., et al. (2017). Mitochondrial genomes reveal recombination in the presumed asexual *Fusarium oxysporum* species complex. *BMC Genomics* 18:735. doi: 10.1186/s12864-017-4116-4115

Brankovics, B., Zhang, H., van Diepeningen, A. D., van der Lee, T. A., Waalwijk, C., and de Hoog, G. S. (2016). GRAbB: selective assembly of genomic regions, a new niche for genomic research. *PLoS Comput. Biol.* 12:e1004753. doi: 10.1371/journal.pcbi.1004753

Del Ponte, E. M., Spolti, P., Ward, T. J., Gomes, L. B., Nicolli, C. P., Kuhnem, P. R., et al. (2015). Regional and field-specific factors affect the composition of *fusarium* head blight pathogens in subtropical no-till wheat agroecosystem of Brazil. *Phytopathology* 105, 246–254. doi: 10.1094/PHYTO-04-14-0102-R

D'Mello, J. P. F., Placinta, C. M., and Macdonald, A. M. C. (1999). *Fusarium mycotoxins*: a review of global implications for animal health, welfare and productivity. *Anim. Feed Sci. Technol.* 80, 183–205. doi: 10.1016/s0377-8401(99)00059-50

Edgar, R. C. (2004). MUSCLE: multiple sequence alignment with high accuracy and high throughput. *Nucleic Acids Res.* 32, 1792–1797. doi: 10.1093/nar/gkh340

Gale, L. R., Harrison, S. A., Ward, T. J., O'Donnell, K., Milus, E. A., Gale, S. W., et al. (2011). Nivalenol-type populations of *Fusarium graminearum* and *F. asiaticum* are prevalent on wheat in southern Louisiana. *Phytopathology* 101, 124–134. doi: 10.1094/phyto-03-10-0067

Gale, L. R., Ward, T. J., Balmas, V., and Kistler, H. C. (2007). Population subdivision of *Fusarium graminearum* sensu stricto in the upper midwestern United States. *Phytopathology* 97, 1434–1439. doi: 10.1094/PHYTO-97-11-1434

Gillett, C. P., Crampton-Platt, A., Timmermans, M. J., Jordal, B. H., Emerson, B. C., and Vogler, A. P. (2014). Bulk de novo mitogenome assembly from pooled total DNA elucidates the phylogeny of weevils (Coleoptera: Curculionoidea). *Mol. Biol. Evol.* 31, 2223–2237. doi: 10.1093/molbev/msu154

Goswami, R. S., and Kistler, H. C. (2004). Heading for disaster: *Fusarium graminearum* on cereal crops. *Mol. Plant Pathol.* 5, 515–525. doi: 10.1111/j.1364-3703.2004.00252.X

Haugen, P., Simon, D. M., and Bhattacharya, D. (2005). The natural history of group I introns. *Trends Genet.* 21, 111–119. doi: 10.1016/j.tig.2004.12.007

Jurgenson, J. E., Bowden, R. L., Zeller, K. A., Leslie, J. F., and Plattner, R. D. J. G. (2002). A genetic map of *Gibberella zeae* (*Fusarium graminearum*). *Genetics* 160, 1451–1460.

Kamvar, Z. N., Tabima, J. F., and Gruenwald, N. J. (2014). Poppr: an R package for genetic analysis of populations with clonal, partially clonal, and/or sexual reproduction. *PeerJ* 2:e281. doi: 10.7717/peerj.281

Kuhnem, P. R., Ward, T. J., Silva, C. N., Spolti, P., Ciliato, M. L., Tessmann, D. J., et al. (2016). Composition and toxigenic potential of the *Fusarium graminearum* species complex from maize ears, stalks and stubble in Brazil. *Plant Pathol.* 65, 1185–1191. doi: 10.1111/ppa.12497

Kulik, T., Brankovics, B., Sawicki, J., and van Diepeningen, A. (2016). The complete mitogenome of *Fusarium culmorum*. *Mitochondrial DNA Part A* 27, 2425–2426. doi: 10.3109/19401736.2015.1030626

Lee, J., Chang, I. Y., Kim, H., Yun, S. H., Leslie, J. F., and Lee, Y. W. (2009). Genetic diversity and fitness of *Fusarium graminearum* populations from rice in Korea. *Appl. Environ. Microbiol.* 75, 3289–3295. doi: 10.1128/AEM.02287-2288

Leigh, J. W., Bryant, D., and Nakagawa, S. (2015). popart: full-feature software for haplotype network construction. *Methods Ecol. Evol.* 6, 1110–1116. doi: 10.1111/2041-210x.12410

Li, Q., Chen, C., Xiong, C., Jin, X., Chen, Z., and Huang, W. (2018a). Comparative mitogenomics reveals large-scale gene rearrangements in the mitochondrial genome of two *Pleurotus* species. *Appl. Microbiol. Biotechnol.* 102, 6143–6153. doi: 10.1007/s00253-018-9082-9086

Li, Q., Wang, Q., Chen, C., Jin, X., Chen, Z., Xiong, C., et al. (2018b). Characterization and comparative mitogenomic analysis of six newly sequenced mitochondrial genomes from ectomycorrhizal fungi (*Russula*) and phylogenetic analysis of the *Agaricomycetes*. *Int. J. Biol. Macromol.* 119, 792–802. doi: 10.1016/j.ijbiomac.2018.07.197

Li, Q., Wang, Q., Jin, X., Chen, Z., Xiong, C., Li, P., et al. (2019). Characterization and comparative analysis of six complete mitochondrial genomes from ectomycorrhizal fungi of the *Lactarius* genus and phylogenetic analysis of the *Agaricomycetes*. *Int. J. Biol. Macromol.* 121, 249–260. doi: 10.1016/j.ijbiomac.2018.10.029

Mantel, N. (1967). The detection of disease clustering and a generalized regression approach. *Cancer Res.* 27, 209–220.

Marchler-Bauer, A., and Bryant, S. H. (2004). CD-Search: protein domain annotations on the fly. *Nucleic Acids Res.* 32, W327–W331. doi: 10.1093/nar/gkh454

Mitchell, A., Chang, H.-Y., Daugherty, L., Fraser, M., Hunter, S., Lopez, R., et al. (2015). The InterPro protein families database: the classification resource after 15 years. *Nucleic Acids Res.* 43, D213–D221. doi: 10.1093/nar/gku1243

Monds, R. D., Cromey, M. G., Lauren, D. R., di Menna, M., and Marshall, J. (2005). *Fusarium graminearum*, *F. cortaderiae* and *F. pseudograminearum* in New Zealand: molecular phylogenetic analysis, mycotoxin chemotypes and co-existence of species. *Mycol. Res.* 109(Pt 4), 410–420. doi: 10.1017/s0953756204002217

Nurk, S., Bankevich, A., Antipov, D., Gurevich, A. A., Korobeynikov, A., Lapidus, A., et al. (2013). Assembling single-cell genomes and mini-metagenomes from chimeric MDA products. *J. Comput. Biol.* 20, 714–737. doi: 10.1089/cmb.2013.0084

O'Donnell, K., Kistler, H. C., Tacke, B. K., and Casper, H. H. (2000). Gene genealogies reveal global phylogeographic structure and reproductive isolation among lineages of *Fusarium graminearum*, the fungus causing wheat scab. *Proc. Natl. Acad. Sci. U.S.A.* 97, 7905–7910. doi: 10.1073/pnas.130193297

Pantou, M. P., Kouvelis, V. N., and Typas, M. A. (2008). The complete mitochondrial genome of *Fusarium oxysporum*: insights into fungal mitochondrial evolution. *Gene* 419, 7–15. doi: 10.1016/j.gene.2008.04.009

Pavesi, A., Conterio, F., Bolchi, A., Dieci, G., and Ottonello, S. (1994). Identification of new eukaryotic tRNA genes in genomic DNA databases by a multistep weight matrix analysis of transcriptional control regions. *Nucleic Acids Res.* 22, 1247–1256. doi: 10.1093/nar/22.7.1247

Peakall, R., and Smouse, P. E. (2012). GenAlEx 6.5: genetic analysis in Excel. Population genetic software for teaching and research-an update. *Bioinformatics* 28, 2537–2539. doi: 10.1093/bioinformatics/bts460

Sarver, B. A. J., Ward, T. J., Gale, L. R., Broz, K., Corby Kistler, H., Aoki, T., et al. (2011). Novel *Fusarium* head blight pathogens from Nepal and Louisiana revealed by multilocus genealogical concordance. *Fungal Genet. Biol.* 48, 1096–1107. doi: 10.1016/j.fgb.2011.09.002

Schmale, D. G., and Bergstrom, G. C. (2003). *Fusarium Head Blight in Wheat [Online]. The Plant Health Instructor*. Available online at: https://www.apsnet.org/edcenter/disandpath/fungalasco/pdlessons/Pages/Fusarium.aspx

Suga, H., Karugia, G. W., Ward, T., Gale, L. R., Tomimura, K., Nakajima, T., et al. (2008). Molecular characterization of the *Fusarium graminearum* species complex in Japan. *Phytopathology* 98, 159–166. doi: 10.1094/phyto-98-2-0159

Talas, F., and McDonald, B. A. (2015). Significant variation in sensitivity to a DMI fungicide in field populations of *Fusarium graminearum*. *Plant Pathol.* 64, 664–670. doi: 10.1111/ppa.12280

van der Lee, T., Zhang, H., van Diepeningen, A., and Waalwijk, C. (2015). Biogeography of *Fusarium graminearum* species complex and chemotypes: a review. *Food Addit. Contam Part A Chem. Anal. Control Exp. Risk Assess.* 32, 453–460. doi: 10.1080/19440049.2014.984244

Waalwijk, C., Kastelein, P., de Vries, I., Kerenyi, Z., van der Lee, T., Hesselink, T., et al. (2003). Major changes in *Fusarium* spp. in wheat in the Netherlands. *Eur. J. Plant Pathol.* 109, 743–754. doi: 10.1023/a:1026086510156

Wang, Q., Jiang, C., Wang, C., Chen, C., Xu, J.-R., and Liu, H. (2017). Characterization of the two-speed subgenomes of *Fusarium graminearum* reveals the fast-speed subgenome specialized for adaption and infection. *Front. Plant Sci.* 8:140. doi: 10.3389/fpls.2017.00140

Ward, T. J., Clear, R. M., Rooney, A. P., O'Donnell, K., Gaba, D., Patrick, S., et al. (2008). An adaptive evolutionary shift in *Fusarium* head blight pathogen populations is driving the rapid spread of more toxigenic *Fusarium graminearum* in North America. *Fungal Genet. Biol.* 45, 473–484. doi: 10.1016/j.fgb.2007.10.003

Yang, L., van der Lee, T., Yang, X., Yu, D., and Waalwijk, C. (2008). *Fusarium* populations on chinese barley show a dramatic gradient in mycotoxin profiles. *Phytopathology* 98, 719–727. doi: 10.1094/phyto-98-6-0719

Yang, M., Zhang, H., Kong, X., van der Lee, T., Waalwijk, C., van Diepeningen, A., et al. (2018). Host and cropping system shape the *Fusarium* population: 3ADON-producers are ubiquitous in wheat whereas NIV-producers are more prevalent in rice. *Toxins* 10:115. doi: 10.3390/toxins10030115

Yuen, J., and Mila, A. (2015). Landscape-scale disease risk quantification and prediction. *Annu. Rev. Phytopathol.* 53, 471–484. doi: 10.1146/annurev-phyto-080614-120406

Zeng, F., An, H., and Tang, T. (2011). Diversity of crops in China. *Hubei Agricult. Sci.* 50, 2377–2380. doi: 10.3969/j.issn.0439-8114.2011.12.001

Zhang, H., Brankovics, B., Luo, W., Xu, J., Xu, J. S., Guo, C., et al. (2016a). Crops are a main driver for species diversity and the toxigenic potential of *Fusarium* isolates in maize ears in China. *World Mycotoxin J.* 9, 701–715. doi: 10.3920/wmj2015.2004

Zhang, H., Brankovics, B., van der Lee, T. A., Waalwijk, C., van Diepeningen, A. A., Xu, J., et al. (2016b). A single-nucleotide-polymorphism-based genotyping assay for simultaneous detection of different carbendazim-resistant genotypes in the *Fusarium graminearum* species complex. *PeerJ* 4:e2609. doi: 10.7717/peerj.2609

Zhang, H., Van der Lee, T., Waalwijk, C., Chen, W., Xu, J., Xu, J., et al. (2012). Population analysis of the *Fusariumgraminearum* species complex from wheat in china show a shift to more aggressive isolates. *PLoS One* 7:e31722. doi: 10.1371/journal.pone.0031722

Zhang, H., Zhang, Z., van der Lee, T., Chen, W. Q., Xu, J., Xu, J. S., et al. (2010). Population genetic analyses of *Fusarium asiaticum* populations from barley suggest a recent shift favoring 3ADON producers in Southern China. *Phytopathology* 100, 328–336. doi: 10.1094/phyto-100-4-0328

Zhang, J.-B., Li, H.-P., Dang, F.-J., Qu, B., Xu, Y.-B., Zhao, C.-S., et al. (2007). Determination of the trichothecene mycotoxin chemotypes and associated geographical distribution and phylogenetic species of the *Fusarium graminearum* clade from China. *Mycol. Res.* 111, 967–975. doi: 10.1016/j.mycres.2007.06.008

Conflict of Interest: The authors declare that the research was conducted in the absence of any commercial or financial relationships that could be construed as a potential conflict of interest.

frontiers in Microbiology

ORIGINAL RESEARCH
published: 08 May 2020
doi: 10.3389/fmicb.2020.00863

The Mitochondrial Genome of the Phytopathogenic Fungus *Bipolaris sorokiniana* and the Utility of Mitochondrial Genome to Infer Phylogeny of Dothideomycetes

Nan Song, Yuehua Geng* and Xinghao Li*

College of Plant Protection, Henan Agricultural University, Zhengzhou, China

OPEN ACCESS

Edited by:
Tomasz Kulik, University of Warmia and Mazury in Olsztyn, Poland

Reviewed by:
Johannes Wöstemeyer, Friedrich Schiller University Jena, Germany
Yongjie Zhang, Shanxi University, China
Bruno Andrade, Universidade Estadual do Sudoeste da Bahia, Brazil

***Correspondence:**
Nan Song
songnan@henau.edu.cn
Yuehua Geng
gyh@henau.edu.cn

Specialty section:
This article was submitted to Fungi and Their Interactions, a section of the journal Frontiers in Microbiology

Received: *27 January 2020*
Accepted: *09 April 2020*
Published: *08 May 2020*

Citation:
Song N, Geng Y and Li X (2020) The Mitochondrial Genome of the Phytopathogenic Fungus Bipolaris sorokiniana and the Utility of Mitochondrial Genome to Infer Phylogeny of Dothideomycetes. Front. Microbiol. 11:863. doi: 10.3389/fmicb.2020.00863

A number of species in *Bipolaris* are important plant pathogens. Due to a limited number of synapomorphic characters, it is difficult to perform species identification and to estimate phylogeny of *Bipolaris* based solely on morphology. In this study, we sequenced the complete mitochondrial genome of *Bipolaris sorokiniana*, and presented the detailed annotation of the genome. The *B. sorokiniana* mitochondrial genome is 137,775 bp long, and contains two ribosomal RNA genes, 12 core protein-coding genes, 38 tRNA genes. In addition, two ribosomal protein genes (*rps3* gene and *rps5* gene) and the fungal mitochondrial RNase P gene (*rnpB*) are identified. The large genome size is mostly determined by the presence of numerous intronic and intergenic regions. A total of 28 introns are inserted in eight core protein-coding genes. Together with the published mitochondrial genome sequences, we conducted a preliminary phylogenetic inference of Dothideomycetes under various datasets and substitution models. The monophyly of *Capnodiales*, *Botryosphaeriales* and *Pleosporales* are consistently supported in all analyses. The *Venturiaceae* forms an independent lineage, with a distant phylogenetic relationship to *Pleosporales*. At the family level, the *Mycosphaerellaceae*, *Botryosphaeriaceae*. *Phaeosphaeriaceae*, and *Pleosporaceae* are recognized in the majority of trees.

Keywords: fungi, Ascomycota, *Pleosporales*, next-generation sequencing, mitogenome, phylogenetic

INTRODUCTION

The genus *Bipolaris* belongs to the family *Pleosporaceae* (Ascomycota, Dothideomycetes, *Pleosporales*). Shoemaker (1959) originally established the generic *Bipolaris*. The species of *Bipolaris* were once classified in *Helminthosporium* (Link, 1824). Subramanian (1971) provided a key to separate the species of *Bipolaris* from members of the *Helminthosporium*. Further study divided the *Helminthosporium* into several genera including *Bipolaris*, *Curvularia*, *Drechslera*, and *Exserohilum* (Sivanesan, 1987). Modern descriptions and illustrations for the species in the genus *Bipolaris* were given in the studies of Manamgoda et al. (2012, 2014). Many morphological similarities are shared by *Bipolaris* and *Curvularia*, both of which have sexual morphs in the genus *Cochliobolus* (Alcorn, 1983; Manamgoda et al., 2014). The genera *Cochliobolus*, *Bipolaris* and *Curvularia* form

a complex, and the taxonomy of this complex are uncertain with the morphological characters (Manamgoda et al., 2012). A combined analysis of ITS, GPDH, EF1-α and LSU gene sequences resulted in two main groups corresponding to the complex (Manamgoda et al., 2012). One clade included the majority of *Bipolaris* and *Cochliobolus*, and another contained the *Curvularia* and the partial members of *Bipolaris* and *Cochliobolus* (Manamgoda et al., 2012). Manamgoda et al. (2014) recovered *Bipolaris* as a sister group to *Curvularia* based on a combined analysis of ITS, GPDH and EF1-α gene sequences.

Bipolaris sorokiniana (Sacc.) Shoemaker [teleomorph: *Cochliobolus sativus* (Ito and Kuribayashi) Drechs. ex Dastur] is a seed and soil borne pathogen, which causes spot blotch, root rot, leaf spot, seedling blight, head blight, and black point disease in cereal crops (Wiese, 1998; Kumar et al., 2002). Among these diseases, the leaf spot blotch is recognized as the major biotic stress hampering commercial production of wheat, because it results in significant yield losses (Chowdhury et al., 2013; Mina et al., 2016). The type strain was isolated from Russia with number of MBT197973 in 1890, which was originally named as *Helminthosporium sorokinianum*. Several synonyms of *B. sorokiniana* were used as following: *H. sorokinianum*, *H. sativum*, *Drechslera sorokiniana* (Maraite et al., 1998). The detailed description of *B. sorokiniana* can be seen from Commonwealth Mycological Institute's Sivanesan and Holliday (1981). In addition to *B. sorokiniana*, the genus *Bipolaris* contains many other important plant pathogens with worldwide distribution. The distinction of species in *Bipolaris* and the classification of *Bipolaris* with other fungus species appear difficult when only morphological characters are considered. Because some species have overlapping morphological features. Molecular phylogenetic studies based on gene sequences have shown promise in resolving the fungi classification problems (Swann and Taylor, 1995; Berbee et al., 1999; Fitzpatrick et al., 2006; James et al., 2006a,b; Robbertse et al., 2006; Mangold et al., 2008; Wang et al., 2009; Manamgoda et al., 2012, 2014). Ohm et al. (2012) determined 14 dothideomycete whole-genomes, including that from the sexual morph of *B. sorokiniana* (i.e., *Cochliobolus sativus*). Condon et al. (2013) reported three additional whole-genome sequences of *Bipolaris*, namely the *B. victoriae* (as *C. victoriae*), *B. zeicola* (as *C. carbonum*), and *B. maydis* (as *C. heterostrophus*).

Mitochondrial (mt) DNA has been widely used in evolutionary biology and systematics of Fungi (Paquin et al., 1997; Hausner, 2003; Kouvelis et al., 2004; Formighieri et al., 2008; Pantou et al., 2008; Sethuraman et al., 2009; Duo et al., 2012; Aguileta et al., 2014; Lin et al., 2015; Utomo et al., 2019). As a class of molecular markers, mtDNA sequences have some preferable characteristics in resolving systematic issues, such as faster rate of evolution, the virtual absence of recombination, and conserved gene content (Simon et al., 1994, 2006; Caterino et al., 2000; Lin and Danforth, 2004). Recently, development of high-throughput sequencing technologies and related bioinformatics tools have allowed considerably greater numbers of nucleotides to be characterized and the genome-scale data to be more easily assembled. As a case in point, next-generation sequencing (NGS) technologies have been successfully used to reconstruct the fungal mitochondrial genomes (Losada et al., 2014; Mardanov et al., 2014; Salavirta et al., 2014; Torriani et al., 2014; Lin et al., 2015; Kanzi et al., 2016; Nowrousian, 2016; Kang et al., 2017; Deng et al., 2018). Compared to the whole-genome data, mitochondrial genomes are more readily sequenced with broader taxon sampling and a reasonable cost. The fungal mitochondrial genome size varied greatly between species. For example, the mitochondrial genome of *Hanseniaspora uvarum* has a length of 18,844 bp (Pramateftaki et al., 2006), while the *Sclerotinia borealis* has a length of 203,051 bp (Mardanov et al., 2014). Large variation of mitochondrial genome size in fungi is mainly attributed to different lengths of intronic sequences and intergenic regions (Belcour et al., 1997; Hausner, 2003; Formighieri et al., 2008). Despite with the continuously increasing number of fungal mitochondrial genome studies (Paquin et al., 1997; Hausner, 2003; Formighieri et al., 2008; Pantou et al., 2008; Duo et al., 2012; Torriani et al., 2014; Kang et al., 2017; Zaccaron and Bluhm, 2017; Deng et al., 2018; Utomo et al., 2019), the complete mtDNA sequences available for some important lineages are still limited. There are only 16 complete mitochondrial genomes published from the class Dothideomycetes in GenBank as of December 2019. The *Bipolaris cookei* was the first species having complete mtDNA sequence (Zaccaron and Bluhm, 2017) in the genus *Bipolaris*. It provided a reference for further investigation of the *Bipolaris* mitochondrial genomes.

In the present study, we use an NGS based approach to determine a complete mitochondrial genome of *B. sorokiniana*. The description of the mitochondrial genome organization is presented. One of our primary objectives is to explore the utility of mtDNA sequence data in inferring phylogeny of Dothideomycetes.

MATERIALS AND METHODS

Fungal Isolate

The strains of *B. sorokiniana* were obtained from wheat root and leaves in Luyi County (38.48°N, 115.08°E), Henan province, China, with the single spore isolation (Matusinsky et al., 2010). The living strains were harvested in 10% aqueous glycerol in a 2 ml-Eppendorf tube, and then were stored at −80°C. The fungus was cultured on PDA culture medium at 25°C, with ampicillin resistant to bacterial growth. Species identification was based on morphological features and confirmed using ITS sequence. The dried cultures and living cultures of specimen have been deposited in the Herbarium of Henan Agricultural University: Fungi (HHAUF).

DNA Extraction and Genome Sequencing

Total genomic DNA was extracted by using the Cetyl Trimethyl Ammonium Bromide (CTAB) method (Rogers and Bendich, 1985), with minor modification. DNA concentration (avg. 14.20 ng/μL) was determined using a Qubit Flurometer (Invitrogen, United States) and a NanoDrop Spectrophotometer (Thermo Scientific, United States).

Genomic DNA were sent to Shanghai Personal Biotechnology Co., Ltd. for library preparation and high-throughput

sequencing. Library was constructed by using the Illumina TruSeqTM DNA Sample Prep Kit (Illumina, San Diego, CA, United States), with the insert size of 400 bp. The genome sequencing was conducted on an Illumina NovaSeq 6000 platform, with a strategy of 150 paired-end sequencing.

Genome Assembly and Annotation

Raw data set was filtered through AdapterRemoval (Lindgreen, 2012) and SOAPec_v2.01 (Luo et al., 2012). The high-quality reads (Q20 = 97.71%, and Q30 = 93.43%) were used to assemble the mitochondrial contig, with the software MITObim v1.9 (Hahn et al., 2013). The mitochondrial genome of *B. cookei* (Zaccaron and Bluhm, 2017) was used as the reference genome. We also used IDBA-tran v. 1.1.1 (Peng et al., 2013) to conduct *de novo* assembly of *B. sorokiniana*, with the following parameters: the minimum size of contig of 200, an initial k-mer size of 41, an iteration size of 10, and a maximum k-mer size of 91. The assembled result produced by IDBA-tran were used to build a Blast database, using the program makeblastdb implemented in the BLAST package v 2.9.0+ (Camacho et al., 2009). The mitochondrial gene sequences of *B. cookei* were used as queries in Blastn searches against the database. BLAST hit contigs were retrieved through the program blastdbcmd in BLAST package v 2.9.0+ (Camacho et al., 2009).

To check the quality of assembly, we used BWA v. 0.7.5 (Li and Durbin, 2009) to align the sequenced reads to the mtDNA sequence assembled. SAMtools v. 0.1.19 (Li et al., 2009) was used to convert SAM output to a sorted BAM file. Qualimap v. 2.2.1 (Okonechnikov et al., 2016) was applied to calculate correctly mapped reads to the mitochondrial genome.

The mitochondrial genome annotation was conducted in MITOS web (Bernt et al., 2013). The following settings were implemented: Reference, "RefSeq 63 Fungi"; Genetic Code, "4 Mold." We also used the automated organelle genome annotation tool MFannot (Valach et al., 2014) to perform annotation of the mitochondrial genome of *B. sorokiniana*, under the genetic code of "4 Mold, Protozoan, and Coelenterate Mitochondrial; Mycoplasma/Spiroplasma." The gene boundaries were further refined by sequence alignment to the *B. cookei* mitochondrial genome (Zaccaron and Bluhm, 2017). The secondary structures of tRNA genes were predicted by MITOS (Bernt et al., 2013), and redrawn in Adobe Illustrator CS6. The genome structure image (**Figure 1**) was generated using OGDRAW (Greiner et al., 2019). The newly determined mitochondrial genome sequence of *B. sorokiniana* has been submitted to GenBank under the accession number MN978926. Besides the *B. sorokiniana* mitochondrial genome sequenced in this study, all other 19 complete mtDNA sequences (sixteen representing the Dothideomycetes and three representing the Sordariomycetes, see details in **Table 1**) downloaded from GenBank were re-annotated in MITOS web (Bernt et al., 2013) following the settings described above for uniform annotations.

Composition of Mitochondrial Genome

The nucleotide composition of the mtDNA sequence of *B. sorokiniana* and other 16 dothideomycete fungi downloaded from GenBank were computed with MEGA 7 (Kumar et al., 2016). The AT and GC skews were calculated according to the formula AT skew = (A - T)/(A + T) and GC skew = (G - C)/(G + C) (Perna and Kocher, 1995), in order to measure the strand-specific bias of nucleotide composition. Moreover, codon usage in the core mitochondrial protein-encoding genes were analyzed in MEGA 7 (Kumar et al., 2016).

Sequence Alignments

Prior to aligning each mitochondrial gene, we merged the FASTA files generated by MITOS for all species into a single file. Using the custom Perl script (selectSeqs.pl, commands used are provided in **Supplementary File S1**), the annotated genes collected from each species were extracted to compile the matrices. For the core protein-coding gene matrix, we firstly used TranslatorX (Abascal et al., 2010) to construct a preliminary multiple sequence alignment. The following parameters were set: Genetic code = "Mold mitochondrial," and Protein alignment = "MAFFT." Because many protein-coding genes were split into fragments by introns, the initial alignment contained many long gap sequences. In order to remove these gap sequences, we divided an alignment into several shorter ones based on the sequence homology checked by eye. After removal of long gap sequences, the alignments were concatenated into a single matrix, with the Perl script FASconCAT_v1.0 (Kuck and Meusemann, 2010). Ambiguous positions in the genes' alignment were trimmed with Gblocks (Talavera and Castresana, 2007), under less stringent options. Stop codons in each alignment were checked in MEGA 7 (Kumar et al., 2016) and deleted. Individual gene alignments were concatenated into an alignment comprising all 13 core protein-coding genes but *atp8*. Because this gene is missing in nine out of 20 fungal mitochondrial genomes analyzed. The mitochondrial rRNA and tRNA genes were individually aligned using MAFFT online server with E-INS-i strategy (Katoh and Standley, 2013). For the tRNA gene with more than one copy, only the one most similar to other species was used in the sequence alignment. Poorly aligned sections were eliminated by Gblocks (Talavera and Castresana, 2007). The individual alignments were concatenated to create the data matrices of rRNA gene (rrn) and tRNA gene (trn), respectively.

Characteristics of Sequence Alignments

Sequence potential saturation was assessed in DAMBE software (Xia, 2013). Sequence divergence heterogeneity was evaluated using AliGROOVE (Kuck et al., 2014), with the default sliding window size. Indels in nucleotide data set were treated as ambiguity and a BLOSUM62 matrix was used as default amino acid substitution matrix. The number of synonymous substitutions per synonymous site (*Ks*) and the number of non-synonymous substitutions per non-synonymous site (*Ka*) for protein-coding genes were estimated with DnaSP v5 (Librado and Rozas, 2009), under the genetic code of mtDNA Mold-Protozoan. Congruence between different gene type alignments (protein-coding genes, rRNA genes, and tRNA genes) was assessed by using the Incongruence Length Difference (ILD) tests (Farris et al., 1994) implemented in PAUP*4.0b10 (Swofford,

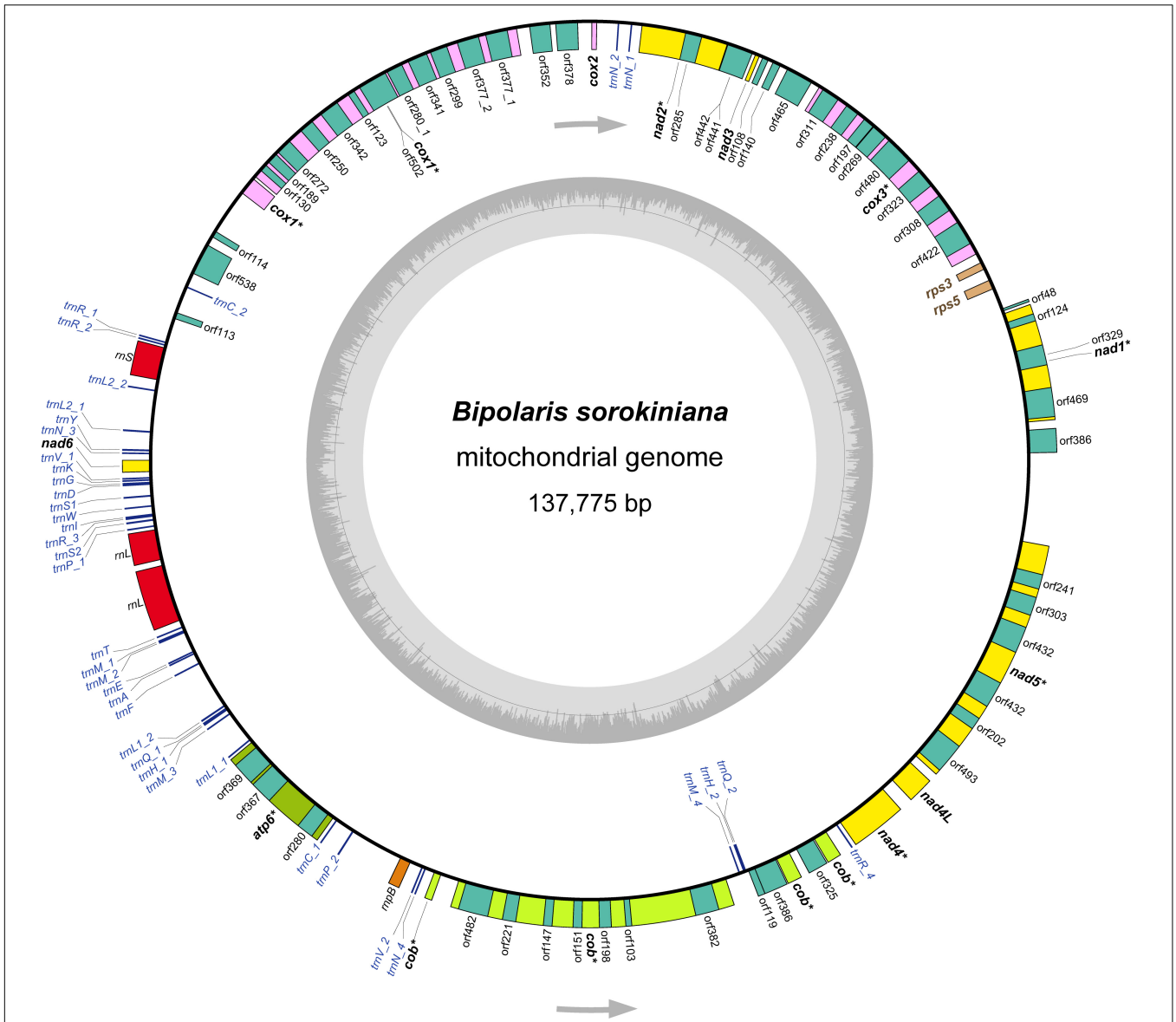

FIGURE 1 | The structure of the mitochondrial genome of *Bipolaris sorokiniana*. Arrows indicate the direction of gene transcription. The inner circles show the GC content. All genes identified are indicated in italics. The core 12 protein-coding genes are highlighted in bold. Of which, eight protein-coding genes including introns are denoted by asterisk. The detailed annotation of the mitochondrial genome of *B. sorokiniana* are shown in **Supplementary Table S2**.

2002), under the parsimony optimality criterion and using 1,000 additional replicates.

Phylogenetic Reconstructions

In the phylogenetic analyses, our taxon sample included 17 fungus species representing eight families of Dothideomycetes, namely *Venturiaceae*, *Mycosphaerellaceae*, *Botryosphaeriaceae*, *Astrosphaeriellaceae*, *Didymellaceae*, *Phaeosphaeriaceae*, *Coniothyriaceae*, and *Pleosporaceae* (**Table 1**). In addition, three mitochondrial genome sequences from the class Sordariomycetes were selected as outgroups (Fourie et al., 2013; Kulik et al., 2016).

A total of five concatenated datasets were compiled as following: (1) PCG_nt (10,561 nucleotide sites), nucleotide alignment including 12 protein-coding genes; (2) PCG_aa (3,364 amino acid sites), amino acid alignment including 12 protein-coding genes; (3) PCG-rrn (14,612 nucleotide sites), nucleotide alignment including 12 protein-coding genes and two rRNA genes; (4) rrn (4,051 nucleotide sites), nucleotide alignment including *rrnL* and *rrnS* genes; and (5) trn (1,637 nucleotide sites), nucleotide alignment including 22 tRNA genes. The sequence alignments supporting the phylogenetic results of this article are presented in **Supplementary File S2**.

Phylogenetic trees were built using maximum likelihood (ML) method and Bayesian inference (BI) method. For the combined datasets of PCG_nt, PCG_aa, and PCG-rrn, data partition schemes and best-fitting substitution models (**Supplementary**

TABLE 1 | Species included in the phylogenetic analyses.

Item	Phylum	Class	Order	Family	Species	Accession number
Outgroup	Ascomycota	Sordariomycetes	*Hypocreales*	*Nectriaceae*	*Fusarium culmorum*	KP827647
	Ascomycota	Sordariomycetes	*Hypocreales*	*Nectriaceae*	*Fusarium circinatum*	JX910419
	Ascomycota	Sordariomycetes	*Hypocreales*	*Nectriaceae*	*Fusarium oxysporum*	KR952337
Ingroup	Ascomycota	Dothideomycetes	*Venturiales*	*Venturiaceae*	*Venturia effusa*	CP042205
	Ascomycota	Dothideomycetes	*Capnodiales*	*Mycosphaerellaceae*	*Zymoseptoria tritici*	MH374028
	Ascomycota	Dothideomycetes	*Capnodiales*	*Mycosphaerellaceae*	*Zasmidium cellare*	NC_030334
	Ascomycota	Dothideomycetes	*Capnodiales*	*Mycosphaerellaceae*	*Pseudocercospora mori*	NC_037198
	Ascomycota	Dothideomycetes	*Capnodiales*	*Mycosphaerellaceae*	*Pseudocercospora fijiensis*	NC_044132
	Ascomycota	Dothideomycetes	*Botryosphaeriales*	*Botryosphaeriaceae*	*Botryosphaeria dothidea*	KY801668
	Ascomycota	Dothideomycetes	*Botryosphaeriales*	*Botryosphaeriaceae*	*Botryosphaeria kuwatsukai*	MG593780
	Ascomycota	Dothideomycetes	*Pleosporales*	*Astrosphaeriellaceae*	*Pithomyces chartarum*	NC_035636
	Ascomycota	Dothideomycetes	*Pleosporales*	*Didymellaceae*	*Didymella pinodes*	NC_029396
	Ascomycota	Dothideomycetes	*Pleosporales*	*Phaeosphaeriaceae*	*Phaeosphaeria nodorum*	CM017955
	Ascomycota	Dothideomycetes	*Pleosporales*	*Phaeosphaeriaceae*	*Shiraia bambusicola*	NC_026869
	Ascomycota	Dothideomycetes	*Pleosporales*	*Coniothyriaceae*	*Coniothyrium glycines*	NC_040008
	Ascomycota	Dothideomycetes	*Pleosporales*	*Pleosporaceae*	*Pyrenophora teres*	CM017819
	Ascomycota	Dothideomycetes	*Pleosporales*	*Pleosporaceae*	*Alternaria alternata*	MF669499
	Ascomycota	Dothideomycetes	*Pleosporales*	*Pleosporaceae*	*Stemphylium lycopersici*	NC_036039
	Ascomycota	Dothideomycetes	*Pleosporales*	*Pleosporaceae*	*Bipolaris sorokiniana*	MN978926
	Ascomycota	Dothideomycetes	*Pleosporales*	*Pleosporaceae*	*Bipolaris cookei*	MF784482

Table S1) were estimated using PartitionFinder 2 (Lanfear et al., 2012). Data blocks were predefined by genes. The PartitionFinder 2 analyses were run using a greedy search scheme (Lanfear et al., 2012), with all models considered under the Akaike information criteria.

For ML inferences, we conducted separate analyses of each protein-coding gene (i.e., *atp6*, *cob*, *cox1-3*, and *nad1-6*), and then performed combined analysis based on the dataset of PCG_nt. In addition, other four concatenated datasets (i.e., PCG_aa, PCG-rrn, rrn, and trn) were also used in the ML analyses. ML tree searches were performed in IQ-TREE 1.6.10 (Nguyen et al., 2015) implemented in the Cipres Science Gateway (Miller et al., 2010). Partitioned analyses were conducted for datasets of PCG_nt, PCG_aa, and PCG-rrn, with the data partitions and the best-fitting models selected by PartitionFinder 2 (Lanfear et al., 2012). Allowing partitions to have different speeds (-spp) was selected. Nodal support values (BP) were evaluated through an ultrafast bootstrap approach (Minh et al., 2013), with 10,000 replicates.

To circumvent the long computational time required, only the five concatenated datasets (i.e., PCG_nt, PCG_aa, PCG-rrn, rrn, and trn) were used in Bayesian inferences. Bayesian tree searches were conducted in MrBayes 3.2.6 (Ronquist et al., 2012) implemented in the CIPRES Science Gateway (Miller et al., 2010). We applied the MrBayes blocks for partition definitions generated from PartitionFinder 2 (Lanfear et al., 2012). All model parameters were set as unlinked across partitions. Each analysis involved two independent runs and started from random topology. Each run implemented four Markov chain Monte Carlo chains in parallel for 10 million generations, and sampled every 1,000 generations. The program Tracer 1.7 (Rambaut et al., 2018) was used to analyze the trace files from two Bayesian MCMC runs for monitoring convergence. The first 25% of sampled trees were discarded as burn-in, and the remaining trees were used to calculate a majority-rule consensus tree. Branch support was assessed by clade posterior probabilities (PP).

We also used PhyloBayes (Lartillot et al., 2009) to conduct Bayesian inferences. This software implements the site-heterogeneous CAT-GTR or CAT model accounting for the heterogeneity present in the data. Each analysis involved two independent runs, and started from random topology, respectively. Each run implemented two Markov chain Monte Carlo chains in parallel for at least 20,000 iterations. The CAT-GTR model was used for nucleotide dataset analyses, while the CAT-MTZOA model for amino acid dataset. The "bpcomp" program contained in the package of PhyloBayes was used to calculate the largest (maxdiff) and mean (meandiff) discrepancy observed across all bipartitions. The program "tracecomp" was also used to summarize the discrepancies and the effective sizes estimated for each column of the trace file. When the maxdiff was <0.1 and minimum effective size was >100, the Bayesian runs were recognized to be reached good convergence. The first 1,000 trees of each MCMC were treated as the burn-in, and the majority-rule consensus tree was calculated from the saved trees.

Hypothesis Testing

We tested the statistical robustness of critical nodes defining deep level relationships in Dothideomycetes, by means of the four-cluster likelihood-mapping (FcLM) approach implemented in IQ-TREE 1.6.10 (Nguyen et al., 2015). The datasets of PCG_nt, PCG_aa, PCG-rrn, rrn, and trn were used for this test. The partition schemes and the corresponding best-fitting models were applied as those in the ML tree searches.

RESULTS

Genome Assembly

The total number of raw reads are 22,819,080. After filtering, 22,111,146 high-quality PE reads are produced. A 137,775 bp mitochondrial contig is reconstructed by the assembler MITObim. Statistical analysis from Qualimap show that 465,656 single-mate reads are mapped on this mitochondrial contig. This accounts for 4.2% of the total number of reads. The mean coverage of this mitochondrial contig reach 499.92-fold. Blastn searches against the IDBA-tran assembly identify 19 possible mitochondrial contigs. Twelve contigs with a length larger than 1,000 bp match the 137,775 bp mitochondrial contig assembled by MITObim. Of which, five largest contigs have the length of 42,635, 20,394, 16,519, 7,563, and 5,602 bp, respectively. The IDBA-tran assembly confirms the result from MITObim to some extent. Considering the completeness of the mitochondrial genome assembled, the following sections will focus on the result from the assembler MITObim.

General Features of *B. sorokiniana* Mitochondrial Genome

The *B. sorokiniana* mtDNA sequence shows similar values concerning AT content, AT skew, and GC skew to most other dothideomycete fungi (mean AT content of 70.5%, mean AT skew of 0.0043, and mean GC skew of 0.0203). The mean AT content of the complete mitochondrial genome calculated for *B. sorokiniana* is 69.5%. The AT skew is slightly negative (-0.0043), while the GC skew is positive (0.0263). These results suggest that there is no significant strand-specific bias of nucleotide composition in the mitochondrial genome of *B. sorokiniana*. The gene content of *B. sorokiniana* mitochondrial genome is characteristic of fungal mitochondria (**Figure 1** and **Supplementary Table S2**), including the usual set of genes interrupted by numerous introns (up to 60,277 bp in length) and separated by long intergenic spacers (up to 53,712 bp in length). A total of 12 core mitochondrial protein-coding genes are identified. In addition to the core protein-coding genes, 52 free-standing open reading frames of unknown function (uORFs) are annotated. The remaining conserved genes identified include two ORFs coding for the putative ribosomal protein S3 (*rps3*) gene and the putative ribosomal protein S5 (*rps5*) gene, the fungal mitochondrial RNase P (*rnpB*) gene, 38 tRNA genes and two mitochondrial ribosomal RNA genes (*rrnL* and *rrnS*).

Protein-Coding Genes and Codon Usage

The 12 core protein-coding genes (*atp6*, *cob*, *cox1*, *cox2*, *cox3*, *nad1*, *nad2*, *nad3*, *nad4*, *nad4L*, *nad5*, and *nad6*) are typical to fungal mtDNA, which are related to the mitochondrial oxidative phosphorylation pathway. The *atp8* gene is missing, which resembles that in the mitochondrial genome of *B. cookei*. Five protein-coding genes (*cox1-3* and *nad2-3*) are coded at the light strand, while the remaining seven ones are coded at the heavy strand (**Figure 1**). Eight out of 12 protein-coding genes are interrupted by introns, namely *atp6*, *cob*, *cox1*, *cox3*, *nad1*, *nad2*, *nad4*, and *nad5*. The highest number of intron sequences (8) are present in the *cox1* gene.

In the core protein-coding genes of *B. sorokiniana*, Ile (I), Leu2 (L2), and Phe (F) are among the most frequently found amino acids with the frequency of AUU (14.8%), AUA (5.48%), and AUC (1.40%) for Ile, UUA (10.17%) and UUG (0.82%) for Leu2, UUU (5.63%) and UUC (2.65%) for Phe, respectively. In *B. sorokiniana* mitochondrial genome, 82.33% codons terminate with A or T. The codon usage pattern can be due to the relatively high AT content found in the whole mitochondrial genome. The average AT content of the core protein-coding genes is 70.5%, and the third codon positions have the highest AT content (82.3%).

Ribosomal Protein Genes and Mitochondrial RNase P Gene

The *rps3* gene and the *rps5* gene are found between *cox3* and *nad1*, with the lengths of 399 and 555 bp, respectively. Both genes have the same positions and the similar sequence lengths as those in the mitochondrial genome of *B. cookei*. The genes of *rps3* and *rps5* are coded at the light strand. The AT content of *rps3* gene and *rps5* gene are 78.9 and 73.6%, which are higher than that of the core protein-coding genes. In addition, the fungal mitochondrial RNase P gene (*rnpB*) is identified between *trnP*_2 and *trnV*_2, with a length of 563 bp. The AT content of *rnpB* gene is 73.4%.

Transfer RNA and Ribosomal RNA Genes

A total of 38 tRNA genes are identified in the mitochondrial genome of *B. sorokiniana* coding for 22 amino acids (**Supplementary Figure S1**), with length ranging from 68 bp (*trnC*_1) to 85 bp (*trnY*). Seven tRNA genes (*trnC*, *trnH*, *trnL1*, *trnL2*, *trnP*, *trnQ*, and *trnV*) are duplicated. Four *trnM* genes are present in the mitochondrial genome, as the genes of *trnN* and *trnR*. The majority of tRNA genes are located between *rrnS* and *nad4*, and coded at the heavy strand in an anti-clockwise direction. No introns have been found in tRNA genes. All tRNA genes can be folded into the cloverleaf secondary structure. However, the *trnC*_1 displays an unusual acceptor stem due to nucleotide missing. In addition, the anticodon loop in *trnP*_1 is replaced with a large loop structure due to redundant nucleotides.

Two mitochondrial rRNA genes are identified, namely *rrnL* gene and *rrnS* gene. The *rrnL* gene is 4,440 bp in length, which is placed between *trnP*_1 and *trnT*. The *rrnL* gene is separated into two fragments by an intronic spacer with length of 273 bp. The *rrnS* gene is 1,659 bp, and positioned between *trnR*_2 *and trnL2*_2. The *rrnS* is a complete gene sequence, without intronic spacer identified in this gene. The AT content of *rrnL* and *rrnS* gene are 65.1 and 63.3%, respectively.

Phylogenetic Inference

Partition homogeneity tests showed the dataset of PCG_nt to be congruent with the dataset of rrn (P = 0.13). Therefore, the alignments of PCG_nt and rrn can be combined. The trn alignment is significantly incongruent when evaluated against PCG_nt (P = 0.01) or rrn (P = 0.01).

The separate ML analyses for individual protein-coding genes (**Supplementary Table S3**) recover three order groups, namely,

Capnodiales, *Botryosphaeriales* and *Pleosporales*. The *Venturiales* is often a deeply-diverging clade, while the *Pleosporales* is placed in a relatively derived position. Despite with these results, the relationships among orders vary greatly across separate analyses. The discordance indicates the conflicting signals in the individual protein-coding gene data.

Combined protein-coding gene datasets (i.e., PCG_nt and PCG_aa) and the PCG-rrn dataset also recovered the three order-level lineages outlined above (**Figures 2**, **3** and **Supplementary Figures S2–S4**). Compared to separate ML analyses on individual protein-coding genes, combined analyses yield higher support values for main nodes in Dothideomycetes. Based on the PCG-rrn data, ML analysis and MrBayes analysis result in an identical tree topology (**Figure 2**). In which, the *Venturiales* is supported as the sister group to all other Dothideomycetes. The *Botryosphaeriales* is placed as sister group to *Pleosporales* (*BP* = 62, *PP* = 0.95). This arrangement receive 46.3% quartet support from the FcLM analysis on PCG-rrn data (**Figure 4**). The datasets of PCG_nt and PCG_aa show weaker signal for this relationship (30% of quartets from PCG_nt, and 27.5% of quartets from PCG_aa). Within *Pleosporales*, the family *Astrosphaeriellaceae* is the first clade to diverge, followed by the families *Phaeosphaeriaceae* and *Coniothyriaceae* in a sequential order. The *Pleosporaceae* forms a sister group to *Didymellaceae*. Within *Pleosporaceae*, our analyses maximally support *B. sorokiniana* as a sister group to *B. cookei*. This sister group relationship is also recovered in the analyses of PCG_nt and PCG_aa (*BP* = 100, *PP* = 1), irrespective of method of phylogenetic inference.

Under the site-homogeneous models, trees obtained from the analyses of PCG_nt data (**Supplementary Figures S2A,B**) are identical in the major lineages to those from the PCG-rrn analyses, but varied in the relationships among orders and families. The similar patterns are revealed in the analyses of PCG_aa data (**Supplementary Figures S3A,B**). The ML tree and MrBayes tree inferred from the amino acid data of PCG_aa differ from the nucleotide data of PCG-rrn in that the *Capnodiales* is retrieved as the sister group to *Pleosporales*. This sister group relationship is also recovered in the ML analysis from the nucleotide data of PCG_nt (**Supplementary Figure S2**A). The FcLM results show weak to moderate signal for the placement of *Capnodiales* as sister group to *Pleosporales* (23.8, 42.5, and 63.8% of quartets, PCG-rrn, PCG_nt, and PCG_aa, respectively).

Under the site-heterogeneous models, phylogenetic trees resulting from PhyloBayes analyses based on datasets of PCG_aa, PCG_nt and PCG-rrn consistently place *Botryosphaeriales* as

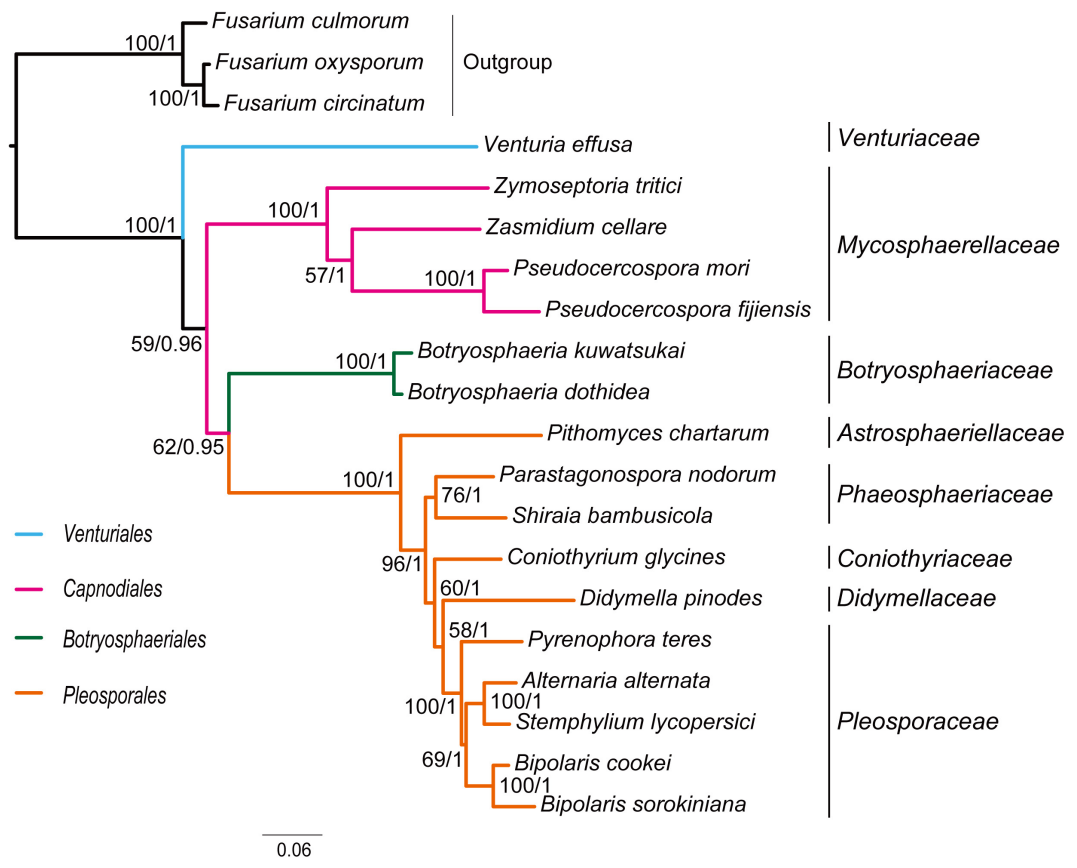

FIGURE 2 | Maximum likelihood tree inferred from the dataset of PCG-rrn using IQ-TREE, under the partition schemes and best-fitting models selected by PartitionFinder 2. Node numbers show bootstrap support values (left) and poster probability values from MrBayes (right).

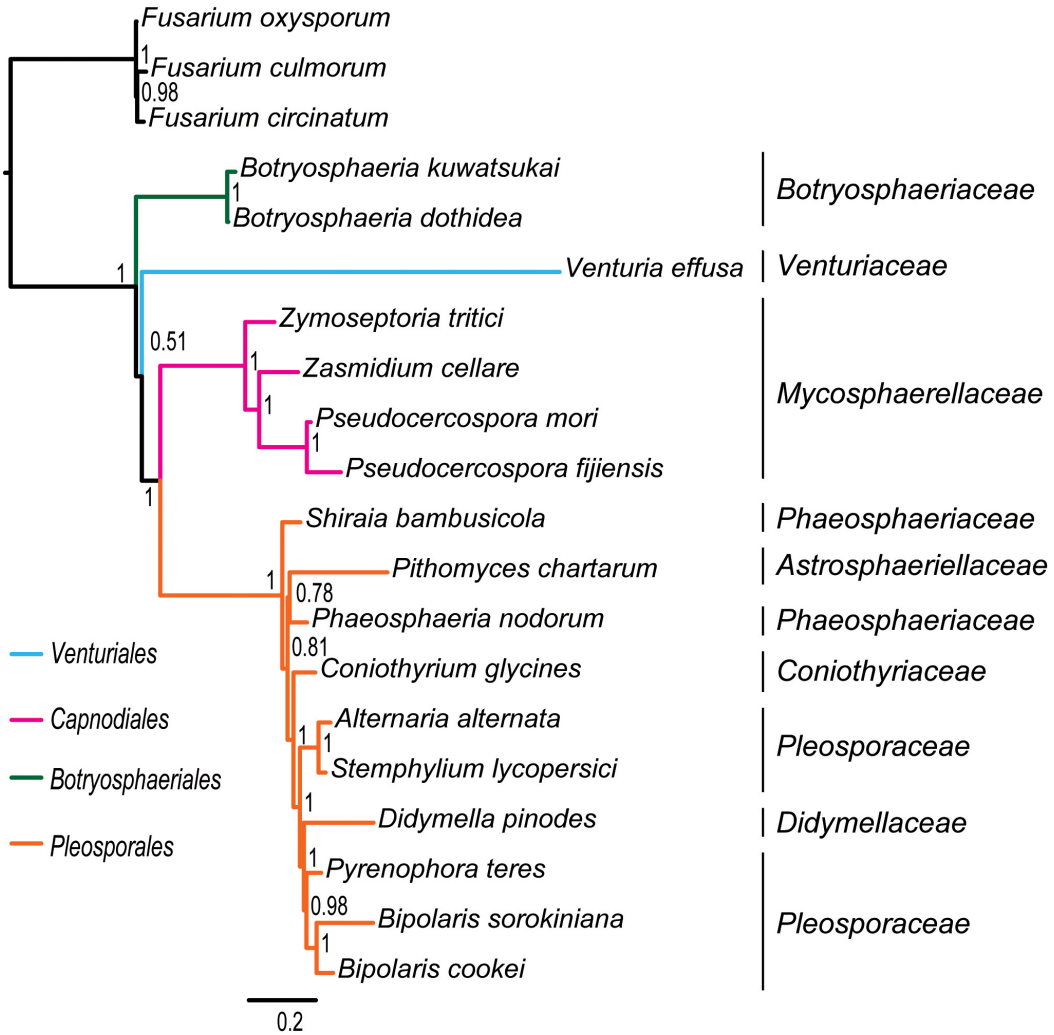

FIGURE 3 | Bayesian tree inferred from the dataset of PCG_aa using PhyloBayes, under the site-heterogeneous CAT-MTZOA model. Node numbers show the poster probability values.

the first diverging clade in Dothideomycetes (**Figure 3** and **Supplementary Figures S4A,B**). In the PhyloBayes trees of PCG_nt and PCG-rrn, *Venturiales* and *Capnodiales* are recovered as sister group. But this relationship lacks significant support from both datasets ($PP \leq 0.62$). By contrast, *Venturiales* is sister to a clade comprising *Capnodiales* and *Pleosporales* in the PhyloBayes trees from PCG_aa (**Figure 3**). Moreover, the *Capnodiales* is supported as a sister-group of *Pleosporales* ($PP = 1$). Within *Pleosporales*, the *Phaeosphaeriaceae* is non-monophyletic. Both *B. sorokiniana* and *B. cookei* are consistently grouped together with strong support ($PP = 1$).

The inference methods do not change the tree topology greatly in the phylogenetic analyses based on the datasets of rrn and trn (**Figures 5**, **6**). Under the ML and MrBayes inferences, the rrn data recovers a very similar inter-order relationship as the PCG-rrn data. The *Venturiales* is the deepest lineage in Dothideomycete, while *Botryosphaeriales* forms a sister-group of *Pleosporales* ($BP = 86$ and $PP = 1$ in **Figure 5**). The trn data also supports a sister-group relationship between *Botryosphaeriales* and *Pleosporales* ($BP = 98$ and $PP = 1$ in **Figure 6**). But it recovers *Venturiales* and *Capnodiales* as sister group, which is not favored in analyses from rrn data. The PhyloBayes trees from the rrn and trn datasets show very similar topological structures as those in the ML and MrBayes trees, but with lower support values for several nodes. The results of the FcLM analyses on the rrn and trn datasets strongly support the (*Botryosphaeriales*, *Pleosporales*) clade (**Supplementary Figure S5**).

DISCUSSION

Thus far, the complete mtDNA sequences available in Dothideomycete are scarce. Compared to animal mitochondrial genomes, fungal mitochondrial genomes have some characteristic features. In particular, presence of numerous introns within the fungal mitochondrial protein-coding genes

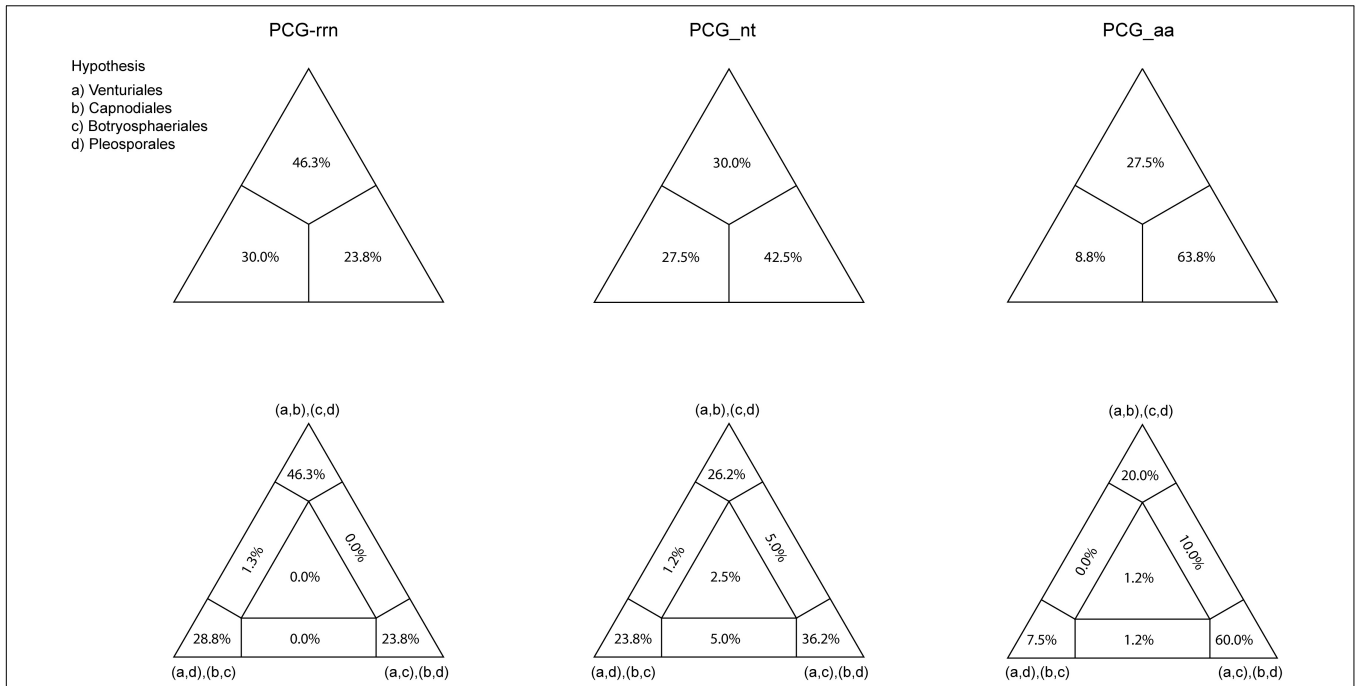

FIGURE 4 | Results obtained from the four-cluster likelihood-mapping analyses on the datasets of PCG-rrn, PCG_nt, and PCG_aa. The triangles above are the three posterior probabilities for the three possible hypotheses; and the triangles down are the two-dimensional simplex graphs supporting different evolutionary information.

makes it difficult to align sequences. This study presents an effective procedure to deal with this problem. Most of the nodes in our phylogenies have maximal statistical support, demonstrating the utility of our approach for generating mitochondrial genome data matrix useful in resolving the relationships in Dothideomycetes.

In addition to the enormous variations in size of mitochondrial genomes, the gene content and gene order may be different among fungal species. The gene content and gene order of the *B. sorokiniana* mitochondrial genome are very similar to those of *B. cookei* (Zaccaron and Bluhm, 2017). The major difference is the occurrence of a variable number of tRNA genes. There are only 28 tRNA genes present in the mitochondrial genome of *B. cookei*, in contrast with 38 tRNA genes in *B. sorokiniana.* Besides tRNA genes, the numbers of unique ORFs, introns inserted in the protein-coding genes and intergenic spacers are different between two *Bipolaris* species. Compared with animal mitochondrial genomes, the *atp9* is an additional gene occurring in many fungi (Paquin et al., 1997; Losada et al., 2014; Salavirta et al., 2014; Torriani et al., 2014; Lin et al., 2015; Ellenberger et al., 2016; Kanzi et al., 2016; Kang et al., 2017; Deng et al., 2018). However, the *atp9* gene is missing in *B. sorokiniana* and in *B. cookei.* Although plasmids and plasmid-like elements have been reported from mitochondria and mitochondrial genomes in some fungal species (Griffiths, 1995; Sakurai et al., 2004; Formighieri et al., 2008; Monteiro-Vitorello et al., 2009), our sequence analysis detected no apparent linear or circular plasmids in *B. sorokiniana*.

Mitochondrial phylogenomic analyses have been extensively used in the studies of animals (Boore, 1999; Garesse and Vallejo, 2001; Xu et al., 2006; Mulcahy et al., 2012; Cameron, 2014; Li et al., 2017; Du et al., 2019; Song F. et al., 2019; Song N. et al., 2019; Tang et al., 2019; Klucnika and Ma, 2020), but few attempts to produce fungal phylogenies based on mitochondrial genome sequences. Dothideomycetes is the largest class of Ascomycota (Hyde et al., 2013), which includes many economically significant plant pathogens. Phylogeny of the Dothideomycetes has attracted systematists' attention in recent years (Schoch et al., 2006, 2009a,b; Shearer et al., 2009; Suetrong et al., 2009; Nelsen et al., 2011a,b; Zhang et al., 2011; Liu et al., 2017). Some authors have initiated studies using single-gene and multi-gene phylogenetic analyses to investigate the relationships of Dothideomycetes (Schoch et al., 2006, 2009a; Shearer et al., 2009; Suetrong et al., 2009; Hyde et al., 2013). These molecular studies more frequently applied nuclear gene sequence data (e.g., nuc SSU rDNA, nuc LSU rDNA, EF1-α and ITS) to establish the phylogenetic framework (Schoch et al., 2006, 2009a,b; Shearer et al., 2009; Hyde et al., 2013; Manamgoda et al., 2012, 2014). Nuclear genes have different mechanisms of inheritance in comparison with mitochondrial genes. In general, nuclear genes show slower rates of evolution than mitochondrial genes (Brown et al., 1979; Moriyama and Powell, 1997; Johnson and Clayton, 2000; San Mauro et al., 2004). Comparisons of phylogenies based on nuclear and mitochondrial gene sequences are essential to our understanding of the phylogenetic affinities of Dothideomycetes.

Traditionally, members of *Venturiaceae* were classified in the order *Pleosporales* (Hyde et al., 2013). Schoch et al. (2009a,b) recovered *Venturiaceae* as a separated clade from the core members of *Pleosporales*, with nuclear gene fragments data.

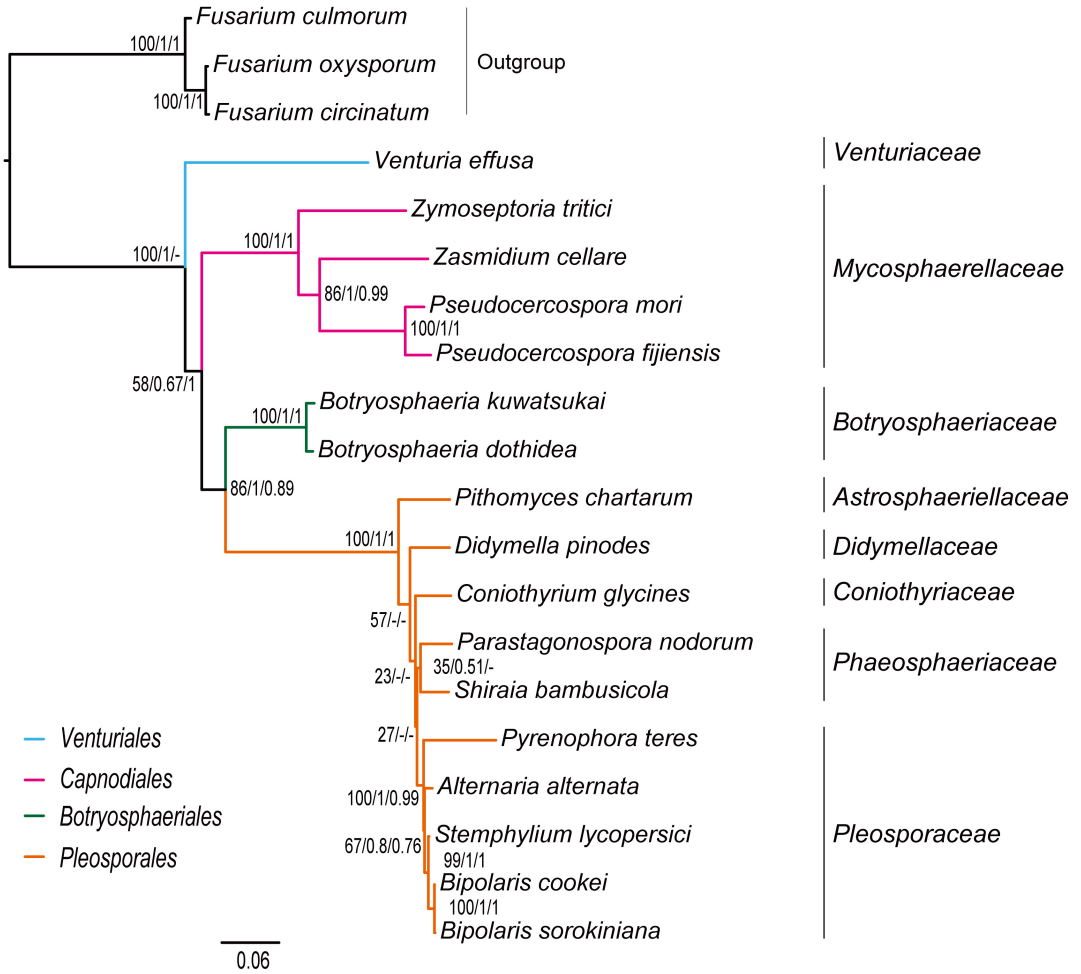

FIGURE 5 | Maximum likelihood tree inferred from the dataset of rrn using IQ-TREE. Node numbers show bootstrap support values (left), poster probability values from MrBayes (middle), and poster probability values from PhyloBayes (right).

Based on combined analysis of molecular, morphological and ecological evidence, Zhang et al. (2011) established the order *Venturiales* comprising *Venturiaceae* and *Sympoventuriaceae*. Our phylogenetic estimates on the mitochondrial genome sequence data consistently support the *Venturiaceae* as an independent clade. The *Botryosphaeriales* is another recently proposed order (Schoch et al., 2006). Based on the PCG-rrn data, ML and MrBayes analyses returned a sister-group relationship between *Botryosphaeriales* and *Pleosporales*. The earlier molecular studies based on the nuclear gene sequences also suggested a relatively close affiliation of *Botryosphaeriales* to *Pleosporales* (Schoch et al., 2006; Hyde et al., 2013). Concerning the deep relationships among four orders surveyed, the branching pattern of {*Venturiales*, [*Capnodiales*, (*Botryosphaeriales*, *Pleosporales*)]} inferred from the PCG-rrn data and the rrn data is congruent with the multi-locus phylogenies from nuclear genes (Schoch et al., 2009a; Hyde et al., 2013).

Our analyses using a variety of datasets and different inference methods largely recover the same substantial clades in Dothideomycetes, albeit with discordant relationships between them. No significant saturation was found in any data type alignments (Iss < Iss.cSym and Iss < Iss.cAsym in **Supplementary Table S4**). The presence of heterogeneous sequences and lineage-specific substitution rates may provide some explanation for the incongruence between gene trees. The instability of the phylogenetic placement of *Venturiales* among analyses deserves special attention. This clade displays the obviously long branch length when compared with other dothideomycete lineages. The sequence heterogeneity analyses revealed that *V. effusa* has the notably higher heterogeneity than other dothideomycete species in the matrix of *rrnL* gene sequences (**Figure 7**). The analyses of synonymous substitution and non-synonymous substitution showed that the *Venturiales* has the elevated frequencies of synonymous substitutions and non-synonymous substitutions (**Table 2**). Both factors may lead to random similarity associated with long-branch effect. In addition to *V. effusa*, four species from *Capnodiales* (*Zymoseptoria tritici*, *Zasmidium cellare*, *Pseudocercospora mori*, and *Pseudocercospora fijiensis*) also have higher synonymous and non-synonymous substitution rates (**Table 2**). Therefore, the

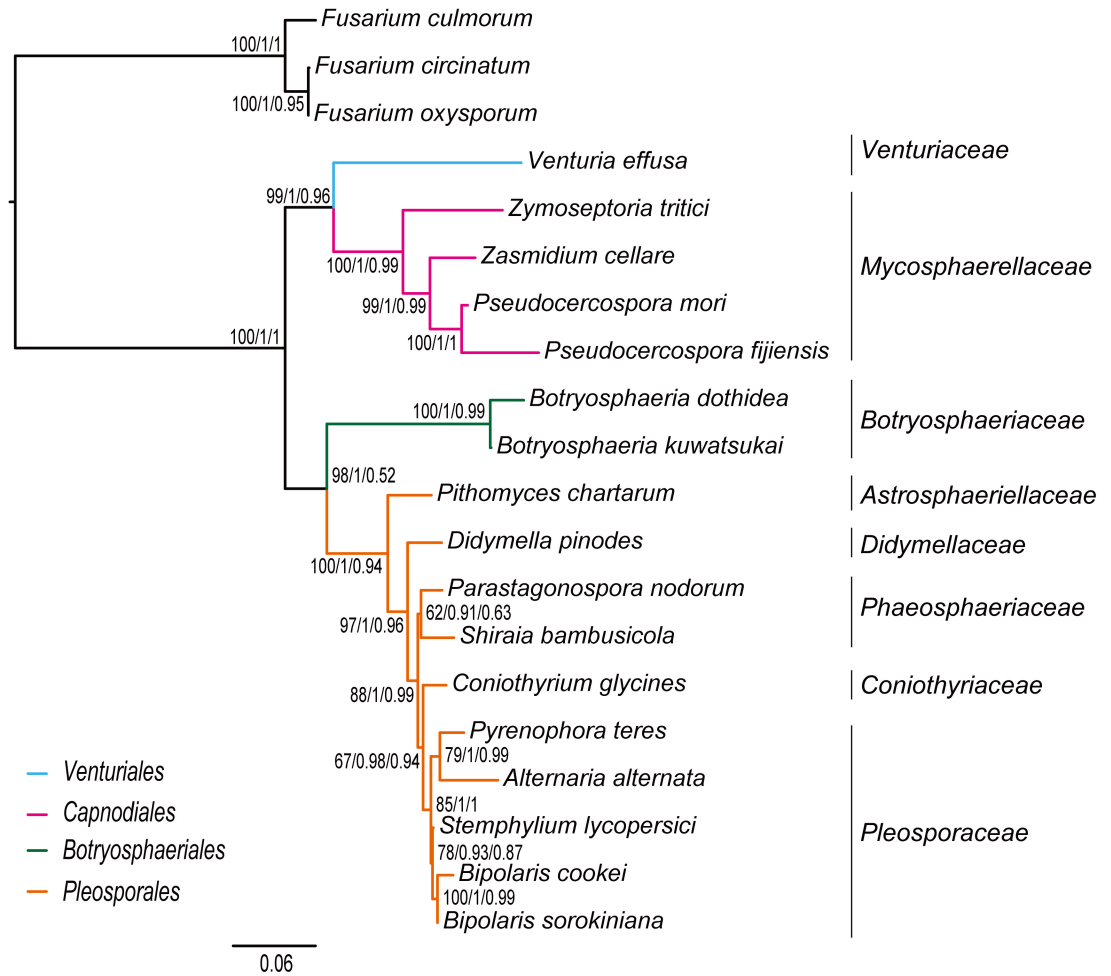

FIGURE 6 | Maximum likelihood tree inferred from the dataset of trn using IQ-TREE. Node numbers show bootstrap support values (left), poster probability values from MrBayes (middle), and poster probability values from PhyloBayes (right).

grouping of *Venturiales* and *Capnodiales* might be the result of long-branch attraction.

Due to rapid evolution of mtDNA (Brown et al., 1979; Simon et al., 2006), long branches occur frequently in the phylogenetic analyses based on mitochondrial genome sequences (Li et al., 2015; Song et al., 2016, Song N. et al., 2019; Timmermans et al., 2016; Liu et al., 2018; Tang et al., 2019). Long branches may have a negative effect on the accuracy of estimation of phylogenetic relationships. Previous studies (Lartillot et al., 2007; Li et al., 2015; Liu et al., 2018; Song F. et al., 2019; Song N. et al., 2019) showed that the site-heterogeneous model implemented in PhyloBayes could reduce the effects of compositional and mutational bias, and further suppress the long-branch attraction artifacts in the animal phylogeny. However, analyzing the current fungal mitochondrial genome data under different models did not resolve the observed incongruence. The PhyloBayes analysis on amino acid data under site-heterogeneous model breaks the grouping of *Venturiales* and *Capnodiales*, and recovers the *Pleosporales* as a sister group to *Capnodiales* (**Figure 3**). The PhyloBayes analyses on nucleotide datasets (PCG_nt and PCG-rrn) still retrieve a sister group of *Venturiales* and *Capnodiales* (**Supplementary Figures S4A,B**).

In contrast to varied results from the datasets compiled by protein-coding genes, consistency between phylogenetic reconstructions at deep level relationships within Dothideomycetes was remarkably improved by the datasets of rRNA gene and tRNA gene. The variable rates of molecular evolution in different gene sequences introduce a significant source of conflict. Slow evolving genes are more suitable for resolving deep level phylogenies (Donoghue and Sanderson, 1992; Giribet, 2002; Nosenko et al., 2013). Rates of evolutionary substitution in rRNA or tRNA genes are unusually lower than those for protein-coding genes (Ochman and Wilson, 1987; Yamamoto and Harayama, 1998; Nosenko et al., 2013). Thus, rRNA or tRNA data partitions are likely to give reliable estimates of the phylogenetic relationships among dothideomycete orders.

The lack of resolution in phylogenetics may be attributed to low levels of phylogenetic signal or highly conflicting phylogenetic signal (Whitfield and Kjer, 2008; Suh, 2016). Our FcLM analyses showed substantial levels of phylogenetic

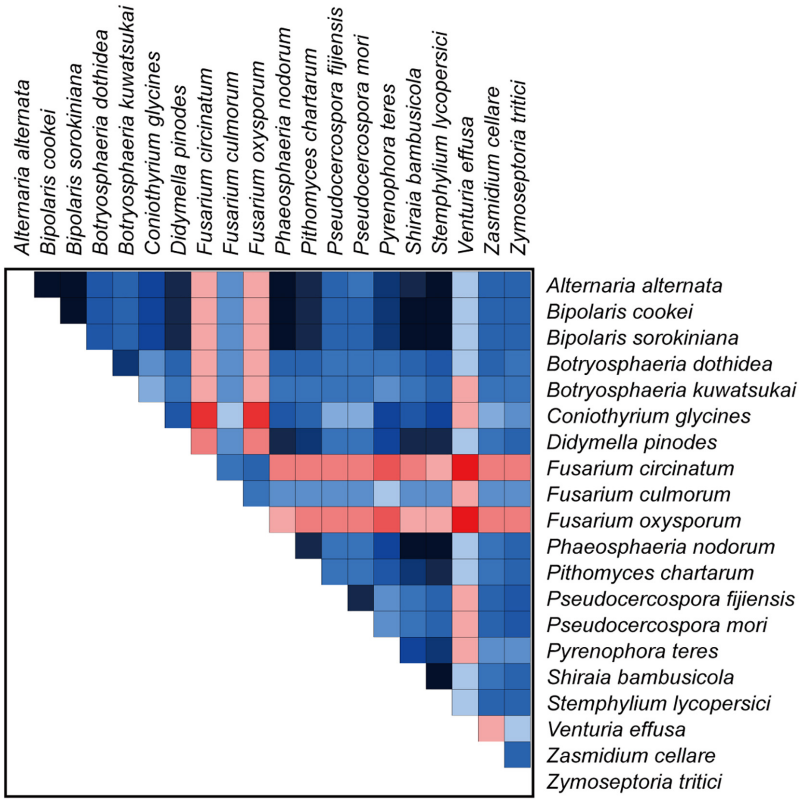

FIGURE 7 | The AliGROOVE graph shows the mean similarity scores between sequences, based on the analysis of the *rrnL* gene alignment. AliGROOVE scores range from −1 (indicating great difference in rates from the remainder of the data set, i.e., red coloring implies the significant heterogeneity) to +1 (indicating rates match all other comparisons). The results from AliGROOVE analyses based on other datasets are shown in **Supplementary Figure S6**.

TABLE 2 | The synonymous and non-synonymous nucleotide substitutions calculated for each species.

Species	*Ks*	*Ka*
Alternaria alternata	0.9016	0.1116
Bipolaris cookei	0.8452	0.1062
Bipolaris sorokiniana	0.8601	0.1312
Botryosphaeria dothidea	1.1755	0.1492
Botryosphaeria kuwatsukai	1.1546	0.1516
Coniothyrium glycines	0.8940	0.1091
Didymella pinodes	1.0238	0.1372
Fusarium circinatum	1.0087	0.1928
Fusarium culmorum	0.9808	0.1981
Fusarium oxysporum	0.9953	0.1923
Phaeosphaeria nodorum	0.9286	0.1066
Pithomyces chartarum	0.9670	0.1301
Pseudocercospora fijiensis	1.2034	0.1578
Pseudocercospora mori	1.2606	0.1452
Pyrenophora teres	0.9070	0.1114
Shiraia bambusicola	0.9158	0.1109
Stemphylium lycopersici	0.8808	0.1105
Venturia effusa	1.4006	0.1979
Zasmidium cellare	1.1401	0.1500
Zymoseptoria tritici	1.5408	0.1484

Ks, number of synonymous substitutions per synonymous site; Ka, number of non-synonymous substitutions per non-synonymous site.

conflict for the interrelationships of four dothideomycete orders. In addition, deficient taxon sampling can also lead to poor resolution of phylogenetic relationships (Nabhan and Sarkar, 2012). We acknowledge the sensitivity of taxon sampling to phylogenetic reconstructions of a highly diverse fungal lineage. Yet, the effectively analytical approaches presented in this study are expected to inspire more mitochondrial phylogenomic analyses of Dothideomycetes. Increasing the available mitogenomic data will inevitably contribute to addressing the persisting phylogenetic uncertainties in this important fungal group.

CONCLUSION

We sequenced and annotated the complete mitochondrial genome of *B. sorokiniana*, which is only the second mitochondrial genome sequence published in the genus *Bipolaris*. The gene content and organization are similar to those of the *B. cookei*. The large number and size of introns and intergenic spacers result in the large genome size. Several order- and family-level taxa are robustly supported by the current mtDNA sequence data. The *Venturiaceae* is consistently recovered to be an independent clade and phylogenetically distant from *Pleosporales*. This result confirms the view of prior studies (Schoch et al., 2009a,b;

Zhang et al., 2011). Incongruence between phylogenies constructed using various data types may stem from conflicting signals and unequal evolutionary rates. Tremendous advances of new DNA sequencing technologies have opened a window into the field of phylogenomic research, which will provide more alternative methods to tackle the problems. An understanding of mitochondrial genome evolution and phylogenetic relationships within Dothideomycetes would require the sequencing of mitochondrial genomes from more members of this group.

DATA AVAILABILITY STATEMENT

The datasets generated for this study can be found in the GenBank under the accession number MN978926.

AUTHOR CONTRIBUTIONS

NS and YG conceived this study. NS analyzed the data, prepared the figures, and drafted the manuscript. YG and XL participated in early analysis of preliminary data and manuscript writing and revision. YG provided suggestion for the research, contributed to the data interpretation, writing, and revising the manuscript critically. All authors have read and approved the final version of the manuscript.

FUNDING

This research was funded by Science and Technology Innovation Fund of Henan Agricultural University (KJCX2019A10) and Key Scientific Research Projects of Henan Province (18B210006).

SUPPLEMENTARY MATERIAL

The Supplementary Material for this article can be found online at: https://www.frontiersin.org/articles/10.3389/fmicb.2020.00863/full#supplementary-material

REFERENCES

Abascal, F., Zardoya, R., and Telford, M. J. (2010). TranslatorX: multiple alignment of nucleotide sequences guided by amino acid translations. *Nucleic Acids Res.* 38, W7–W13. doi: 10.1093/nar/gkq291

Aguileta, G., De Vienne, D. M., Ross, O. N., Hood, M. E., Giraud, T., Petit, E., et al. (2014). High variability of mitochondrial gene order among fungi. *Genome Biol. Evol.* 6, 451–465. doi: 10.1093/gbe/evu028

Alcorn, J. L. (1983). On the genera *Cochliobolus* and *Pseudocochliobolus*. *Mycotaxon* 16, 353–379.

Belcour, L., Rossignol, M., Koll, F., Sellem, C. H., and Oldani, C. (1997). Plasticity of the mitochondrial genome in Podospora. Polymorphism for 15 optional sequences: group-I, group-II introns, intronic ORFs and an intergenic region. *Curr. Genet.* 31, 308–317. doi: 10.1007/s002940050210

Berbee, M., Pirseyedi, M., and Hubbard, S. (1999). *Cochliobolus phylogenetics* and the origin of known, highly virulent pathogens, inferred from ITS and glyceraldehyde-3-phosphate dehydrogenase gene sequences. *Mycologia* 91, 964–977.

Bernt, M., Donath, A., Juhling, F., Externbrink, F., Florentz, C., Fritzsch, G., et al. (2013). MITOS: improved de novo metazoan mitochondrial genome annotation. *Mol. Phylogenet. Evol.* 69, 313–319. doi: 10.1016/j.ympev.2012.08.023

Boore, J. L. (1999). Animal mitochondrial genomes. *Nucleic Acids Res.* 27, 1767–1780.

Brown, W. M., George, M. Jr., and Wilson, A. C. (1979). Rapid evolution of animal mitochondrial DNA. *Proc. Natl. Acad. Sci. U.S.A.* 76, 1967–1971. doi: 10.1098/rspb.2007.0169

Camacho, C., Coulouris, G., Avagyan, V., Ma, N., Papadopoulos, J., Bealer, K., et al. (2009). BLAST+: architecture and applications. *BMC Bioinformatics* 10:421. doi: 10.1186/1471-2105-10-421

Cameron, S. L. (2014). Insect mitochondrial genomics: implications for evolution and phylogeny. *Annu. Rev. Entomol.* 59, 95–117. doi: 10.1146/annurev-ento-011613-162007

Caterino, M. S., Cho, S., and Sperling, F. A. (2000). The current state of insect molecular systematics: a thriving Tower of Babel. *Annu. Rev. Entomol.* 45, 1–54. doi: 10.1146/annurev.ento.45.1.1

Chowdhury, A. K., Singh, G., Tyagi, B. S., Ojha, A., Dhar, T., and Bhattacharya, P. M. (2013). Spot blotch disease of wheat–a new thrust area for sustaining productivity. *J. Wheat Res.* 5, 1–11.

Condon, B. J., Leng, Y. Q., Wu, D. L., Bushley, K. E., Ohm, R. A., Otillar, R., et al. (2013). Comparative genome structure, secondary metabolite, and effector coding capacity across *Cochliobolus pathogens*. *PLoS Genet.* 9:e1003233. doi: 10.1371/journal.pgen.1003233

Deng, Y., Hsiang, T., Li, S., Lin, L., Wang, Q., Chen, Q., et al. (2018). Comparison of the mitochondrial genome sequences of six Annulohypoxylon stygium Isolates suggests short fragment insertions as a potential factor leading to larger genomic size. *Front. Microbiol.* 9:2079. doi: 10.3389/fmicb.2018.02079

Donoghue, M., and Sanderson, M. (1992). "The suitability of molecular and morphological evidence in reconstructing plant phylogeny," in *Molecular Systematics in Plants*, eds P. Soltis, D. Soltis, and J. Doyle (New York: Chapman and Hall), 340–368.

Du, Z., Hasegawa, H., Cooley, J. R., Simon, C., Yoshimura, J., Cai, W., et al. (2019). Mitochondrial genomics reveals shared phylogeographic patterns and demographic history among three periodical cicada species groups. *Mol. Biol. Evol.* 36, 1187–1200. doi: 10.1093/molbev/msz051

Duo, A., Bruggmann, R., Zoller, S., Bernt, M., and Grunig, C. R. (2012). Mitochondrial genome evolution in species belonging to the *Phialocephala fortinii* s.l. - Acephala applanata species complex. *BMC Genomics* 13:166. doi: 10.1186/1471-2164-13-166

Ellenberger, S., Burmester, A., and Wöstemeyer, J. (2016). Complete mitochondrial DNA sequence of the mucoralean fungus *Absidia glauca*, a model for studying host-parasite interactions. *Genome Announc.* 4:e00153-16. doi: 10.1128/genomeA.00153-16

Farris, T. S., Källersjö, M., Kluge, A. G., and Bult, C. (1994). Testing significance of congruence. *Cladistics* 10, 315–319. doi: 10.1111/j.1096-0031.1994.tb00181.x

Fitzpatrick, D. A., Logue, M. E., Stajich, J. E., and Butler, G. (2006). A fungal phylogeny based on 42 complete genomes derived from supertree and combined gene analysis. *BMC Evol. Biol.* 6:99. doi: 10.1186/1471-2148-6-99

Formighieri, E. F., Tiburcio, R. A., Armas, E. D., Medrano, F. J., Shimo, H., Carels, N., et al. (2008). The mitochondrial genome of the phytopathogenic basidiomycete *Moniliophthora perniciosa* is 109 kb in size and contains a stable integrated plasmid. *Mycol. Res.* 112, 1136–1152. doi: 10.1016/j.mycres.2008.04.014

Fourie, G., Van Der Merwe, N. A., Wingfield, B. D., Bogale, M., Tudzynski, B., Wingfield, M. J., et al. (2013). Evidence for inter-specific recombination among the mitochondrial genomes of Fusarium species in the *Gibberella fujikuroi* complex. *BMC Genomics* 14:605. doi: 10.1186/1471-2164-14-605

Garesse, R., and Vallejo, C. G. (2001). Animal mitochondrial biogenesis and function: a regulatory cross-talk between two genomes. *Gene* 263, 1–16. doi: 10.1016/s0378-1119(00)00582-5

Giribet, G. (2002). Current advances in the phylogenetic reconstruction of metazoen evolution. a new paradigm for the cambrian explosion?

Mol. Phylogenet. Evol. 24, 345–357. doi: 10.1016/s1055-7903(02)00206-3

Greiner, S., Lehwark, P., and Bock, R. (2019). OrganellarGenomeDRAW (OGDRAW) version 1.3. 1: expanded toolkit for the graphical visualization of organellar genomes. *Nucleic Acids Res.* 47, W59–W64. doi: 10.1093/nar/gkz238

Griffiths, A. J. F. (1995). Natural plasmids of filamentous fungi. *Microbiol. Rev.* 59, 673–685.

Hahn, C., Bachmann, L., and Chevreux, B. (2013). Reconstructing mitochondrial genomes directly from genomic next-generation sequencing reads-a baiting and iterative mapping approach. *Nucleic Acids Res.* 41, 1–9. doi: 10.1093/nar/gkt371

Hausner, G. (2003). Fungal mitochondrial genomes, plasmids and introns. *Appl. Mycol. Biotech.* 3, 101–131.

Hyde, K. D., Jones, E. B. G., Liu, J. K., Ariyawansa, H., Boehm, E., Boonmee, S., et al. (2013). Families of dothideomycetes. *Fungal Divers.* 63, 1–313.

James, T. Y., Kauff, F., Schoch, C. L., Matheny, P. B., Hofstetter, V., Cox, C. J., et al. (2006a). Reconstructing the early evolution of Fungi using a six-gene phylogeny. *Nature* 443, 818–822. doi: 10.1038/nature05110

James, T. Y., Letcher, P. M., Longcore, J. E., Mozley-Standridge, S. E., Porter, D., Powell, M. J., et al. (2006b). A molecular phylogeny of the flagellated fungi (Chytridiomycota) and description of a new phylum (Blastocladiomycota). *Mycologia* 98, 860–871. doi: 10.3852/mycologia.98.6.860

Johnson, K. P., and Clayton, D. H. (2000). Nuclear and mitochondrial genes contain similar phylogenetic signal for pigeons and doves (Aves: Columbiformes). *Mol. Phylogenet. Evol.* 14, 141–151. doi: 10.1006/mpev.1999.0682

Kang, X., Hu, L., Shen, P., Li, R., and Liu, D. (2017). SMRT Sequencing revealed mitogenome characteristics and mitogenome-wide DNA modification pattern in *Ophiocordyceps sinensis*. *Front. Microbiol.* 8:1422. doi: 10.3389/fmicb.2017.01422

Kanzi, A. M., Wingfield, B. D., Steenkamp, E. T., Naidoo, S., and Van Der Merwe, N. A. (2016). Intron derived size polymorphism in the mitochondrial genomes of closely related chrysoporthe species. *PLoS One* 11:e0156104. doi: 10.1371/journal.pone.0156104

Katoh, K., and Standley, D. M. (2013). MAFFT multiple sequence alignment software version 7: improvements in performance and usability. *Mol. Biol. Evol.* 30, 772–780. doi: 10.1093/molbev/mst010

Klucnika, A., and Ma, H. (2020). Mapping and editing animal mitochondrial genomes: can we overcome the challenges? *Philos. Trans. R. Soc. Lond. B. Biol. Sci.* 375:20190187. doi: 10.1098/rstb.2019.0187

Kouvelis, V. N., Ghikas, D. V., and Typas, M. A. (2004). The analysis of the complete mitochondrial genome of *Lecanicillium muscarium* (synonym *Verticillium lecanii*) suggests a minimum common gene organization in mtDNAs of Sordariomycetes: phylogenetic implications. *Fungal Genet. Biol.* 41, 930–940. doi: 10.1016/j.fgb.2004.07.003

Kuck, P., Meid, S. A., Gross, C., Wagele, J. W., and Misof, B. (2014). AliGROOVE - visualization of heterogeneous sequence divergence within multiple sequence alignments and detection of inflated branch support. *BMC Bioinformatics* 15:294. doi: 10.1186/1471-2105-15-294

Kuck, P., and Meusemann, K. (2010). FASconCAT: convenient handling of data matrices. *Mol. Phylogenet. Evol.* 56, 1115–1118. doi: 10.1016/j.ympev.2010.04.024

Kulik, T., Brankovics, B., Sawicki, J., and Van Diepeningen, A. (2016). The complete mitogenome of *Fusarium culmorum*. *Mitochondrial DNA A* 27, 2425–2426. doi: 10.3109/19401736.2015.1030626

Kumar, J., Schafer, P., Huckelhoven, R., Langen, G., Baltruschat, H., Stein, E., et al. (2002). *Bipolaris sorokiniana*, a cereal pathogen of global concern: cytological and molecular approaches towards better control. *Mol. Plant Pathol.* 3, 185–195. doi: 10.1046/j.1364-3703.2002.00120.x

Kumar, S., Stecher, G., and Tamura, K. (2016). MEGA7: molecular evolutionary genetics analysis version 7.0 for bigger datasets. *Mol. Biol. Evol.* 33, 1870–1874. doi: 10.1093/molbev/msw054

Lanfear, R., Calcott, B., Ho, S. Y. W., and Guindon, S. (2012). PartitionFinder: combined selection of partitioning schemes and substitution models for phylogenetic analyses. *Mol. Biol. Evol.* 29, 1695–1701. doi: 10.1093/molbev/mss020

Lartillot, N., Brinkmann, H., and Philippe, H. (2007). Suppression of long-branch attraction artefacts in the animal phylogeny using a site-heterogeneous model. *BMC Evol. Biol.* 7:S4. doi: 10.1186/1471-2148-7-S1-S4

Lartillot, N., Lepage, T., and Blanquart, S. (2009). PhyloBayes 3: a Bayesian software package for phylogenetic reconstruction and molecular dating. *Bioinformatics* 25, 2286–2288. doi: 10.1093/bioinformatics/btp368

Li, H., and Durbin, R. (2009). Fast and accurate short read alignment with Burrows–Wheeler transform. *Bioinformatics* 25, 1754–1760. doi: 10.1093/bioinformatics/btp324

Li, H., Handsaker, B., Wysoker, A., Fennell, T., Ruan, J., Homer, N., et al. (2009). The sequence alignment/map format and SAMtools. *Bioinformatics* 25, 2078–2079. doi: 10.1093/bioinformatics/btp352

Li, H., Leavengood, J. M. Jr., Chapman, E. G., Burkhardt, D., Song, F., et al. (2017). Mitochondrial phylogenomics of Hemiptera reveals adaptive innovations driving the diversification of true bugs. *Proc. Biol. Sci.* 284:20171223. doi: 10.1098/rspb.2017.1223

Li, H., Shao, R. F., Song, N., Song, F., Jiang, P., Li, Z. H., et al. (2015). Higher-level phylogeny of paraneopteran insects inferred from mitochondrial genome sequences. *Sci. Rep.* 5:8527. doi: 10.1038/srep08527

Librado, P., and Rozas, J. (2009). DnaSP v5: a software for comprehensive analysis of DNA polymorphism data. *Bioinformatics* 25, 1451–1452. doi: 10.1093/bioinformatics/btp187

Lin, C. P., and Danforth, B. N. (2004). How do insect nuclear and mitochondrial gene substitution patterns differ? Insights from Bayesian analyses of combined datasets. *Mol. Phylogenet. Evol.* 30, 686–702. doi: 10.1016/S1055-7903(03)00241-0

Lin, R., Liu, C., Shen, B., Bai, M., Ling, J., Chen, G., et al. (2015). Analysis of the complete mitochondrial genome of *Pochonia chlamydosporia* suggests a close relationship to the invertebrate-pathogenic fungi in Hypocreales. *BMC Microbiol.* 15:5. doi: 10.1186/s12866-015-0341-8

Lindgreen, S. (2012). AdapterRemoval: easy cleaning of next-generation sequencing reads. *BMC Res. Notes* 5:337. doi: 10.1186/1756-0500-5-337

Link, J. H. F. (1824). "Species hyphomycetum et gymnomycetum," in *Species Plantarum*, ed. C. Linne (Germany: G.C. Nauk), 1–33.

Liu, J. K., Hyde, K. D., Jeewon, R., Phillips, A. J. L., Maharachchikumbura, S. S. N., Ryberg, M., et al. (2017). Ranking higher taxa using divergence times: a case study in Dothideomycetes. *Fungal Divers.* 84, 75–99.

Liu, Y., Song, F., Jiang, P., Wilson, J. J., Cai, W., and Li, H. (2018). Compositional heterogeneity in true bug mitochondrial phylogenomics. *Mol. Phylogenet. Evol.* 118, 135–144. doi: 10.1016/j.ympev.2017.09.025

Losada, L., Pakala, S. B., Fedorova, N. D., Joardar, V., Shabalina, S. A., Hostetler, J., et al. (2014). Mobile elements and mitochondrial genome expansion in the soil fungus and potato pathogen *Rhizoctonia solani* AG-3. *FEMS Microbiol. Lett.* 352, 165–173. doi: 10.1111/1574-6968.12387

Luo, R., Liu, B., Xie, Y., Li, Z., Huang, W., Yuan, J., et al. (2012). SOAPdenovo2: an empirically improved memory-efficient short-read de novo assembler. *Gigascience* 1:18. doi: 10.1186/s13742-015-0069-2

Manamgoda, D. S., Cai, L., Mckenzie, E. H. C., Crous, P. W., Madrid, H., Chukeatirote, E., et al. (2012). A phylogenetic and taxonomic re-evaluation of the Bipolaris - Cochliobolus - curvularia complex. *Fungal Divers.* 56, 131–144.

Manamgoda, D. S., Rossman, A. Y., Castlebury, L. A., Crous, P. W., Madrid, H., Chukeatirote, E., et al. (2014). The genus *Bipolaris*. *Stud. Mycol.* 79, 221–288. doi: 10.1016/j.simyco.2014.10.002

Mangold, A., Martin, M. P., Lucking, R., and Lumbsch, T. (2008). Molecular phylogeny suggests synonymy of Thelotremataceae within Graphidaceae (Ascomycota: Ostropales). *Taxon* 57, 476–486. doi: 10.1016/j.ympev.2011.04.025

Maraite, H., Di Zinno, T., Longrée, H., Daumerie, V., and Duveiller, E. (1998). "Fungi associated with foliar blight of wheat in warmer areas," in *Proceedings of the International Workshop on Helminthosporium Diseases of Wheat: Spot Blotch and Tan Spot*, eds E. Duveiller, H. J. Dubin, J. Reeves, and A. McNab (Mexico: CIMMYT, El Batán), 293–300.

Mardanov, A. V., Beletsky, A. V., Kadnikov, V. V., Ignatov, A. N., and Ravin, N. V. (2014). The 203 kbp mitochondrial genome of the phytopathogenic fungus *Sclerotinia borealis* reveals multiple invasions of introns and genomic duplications. *PLoS One* 9:e107536. doi: 10.1371/journal.pone.0107536

Matusinsky, P., Frei, P., Mikolasova, R., Svacinova, I., Tvaruzek, L., and Spitzer, T. (2010). Species-specific detection of *Bipolaris sorokiniana* from wheat and barley tissues. *Crop Prot.* 29, 1325–1330.

Miller, M., Pfeiffer, W., and Schwartz, T. (2010). Creating the CIPRES Science Gateway for inference of large phylogenetic trees. *Gateway Comput. Environ. Workshop* 14, 1–8.

Mina, U., Fuloria, A., and Aggarwal, R. (2016). Effect of ozone and antioxidants on wheat and its pathogen - *Bipolaris sorokininana*. *Cereal Res. Commun.* 44, 594–604.

Minh, B. Q., Nguyen, M. A. T., and Von Haeseler, A. (2013). Ultrafast approximation for phylogenetic bootstrap. *Mol. Biol. Evol.* 30, 1188–1195. doi: 10.1093/molbev/mst024

Monteiro-Vitorello, C. B., Hausner, G., Searles, D. B., Gibb, E. A., Fulbright, D. W., and Bertrand, H. (2009). The *Cryphonectria parasitica* mitochondrial rns gene: plasmid-like elements, introns and homing endonucleases. *Fungal Genet. Biol.* 46, 837–848. doi: 10.1016/j.fgb.2009.07.005

Moriyama, E. N., and Powell, J. R. (1997). Synonymous substitution rates in *Drosophila*: mitochondrial versus nuclear genes. *J. Mol. Evol.* 45, 378–391. doi: 10.1007/pl00006243

Mulcahy, D. G., Noonan, B. P., Moss, T., Townsend, T. M., Reeder, T. W., Sites, J. W. Jr., et al. (2012). Estimating divergence dates and evaluating dating methods using phylogenomic and mitochondrial data in squamate reptiles. *Mol. Phylogenet. Evol.* 65, 974–991. doi: 10.1016/j.ympev.2012.08.018

Nabhan, A. R., and Sarkar, I. N. (2012). The impact of taxon sampling on phylogenetic inference: a review of two decades of controversy. *Brief. Bioinform.* 13, 122–134. doi: 10.1093/bib/bbr014

Nelsen, M. P., Lucking, R., Mbatchou, J. S., Andrew, C. J., Spielmann, A. A., and Lumbsch, H. T. (2011a). New insights into relationships of lichen-forming Dothideomycetes. *Fungal Divers.* 51, 155–162.

Nelsen, M. P., Plata, E. R., Andrew, C. J., Lucking, R., and Lumbsch, H. T. (2011b). Phylogenetic diversity of Trentepohlialean Algae associated with lichen-forming fungi. *J. Phycol.* 47, 282–290. doi: 10.1111/j.1529-8817.2011.00962.x

Nguyen, L. T., Schmidt, H. A., Von Haeseler, A., and Minh, B. Q. (2015). IQ-TREE: a fast and effective stochastic algorithm for estimating maximum-likelihood phylogenies. *Mol. Biol. Evol.* 32, 268–274. doi: 10.1093/molbev/msu300

Nosenko, T., Schreiber, F., Adamska, M., Adamski, M., Eitel, M., Hammel, J., et al. (2013). Deep metazoan phylogeny: when different genes tell different stories. *Mol. Phylogenet. Evol.* 67, 223–233. doi: 10.1016/j.ympev.2013.01.010

Nowrousian, M. (2016). Complete mitochondrial genome sequence of the Pezizomycete *Pyronema confluens*. *Genome Announc.* 4:e00355-16. doi: 10.1128/genomeA.00355-16

Ochman, H., and Wilson, A. C. (1987). Evolution in bacteria: evidence for a universal substitution rate in cellular genomes. *J. Mol. Evol.* 26, 74–86. doi: 10.1007/bf02111283

Ohm, R. A., Feau, N., Henrissat, B., Schoch, C. L., Horwitz, B. A., Barry, K. W., et al. (2012). Diverse lifestyles and strategies of plant pathogenesis encoded in the genomes of eighteen *Dothideomycetes* fungi. *PLoS Pathog.* 8:e1003037. doi: 10.1371/journal.ppat.1003037

Okonechnikov, K., Conesa, A., and García-Alcalde, F. (2016). Qualimap 2: advanced multisample quality control for high-throughput sequencing data. *Bioinformatics* 32, 292–294. doi: 10.1093/bioinformatics/btv566

Pantou, M. P., Kouvelis, V. N., and Typas, M. A. (2008). The complete mitochondrial genome of *Fusarium oxysporum*: insights into fungal mitochondrial evolution. *Gene* 419, 7–15. doi: 10.1016/j.gene.2008.04.009

Paquin, B., Laforest, M. J., Forget, L., Roewer, I., Wang, Z., Longcore, J., et al. (1997). The fungal mitochondrial genome project: evolution of fungal mitochondrial genomes and their gene expression. *Curr. Genet.* 31, 380–395. doi: 10.1007/s002940050220

Peng, Y., Leung, H. C., Yiu, S. M., Lv, M. J., Zhu, X. G., and Chin, F. Y. (2013). IDBA-tran: a more robust de novo de Bruijn graph assembler for transcriptomes with uneven expression levels. *Bioinformatics* 29, i326–i334. doi: 10.1093/bioinformatics/btt219

Perna, N. T., and Kocher, T. D. (1995). Patterns of nucleotide composition at fourfold degenerate sites of animal mitochondrial genomes. *J. Mol. Evol.* 41, 353–358. doi: 10.1007/bf00186547

Pramateftaki, P. V., Kouvelis, V. N., Lanaridis, P., and Typas, M. A. (2006). The mitochondrial genome of the wine yeast *Hanseniaspora uvarum*: a unique genome organization among yeast/fungal counterparts. *FEMS Yeast Res.* 6, 77–90. doi: 10.1111/j.1567-1364.2005.00018.x

Rambaut, A., Drummond, A. J., Xie, D., Baele, G., and Suchard, M. A. (2018). Posterior summarization in Bayesian phylogenetics using Tracer 1.7. *Syst. Biol.* 67, 901–904. doi: 10.1093/sysbio/syy032

Robbertse, B., Reeves, J. B., Schoch, C. L., and Spatafora, J. W. (2006). A phylogenomic analysis of the Ascomycota. *Fungal Genet. Biol.* 43, 715–725.

Rogers, S. O., and Bendich, A. J. (1985). Extraction of DNA from milligram amounts of fresh, herbarium, and mummified plant tissues. *Plant Mol. Biol.* 5, 69–76. doi: 10.1007/BF00020088

Ronquist, F., Teslenko, M., Van Der Mark, P., Ayres, D. L., Darling, A., Hohna, S., et al. (2012). MrBayes 3.2: efficient Bayesian phylogenetic inference and model choice across a large model space. *Syst. Biol.* 61, 539–542. doi: 10.1093/sysbio/sys029

Sakurai, T., Nomura, H., Moriyam, Y., and Kawano, S. (2004). The mitochondrial plasmid of the true slime mold *Physarum polycephalum* bypasses uniparental inheritance by promoting mitochondrial fusion. *Curr. Genet.* 46, 103–114. doi: 10.1007/s00294-004-0512-x

Salavirta, H., Oksanen, I., Kuuskeri, J., Makela, M., Laine, P., Paulin, L., et al. (2014). Mitochondrial genome of *Phlebia radiata* is the second largest (156 kbp) among Fungi and features signs of genome flexibility and recent recombination events. *PLoS One* 9:e97141. doi: 10.1371/journal.pone.0097141

San Mauro, D., Gower, D. J., Oommen, O. V., Wilkinson, M., and Zardoya, R. (2004). Phylogeny of *Caecilian amphibians* (Gymnophiona) based on complete mitochondrial genomes and nuclear RAG1. *Mol. Phylogenet. Evol.* 33, 413–427. doi: 10.1016/j.ympev.2004.05.014

Schoch, C. L., Crous, P. W., Groenewald, J. Z., Boehm, E. W., Burgess, T. I., De Gruyter, J., et al. (2009a). A class-wide phylogenetic assessment of Dothideomycetes. *Stud. Mycol.* 64, 1–15.

Schoch, C. L., Shoemaker, R. A., Seifert, K. A., Hambleton, S., Spatafora, J. W., and Crous, P. W. (2006). A multigene phylogeny of the Dothideomycetes using four nuclear loci. *Mycologia* 98, 1041–1052. doi: 10.3852/mycologia.98.6.1041

Schoch, C. L., Sung, G. H., Lopez-Giraldez, F., Townsend, J. P., Miadlikowska, J., Hofstetter, V., et al. (2009b). The Ascomycota tree of life: a phylum-wide phylogeny clarifies the origin and evolution of fundamental reproductive and ecological traits. *Syst. Biol.* 58, 224–239. doi: 10.1093/sysbio/syp020

Sethuraman, J., Majer, A., Iranpour, M., and Hausner, G. (2009). Molecular evolution of the mtDNA encoded rps3 gene among filamentous ascomycetes fungi with an emphasis on the ophiostomatoid fungi. *J. Mol. Evol.* 69, 372–385. doi: 10.1007/s00239-009-9291-9

Shearer, C. A., Raja, H. A., Miller, A. N., Nelson, P., Tanaka, K., Hirayama, K., et al. (2009). The molecular phylogeny of freshwater Dothideomycetes. *Stud. Mycol.* 64, 145–153.

Shoemaker, R. A. (1959). Nomenclature of *Drechslera* and *Bipolaris*, grass parasites segregated from Helminthosporium. *Can. J. Bot.* 37, 879–887.

Simon, C., Buckley, T. R., Frati, F., Stewart, J. B., and Beckenbach, A. T. (2006). Incorporating molecular evolution into phylogenetic analysis, and a new compilation of conserved polymerase chain reaction primers for animal mitochondrial DNA. *Annu. Rev. Ecol. Evol. Syst.* 37, 545–579.

Simon, C., Frati, F., Beckenbach, A., Crespi, B., Liu, H., and Flook, P. (1994). Evolution, weighting, and phylogenetic utility of mitochondrial gene sequences and a compilation of conserved polymerase chain reaction primers. *Ann. Entomol. Soci. Am.* 87, 651–701.

Sivanesan, A. (1987). Graminicolous species of *Bipolaris*, *Curvularia*, *Drechslera*, *Exserohilum* and their teleomorphs. *Mycol. Pap.* 158, 1–261. doi: 10.1094/PDIS.2001.85.11.1206B

Sivanesan, A., and Holliday, P. (1981). *CMI Descriptions of Pathogenic Fungi and Bacteria Sheet-No. 701*. London: CAB—International Mycological Institute.

Song, F., Li, H., Jiang, P., Zhou, X. G., Liu, J. P., Sun, C. H., et al. (2016). Capturing the phylogeny of Holometabola with mitochondrial genome data and Bayesian site-heterogeneous mixture models. *Genome Biol. Evol.* 8, 1411–1426. doi: 10.1093/gbe/evw086

Song, F., Li, H., Liu, G. H., Wang, W., James, P., Colwell, D. D., et al. (2019). Mitochondrial genome fragmentation unites the parasitic lice of Eutherian mammals. *Syst. Biol.* 68, 430–440. doi: 10.1093/sysbio/syy062

Song, N., Zhang, H., and Zhao, T. (2019). Insights into the phylogeny of Hemiptera from increased mitogenomic taxon sampling. *Mol. Phylogenet. Evol.* 137, 236–249. doi: 10.1016/j.ympev.2019.05.009

Subramanian, C. V. (1971). "Bipolaris shoemaker," in *Hyphomycetes: An Account of Indian Species, Except Cercosporae*, ed. C. V. Subramanian (New Delhi: Indian Council of Agricultural Research).

Suetrong, S., Schoch, C. L., Spatafora, J. W., Kohlmeyer, J., Volkmann-Kohlmeyer, B., Sakayaroj, J., et al. (2009). Molecular systematics of the marine Dothideomycetes. *Stud. Mycol.* 64, 155–173.

Suh, A. (2016). The phylogenomic forest of bird trees contains a hard polytomy at the root of Neoaves. *Zool. Scr.* 45, 50–62.

Swann, E. C., and Taylor, J. W. (1995). Phylogenetic perspectives on Basidiomycete systematics - evidence from the 18s ribosomal-rna gene. *Can. J. Bot.* 73, S862–S868.

Swofford, D. L. (2002). *PAUP*, Phylogenetic Analysis Using Parsimony (*and other methods). Version. 4.* Sunderland, MA: Sinauer Associates.

Talavera, G., and Castresana, J. (2007). Improvement of phylogenies after removing divergent and ambiguously aligned blocks from protein sequence alignments. *Syst. Biol.* 56, 564–577. doi: 10.1080/10635150701472164

Tang, P., Zhu, J. C., Zheng, B. Y., Wei, S. J., Sharkey, M., Chen, X. X., et al. (2019). Mitochondrial phylogenomics of the Hymenoptera. *Mol. Phylogenet. Evol.* 131, 8–18.

Timmermans, M., Barton, C., Haran, J., Ahrens, D., Culverwell, C. L., Ollikainen, A., et al. (2016). Family-level sampling of mitochondrial genomes in Coleoptera: compositional heterogeneity and phylogenetics. *Genome Biol. Evol.* 8, 161–175. doi: 10.1093/gbe/evv241

Torriani, S. F., Penselin, D., Knogge, W., Felder, M., Taudien, S., Platzer, M., et al. (2014). Comparative analysis of mitochondrial genomes from closely related *Rhynchosporium* species reveals extensive intron invasion. *Fungal Genet. Biol.* 62, 34–42. doi: 10.1016/j.fgb.2013.11.001

Utomo, C., Tanjung, Z. A., Aditama, R., Buana, R. F. N., Pratomo, A. D. M., Tryono, R., et al. (2019). Complete mitochondrial genome dequence of the phytopathogenic Basidiomycete *Ganoderma boninense* Strain G3. *Microbiol. Resour. Announc.* 8:e00968-18. doi: 10.1128/MRA.00968-18

Valach, M., Burger, G., Gray, M. W., and Lang, B. F. (2014). Widespread occurrence of organelle genome-encoded 5S rRNAs including permuted molecules. *Nucleic Acids Res.* 42, 13764–13777. doi: 10.1093/nar/gku1266

Wang, H., Xu, Z., Gao, L., and Hao, B. L. (2009). A fungal phylogeny based on 82 complete genomes using the composition vector method. *BMC Evol. Biol.* 9: 195. doi: 10.1186/1471-2148-9-195

Whitfield, J. B., and Kjer, K. M. (2008). Ancient rapid radiations of insects: challenges for phylogenetic analysis. *Annu. Rev. Entomol.* 53, 449–472. doi: 10.1146/annurev.ento.53.103106.093304

Wiese, M. V. (1998). *Compendium of Wheat Diseases*, 3rd Edn. St. Paul: APS Press.

Xia, X. H. (2013). DAMBE5: a comprehensive software package for data analysis in Mol. *Biol. Evol.* 30, 1720–1728. doi: 10.1007/s12539-016-0158-7

Xu, W., Jameson, D., Tang, B., and Higgs, P. G. (2006). The relationship between the rate of molecular evolution and the rate of genome rearrangement in animal mitochondrial genomes. *J. Mol. Evol.* 63, 375–392. doi: 10.1007/s00239-005-0246-5

Yamamoto, S., and Harayama, S. (1998). Phylogenetic relationships of *Pseudomonas* putida strains deduced from the nucleotide sequences of gyrB, rpoD and 16S rRNA genes. *Int. J. Syst. Bacteriol.* 48, 813–819. doi: 10.1099/00207713-48-3-813

Zaccaron, A. Z., and Bluhm, B. H. (2017). The genome sequence of *Bipolaris cookei* reveals mechanisms of pathogenesis underlying target leaf spot of sorghum. *Sci. Rep.* 7:17217. doi: 10.1038/s41598-017-17476-x

Zhang, Y., Crous, P. W., Schoch, C. L., Bahkali, A. H., Guo, L. D., and Hyde, K. D. (2011). A molecular, morphological and ecological re-appraisal of Venturiales - a new order of Dothideomycetes. *Fungal Divers.* 51, 249–277. doi: 10.1007/s13225-011-0141-x

Conflict of Interest: The authors declare that the research was conducted in the absence of any commercial or financial relationships that could be construed as a potential conflict of interest.

frontiers in Microbiology

ORIGINAL RESEARCH
published: 25 May 2020
doi: 10.3389/fmicb.2020.01002

Diversity of Mobile Genetic Elements in the Mitogenomes of Closely Related *Fusarium culmorum* and *F. graminearum* sensu stricto Strains and Its Implication for Diagnostic Purposes

Tomasz Kulik[1], Balazs Brankovics[2], Anne D. van Diepeningen[2], Katarzyna Bilska[1], Maciej Żelechowski[1], Kamil Myszczyński[1,3], Tomasz Molcan[4], Alexander Stakheev[5], Sebastian Stenglein[6,7], Marco Beyer[8], Matias Pasquali[9], Jakub Sawicki[1], Joanna Wyrębek[1] and Anna Baturo-Cieśniewska[10]*

[1] Department of Botany and Nature Protection, University of Warmia and Mazury in Olsztyn, Olsztyn, Poland, [2] Biointeractions & Plant Health, Wageningen Plant Research, Wageningen, Netherlands, [3] Molecular Biology Laboratory, Institute of Animal Reproduction and Food Research, Polish Academy of Sciences, Olsztyn, Poland, [4] Department of Animal Anatomy and Physiology, Faculty of Biology and Biotechnology, University of Warmia and Mazury in Olsztyn, Olsztyn, Poland, [5] Shemyakin and Ovchinnikov Institute of Bioorganic Chemistry, Russian Academy of Sciences, Moscow, Russia, [6] National Scientific and Technical Research Council, Godoy Cruz, Argentina, [7] Universidad Nacional del Centro de la Provincia de Buenos Aires, Tandil, Argentina, [8] Department of Environmental Research and Innovation, Agro-Environmental Systems, Luxembourg Institute of Science and Technology, Belval, Luxembourg, [9] Department of Food, Environmental and Nutritional Sciences, University of Milan, Milan, Italy, [10] Laboratory of Phytopathology and Molecular Mycology, Department of Biology and Plant Protection, UTP University of Science and Technology, Bydgoszcz, Poland

OPEN ACCESS

Edited by:
James Bernard Konopka, Stony Brook University, United States

Reviewed by:
Gerard Barroso, Université de Bordeaux, France
Shu Zhang, Shanxi University, China

***Correspondence:**
Tomasz Kulik
tomaszkulik76@gmail.com

Specialty section:
This article was submitted to Fungi and Their Interactions, a section of the journal Frontiers in Microbiology

Received: *19 February 2020*
Accepted: *24 April 2020*
Published: *25 May 2020*

Citation:
Kulik T, Brankovics B, van Diepeningen AD, Bilska K, Żelechowski M, Myszczyński K, Molcan T, Stakheev A, Stenglein S, Beyer M, Pasquali M, Sawicki J, Wyrębek J and Baturo-Cieśniewska A (2020) Diversity of Mobile Genetic Elements in the Mitogenomes of Closely Related Fusarium culmorum and F. graminearum sensu stricto Strains and Its Implication for Diagnostic Purposes. Front. Microbiol. 11:1002. doi: 10.3389/fmicb.2020.01002

Much of the mitogenome variation observed in fungal lineages seems driven by mobile genetic elements (MGEs), which have invaded their genomes throughout evolution. The variation in the distribution and nucleotide diversity of these elements appears to be the main distinction between different fungal taxa, making them promising candidates for diagnostic purposes. Fungi of the genus *Fusarium* display a high variation in MGE content, from MGE-poor (*Fusarium oxysporum* and *Fusarium fujikuroi* species complex) to MGE-rich mitogenomes found in the important cereal pathogens *F. culmorum* and *F. graminearum* sensu stricto. In this study, we investigated the MGE variation in these latter two species by mitogenome analysis of geographically diverse strains. In addition, a smaller set of *F. cerealis* and *F. pseudograminearum* strains was included for comparison. Forty-seven introns harboring from 0 to 3 endonucleases (HEGs) were identified in the standard set of mitochondrial protein-coding genes. Most of them belonged to the group I intron family and harbored either LAGLIDADG or GIY-YIG HEGs. Among a total of 53 HEGs, 27 were shared by all fungal strains. Most of the optional HEGs were irregularly distributed among fungal strains/species indicating ancestral mosaicism in MGEs. However, among optional MGEs, one exhibited species-specific

conservation in *F. culmorum.* While in *F. graminearum* s.s. MGE patterns in *cox3* and in the intergenic spacer between *cox2* and *nad4L* may facilitate the identification of this species. Thus, our results demonstrate distinctive traits of mitogenomes for diagnostic purposes of Fusaria.

Keywords: *Fusarium graminearum* sensu stricto, *F. culmorum*, mitogenome, mobile genetic elements, mitochondrial introns, homing endonucleases

INTRODUCTION

Most fungi contain mitochondria, organelles playing a key role in the generation of metabolic energy. Besides, fungal mitochondria have been shown to contribute to diverse cellular and organismal functions including senescence, quiescence, biofilm regulation and hyphal growth (Chatre and Ricchetti, 2014; Calderone et al., 2015; Bartelli et al., 2018; Sandor et al., 2018). They may also be involved in antifungal drug resistance, as well as in fungal virulence and pathogenicity (Shingu-Vazquez and Traven, 2011; Sandor et al., 2018). It is therefore not surprising that mitochondrial structure and function, as well as mitogenomes of fungi, have been studied intensively since the 2000s (Hausner, 2003; Chatre and Ricchetti, 2014).

Mitogenomes are expected to provide new insights for understanding the phylogenetic relationships and evolutionary biology of fungi (Aguileta et al., 2014; Lin et al., 2015; Franco et al., 2017). The reason for this is that fungal mitogenomes are highly divergent among even closely related lineages (Yin et al., 2012; Pogoda et al., 2019). This fact opens entirely new perspectives in diagnostics of fungi. The concept of applying mitogenomes for the identification of species mainly derives from their higher DNA copy number compared with nuclear DNA, and hence higher recovery and amplification success (Santamaria et al., 2009). However, for many fungal lineages, the characterization of mitochondrial DNA (mtDNA) has been largely limited by a low number of mitochondrial sequences in the GenBank database.

Fungal mitogenomes are double-stranded DNA molecules with relatively simple genetic structures often containing a set of 14 protein-coding genes, two rRNA coding genes and a large group of tRNA coding genes. The set of 14 core-genes encoding proteins is involved in the respiratory chain: the apocytochrome b (*cob*), 3 subunits of the cytochrome c oxidase (*cox* genes), 7 subunits of the NADH dehydrogenase (*nad* genes) and 3 components of the ATP synthase (*atp* genes). The two conserved rRNA genes encode the small (rns) and large (rnl) ribosomal RNA (rRNA) subunits (Bullerwell and Lang, 2005). In addition, fungal mitogenomes harbor a variable number of mobile genetic elements (MGEs) such as introns and associated homing endonucleases (HEGs), which have invaded the mitogenomes throughout the evolution (Basse, 2010; Joardar et al., 2012; Pogoda et al., 2019).

Surveys of intron distribution among different filamentous fungi have pinpointed a surprisingly high variation in MGE content, from the single-intron mitogenome of *Fusarium proliferatum* (Brankovics et al., 2017) to MGE-rich mitogenome of *Rhizoctonia solani* containing several dozens of MGEs (Losada et al., 2014). Most of the MGE insertion sites are highly conserved (Hausner, 2003) and occur in mitochondrial protein-coding genes, but certain genes can display remarkably different MGE densities (Hausner, 2003; Yin et al., 2012; Aguileta et al., 2014; Franco et al., 2017). In addition, the same MGEs can be irregularly distributed in evolutionarily distant species and mosaicism in MGE patterns can be found between different populations or even strains of the same species driving large genome size differences among them (Yin et al., 2012; Kolesnikova et al., 2019).

The widespread distribution of MGEs in fungi can be explained by an intron-rich progenitor of major eukaryotic lineages from which extensive and lineage-dependent intron loss has occurred. The most frequently assumed mechanism of intron loss considers the replacement of intron-containing genes with their intronless versions through homologous recombination between intronless cDNA and the corresponding genomic DNA (Hausner, 2003; Yin et al., 2012; Pogoda et al., 2019). In addition to intron/HEG loss, the infective nature of HEGs, which can propagate horizontally between different lineages is often suggested to drive the observed variation in MGE content. The mobility of HEGs is primarily explained by their transfer and site-specific integration, which usually involves three steps: recognition of an intronless allele, cleaving, and insertion of the HEG (Haugen et al., 2005; Yin et al., 2012). In addition, HEGs themselves may propagate over a variety of lineages independently from their host intron, resembling free-standing HEGs, which frequently occur in genomes of phages (Edgell, 2009; Franco et al., 2017). This type of mobility, although not frequently documented, drives variation in size and nucleotide content of introns (Wu and Hao, 2014).

Several recent studies addressed the comprehensive analyses of mitogenomes in important plant pathogenic *Fusarium* species (Al-Reedy et al., 2012; Fourie et al., 2013; Brankovics et al., 2017, 2018). Mitogenomes of Fusaria pose a typical set of mitochondrial genes with identical gene order. A unique feature apparently common in all *Fusarium* species is the presence of a large open reading frame with unknown function (LV-uORF) firstly described in mitogenomes of *F. graminearum*, *F. verticillioides* and *F. solani* (Al-Reedy et al., 2012). *Fusarium* mitogenomes have been shown to vary considerably in size. So far, *Fusarium pseudograminearum* contains the largest mitogenome of 110,526 bp long (described in this study), while the smallest proved only 30,629 bp long in *F. oxysporum* (Pantou et al., 2008). Such large size differences are caused primary by the irregular distribution of MGEs (Al-Reedy et al., 2012; Fourie et al., 2013; Brankovics et al., 2018). In *F. graminearum* sensu stricto (s.s.), MGEs comprise more than half of the mitogenome. Diversity in MGE content contributed to

remarkable variation among geographically diverse strains which raised the question of the feasibility of using this type of variation in mitochondrial population genetic studies of *Fusarium* field populations (Brankovics et al., 2018).

Fusarium graminearum s.s. and *F. culmorum* are important and closely related plant pathogens exhibiting a mainly necrotrophic lifestyle after a short biotrophic infection stage and can be described as generalists based on their broad host ranges. Fusarium Head Blight (FHB) and Fusarium Crown Rot (FCR) are among the most important diseases of cereals caused by these pathogens. Both have led to major economic losses for the cereal-based feed and food supply chains. Besides these two species, other closely related fungi such as *F. cerealis* and *F. pseudograminearum* can be involved in cereal diseases (Leslie and Summerell, 2008).

All four pathogens exhibit a similar toxigenic potential by the production of type B trichothecenes and zearalenone (ZEA). These compounds are nowadays among the most frequently detected mycotoxins in different wheat- and barley-growing regions of the world (Desjardins, 2006). Trichothecenes have been found to induce mycotoxicoses in humans and animals and play a role in the virulence of fungal strains (Desjardins, 2006). ZEA is a non-steroidal estrogen that may cause female reproductive changes due to its strong estrogenic activity (Hueza et al., 2014).

However, despite the aforementioned similarities, all four *Fusarium* species appear to exhibit considerable variation in distribution and frequency in agroecosystems. The most noticeable, despite their frequent co−existence, is the dramatic prevalence of *F. graminearum* s.s. in many cropping regions of the world (van der Lee et al., 2015). The emergence of *F. graminearum* s.s. resulted in the continuous displacement of other FHB causing *Fusarium* species. The best example illustrating this displacement is the gradual decrease of *F. culmorum*, which has been traditionally reported as the primary cause of FHB in Northern, Central and Western Europe (Waalwijk et al., 2003; Scherm et al., 2013; Bilska et al., 2018a). *F. cerealis* causes root rots and seedling blights, but can also be found on corn cobs and as emerging, mycotoxigenic FHB pathogen in temperate regions (Amarasinghe et al., 2015). While the predominance of *F. pseudograminearum* has been linked to the rather warm and dry environmental conditions (Kazan and Gardiner, 2018).

Even when using a software package designed for patch characterization in images, *Fusarium cerealis* could neither be distinguished unambiguously from *F. sambucinum* nor from *F. graminearum s.s.* based on their morphological spore shape parameters (Dubos et al., 2012). All of them produce similar banana-shaped macroconidia and chlamydospores. *F. graminearum* s.s. is morphologically identical to *F. pseudograminearum*, while *F. culmorum* can easily be confused with *F. cerealis* (Leslie and Summerell, 2008). More reliable identification of these four species could be achieved by using molecular markers, especially with methods employing species-specific primers in either end point (conventional PCR) or qPCR (Waalwijk et al., 2004; Nicolaisen et al., 2009). A more laborious method of species discrimination is based on multi-locus sequencing (MLST) (Geiser et al., 2004; Wang et al., 2011). However, the major disadvantage of nuclear markers is their reduced detection limits mostly due to the targeted nuclear single-copy genes (Kulik et al., 2015; Bilska et al., 2018b). Amongst the most promising solutions is targeting repeated genomic sequences such as mitochondrial DNA. However, the low number of available mtDNA sequences from Fusaria so far limited the evaluation of mitochondrial DNA as a diagnostic marker.

Today, the growing body of mitogenome data suggests that variation in MGE number can follow the divergence of different fungal taxa (Brankovics et al., 2017; Liang et al., 2017; Fourie et al., 2018), offering great perspectives for future diagnostic purposes. Brankovics et al. (2017) showed that mosaicism in intron patterns can support the separation of three phylogenetic species in *F. oxysporum*. Fourie et al. (2018) revealed significant differences in intron patterns among species from the *Fusarium fujikuroi* species complex (FFSC). Beyond *Fusarium*, recent studies on *Colletotrichum* mitogenomes indicated that intron content variation could improve cryptic species delimitation within this genus (Liang et al., 2017).

This study demonstrates that the variable landscape of MGEs is the most prominent type of variation among mitogenomes of closely related *F. graminearum* s.s. and *F. culmorum*. The major objective of this study was to discover if the pattern of MGE diversity might facilitate the delimitation of these species.

Therefore, we sequenced, assembled and annotated the mitogenomes from geographically diverse strains. Mitogenomes of the studied Fusaria were MGE-rich and most of them were present in all studied strains. Protein homology searches in GenBank database revealed a number of HEG orthologs shared with other fungal species with considerable variation in protein identity scores. Among the total of 53 identified HEGs, one showed species-specific conservation in *F. culmorum*. *F. graminearum* s.s. did not harbor unique MGEs throughout the mitogenome, however, we found that MGE patterns in *cox3* and in the intergenic spacer between *cox2* and *nad4L* that can serve as potential markers for the identification of this species.

MATERIALS AND METHODS

Fungal Strains

Supplementary File 1 provides characteristics of all fungal strains used in this study. A more detailed description of the strains can be found in the ToxGen database (Kulik et al., 2017). The mitogenomes of 78 strains of *F. graminearum* s.s. and 33 strains of *F. culmorum* were included into the analyses. In addition, 8 strains of *F. cerealis* and 4 strains of *F. pseudograminearum* were included for comparison. Moreover, 23 complete mitogenomes of *F. graminearum* s.s. previously described by Brankovics et al. (2018) and one mitogenome of *F. culmorum* (Kulik et al., 2016a) were also included.

DNA Extraction and Sequencing

For DNA extraction, fungal strains were incubated on Petri plates (Ø 80 mm) with PDA medium at 24°C for 6 days.

DNA from fungal strains was extracted from 0.1 g of mycelium with the use of the Quick-DNA Plant/Seed Miniprep Kit (Zymo Research, Irvine, CA, United States) according to the manufacturer's protocol.

Whole-genome sequencing was performed at Macrogen (Seoul, South Korea). Genome libraries were constructed using a TruSeq DNA PCR-free library preparation kit (Illumina, San Diego, CA, United States). An Illumina HiSeq X Ten platform was used to sequence the genomes using a paired-end read length of 2 × 150 bp with an insert size of 350 bp.

Assembly and Annotation of Mitogenomes

NOVOPlasty 2.7.2 (Dierckxsens et al., 2017) was used for *de novo* assembly of fungal mitogenomes from whole-genome data. HEGs were identified using NCBI's ORF Finder[1], Blast+ (v. 2.9.0) (Johnson et al., 2008) and Geneious Prime software (Biomatters Ltd., New Zealand). Annotations were performed using MFannot[2], InterPro (Mitchell et al., 2015), CD-Search (Marchler-Bauer and Bryant, 2004) and Geneious Prime software (Biomatters Ltd., New Zealand). Annotation of tRNA genes was improved using tRNAscan-SE (Pavesi et al., 1994).

Complete mitogenomes have been deposited in the NCBI database under the GenBank accession numbers MT036635-757 (**Supplementary File 1**).

Alignment

Mitogenome comparison included a total of 147 complete mitogenomes. Multiple sequence alignments of the complete mitogenomes were performed with progressive Mauve (Darling et al., 2010) implemented in the Geneious Prime software (Biomatters Ltd., New Zealand) to examine the distribution of MGEs in fungal mitogenomes.

BlastP Analyses

To reveal the distribution and the diversity of HEGs, blastP searches were performed using the BLAST program available at the National Center for Biotechnology Information web page https://www.ncbi.nlm.nih.gov/. Hits were retained only if they had an *e*-value cut off lower than 0.001 and which covered at least 70% of the query sequence with >60% identity.

Phylogenetic Analysis

HEGs showing higher protein similarity to sequences from distantly related species than to those found in other Fusaria were subjected for phylogenetic analysis. Protein sequences were aligned using the Muscle algorithm implanted in the software package Geneious Prime (Biomatters Ltd., New Zealand). An optimal evolutionary model was estimated using MEGA X (Kumar et al., 2018). The trees were constructed using the Maximum Likelihood method as implemented in Mega X with JTT + G + F model and 2000 bootstrap replicates.

[1]https://www.ncbi.nlm.nih.gov/orffinder/

[2]http://megasun.bch.umontreal.ca/cgi-bin/mfannot/mfannotInterface.pl

RESULTS

General Features of Fungal Mitogenomes

The mitochondrial genomes of all strains contained a conserved set of genes in the same order and orientation; a set of 14 protein-coding genes, 2 rRNA genes (*rns* and *rnl*) and 28 tRNA genes. The four *Fusarium* species displayed a similar GC content of 31.6–32.0% within their mitogenomes; clearly in the middle limit of the GC content range for fungal mitogenomes (8.4–52.7%, estimated from sequence data deposited in the GenBank database of the NCBI by April 2019).

Mitogenome sizes ranged from of 92.816 bp (*F. cerealis* strain 64722) to 110.526 bp for (*F. pseudograminearum* strain CBS 109956) (**Supplementary File 1**). These sizes of mitogenomes are well in between the current size limits of the fungal mitogenomes ranging from 12 kb to over 235 kb (based on GenBank database by April 2019). To date, the mitogenome of *F. pseudograminearum* remains the largest among fungi of the genus *Fusarium*.

Besides genes with functional predictions, *Fusarium* mitogenomes contained a large open reading frame with unknown function (LV-uORF). This ORF is located in the intergenic spacer between *rnl* and the *nad2* gene (Al-Reedy et al., 2012). The GC content of the LV-uORF is higher than the usual set of mitochondrial genes suggesting its horizontal acquisition by a common ancestor of *Fusarium* species (Al-Reedy et al., 2012).

Our results showed a highly conserved distribution of LV-uORF in four studied species (**Supplementary File 1**). We found that LV-uORF is present in all examined strains in the same position and orientation. However, we found considerable variation within LV-uORF mainly due to multiple indel mutations altering its length, which ranged from 4.155 to 6.390 bp (**Figure 1**). The apparently conserved placement of indels within LV-uORF and their irregular distribution among strains and species suggests that most of these events occurred prior to the divergence of the *Fusarium* species.

Mobile Genetic Elements

A total of 47 introns has been identified in the basic set of mitochondrial protein-coding genes of the studied strains (**Supplementary Files 1, 2a–6a**). All introns belonged to the group I intron family with two exceptions: the first one was *iIIcob* intron, which was classified to the group II introns and encodes a protein of the reverse transcriptase family (**Supplementary File 2a**). Notably, the distribution of this intron within studied Fusaria seems to be very limited. We detected its presence in only 2 *F. graminearum* s.s. strains (16-462-z and INRA-156). The second exception was the *i4cox2* intron, which lacked distinguishable features for classification (**Supplementary File 3a**).

Most introns harbored HEGs, either of the LAGLIDADG or GIY-YIG type, which are determined based on the differences in conserved amino acid motifs. Among 53 distinct HEGs, 36 were assigned as LAGLIDADG endonucleases being present

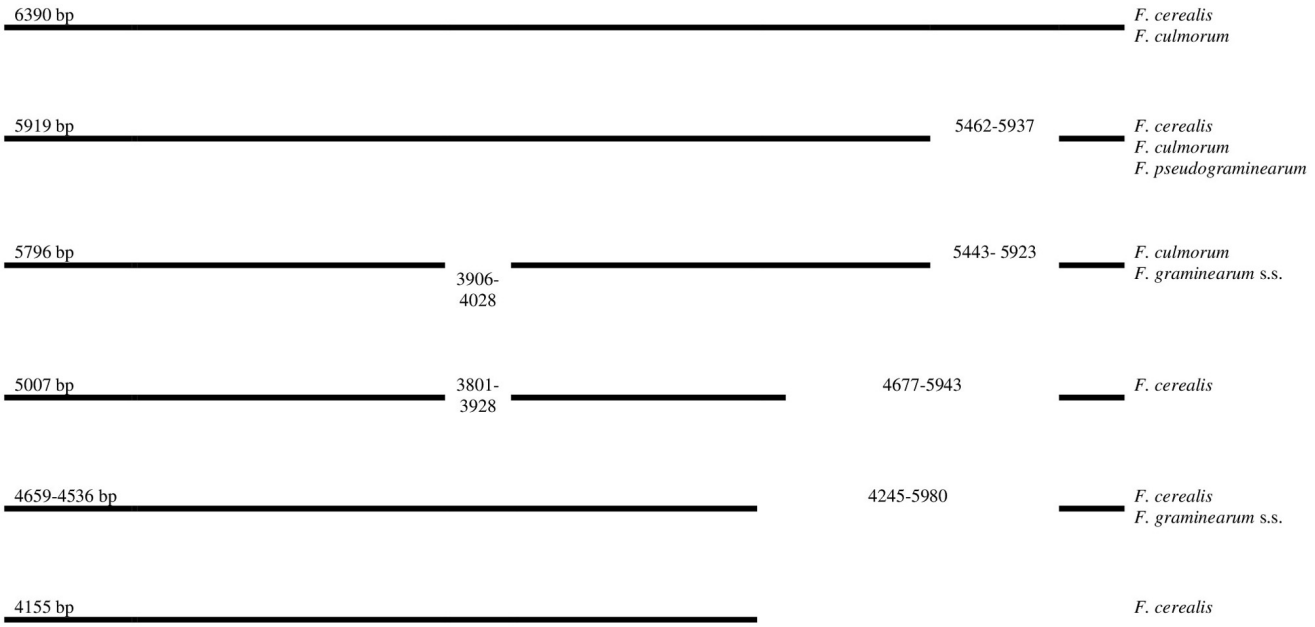

FIGURE 1 | Schematic position of indels in LV-uORF in four Fusarium species. Position of indels (bp) are referred to *F. cerealis* (GenBank accession number MT036645, CBS 110268 strain).

in 9 out of 11 intron-rich genes. GIY-YIG endonucleases appear to be less commonly occurring HEGs in mitogenomes of Fusaria. We identified 15 distinct GIY-YIG endonucleases in only six out of eleven protein-coding genes. However, two HEGs [*i4cob* HEG (112 aa) and *i6cob* HEG (472 aa)] could not be precisely predicted through similarity searches with blastP, presumably due to loss of conserved amino acid motifs that reflect these functional differences. We found that orthologs of *i4cob* HEG present in GenBank are much larger in the other species; e.g., in *Podospora comata* this HEG is 314 aa in length (YP_009550007.1), while in *Neurospora crassa* – 477 aa (YP_009126715.1), which suggests deletion events during the divergence of Fusaria. The second *i6cob* HEG showed the highest identity (73.8 – 75.5%) to unclassified mitochondrial proteins (ATI20208.1, ATI20295.1, ATI20458.1) found in *Juglanconis* sp. (q-cover = 99-100%, *E* value = 0).

More than half of the introns (n = 26) identified in Fusaria were located in 3 subunits of the cytochrome c oxidase (*cox* genes): 17 in *cox1*, 5 in *cox2*, and 4 in *cox3* (**Supplementary Files 2a–6a**). Positions of MGEs were highly conserved among different strains, however, with one exception. We found that two different introns *icox1a* and *icox1b* can share the same location in *cox1* (**Supplementary File 4a**). Intron *icox1a* harbored a LAGLIDADG motif and was present in *F. cerealis*, while *icox1b* contained a GIY-YIG motif and was found in all strains of *F. culmorum*, *F. graminearum* s.s. and *F. pseudograminearum*. Further analyses of a larger collection of strains could confirm whether the LAGLIDAD HEG found in *icox1a* is fixed in *F. cerealis*.

HEGs drive mobility of MGEs, which can move across species, genera or even kingdoms (Koufopanou et al., 2002; Wu and Hao, 2014). We performed comprehensive blastP searches against GenBank to gather information on their distribution and the diversity among species. BlastP analyses revealed that most of the identified HEGs can be found in other *Fusarium* species as well as in species out of the genus *Fusarium*, however, with considerable variation in protein identity scores (**Supplementary Files 2b–6b**). Notably, for most HEGs (49 out of 53), protein identity was greater within than outside the genus *Fusarium*, which indicates their ancestral acquisition in the genus *Fusarium*. However, 4 HEGs showed higher similarity to sequences from distantly related species than to those found in the other Fusaria, suggesting their more recent acquisitions from distantly related donors. These include LAGLIDADG HEGs found in introns: *i1nad5, i3cox1*, *i13cox1* and single *i14cox1* GIY-YIG HEG. To test their horizontal transfer, we attempted to construct maximum-likelihood (ML) amino acid trees using GenBank records covering at least 85% of the query protein sequence (**Figures 2–5**).

Phylogenetic analyses provided strong evidence for horizontal gene transfer in the case of *i1nad5* LAGLIDADG HEG (**Figure 2**). On this particular tree, the LAGLIDADGs from different Fusaria are scattered in three different well-supported clades together with HEGs harbored by more distantly fungi such as *Bipolaris cookei*, *Chrysoporthe austroafricana*, *Coniothyrium glycines*, *Pithomyces chartarum*, and *Scytalidium* sp. Maximum Likelihood analyses also provided strong evidence for different evolutionary histories of two *i3cox1* LAGLIDADG HEGs present in *F. pseudograminearum* and in *F. solani*. Phylogenetic trees depict that both HEGs cluster into a different clades (**Figure 3**).

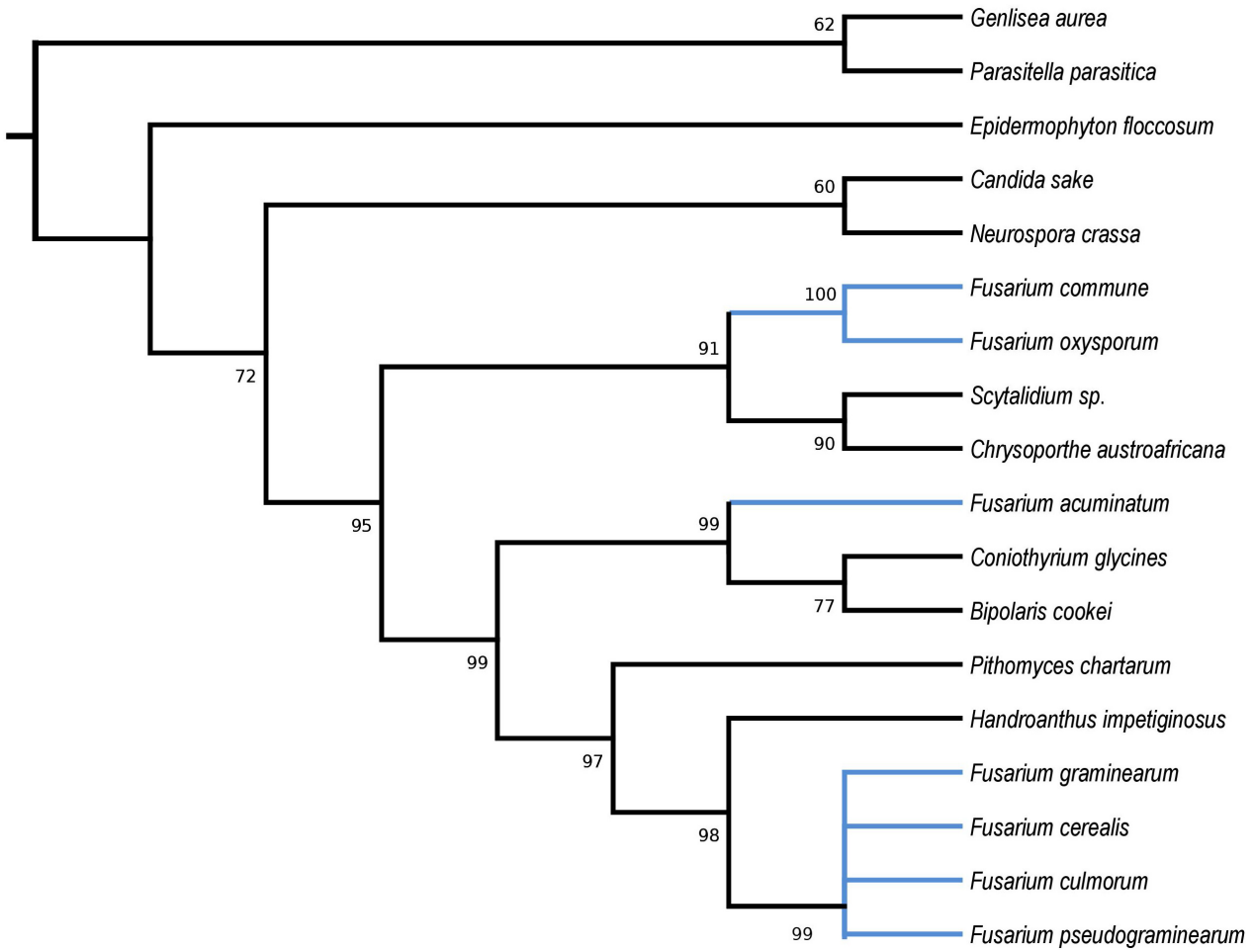

FIGURE 2 | Maximum Likelihood tree inferred from *i1nad5* LAGLIDADG HEG. GenBank accession numbers are given in brackets *Bipolaris cookie* (YP_009445560.1), *Candida sake* (YP_008475145.1), *Chrysoporthe austroafricana* (YP_009262028.1), *Coniothyrium glycines* (YP_009543504.1), *Epidermophyton floccosum* (YP_313631.1), *Fusarium acuminatum* (CDL73463.1), *Fusarium cerealis* (YP_009741100.1), *Fusarium commune* (YP_009437834.1), *Fusarium culmorum* (CDL73494.1), *Fusarium graminearum* (YP_001249315.1), *Fusarium oxysporum* (ATG24573.1), *Fusarium pseudograminearum* (CDL72485.1), *Genlisea aurea* (EPS67323.1), *Handroanthus impetiginosus* (PIM96989.1), *Neurospora crassa* (YP_009126712.1), *Parasitella parasitica* (YP_009059710.1), *Pithomyces chartarum* (YP_009415186.1), and *Scytalidium* sp. (QDG01253.1).

The HEG found in *F. pseudograminearum* forms a single cluster with *Hypomyces aurantius*, while the *F. solani* HEG shows its closest relationship to orthologs found in *Aspergillus* spp. However, phylogenetic analysis failed to support a different phylogenetic history of *i13cox1* HEG in Fusaria. Many nodes on the tree had low bootstrap support (**Figure 4**). **Supplementary File 4b** depicts distribution of this HEG among fungal lineages. It displays high conservation among *F. cerealis*, *F. culmorum*, *F. graminearum* s.s., *F. pseudograminearum, F. circinatum* and *F. temperatum* (Identity = 90–100%, q-cover = 89–100%, *E*-value = 0), but only 61% identity to HEG found in *F. acuminatum*. BlastP analyses indicated its higher similarity (70–76%) to orthologs present in more distantly species such as *Hypomyces aurantius*, *Ceratocystis cacaofunesta*, *Peltigera malacea*, *Arthrobotrys* spp., *Glarea lozoyensis*, *Cladonia* spp., *Termitomyces* sp., *Rhynchosporium* spp. and *Pithomyces chartarum*. We hypothesize that the incorrect conclusion from this phylogenetic analysis may be likely due to high divergence within groups and a reduced number of taxa in the data set. The evidence for horizontal transfer of HEG between different fungal species is also indicated in the case of the *i14cox1* GIY-YIG HEG tree by demonstrating a closer relationship of *F. circinatum*/*F. temperatum* to *Epichloe typhina* than to the remaining Fusaria (**Figure 5**).

The Majority of MGEs Show Highly Conserved Distribution in *Fusarium* Strains/Species

Twenty-six introns and 27 HEGs were shared by all fungal strains. The majority of them showed high sequence conservation. Eleven from these introns showed very high similarity with no size variation and pairwise identity ranging from 99.9 to 100%.

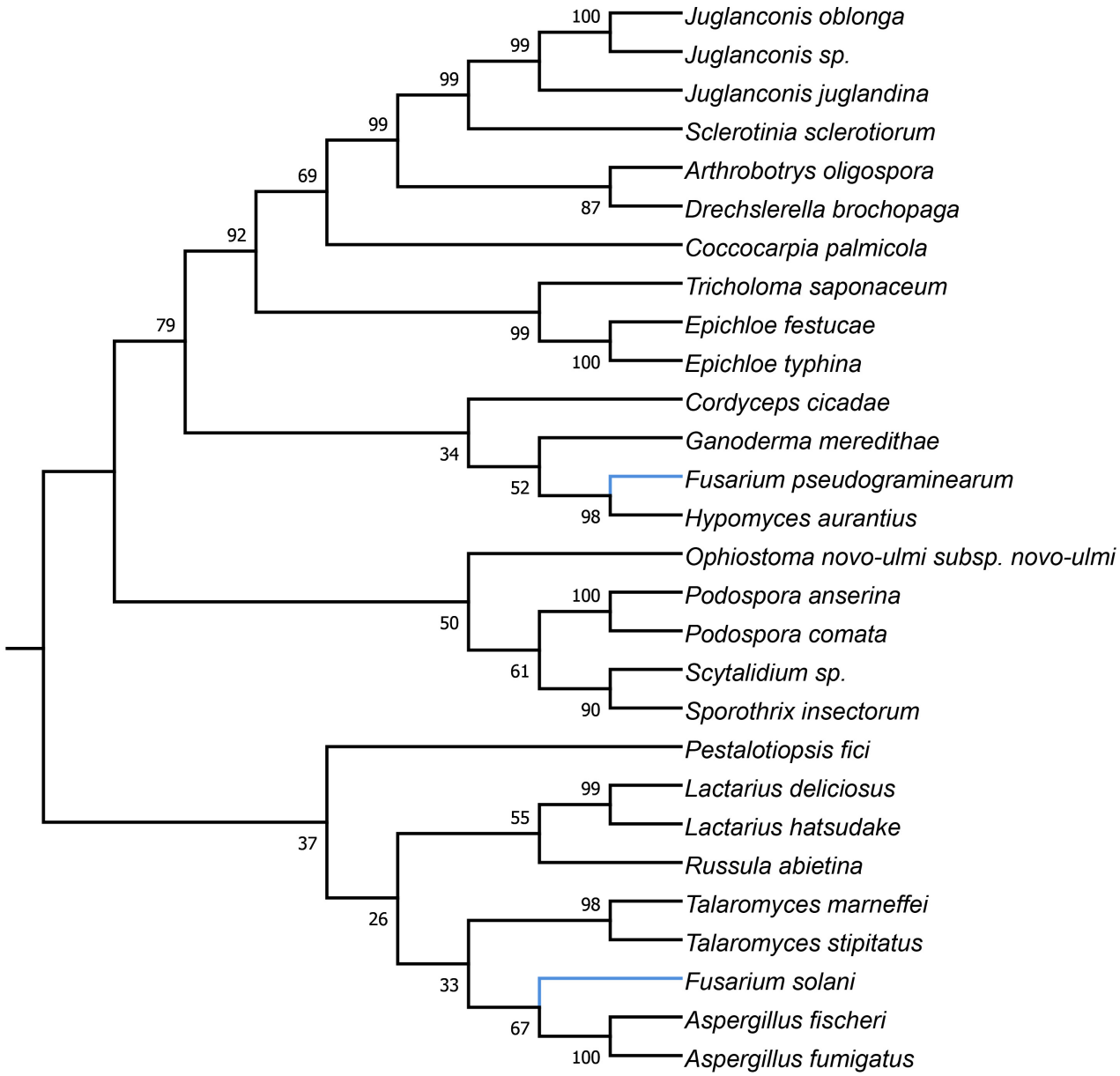

FIGURE 3 | Maximum Likelihood tree inferred from *i3cox1* LAGLIDADG HEG. GenBank accession numbers are given in brackets *Arthrobotrys oligospora* (QID02895.1), *Aspergillus fischeri* (AFD95944.1), *Aspergillus fumigatus* (YP_005353060.1), *Coccocarpia palmicola* (YP_009355407.1), *Cordyceps cicadae* (YP_009577892.1), *Drechslerella brochopaga* (QCW06877.1), *Drechslerella brochopaga* (YP_009568474.1), *Epichloe festucae* (YP_009327861.1), *Epichloe typhina* (YP_009327804.1), *Fusarium pseudograminearum* (QID41639.1), *Fusarium solani* (YP_005088111.1), *Ganoderma meredithae* (YP_009129958.1), *Hypomyces aurantius* (YP_009254043.1), *Juglanconis juglandina* (ATI20474.1), *Juglanconis oblonga* (ATI20215.1), *Juglanconis* sp. (ATI20300.1), *Lactarius deliciosus* (YP_009498182.1), *Lactarius hatsudake* (YP_009504192.1), *Ophiostoma novo-ulmi* (AVD96803.1), *Pestalotiopsis fici* (YP_009317077.1), *Podospora anserina* (NP_074927.1), *Podospora comata* (YP_009550011.1), *Russula abietina* (YP_009487192.1), *Sclerotinia sclerotiorum* (YP_009389070.1), *Scytalidium* sp. (QDG01205.1), *Sporothrix insectorum* (QGX43780.1), *Talaromyces marneffei* (NP_943724.1), *Talaromyces stipitatus* (AFD95918.1), and *Tricholoma saponaceum* (QIC20272.1).

12 introns displayed some size variation due to small, strain-dependent indels mostly below 100 bp in size. When excluding indel variation, their nucleotide diversity was very low, with pairwise identity above 99%. The last three introns: the *i11cox1*, the *i4cob* intron, and the *i1atp6* intron showed huge size variation (**Supplementary Files 2a, 4a, 5a**). Among these conserved introns, all contained two LAGLIDADGs among which the first was conserved (invariably present in all studied strains), while the second one (optional) was irregularly distributed among the strains, presumably due to independent of introns spread of HEGs. However, the distribution of optional HEGs across multiple strains was low. An optional *i11bcox1* LAGLIDADG

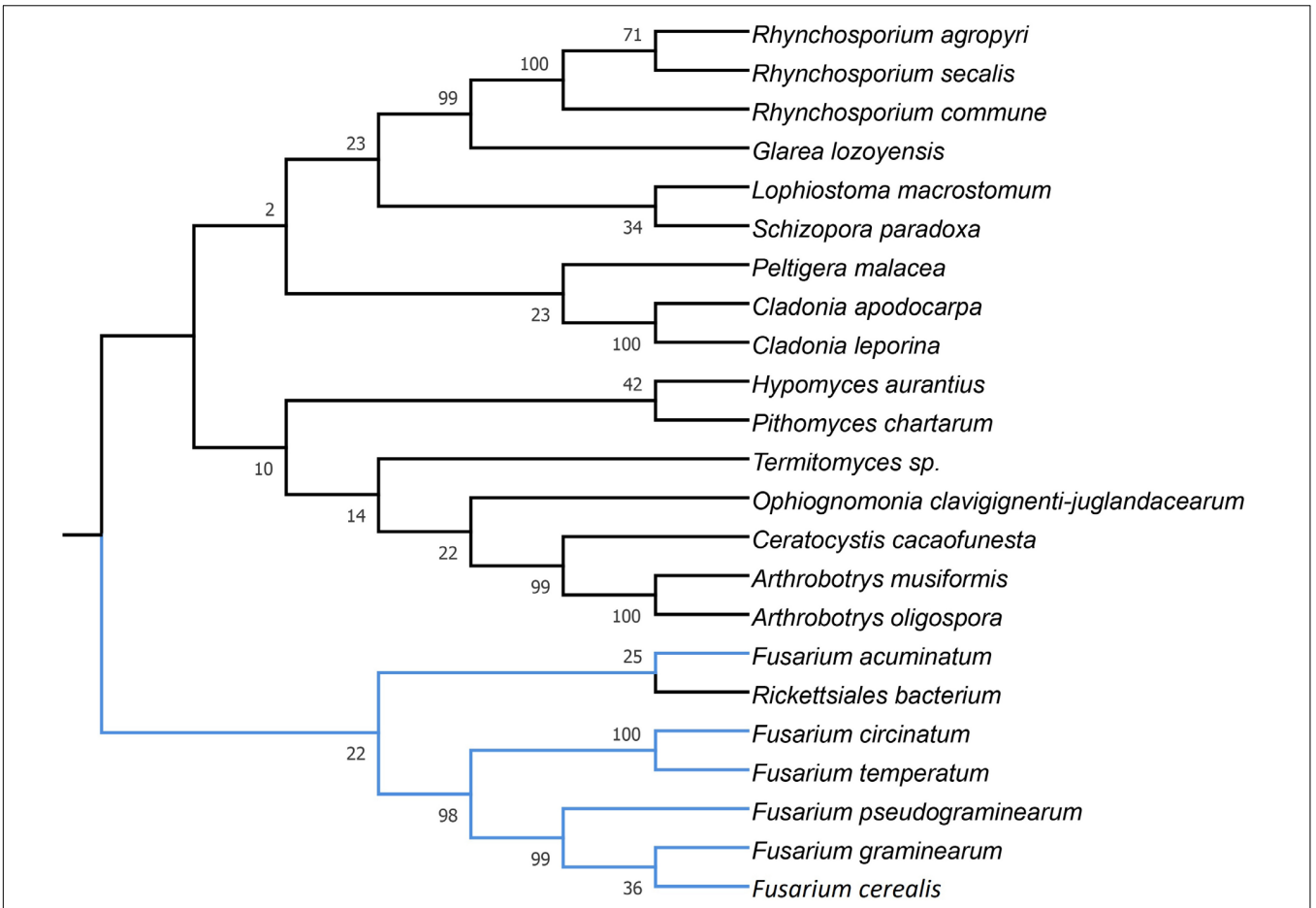

FIGURE 4 | Maximum Likelihood tree inferred from *i13cox1* LAGLIDADG HEG. GenBank accession numbers are given in brackets *Arthrobotrys musiformis* (YP_009574367.1), *Arthrobotrys oligospora* (QID02793.1), *Ceratocystis cacaofunesta* (YP_007507075.1), *Ceratocystis cacaofunesta* (YP_007507075.1), *Cladonia apodocarpa* (YP_009514117.1), *Cladonia leporina* (YP_009526663.1), *Fusarium acuminatum* (CDL73453.1), *Fusarium circinatum* (YP_008757706.1), *Fusarium cerealis* (YP_009741121.1), *Fusarium graminearum* (YP_001249335.1), *Fusarium pseudograminearum* (CDL72517.1), *Fusarium temperatum* (AKM98021.1), *Glarea lozoyensis* (AGN74496.1), *Glarea lozoyensis* (YP_009306750.1), *Hypomyces aurantius* (YP_009254047.1), *Lophiostoma macrostomum* (KAF2647136.1), *Ophiognomonia clavigignenti-juglandacearum* (ATI20563.1), *Peltigera malacea* (YP_005351183.1), *Pithomyces chartarum* (YP_009415166.1), *Rhynchosporium agropyri* (YP_008965308.1), *Rhynchosporium commune* (YP_008965356.1), *Rhynchosporium secalis* (YP_008965429.1), *Rickettsiales bacterium* (RYE15942.1), *Schizopora paradoxa* (YP_009690425.1), and *Termitomyces* sp. (AYE93211.1).

HEG (318 aa) was found in only one fungal mitogenome (CBS 119173). Only four fungal strains (all *F. pseudograminearum*) harbored optional LAGLIDADG HEG (387 aa) in the *atp6* gene. The occurrence of the third optional *i4cob* LAGLIDADG HEG (252 aa) was more frequent, but still low, being found in 14% of strains. We also found that the unexceptionally short (112 aa) *i4cob* HEG displays optional distribution among fungal strains and was more frequent than the other optional HEGs being found in 27% of strains (**Supplementary Files 1, 2a**).

HEG Content Variation Between in *F. culmorum* and in *F. graminearum* s.s.

Among 53 HEGs identified in introns, 26 were optional (irregularly distributed among all strains). We analyzed their distribution in the context of species-specific occurrence in *F. culmorum* and in *F. graminearum* s.s. Mitogenomes of *F. cerealis* and *F. pseudograminearum* were not analyzed in the context of species-specific distribution of MGEs due to low number of representative strains. We found that among these optional HEGs, one located in *i3acox2* intron was fixed in *F. culmorum* (**Supplementary Files 3a,b**). We also found another *i4cox3* LAGLIDADG HEG in *F. culmorum* which was absent in four closely related Fusaria, but BlastP searches indicated its presence in other, more distantly *F. solani* (**Supplementary Files 3a,b**), however, with 23% difference in protein identity scores. Noteworthy, its nucleotide sequence appears to be highly conserved in *F. culmorum* fulfilling criterion of diagnostic marker, which should display enough conservation to achieve less variability within species than between species (Raja et al., 2017).

The absence of unique MGEs in *F. graminearum* s.s. prompted us to search for unique MGE patterns in *F. graminearum* s.s. Among protein-coding genes, we found that intron content

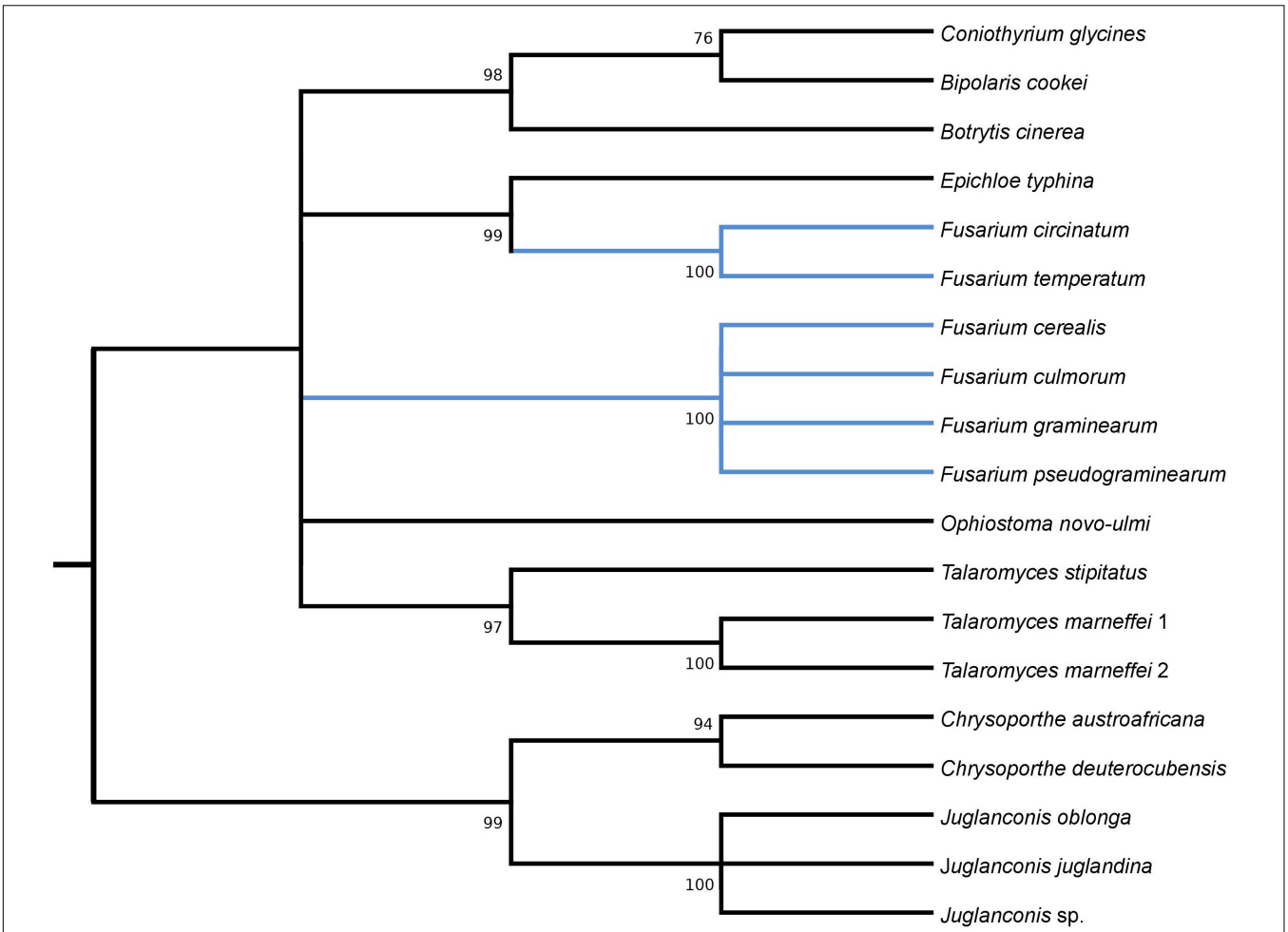

FIGURE 5 | Maximum Likelihood tree inferred from *i14cox1* GIY-YIG HEG. GenBank accession numbers are given in brackets *Bipolaris cookei* (YP_009445523.1), *Botrytis cinerea* (AGN49010.1), *Chrysoporthe austroafricana* (YP_009262000.1), *Chrysoporthe deuterocubensis* (YP_009262086.1), *Coniothyrium glycines* (YP_009543497.1), *Epichloe typhina* (YP_009327808.1), *Fusarium cerealis* (YP_009741122.1), *Fusarium culmorum* (CDL73523.1), *Fusarium graminearum* (YP_001249336.1), *Fusarium pseudograminearum* (QID41650.1), *Fusarium circinatum* (YP_008757707.1), *Fusarium temperatum* (AKM98023.1), *Juglanconis juglandina* (ATI20489.1), *Juglanconis oblonga* (ATI20223.1), *Juglanconis* sp. (ATI20312.1), *Ophiostoma novo-ulmi* (AVD96809.1), *Talaromyces marneffei* 1 (AFD95988.1), *Talaromyces marneffei* 2 (NP_943730.1), and *Talaromyces stipitatus* (AFD95924.1).

variation in *cox3* exhibits unique mosaicism in *F. graminearum* s.s. *Cox3* contains four introns (**Supplementary File 3a**), among which two: *i1cox3* and *i2cox3* are present in all species. The third *i3cox3* intron is present in *F. cerealis* and *F. pseudograminearum*, while the fourth the *i4cox3* is uniquely present in *F. culmorum*. Thus, the lack of these last two introns in *F. graminearum* s.s. determines a unique MGE pattern in *F. graminearum* s.s.

Besides HEGs found in protein-coding genes, the mitogenomes of three Fusaria (*F. cerealis, F. culmorum*, and *F. pseudograminearum*) contained an approximately 1895 bp insertion between *cox2* and *nad4L*, which is absent in *F. graminearum* s.s. This insertion harbors two ORFs: ORF 313 (942 bp) and ORF 132 (399 bp), both encoding LAGLIDADG HEGs. From a diagnostic point of view, the absence of these two HEGs in *F. graminearum* s.s. also appears to be promising diagnostic features separating *F. graminearum* s.s. from the remaining three species.

DISCUSSION

Highly sensitive and precise detection and quantification of fungi are critical to support diagnosis for disease surveillance. Therefore, this research field has been revolutionized by the advent of molecular markers (Tsui et al., 2011). However, the detection of fungi is still a challenge, because fungal biomass is often present at very low and uneven concentrations in environmental or clinical samples. For that reason, the use of DNA extraction methods facilitating efficient recovery of fungal DNA is highly recommended, however, with even highly efficient extraction techniques, low amounts of fungal DNA are often extracted in the presence of large amounts of

background DNA, hampering largely the sensitivity of the assays (Wickes and Wiederhold, 2018).

The use of assays targeting repeated genomic sequences such as internal transcribed spacer (ITS) of the rRNA region (official fungal barcode) provides one of the best solutions to this problem (Yang et al., 2018). Unfortunately, ITS fails to delineate most agriculturally important *Fusarium* species (Schoch et al., 2012). Consequently, for most Fusaria, diagnostic markers enabling their species-specific identification, have been developed based on single-copy nuclear loci (Nicolaisen et al., 2009; O'Donnell et al., 2015), which can limit successful detection of low amounts of fungal biomass (Kulik et al., 2015; Bilska et al., 2018b).

Targeting mitochondrial DNA could be a viable solution due to its high copy number in fungal cells (Krimitzas et al., 2013). The use of mtDNA for barcoding of fungi has been studied more than a decade ago (Seifert et al., 2007). In one of the first in-depth studies, it was demonstrated that the standard animal barcode *cox1* could be highly effective in the resolution of *Penicillium* species. However, *cox1* showed significant diagnostic limitations for *Fusarium* fungi (Gilmore et al., 2009) mostly due to the presence of paralogous copies of *cox1* in studied strains and low species resolution. Besides, one of the major shortcomings of mitogenome-based studies in fungi is the difficulty in obtaining amplicons for further sequencing, mainly due to large indel polymorphism associated with irregular distribution of MGEs. Further study of Santamaria et al. (2009) showed that most mitochondrial genes of *Ascomycota* fungi contain MGEs, which largely limits their potential use for barcoding purposes.

Emerging next-generation sequencing provides a new opportunity for the rapid characterization of fungal mitogenomes. Mitogenomes can be assembled from the whole genome reads via either *de novo* assemblies or mapping to a reference genome (Tenaillon et al., 2011) providing an unbiased look into the patterns of MGE diversity. It is worth noting that exploration of this type of diversity on species or population level was previously not possible due to low numbers of complete mitogenomes. In one of the first large-scale studies on budding yeast, *Saccharomyces cerevisiae*, Wolters et al. (2015) revealed that the distribution of certain MGEs follows species divisions and even exhibits population-specific profiles. Further, but still, very limited studies on plant pathogenic fungi appeared to support this evidence. Despite the observed strain-dependent variation in MGE content, some of these elements appear to show species-specific occurrence in *F. oxysporum* (Brankovics et al., 2017), *Fusarium fujikuroi* species complex (FFSC) (Fourie et al., 2018) or more distantly related *Colletotrichum* spp. (Liang et al., 2017). In this study, we identified a single *i3acox2* HEG displaying species-specific conservation in *F. culmorum* (**Supplementary Files 3a,b**). A previous study by Bilska et al. (2018b) demonstrated that targeting of this HEG through qPCR technology offers highly specific and sensitive quantification of *F. culmorum*.

We found that positions of MGEs were highly conserved among different strains. More than half of introns ($n = 26$) were found in *cox* genes (**Supplementary Files 2a–6a**), which is in line with accumulating evidence from various fungal lineages confirming remarkably high density in MGE content in especially *cox1* (Sandor et al., 2018; Zubaer et al., 2018; Pogoda et al., 2019). This, however, is notably in contrast to recent findings which showed that other Fusaria display rather low intron density within their *cox* genes, which can be even intronless in species from *F. oxysporum* (Brankovics et al., 2017) and *Fusarium fujikuroi* species complex (FFSC) (Fourie et al., 2018). However, it is worth to note that mitogenomes of the strains analyzed in our study are MGE−rich in comparison with previously studied Fusaria (Brankovics et al., 2017; Fourie et al., 2018). Notably, there were large differences in frequency distribution of MGEs. The vast majority of them occur at relatively higher frequencies compared to others, such as the *iIIcob* intron or the *i11bcox1* LAGLIDADG HEG (318 aa), raising the question on their role in gene regulation and their maintenance through selection (Guha et al., 2018; Zubaer et al., 2018).

We found that among 53 HEGs identified in introns, 9 showed irregular distribution within *F. graminearum* s.s., and only 4 within *F. culmorum* (**Supplementary Files 2a–6a**). The increased variation in HEG content within *F. graminearum* s.s. may be explained by its recombining reproductive behavior (outcrossing) (Trail, 2009; Talas and McDonald, 2015), which is assumed to favor intron mobility (Hausner, 2003). Unlike in *F. graminearum* s.s., no evidence of sexual reproduction was found in both *F. culmorum* and *F. cerealis* (Leslie and Summerell, 2008; Scherm et al., 2013). Sexual recombination can occur in *F. pseudograminearum*; however, it was rarely observed under field conditions (Summerell et al., 2001). Previous population genomic analyses by Kelly and Ward (2018) (restricted to North American populations) showed that in *F. graminearum* s.s., gene content variation in the nuclear genome displays population-specific patterns of conservation. We attempted to find out if variation in the MGE content shows population-specific profiles. To achieve it, we investigated if the distribution of optional HEGs reflects the geographic origin of the strains. We found that such a link does not exist. The same HEG patterns could be found in strains originated from distant geographic locations as in strains isolated from the same and even relatively small geographic locations (e.g., Luxembourg), which is indicative of low mobility of ancestrally acquired MGEs shared by different populations of this phylogenetic species. Our findings are, however, in sharp contrast to previous survey on *Saccharomyces cerevisiae* showing that the MGEs can be distributed in a population-specific manner (Wolters et al., 2015).

Assuming low mobility of MGEs in Fusaria, it could be speculated that HEG content variation will not follow cryptic divergence of other phylogenetic species from the *Fusarium graminearum* species complex (FGSC). Until now, only one complete mitogenome of *F. gerlachii* (Kulik et al., 2016b) is available in the GenBank database. Indeed, analysis of its mitogenome did not reveal unique MGEs separating *F. gerlachii* from *F. graminearum* s.s. (**Supplementary Files 2b–6b**). Besides MGE content variation, we previously showed that SNP polymorphism found in conserved introns can facilitate design of species-specific markers in FGSC. A previously developed mitochondrial-based qPCR assay has been designed based on such a polymorphism for species-specific detection and quantification of *F. graminearum* s.s. (Kulik et al., 2015).

The assay has been demonstrated not to interfere with other phylogenetic species from FGSC, which indicates that this type of polymorphism could be useful in the assessment of cryptic diversity in Fusaria. This issue will need to be fully addressed in our further studies by analysis of mitogenomes from all known cryptic species from FGSC.

Blast alignments are commonly employed to reveal different evolutionary histories of genes (Zhu et al., 2014). In this study, protein homology searches in GenBank database showed that most HEGs found in four *Fusarium* species are shared with other fungal species (**Supplementary Files 2b–6b**). This variation was very low when comparing HEG orthologs from closely related *F. cerealis*, *F. culmorum*, *F. gerlachii*, *F. graminearum* s.s. and *F. pseudograminearum*, and increased when including other Fusaria. In most cases variation in protein identity scores was highest for HEG orthologs from other fungal genera, which is indicative of an ancestral acquisition of HEGs in the genus *Fusarium*.

MGEs, when fixed in population, are susceptible to degeneration. To ensure their survival, these elements can spread to new populations or even horizontally across species (Koufopanou et al., 2002; Wu and Hao, 2014). HEGs are well-adapted for horizontal transmission by the maintenance of highly conserved recognition sequences and the conserved nucleotide sites most critical for homing (Koufopanou et al., 2002). However, in this study, we found, that among a total of 53 HEGs, only 4 showed hallmarks of horizontal mobility across different fungi (**Figures 2**–**5**). Our analyses also suggest two cross-kingdom horizontal gene transfer events (**Figures 2**, **4**). The first one is indicated by a higher (66.91%) protein identity (q-cover = 88%, *E* value = 3e-115) of *i1nad5* LAGLIDADG HEG (**Supplementary Files 6a,b**) to the plant ortholog (PIM96989.1) found in *Handroanthus impetiginosus* than to the other fungal orthologs. The second event is indicated by higher (63.6%) identity of *i13cox1* LAGLIDADG HEG (**Supplementary Files 4a,b**) to ortholog found in *Rickettsiales bacterium* (RYE15942.1) (q-cover = 94%, *E* value = 9e-174) than to the other fungal derived orthologs. BlastP searches showed that both HEGs gave no significant BLAST hits in species outside fungi, which suggests a cross-kingdom jump from a fungal donors to the plants (PIM96989.1) and alphaproteobacteria (RYE15942.1).

Overall, our results presented in this study demonstrate that the MGE diversity in fungal mitogenomes may lead to the development of novel diagnostic markers offering improved detection of fungi. Diagnostic markers for pathogenic fungi need to be tested against the range of strains from different geographical origins to ensure their uniformity. The geographically diverse mitogenomes provide valuable resources for the marker design. However, in case of *F. cerealis* and *F. pseudograminearum* more strains are needed for robust conclusions. Today, mitochondrial-based qPCR assays are available for both *F. culmorum* and *F. graminearum* s.s. (Kulik et al., 2015; Bilska et al., 2018b). qPCR remains a valuable option due to the ability to quantify fungal DNA, especially from difficult food or environmental samples from which extraction of high-molecular-weight DNA is problematic. In addition, the increased sensitivity of mitochondrial-based markers may reduce the incidence of scoring errors, making interpretation qPCR results less error-prone. Besides qPCR, other promising techniques such as loop-mediated isothermal amplification (LAMP) may be also considered (Panek and Frac, 2019). Among a number of molecular methods for the identification of fungi, barcoding DNA provides the best potential for biodiversity monitoring (Begerow et al., 2010). However, it would require multiple group-specific primers for sequencing of MGEs-barcodes, which is nowadays time-consuming and cost-intensive. Whatever the method, the revealed strong evidence for species-specific polymorphism in fungal mitogenomes opens entirely new perspectives to fungal diagnostics, which can be of great benefit in the field of agriculture and food security when highly sensitive detection of fungi is needed.

CONCLUSION

Mitogenomes of *F. culmorum* and *F. graminearum* s.s. are MGE-rich and harbor especially group I introns encoding LAGLIDADG and GIY-YIG HEGs. The majority of mitochondrial MGEs showed a highly conserved distribution in all studied strains. MGEs present in these species can be found in other Fusaria and in other fungal genera with considerable variation in protein identity scores. Intraspecies variation in MGE content is more evident in *F. graminearum* s.s. than in *F. culmorum* but is indicative of ancestral mosaicism of HEGs shared by different fungal populations. Among optional HEGs, one exhibits species-specific conservation in *F. culmorum*. *F. graminearum* s.s. does not harbor unique MGEs throughout the mitogenome, however, MGE patterns in *cox3* and in the intergenic spacer between *cox2* and *nad4L* may support identification of this species.

DATA AVAILABILITY STATEMENT

The datasets generated for this study can be found in the NCBI GenBank database. MT036635, MT036636, MT036637, MT036638, MT036639, MT036640, MT036641, MT036642, MT036643, MT036644, MT036645, MT036646, MT036647, MT036648, MT036649, MT036650, MT036651, MT036652, MT036653, MT036654, MT036655, MT036656, MT036657, MT036658, MT036659, MT036660, MT036661, MT036662, MT036663, MT036664, MT036665, MT036666, MT036667, MT036668, MT036669, MT036670, MT036671, MT036672, MT036673, MT036674, MT036675, MT036676, MT036677, MT036678, MT036679, MT036680, MT036681, MT036682, MT036683, MT036684, MT036685, MT036686, MT036687, MT036688, MT036689, MT036690, MT036691, MT036692, MT036693, MT036694, MT036695, MT036696, MT036697, MT036698, MT036699, MT036701, MT036702, MT036703, MT036704, MT036705, MT036706, MT036707, MT036708, MT036709, MT036710, MT036711, MT036712, MT036713, MT036714, MT036715, MT036716, MT036717, MT036718, MT036719, MT036720, MT036721, MT036722, MT036723, MT036724, MT036725, MT036726, MT036727, MT036728,

MT036729, MT036730, MT036731, MT036732, MT036733, MT036734, MT036735, MT036736, MT036737, MT036738, MT036739, MT036740, MT036741, MT036742, MT036743, MT036744, MT036745, MT036746, MT036747, MT036748, MT036749, MT036750, MT036751, MT036752, MT036753, MT036754, MT036755, MT036756, and MT036757.

AUTHOR CONTRIBUTIONS

TK was responsible for the study design and wrote the manuscript. TK, AD, KB, MŻ, AS, SS, MB, MP, and AB-C contributed the isolation and strain growth. KB and MŻ extracted fungal DNA and prepared a library for whole-genome sequencing. TK and BB assembled the mitogenomes. BB, KM, and TM performed the mitogenome annotation. JS performed the phylogenetic analysis. AD, AS, KB, MB, MP, MŻ, and JS contributed the manuscript editing of relevant sections. JW edited supplementary files.

FUNDING

This research was funded by the National Science Center, Poland, grant number 2015/19/B/NZ9/01329. MB acknowledges the financial support of the project "Sentinelle" by the Administration des Services Techniques de l'Agriculture of Luxembourg.

SUPPLEMENTARY MATERIAL

The Supplementary Material for this article can be found online at: https://www.frontiersin.org/articles/10.3389/fmicb.2020.01002/full#supplementary-material

REFERENCES

Aguileta, G., de Vienne, D. M., Ross, O. N., Hood, M. E., Giraud, T., Petit, E., et al. (2014). High variability of mitochondrial gene order among fungi. *Genome Biol. Evol.* 6, 451–465. doi: 10.1093/gbe/evu028

Al-Reedy, R. M., Malireddy, R., Dillman, C. B., and Kennell, J. C. (2012). Comparative analysis of *Fusarium* mitochondrial genomes reveals a highly variable region that encodes an exceptionally large open reading frame. *Fungal Genet. Biol.* 49, 2–14. doi: 10.1016/j.fgb.2011.11.008

Amarasinghe, C. C., Tittlemier, S. A., and Fernando, W. G. D. (2015). Nivalenol-producing *Fusarium cerealis* associated with *fusarium* head blight in winter wheat in Manitoba, Canada. *Plant Pathol.* 64, 988–995. doi: 10.1111/ppa.12329

Bartelli, T. F., Bruno, D. C. F., and Briones, M. R. S. (2018). Evidence for mitochondrial genome methylation in the yeast *Candida albicans*: a potential novel epigenetic mechanism affecting adaptation and pathogenicity? *Front. Genet.* 9:166. doi: 10.3389/fgene.2018.00166

Basse, C. W. (2010). Mitochondrial inheritance in fungi. *Curr. Opin. Microbiol.* 13, 321–326. doi: 10.1016/j.mib.2010.09.003

Begerow, D., Nilsson, H., Unterseher, M., and Maier, W. (2010). Current state and perspectives of fungal DNA barcoding and rapid identification procedures. *Appl. Microbiol. Biotechnol.* 87, 99–108. doi: 10.1007/s00253-010-2585-4

Bilska, K., Jurczak, S., Kulik, T., Ropelewska, E., Olszewski, J., Zelechowski, M., et al. (2018a). Species composition and trichothecene genotype profiling of *Fusarium* field isolates recovered from wheat in Poland. *Toxins* 10:325. doi: 10.3390/toxins10080325

Bilska, K., Kulik, T., Ostrowska-Kolodziejczak, A., Busko, M., Pasquali, M., Beyer, M., et al. (2018b). Development of a highly sensitive FcMito qPCR assay for the quantification of the toxigenic fungal plant pathogen *Fusarium culmorum*. *Toxins* 10:211. doi: 10.3390/toxins10050211

Brankovics, B., Kulik, T., Sawicki, J., Bilska, K., Zhang, H., de Hoog, G. S., et al. (2018). First steps towards mitochondrial pan-genomics: detailed analysis of *Fusarium graminearum* mitogenomes. *PeerJ* 6:e5963. doi: 10.7717/peerj.5963

Brankovics, B., van Dam, P., Rep, M., de Hoog, G. S., van der Lee, T. A. J., Waalwijk, C., et al. (2017). Mitochondrial genomes reveal recombination in the presumed asexual *Fusarium oxysporum* species complex. *BMC Genomics* 18:735. doi: 10.1186/s12864-017-4116-5

Bullerwell, C. E., and Lang, B. F. (2005). Fungal evolution: the case of the vanishing mitochondrion. *Curr. Opin. Microbiol.* 8, 362–369. doi: 10.1016/j.mib.2005.06.009

Calderone, R., Li, D. M., and Traven, A. (2015). System-level impact of mitochondria on fungal virulence: to metabolism and beyond. *FEMS Yeast Res.* 15:fov027. doi: 10.1093/femsyr/fov027

Chatre, L., and Ricchetti, M. (2014). Are mitochondria the Achilles' heel of the Kingdom Fungi? *Curr. Opin. Microbiol.* 20, 49–54. doi: 10.1016/j.mib.2014.05.001

Darling, A. E., Mau, B., and Perna, N. T. (2010). progressiveMauve: multiple genome alignment with gene gain, loss and rearrangement. *PLoS One* 5:e11147. doi: 10.1371/journal.pone.0011147

Desjardins, A. E. (2006). *Fusarium* mycotoxins: chemistry, genetics, and biology. *Am. Phytopathol. Soc.* 56:337. doi: 10.1111/j.1365-3059.2006.01505.x

Dierckxsens, N., Mardulyn, P., and Smits, G. (2017). NOVOPlasty: de novo assembly of organelle genomes from whole genome data. *Nucleic Acids Res.* 45:e18. doi: 10.1093/nar/gkw955

Dubos, T., Pogoda, F., Ronellenfitsch, F. K., Junk, J., Hoffmann, L., and Beyer, M. (2012). Fractal dimension and shape parameters of asexual *Fusarium* spores from selected species: Which can be distinguished? *J. Plant Dis. Prot.* 119, 8–14. doi: 10.1007/BF03356413

Edgell, D. R. (2009). Selfish DNA: homing endonucleases find a home. *Curr. Biol.* 19, R115–R117. doi: 10.1016/j.cub.2008.12.019

Fourie, G., van der Merwe, N. A., Wingfield, B. D., Bogale, M., Tudzynski, B., Wingfield, M. J., et al. (2013). Evidence for inter-specific recombination among the mitochondrial genomes of *Fusarium* species in the *Gibberella fujikuroi* complex. *BMC Genomics* 14:605. doi: 10.1186/1471-2164-14-605

Fourie, G., Van der Merwe, N. A., Wingfield, B. D., Bogale, M., Wingfield, M. J., and Steenkamp, E. T. (2018). Mitochondrial introgression and interspecies recombination in the *Fusarium* fujikuroi species complex. *IMA Fungus* 9, 37–48. doi: 10.5598/imafungus.2018.09.01.04

Franco, M. E. E., Lopez, S. M. Y., Medina, R., Lucentini, C. G., Troncozo, M. I., Pastorino, G. N., et al. (2017). The mitochondrial genome of the plant-pathogenic fungus *Stemphylium lycopersici* uncovers a dynamic structure due to repetitive and mobile elements. *PLoS One* 12:e0185545. doi: 10.1371/journal.pone.0185545

Geiser, D. M., Jimenez-Gasco, M. D., Kang, S. C., Makalowska, I., Veeraraghavan, N., Ward, T. J., et al. (2004). *FUSARIUM*-ID v. 1.0: a DNA sequence database for identifying *Fusarium*. *Eur. J. Plant Pathol.* 110, 473–479. doi: 10.1023/B:EJPP.0000032386.75915.a0

Gilmore, S. R., GrÄfenhan, T., Louis-Seize, G., and Seifert, K. A. (2009). Multiple copies of cytochrome oxidase 1 in species of the fungal genus *Fusarium*. *Mol. Ecol. Resour.* 9, 90–98. doi: 10.1111/j.1755-0998.2009.02636.x

Guha, T. K., Wai, A., Mullineux, S. T., and Hausner, G. (2018). The intron landscape of the mtDNA cytb gene among the Ascomycota: introns and intron-encoded open reading frames. *Mitochondrial DNA Part A* 29, 1015–1024. doi: 10.1080/24701394.2017.1404042

Haugen, P., Simon, D. M., and Bhattacharya, D. (2005). The natural history of group I introns. *Trends Genet.* 21, 111–119. doi: 10.1016/j.tig.2004.12.007

Hausner, G. (2003). Fungal mitochondrial genomes, plasmids and introns. *Appl. Mycol. Biotechnol.* 3, 101–131. doi: 10.1016/S1874-5334(03)80009-6

Hueza, I. M., Raspantini, P. C. F., Raspantini, L. E. R., Latorre, A. O., and Gorniak, S. L. (2014). Zearalenone, an estrogenic mycotoxin, is an immunotoxic compound. *Toxins* 6, 1080–1095. doi: 10.3390/toxins6031080

Joardar, V., Abrams, N. F., Hostetler, J., Paukstelis, P. J., Pakala, S., Pakala, S. B., et al. (2012). Sequencing of mitochondrial genomes of nine *Aspergillus* and *Penicillium* species identifies mobile introns and accessory genes as main sources of genome size variability. *BMC Genomics* 13:698. doi: 10.1186/1471-2164-13-698

Johnson, M., Zaretskaya, I., Raytselis, Y., Merezhuk, Y., McGinnis, S., and Madden, T. L. (2008). NCBI BLAST: a better web interface. *Nucleic Acids Res.* 36, 5–9. doi: 10.1093/nar/gkn201

Kazan, K., and Gardiner, D. M. (2018). *Fusarium* crown rot caused by *Fusarium pseudograminearum* in cereal crops: recent progress and future prospects. *Mol. Plant Pathol.* 19, 1547–1562. doi: 10.1111/mpp.12639

Kelly, A. C., and Ward, T. J. (2018). Population genomics of *Fusarium graminearum* reveals signatures of divergent evolution within a major cereal pathogen. *PLoS One* 13:e0194616. doi: 10.1371/journal.pone.0194616

Kolesnikova, A. I., Putintseva, Y. A., Simonov, E. P., Biriukov, V. V., Oreshkova, N. V., Pavlov, I. N., et al. (2019). Mobile genetic elements explain size variation in the mitochondrial genomes of four closely-related *Armillaria* species. *BMC Genomics* 20:351. doi: 10.1186/s12864-019-5732-z

Koufopanou, V., Goddard, M. R., and Burt, A. (2002). Adaptation for horizontal transfer in a homing endonuclease. *Mol. Biol. Evol.* 19, 239–246. doi: 10.1093/oxfordjournals.molbev.a004077

Krimitzas, A., Pyrri, I., Kouvelis, V. N., Kapsanaki-Gotsi, E., and Typas, M. A. (2013). A phylogenetic analysis of greek isolates of *Aspergillus* species based on morphology and nuclear and mitochondrial gene sequences. *Biomed Res. Int.* 2013:260395. doi: 10.1155/2013/260395

Kulik, T., Abarenkov, K., Buśko, M., Bilska, K., van Diepeningen, A. D., Ostrowska-Kołodziejczak, A., et al. (2017). ToxGen: an improved reference database for the identification of type B-trichothecene genotypes in *Fusarium*. *PeerJ* 5:e2992. doi: 10.7717/peerj.2992

Kulik, T., Brankovics, B., Sawicki, J., and van Diepeningen, A. (2016a). The complete mitogenome of *Fusarium culmorum*. *Mitochondrial DNA Part A* 27, 2425–2426. doi: 10.3109/19401736.2015.1030626

Kulik, T., Brankovics, B., Sawicki, J., and van Diepeningen, A. D. (2016b). The complete mitogenome of *Fusarium gerlachii*. *Mitochondrial DNA Part A* 27, 1895–1896. doi: 10.3109/19401736.2014.971275

Kulik, T., Ostrowska, A., Busko, M., Pasquali, M., Beyer, M., Stenglein, S., et al. (2015). Development of an FgMito assay: a highly sensitive mitochondrial based qPCR assay for quantification of *Fusarium graminearum* sensu stricto. *Int. J. Food Microbiol.* 210, 16–23. doi: 10.1016/j.ijfoodmicro.2015.06.012

Kumar, S., Stecher, G., Li, M., Knyaz, C., and Tamura, K. (2018). MEGA X: molecular evolutionary genetics analysis across computing platforms. *Mol. Biol. Evol.* 35, 1547–1549. doi: 10.1093/molbev/msy096

Leslie, J. F., and Summerell, B. A. (2008). *The Fusarium Laboratory Manual*. New York, NY: John Wiley & Sons.

Liang, X. F., Tian, X. L., Liu, W. K., Wei, T. Y., Wang, W., Dong, Q. Y., et al. (2017). Comparative analysis of the mitochondrial genomes of Colletotrichum gloeosporioides sensu lato: insights into the evolution of a fungal species complex interacting with diverse plants. *BMC Genomics* 18:171. doi: 10.1186/s12864-016-3480-x

Lin, R. M., Liu, C. C., Shen, B. M., Bai, M., Ling, J., Chen, G. H., et al. (2015). Analysis of the complete mitochondrial genome of *Pochonia chlamydosporia* suggests a close relationship to the invertebrate-pathogenic fungi in Hypocreales. *BMC Microbiol.* 15:5. doi: 10.1186/s12866-015-0341-8

Losada, L., Pakala, S. B., Fedorova, N. D., Joardar, V., Shabalina, S. A., Hostetler, J., et al. (2014). Mobile elements and mitochondrial genome expansion in the soil fungus and potato pathogen Rhizoctonia solani AG-3. *FEMS Microbiol. Lett.* 352, 165–173. doi: 10.1111/1574-6968.12387

Marchler-Bauer, A., and Bryant, S. H. (2004). CD-Search: protein domain annotations on the fly. *Nucleic Acids Res.* 32, W327–W331. doi: 10.1093/nar/gkh454

Mitchell, A., Chang, H. Y., Daugherty, L., Fraser, M., Hunter, S., Lopez, R., et al. (2015). The InterPro protein families database: the classification resource after 15 years. *Nucleic Acids Res.* 43, D213–D221. doi: 10.1093/nar/gku1243

Nicolaisen, M., Supronien, S., Nielsen, L. K., Lazzaro, I., Spliid, N. H., and Justesen, A. F. (2009). Real-time PCR for quantification of eleven individual *Fusarium* species in cereals. *J. Microbiol. Methods* 76, 234–240. doi: 10.1016/j.mimet.2008.10.016

O'Donnell, K., Ward, T. J., Robert, V., Crous, P. W., Geiser, D. M., and Kang, S. (2015). DNA sequence-based identification of *Fusarium*: current status and future directions. *Phytoparasitica* 43, 583–595. doi: 10.1007/s12600-015-0484-z

Panek, J., and Frac, M. (2019). Loop-mediated isothermal amplification (LAMP) approach for detection of heat-resistant Talaromyces flavus species. *Sci. Rep.* 9:5846. doi: 10.1038/s41598-019-42275-x

Pantou, M. P., Kouvelis, V. N., and Typas, M. A. (2008). The complete mitochondrial genome of *Fusarium oxysporum*: insights into fungal mitochondrial evolution. *Gene* 419, 7–15. doi: 10.1016/j.gene.2008.04.009

Pavesi, A., Conterio, F., Bolchi, A., Dieci, G., and Ottonello, S. (1994). Identification of new eukaryotic tRNA genes in genomic DNA databases by a multistep weight matrix anaylsis of transcriptional control regions. *Nucleic Acids Res.* 22, 1247–1256. doi: 10.1093/nar/22.7.1247

Pogoda, C. S., Keepers, K. G., Nadiadi, A. Y., Bailey, D. W., Lendemer, J. C., Tripp, E. A., et al. (2019). Genome streamlining via complete loss of introns has occurred multiple times in lichenized fungal mitochondria. *Ecol. Evol.* 9, 4245–4263. doi: 10.1002/ece3.5056

Raja, H. A., Miller, A. N., Pearce, C. J., and Oberlies, N. H. (2017). Fungal identification using molecular tools: a primer for the natural products research community. *J. Nat. Prod.* 80, 756–770. doi: 10.1021/acs.jnatprod.6b01085

Sandor, S., Zhang, Y. J., and Xu, J. P. (2018). Fungal mitochondrial genomes and genetic polymorphisms. *Appl. Microbiol. Biotechnol.* 102, 9433–9448. doi: 10.1007/s00253-018-9350-5

Santamaria, M., Vicario, S., Pappada, G., Scioscia, G., Scazzocchio, C., and Saccone, C. (2009). Towards barcode markers in Fungi: an intron map of Ascomycota mitochondria. *BMC Bioinformatics* 10:S15. doi: 10.1186/1471-2105-10-s6-s15

Scherm, B., Balmas, V., Spanu, F., Pani, G., Delogu, G., Pasquali, M., et al. (2013). *Fusarium culmorum*: causal agent of foot and root rot and head blight on wheat. *Mol. Plant Pathol.* 14, 323–341. doi: 10.1111/mpp.12011

Schoch, C. L., Seifert, K. A., Huhndorf, S., Robert, V., Spouge, J. L., Levesque, C. A., et al. (2012). Nuclear ribosomal internal transcribed spacer (ITS) region as a universal DNA barcode marker for Fungi. *Proc. Natl. Acad. Sci. U.S.A.* 109, 6241–6246. doi: 10.1073/pnas.1117018109

Seifert, K. A., Samson, R. A., DeWaard, J. R., Houbraken, J., Lévesque, C. A., Moncalvo, J. M., et al. (2007). Prospects for fungus identification using CO1 DNA barcodes, with *Penicillium* as a test case. *Proc. Natl. Acad. Sci. U.S.A.* 104, 3901–3906. doi: 10.1073/pnas.0611691104

Shingu-Vazquez, M., and Traven, A. (2011). Mitochondria and fungal pathogenesis: drug tolerance, virulence, and potential for antifungal therapy. *Eukaryot. Cell* 10, 1376–1383. doi: 10.1128/ec.05184-11

Summerell, B. A., Burgess, L. W., Backhouse, D., Bullock, S., and Swan, L. J. (2001). Natural occurrence of perithecia of *Gibberella coronicola* on wheat plants with crown rot in Australia. *Australas. Plant Pathol.* 30, 353–356. doi: 10.1071/ap01045

Talas, F., and McDonald, B. A. (2015). Genome-wide analysis of *Fusarium graminearum* field populations reveals hotspots of recombination. *BMC Genomics* 16:996. doi: 10.1186/s12864-015-2166-0

Tenaillon, M. I., Hufford, M. B., Gaut, B. S., and Ross-Ibarra, J. (2011). Genome size and transposable element content as determined by high-throughput sequencing in maize and *Zea luxurians*. *Genome Biol. Evol.* 3, 219–229. doi: 10.1093/gbe/evr008

Trail, F. (2009). For blighted waves of grain: *Fusarium graminearum* in the postgenomics era. *Plant Physiol.* 149, 103–110. doi: 10.1104/pp.108.129684

Tsui, F., Wagner, M., Cooper, G., Que, J., Harkema, H., Dowling, J., et al. (2011). Probabilistic case detection for disease surveillance using data in electronic medical records. *Online J. Public Health Inform.* 3:ojhi.v3i3.3793. doi: 10.5210/ojphi.v3i3.3793

van der Lee, T., Zhang, H., van Diepeningen, A., and Waalwijk, C. (2015). Biogeography of *Fusarium graminearum* species complex and chemotypes: a review. *Food Addit. Contam. Part A Chem. Anal. Control Expo. Risk Assess.* 32, 453–460. doi: 10.1080/19440049.2014.984244

Waalwijk, C., Kastelein, P., de Vries, I., Kerenyi, Z., van der Lee, T., Hesselink, T., et al. (2003). Major changes in *Fusarium* spp. in wheat in the Netherlands. *Eur. J. Plant Pathol.* 109, 743–754. doi: 10.1023/a:1026086510156

Waalwijk, C., van der Heide, R., de Vries, I., van der Lee, T., Schoen, C., Costrel-de Corainville, G., et al. (2004). Quantitative detection of *Fusarium* species in wheat using TaqMan. *Eur. J. Plant Pathol.* 110, 481–494. doi: 10.1023/b:ejpp.0000032387.52385.13

Wang, H., Xiao, M., Kong, F. R., Chen, S., Dou, H. T., Sorrell, T., et al. (2011). Accurate and practical identification of 20 *Fusarium* species by seven-locus sequence analysis and reverse line blot hybridization, and an in vitro antifungal susceptibility study. *J. Clin. Microbiol.* 49, 1890–1898. doi: 10.1128/jcm.02415-10

Wickes, B. L., and Wiederhold, N. P. (2018). Molecular diagnostics in medical mycology. *Nat. Commun.* 9:5135. doi: 10.1038/s41467-018-07556-5

Wolters, J. F., Chiu, K., and Fiumera, H. L. (2015). Population structure of mitochondrial genomes in Saccharomyces cerevisiae. *BMC Genomics* 16:451. doi: 10.1186/s12864-015-1664-4

Wu, B. J., and Hao, W. L. (2014). Horizontal transfer and gene conversion as an important driving force in shaping the landscape of mitochondrial introns. *G3* 4, 605–612. doi: 10.1534/g3.113.009910

Yang, R. H., Su, J. H., Shang, J. J., Wu, Y. Y., Li, Y., Bao, D. P., et al. (2018). Evaluation of the ribosomal DNA internal transcribed spacer (ITS), specifically ITS1 and ITS2, for the analysis of fungal diversity by deep sequencing. *PLoS One* 13:e206428. doi: 10.1371/journal.pone.0206428

Yin, L. F., Hu, M. J., Wang, F., Kuang, H. H., Zhang, Y., Schnabel, G., et al. (2012). Frequent gain and loss of introns in fungal cytochrome b genes. *PLoS One* 7:e49096. doi: 10.1371/journal.pone.0049096

Zhu, Q., Kosoy, M., and Dittmar, K. (2014). HGTector: an automated method facilitating genome-wide discovery of putative horizontal gene transfers. *BMC Genomics* 15:717. doi: 10.1186/1471-2164-15-717

Zubaer, A., Wai, A., and Hausner, G. (2018). The mitochondrial genome of *Endoconidiophora resinifera* is intron rich. *Sci. Rep.* 8:17591. doi: 10.1038/s41598-018-35926-y

Conflict of Interest: The authors declare that the research was conducted in the absence of any commercial or financial relationships that could be construed as a potential conflict of interest.

frontiers in Microbiology

REVIEW
published: 29 May 2020
doi: 10.3389/fmicb.2020.00978

Fungal Mitogenomes: Relevant Features to Planning Plant Disease Management

*Rocio Medina[1], Mario Emilio Ernesto Franco[2], Laura Cecilia Bartel[1], Virginia Martinez Alcántara[3], Mario Carlos Nazareno Saparrat[3,4] and Pedro Alberto Balatti[1]**

[1] Centro de Investigaciones de Fitopatología, Comisión de Investigaciones Científicas de la Provincia de Buenos Aires (CIDEFI-CICPBA), Facultad de Ciencias Agrarias y Forestales, Universidad Nacional de La Plata, La Plata, Argentina, [2] Department of Biosystems Engineering, The University of Arizona, Tucson, AZ, United States, [3] Cátedra de Microbiología Agrícola, Facultad de Ciencias Agrarias y Forestales, Universidad Nacional de La Plata, La Plata, Argentina, [4] Instituto de Fisiología Vegetal (INFIVE), Consejo Nacional de Investigaciones Científicas y Técnicas (CONICET), Universidad Nacional de La Plata, La Plata, Argentina

Mitochondrial genomes (mt-genomes) are characterized by a distinct codon usage and their autonomous replication. Mt-genomes encode highly conserved genes (mt-genes), like proteins involved in electron transport and oxidative phosphorylation but they also carry highly variable regions that are in part responsible for their high plasticity. The degree of conservation of their genes is such that they allow the establishment of phylogenetic relationships even across distantly related species. Here, we describe the mechanisms that generate changes along mt-genomes, which play key roles at enlarging the ability of fungi to adapt to changing environments. Within mt-genomes of fungal pathogens, there are dispensable as well as indispensable genes for survival, virulence and/or pathogenicity. We also describe the different complexes or mechanisms targeted by fungicides, thus addressing a relevant issue regarding disease management. Despite the controversial origin and evolution of fungal mt-genomes, the intrinsic mechanisms and molecular biology involved in their evolution will help to understand, at the molecular level, the strategies for fungal disease management.

Keywords: fungal mitogenome, plant disease management, mobile elements, pathogens, virulence, pathogenesis, fungal interactions

OPEN ACCESS

Edited by:
Georg Hausner, University of Manitoba, Canada

Reviewed by:
Yongjie Zhang, Shanxi University, China
Xingzhong Liu, Institute of Microbiology (CAS), China
John Carlyle Kennell, Saint Louis University, United States

****Correspondence:***
Pedro Alberto Balatti
pbalatti@gmail.com

Specialty section:
This article was submitted to Fungi and Their Interactions, a section of the journal Frontiers in Microbiology

Received: *28 January 2020*
Accepted: *23 April 2020*
Published: *29 May 2020*

Citation:
Medina R, Franco MEE, Bartel LC, Martinez Alcántara V, Saparrat MCN and Balatti PA (2020) Fungal Mitogenomes: Relevant Features to Planning Plant Disease Management. Front. Microbiol. 11:978. doi: 10.3389/fmicb.2020.00978

ORIGIN AND EVOLUTION OF MITOCHONDRIA

Mitochondria are highly dynamic organelles with a double-membrane that carries the respiratory complex that generates adenosine triphosphate (ATP), the chemical energy currency of cells (Roger et al., 2017). Several processes occur within mitochondria, like the aerobic citric acid cycle (TCA), electron transport system that results in the synthesis of ATP, the biosynthesis of metabolites like amino acids, the heme group, and the Fe-S centers as well as reactions that regulate cellular iron homeostasis (Verma et al., 2018; **Figure 1**). In addition to this, mitochondria play crucial roles in resistance to microbial antagonists as well as in host pathogen interactions (Rudel et al., 2010; Hadwiger and Polashock, 2013).

In 1970, Margulis hypothesized that eukaryotic organelles like mitochondria evolved from endosymbiotic bacteria (Margulis, 1970). The development of biotechnological tools together with

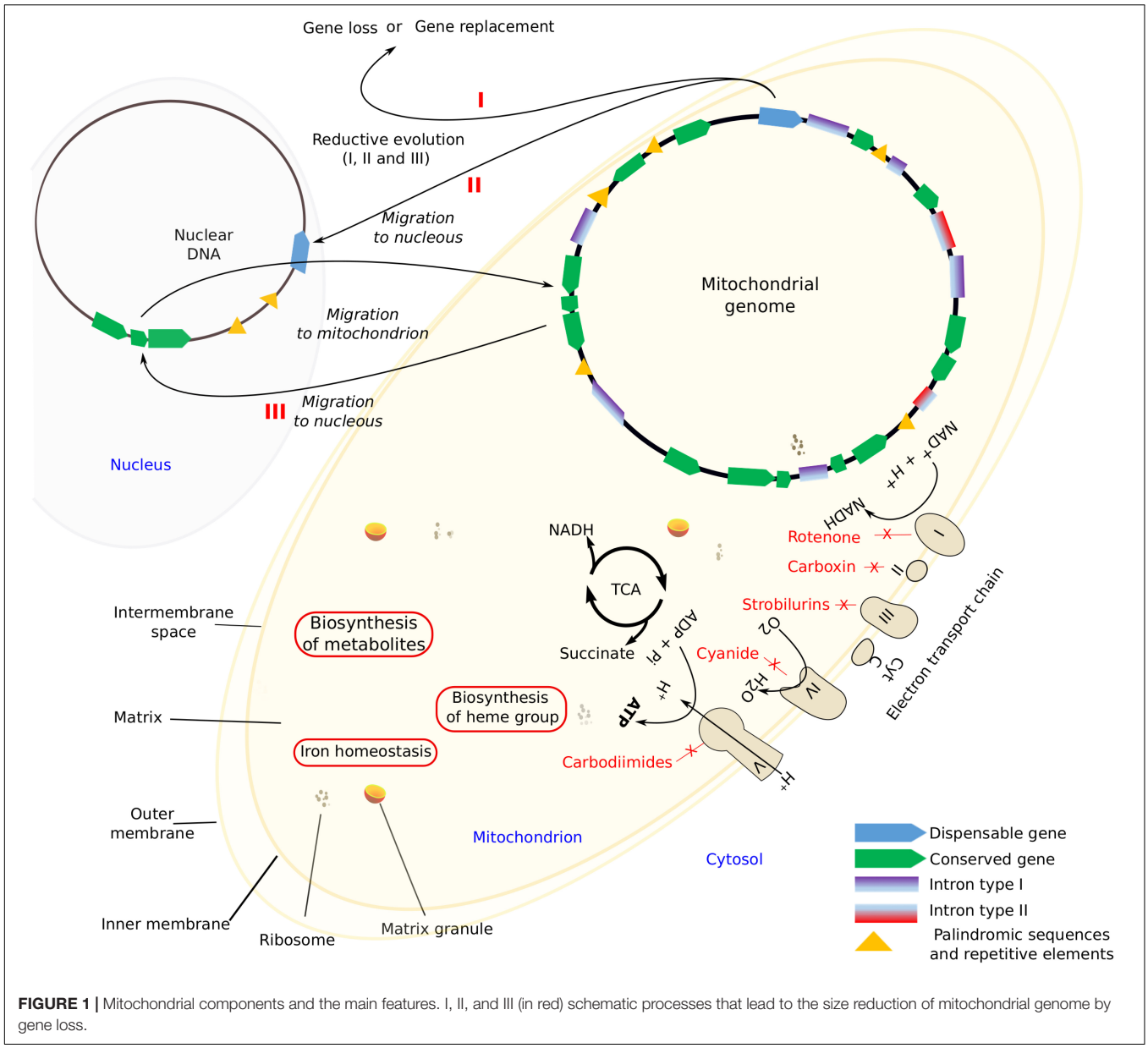

FIGURE 1 | Mitochondrial components and the main features. I, II, and III (in red) schematic processes that lead to the size reduction of mitochondrial genome by gene loss.

the development of phylogenetic analysis software allowed researchers to focus their studies on the origin of mitochondria that consisted in the full integration of an alphaproteobacterium into a host cell that was related to Asgard, an Archaea that produces an organelle capable of aerobic respiration as well as other biochemical functions that also occur in mitochondria (Szklarczyk and Huynen, 2010; Wang and Wu, 2014; Gray, 2015). Also, several researchers suggest that mitochondria originated in subsequent temporary events, essentially at the same time as the nucleus of eukaryotic cells rather than from a common protomitochondrial ancestor (Gray and Spencer, 1996; Andersson et al., 1998; Gray et al., 1999). Eukaryotic evolution started with the last eukaryotic common ancestor (LECA) (Koonin, 2010; Klöpper et al., 2012). One of the earliest branches of eukaryotes is a population of amitochondriate organisms that diverged away from the mainline before the advent of mitochondria (Martin and Müller, 1998; Müller et al., 2012). Recently, a study considered that LECA might not be a pangenomic population (O'Malley et al., 2019). So, an ancestral mitochondrial genome (mt-genome) might be defined as the one that retained vestiges of its eubacterial ancestry (Gray et al., 1999). Regarding mt-genomes, a study based on 14 mitochondrial genes demonstrated that *Ascomycetes* started to diverge earlier than *Basidiomycetes* (Wang et al., 2019). Within Dikarya, in general *Basidiomycetes* mt-genomes are highly variable in gene order compared to *Ascomycetes*. Furthermore, while in *Basidiomycetes* genes are usually encoded on both strands, in *Ascomycetes* they are in only one.

Regarding evolution, most fungal mt-genomes are characterized by gene loss (Spanu et al., 2010), marked

divergence in ribosomal DNA and rRNA structures (Lang et al., 1999; Petrov et al., 2018), adoption of a highly biased codon usage strategy in protein genes (Gray et al., 1999), elimination of certain codons (Nedelcu and Lee, 1998), and also the introduction of non-standard codon assignments (Sengupta et al., 2007). Interestingly, evolution within genes encoding typical mitochondrial proteins was observed in nuclear genomes of amitochondriate protists (Timmis et al., 2004). Furthermore, hydrogenosomes, organelles that generate ATP anaerobically and are characteristic of obligate anaerobic fungi that live within the gut of mammals, known as Neocallimastigales, contained mitochondrial proteins (Hackstein et al., 2019). Mitosomes are highly reduced and cryptic organelles of Microsporidia, that do not produce ATP. They are related either to the iron-sulfur cluster assembly (Burri et al., 2006; Müller et al., 2012) or linked to mitochondria-related organelles in anaerobic and microaerophilic lineages (Burki, 2016). The gene loss that led to a reductive mitochondrial evolution and mitochondrion related organelles is neither a result of functional redundancy nor of gene selection, it is mostly a structural adaptation. Proof of this is that hydrogenosomes and mitochondria have a common evolutionary origin and that amitochondriate eukaryotes once had mitochondria (Henze et al., 1995; Müller, 1997; Doolittle, 1998).

Evolutionary divergent processes might be relatively rapid and might lead to an extensive loss of mt-genes. Adams and Palmer (2003) established three alternative reductive processes, namely: the loss of non-essential functions, substitution, and gene transference to the nucleus (**Figure 1**). Franco et al. (2017) found that in *Stemphylium lycopersici* (Pleosporales, Ascomycota) the widely conserved mt-genes *atp8* and *atp9* migrated to the nucleus. Such transference might transform a non-functional protein into a functional one, otherwise pseudogenization may occur, whereas the opposite, that is, the replacement of mt-genes by nuclear ones of similar function can also occur. However, it is possible that, the non-standard genetic mitochondrial code is probably preventing further gene transfers of functional proteins (Boore, 1999). In any case, all these processes lead to a size reduction of mt-genomes.

CHARACTERISTICS OF FUNGAL MITOGENOMES

Fungal mt-genomes are highly diverse in conformation and size (Lang et al., 2007; Aguileta et al., 2014), gene content, order, and expression (Adams and Palmer, 2003; Shao et al., 2003). Most of them exhibit a circular-mapping topology, like a typical bacterial genome, however, some are linear concatemeric structures (**Figure 2**), that are most likely products of a rolling-circle mechanism of replication, which is frequent in organisms with linear mt-genomes (Maleszka et al., 1991; Maleszka and Clark-Walker, 1992; Bendich, 1993, 1996; Ling and Shibata, 2002; Hausner, 2003; Salavirta et al., 2014). Within the phylum Chytridiomycota, *Synchytrium endobioticum*, an obligate biotrophic pathogen of potato, and *Hyaloraphidium curvatum* have both linear mt-genomes, though the later one with terminal inverted repeats (Forget et al., 2002; van de Vossenberg et al., 2018). This raises a question as to whether linearity or circularization is related to evolution or if this is a step within evolution that separated organisms in different evolutionary branches.

Fungal mt-genomes are characterized by a high AT-content and an ample range of genome sizes. *Spizellomyces punctatus* (Chytridiomycota), a saprotrophic representative that is also found in association with a range of mycorrhizal fungi, mildews, plants, and soil nematodes (Russ et al., 2016), has a mitogenome composed of three chromosomes, and only one of them has 1136 bp. The mt-genome encodes only 8 tRNAs, while they normally carry 24–25 tRNAs (Laforest et al., 1997). On the other extreme, the mitogenome of *Morchella importuna* (Ascomycota), the largest one known, has 272,238 bp long and encodes a set of 32 different tRNAs (Liu et al., 2020). The size of the mt-genome is probably the result of (i) length and organization of intergenic regions; (ii) presence of introns (type I and II) of various sizes and numbers (Burger et al., 2003); (iii) intron-encoded open reading frames and AT-rich intergenic spacers (Hausner, 2003); (iv) palindromic sequences scattered throughout AT-rich intergenic spacers (Yin et al., 1981); (v) tandem-repeat arrays; (vi) stem-loop motifs (Paquin and Lang, 1996); (vii) ultra-short elements (Hausner, 2003); and (viii) evolutionary divergent processes.

Group I and II introns and maybe other introns as well are self-splicing DNA sequences that play a major role in genome evolution (Schuster et al., 2017). They are distinguished by their splicing mechanisms and secondary structures. Frequently, they contain in their loop regions open reading frames (ORFs) that encode different site-specific homing endonuclease genes (HEGs, Schäfer, 2003). Most group I introns include HEGs, with a conserved single or double LAGLIDADG amino-acid sequence motif. In contrast, group II introns encode mostly reverse transcriptase-like (RT) ORFs (Hausner, 2012). While the latter group of introns seems to thrive especially in plants, introns type I mainly occur within fungi (Santamaria et al., 2009; Férandon et al., 2010; Hafez and Hausner, 2012; Li et al., 2015). Other mobile elements identified in fungal mt-genomes are plasmid and plasmid-like DNA sequences. While the former ones are linear or circular DNA with no homology with the mt-genome, the latter are covalently closed DNA sequences homologous to regions within the mt-genome (Hausner, 2003). Plasmid elements usually have been associated with nuclear or mitochondrial mutations (Férandon et al., 2010; Beaudet et al., 2013) and provoke changes in the mt-genome architecture. Mt-genomes also contain palindromic sequences scattered throughout AT-rich intergenic spacers that frequently form long highly stable hairpin structures, where DNA recombination (Hausner, 2003) or replication or transcription initiation occur that might be the primary sites for processing transcripts (Gross et al., 1989a,b). Also, mt-genomes contain ultra-short elements (MUSEs) that are highly repeated recombinant sequences that are associated with excision and amplification of short mitochondrial segments. These processes often occur during the phenomenon of degenerative senescence in *Podospora anserina* (Koll et al., 1996) and consist in a progressive loss of growth potential culminating in hyphal death. MUSEs are highly invasive and contribute to the mt-genome evolution. Additionally, mt-genomes contain

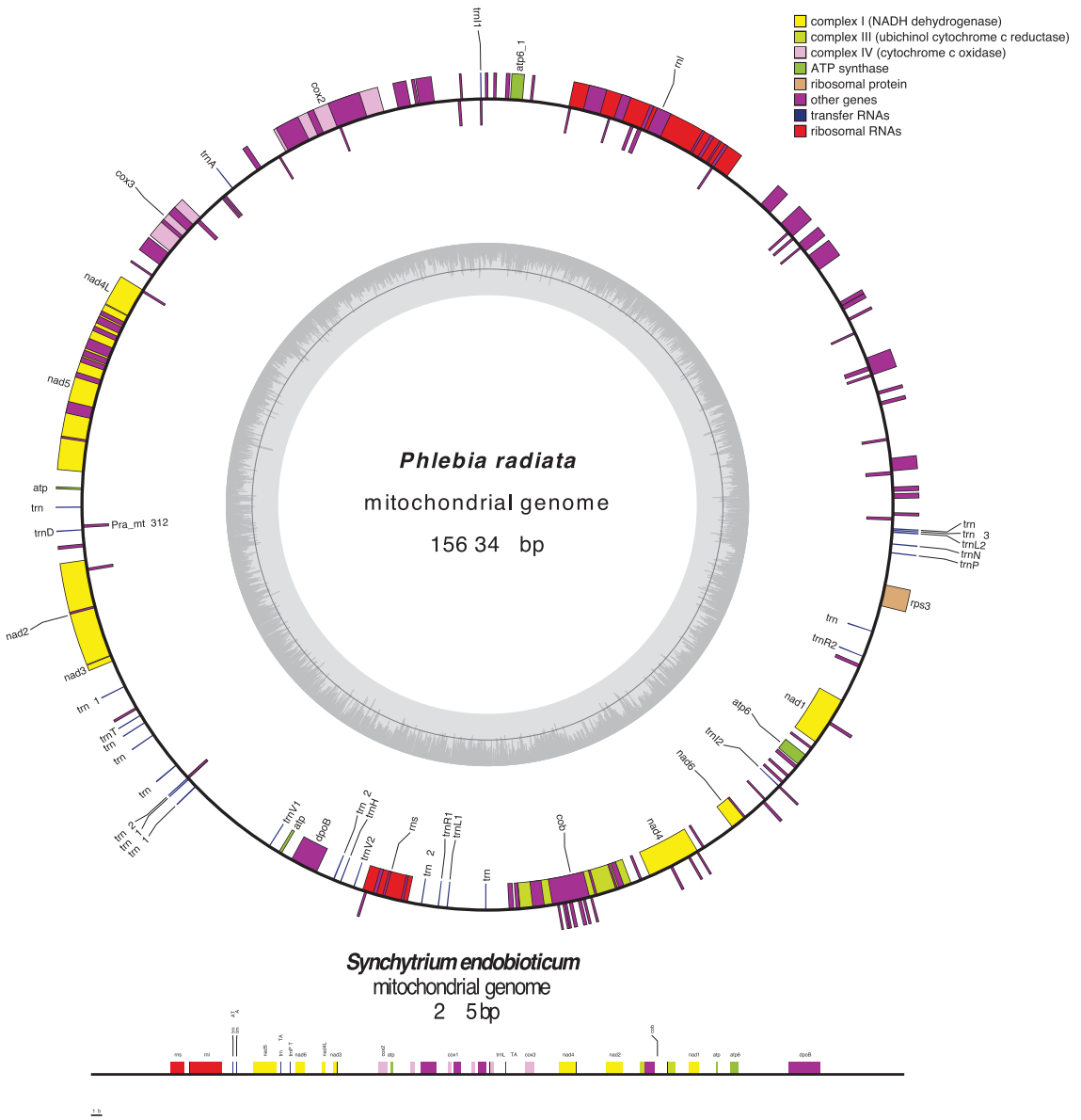

FIGURE 2 | Array and orientation of core genes, the untranslated genes of small and large ribosomal RNA subunits, and the AT/GC content of the circular mt-genome of *Phlebia radiata* (NC_020148, Basidiomycota) and the linear mt-genome of *Synchytrium endobioticum* (NC_042370, Chytridiomycota). Figure was made using OrganellarGenomeDRAW (OGDRAW) version 1.3.1 (Greiner et al., 2019).

introns that have been associated with mt-genome defects (Hausner, 2012), rearrangements (Wu et al., 2015), and diversity of sequences flanking introns (Repar and Warnecke, 2017).

Mobile elements play a key role in the expansion of fungal mt-genomes. Organisms like *Endoconidiophora resinifera,* (Microascales, Ascomycota), a fungus associated with blue-stain on sapwood, and *Phlebia radiata* (Polyporales, Basidiomycota), a fungus that colonizes wood associated with white-rots, have large mitogenomes >220,000 bp and 156,348 bp, respectively. While *E. resinifera* has a large number of intron insertions within coding sequences of the mt-genome (Zubaer et al., 2018), *P. radiata* has many introns as well as intergenic regions that account for 80% of mt-genome (Salavirta et al., 2014). Both, introns and short repetitive sequences, are dispersed and sometimes overlap and/or interrupt conserved genes (*cox1, cox2, cox3*; *cob*; *nad1, nad2, nad4, nad4L, nad5*; *rnl* and *rns*). Another example is *Rhizoctonia solani* (Cantharellales, Basidiomycota), a potato pathogen, whose mt-genome, that is one of the largest one within filamentous fungi, accumulated introns and repeated sequences (**Figure 3**; Losada et al., 2014). It appears that mobile elements like introns and repetitive sequences are responsible for mt-genome expansion, mostly due to the accumulation of repeated sequences and AT-rich intergenic spacers, mobile elements, and introns (Hausner, 2012). Even within a fungal genus, the length

of non-coding intergenic regions in the mt-genome can vary considerably and introns might be splitting genes (Salavirta et al., 2014). Future studies should be aimed at studying if evolution is mostly related to the effect repetitive or mobile elements have on gaining abilities or with the identification of unknown capacities.

Mt-genomes have more unusual gene organizations, like gene fusions (Burger et al., 2003), and order that is poorly conserved due to the loss, transfer and/or gene rearrangements that occur due to insertions, deletions or recombination, that follow specific rules owing to the multicopy character of mt-genomes. Still, the ancestral arrangement in some mt-genomes is quite evident (Paquin and Lang, 1996). Franco et al. (2017) while studying the systematic of the subphylum Pezizomycotina using the amino acid sequences of 12 conserved mt-genes that code for proteins of the oxidative phosphorylation and electron transport system showed that Pezizomycotina is a monophyletic subphylum, which was in agreement with the nuclear phylogeny described by Spatafora et al. (2006). In a way, this shows the importance conservation has within the mt-genome but at the same time, that plasticity is essential since it allows the occurrence of changes, evading in this way quite frequent lethal phenotypes that might arise along the process.

Fungal mt-genomes usually harbor 14 core-genes encoding proteins of the electron transport and oxidative phosphorylation pathway, including the apocytochrome b (*cob*), 3 subunits of the cytochrome c oxidase (*cox1*, *cox2*, *cox3*), 7 subunits of the reduced nicotinamide adenine dinucleotide ubiquinone oxidoreductase (*nad1*, *nad2*, *nad3*, *nad4*, *nad4L*, *nad5*, and *nad6*), and 3 subunits of the ATP synthase (*atp6*, *atp8*, *atp9*) (**Figure 2**). Untranslated genes of the small and large ribosomal RNA (rRNA) subunits (*rns* and *rnl*, respectively) and a set of transfer RNA (tRNA) genes also are part of the mt-genome. Other genes occasionally found are those encoding the ribosomal protein S3 (RPS3, coded by *rps3*), a component of the 40S subunit that plays a critical role in the initiation of protein translation and the RNA subunit of the mitochondrial RNase P (*rnpB*; Adams and Palmer, 2003; Férandon et al., 2013; Franco et al., 2017; **Table 1**). Additionally, Paquin et al. (1997) showed that fungal mitochondrial tRNA genes were processed suggesting that such mismatch repair prevents tRNA processing by RNAse P and/or other enzymes. In line with this, in *S. cerevisiae* homing endonucleases, encoded within the group I intron, can generate a double-stranded break, which is a key step at the beginning of the repair process that involves unidirectional homologous recombination (Dujon et al., 1989). The ribosomal protein S3 (RPS3) is a multi-functional protein encoded within the group I intron or by a free-standing gene sequence (Zimmer et al., 1991; Wool, 1996). RPS3 is involved in DNA repair due to their DNA endonuclease activity (Kim et al., 1995), a function dependent on the level of phosphorylation by PKCδ, which phosphorylates serine 6 and threonine 221 in response to DNA-damaging agents (Kim et al., 2009). RPS3 also plays a role in cell signaling, apoptosis/survival, and transcriptional regulation (Kim et al., 2013). Interestingly, RPS3 is highly conserved among fungal mt-genomes and can be translocated into the nuclear genome through a "cycling" mechanism (Wai et al., 2019). DNA maintenance and/or repair mechanisms in fungal mt-genomes should be deepened to understand their biological significance and to develop new strategies to manage the attack of phytopathogenic fungi.

Hence, the mt-genome uses particular genetic mechanisms of recombination mediated by mobile elements. Furthermore, mt-genes can migrate to the nucleus or be lost after a short time or they might be transiently expressed, unless they are stably integrated into the mt-genome. Besides, point mutations may inactivate genes, and this inactivation may be transient due to the mitochondrial mismatch repair. In summary, it is necessary to know the process that governs the dynamics of the mt-genome as well as its effect on the genetic environment it creates within the mt-genome and its impact in nature.

CONSERVATION VS. PLASTICITY

Fungal mt-genomes generally show the right trade-off between conservation and plasticity that makes them suitable tools for phylogenetic, population, and comparative analyses. On the one hand, they harbor a set of genes that code for proteins involved in the electron transport-oxidative phosphorylation system. Given their vital role in cell physiology, such genes are highly conserved even across distantly related species. For this reason, the use of amino acid sequences of core mt-genes has become a standard practice in mitochondrial-based phylogeny (Burger et al., 2003; Kouvelis et al., 2005; Pantou et al., 2006). In fact, they proved to be useful in solving many unclear phylogenies (Bullerwell et al., 2003; van de Sande, 2012). On the other hand, fungal mt-genomes frequently contain repetitive and mobile elements within introns and intergenic regions between conserved genes, that usually are highly polymorphic. These characteristics make them useful tools to study diversity among or within populations (Formey et al., 2012; Joardar et al., 2012; Zhang et al., 2015). Moreover, the relatively small size, circular-mapping topology, and multi-copy nature of the mt-DNA simplify not only the sequencing but also their assembly, enabling the implementation of robust comparative analyses.

The mt-genome of *Tolypocladium inflatum* (Hypocreales, Ascomycota) is one of the smallest ones carrying a limited number of highly conserved key genes among organisms with similar lifestyles. Such compact mt-genome is the result of several non-typical repetitive elements suggesting that gene transfer occurred from the nucleus to the mitochondria. Interestingly, this mt-genome has a lower level of intraspecific variation compared to the nucleus (Zhang et al., 2017; Muthabathula et al., 2019). In line with this, the mt-genome of *Hypomyces aurantius*, a mycoparasite that causes cobweb disease, share several features like introns and gene arrangement with the mt-genomes of other members of the Hypocreales order, except for *Acremonium chrysogenum* and *Acremonium implicatum*. Still, the mt-genome of *H. aurantius* was larger due to the presence of 17 introns in six conserved genes, *cox1*, *rnl*, *cob*, *atp6*, *cox3*, and *cox2* (Deng et al., 2016). The mt-genome of related species such as *S. endobioticum* and *S. microbalum* (Synchytriales) presented polymorphic mt-genomes with no conserved organization and/or orientation of genes even though they are related (van de Vossenberg

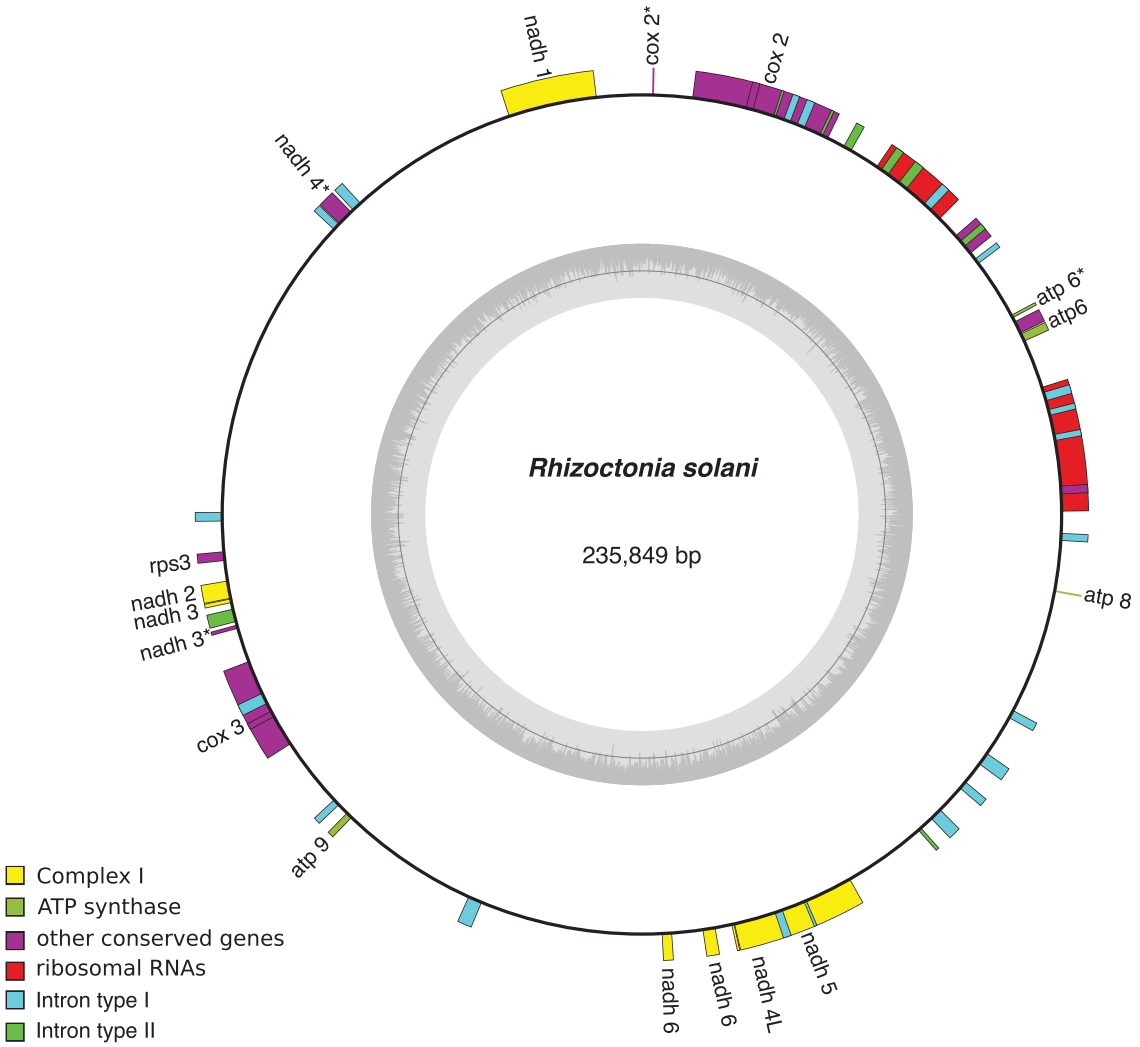

FIGURE 3 | *Rhizoctonia solani* mitochondrial genome and the type and number of introns present. The complete mt-genome is 235,849 bp long and encodes 15 conserved genes (showed in yellow). Group I introns are in red whereas group II are in blue. NCBI Reference Sequence: NC_021436.1. Figure was made using OrganellarGenomeDRAW (OGDRAW) version 1.3.1 (Greiner et al., 2019).

TABLE 1 | Conserved genes encoded in the fungal mtDNA.

	gene	Biological process
apocytochrome *b*	*cob*	Electron transport
cytochrome c oxidase	*cox1, cox2, cox3*	Oxidative phosphorylation
reduces nicotinamide adenine dinucleotide ubiquinone oxidoreductase	*nad1, nad2, nad3, nad4, nad4L, nad5, and nad6*	
ATP synthase	*atp6, atp8, atp9*	ATP synthesis
r RNA	*rns, rnl*	Small and large ribosomal RNA
tRNA	*tRNA*	Transfer RNA
Ribosomal protein	*rps3*	Component of the 40S subunit, initiation of protein translation, cell signaling, apoptosis/survival, transcriptional regulation, and DNA repair
RNAseP	*rnpB*	Subunit of the mitochondrial RNAsP

et al., 2018) and recently suffered a process of linearization and expansion. Another example of mt-genome plasticity is the mt-genome of *Laetiporus sulphureus* (Polyporales, Basidiomycota) that carry 38 coding sequences and 2 rRNA and 25 tRNA genes most probably due to horizontal transfer. As a consequence of this, tandem repeats accumulated in the mt-genome, leading this

to its expansion, which has been crucial to proceed to differentiate species or study evolution (Li et al., 2018a). Interestingly, the GC content of the mt-genome of *L. sulphureus* was, compared to other species of Polyporales, the highest one. In this genome, only *cox1*, *cob*, and *rnl* appeared as potentially useful molecular markers since the other conserved genes were exposed to a purifying selection. So, the degree of gene conservation and ordination within fungal mt-genome seemed to be dependent upon the fungal group studied. In this regard, an exhaustive analysis should be performed before selecting the phylogenetic molecular markers.

Regarding the mt-genome variation within isolates of the same species, results are controversial. While strains of the arbuscular mycorrhizal fungus, *Rhizophagus irregularis* (Glomerales, Glomeromycota), as well as of *T. inflatum* (Hypocreales) presented single-nucleotide polymorphism within the nuclear genome, the mt-genome presented not even one (Formey et al., 2012; Zhang et al., 2017). Besides, closely related yeast species presented a lower level of mitochondrial nucleotide diversity than the orthologous nuclear genes (Freel et al., 2014). On average, mt-genomes had a higher sequence identity than nuclear coding sequences, which is probably due to a lower rate of mitochondrial evolution (Gaillardin et al., 2012). Conversely, the mt-genome of four closely related crop pathogens of the genus *Rhynchosporium* (Heliotiales, Ascomycota) presented 77 times higher variation than the nuclear genomes (Torriani et al., 2014). The analysis of the mt-genome of representatives of the *Hymenochaetales* (Basidiomycota) indicated that evolution is usually lineage-specific, though chimeric mitotypes are frequent, suggesting that the evolutionary processes shaping mitogenomes are similar to those described in other *basidiomycetes* (Lee et al., 2019).

Mobile elements within fungal mt-genome may be potential tools for the genetic engineering of fungi. Introns, containing only genes coding endonucleases, facilitate recombination of intron-containing genes since they occur due to the activity of an intron homing mechanism that facilitates recombination, such regions might turn out to be recombination hotspots (Wu and Hao, 2019). Stand-alone endonucleases (SAEs) are other mobile elements of fungal mt-genomes (Beaudet et al., 2013; Franco et al., 2017). Wu and Hao (2019) studied the mechanisms of recombination in mitochondria and found that SAEs mediate gene conversion of adjacent intron-lacking genes. In line with this, they proposed the mechanism described in **Figure 4**.

The diverse size as well as the structure of fungal mt-genomes is an area that deserves special attention. The mt-genome of the acaropathogenic fungus *Hirsutella thompsonii* (Hypocreales) ranges in size between 60.3 and 66.4 kb and such differences were due to the presence of a variable number of introns. Among the 15 intron *loci* identified, more likely four were acquired by horizontal transfer from other fungi, suggesting this that their genomes are highly dynamic (Wang et al., 2018). On the other hand, the mt-genome of isolates of *Annulohypoxylon stygium* (Xylariales, Ascomycota), a cellulolytic fungus, ranged between 132 and 147 kb but they code for the same sets of conserved protein, tRNA and rRNA genes. Furthermore, even though they shared the arrangement and orientation, the content and distribution of introns are highly variable, which can be explained by movements, within introns, of short fragments that probably affected or hindered their activity. This probably contributed to the accumulation of introns within the mt-genomes (Deng et al., 2018).

The circular mt-genome of the ectomycorrhizal fungus *Cantharellus* (*Agaricomycetes*) is another example of conservation and plasticity. It contains 15 protein-coding genes that are variable in length and GC content probably because they are under a purifying selection (Li et al., 2018b). Furthermore, rearrangements occurred between repetitive sequences and because of this tRNAs changed their positions. A similar process of purifying selection included repetitive sequences within 14 protein-coding genes in the mt-genome of *Hypsizygus marmoreus* (*Agaricomycetes*), another cellulolytic fungus, which probably was due to a positive selection that leads to a faster rate of evolution (Wang et al., 2019). Another example of conservation and plasticity was observed within the mt-genome of *Fusarium oxysporum* species complex (Hypocreales), which includes plant pathogens causing vascular wilts, rots, and damping-off on a broad range of crops. Within phylogenetically related isolates of the *F. oxysporum* species complex, mt-genomes undergo recombination which suggests that a parasexual cycle may exist (Brankovics et al., 2017). Regarding diversification of mt-genomes, Li et al. (2018c) showed that *Pleurotus citrinopileatus* and *Pleurotus platypus* (Agaricales) presented different numbers and sequences of introns, indicating that evolutionary events most probably include gene rearrangements and inversions. Also, *Ganoderma* and *Lyophyllum* (*Agaricomycetes*) had rearranged mt-genomes (Li et al., 2019a,b). Mobile elements play a crucial role in building the mt-genome architecture, but reshuffling appears to be characteristic of an organism or a group of them.

Researchers unsuccessfully tried to relate the size and structure of fungal mt-genomes with the organisms environmental requirements. Reductions in their size and/or complexity are hallmarks of pathogenic or mutualistic symbiotic relationships (Moran and Bennett, 2014). Pogoda et al. (2018) compared the mt-genome of 22 lichenized fungi with 167 mt-genomes of non-lichenized ones and found that the former ones lost the *atp9* gene. Simon et al. (2017) also found that the mt-genomes of the lichenized fungi *Ricasolia amplissima* and *Peltigera* sp. were identical regarding protein-coding genes but they were rearranged. The mt-genome of *Paramicrosporidium saccamoebae* (Rozellomycota), an intranuclear parasite of amoeba, has a gene content similar to Macrosporidia, suggesting that evolution in both groups was affected by repeated and independent gene losses, either due to variations in their parasitic strategies (e.g., host and subcellular localization) or to multiple transitions to parasitism (Quandt et al., 2017; Melnikov et al., 2018). On the other hand, within Mycosphaerellaceae (Capnodiales, Ascomycota), a family that includes many plant pathogens of economically important crops, mt-genomes are significantly expanded at least due to five independent intron insertions within genes of the electron transport chain (Arcilla et al., 2019). As a result of this, the mt-genome of closely related organisms is highly variable in size and gene order and contain

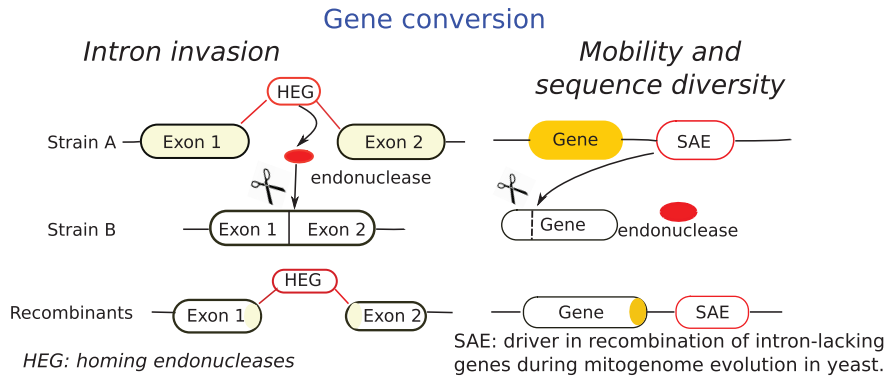

FIGURE 4 | Scheme of gene conversion through intron invasion and mobility and diversification adapted from Wu and Hao (2019). SAE mechanisms, known as intronless homing is compared with intron homing mechanism (HEG). Intron homing is facilitated by intron-encoded endonuclease and occurs into homologous intron-minus genes. SAE occurs in adjacent intron-lacking genes and facilitate gene conversion of their neighboring genes. The horizontal lines indicate endonuclease site.

truncated extra gene copies as well as accessory genes. The mt-genome of *S. lycopersici* and *Pyrenophora tritici-repentis*, two necrotrophic fungal plant pathogens that belong to the order Pleosporales, harbor 12 and 13 genes, respectively. Unlike the mt-genome of other fungi, they also have the *atp8* and *atp9* genes within the nuclear genome (Franco et al., 2017; Moolhuijzen et al., 2018). The mt-genomes of these fungi regarding the order, number, and gene orientation suggest they are plastic, which seems to be due at least in part to the action of homing endonucleases as well as repetitive elements, which provides more pieces of evidences of the crucial role these elements play in shaping the mt-genome architecture.

The mt-genome of another member of the Pleosporales, *Coniothyrium glycines*, the causal agent of soybean red leaf blotch, contains 12 mt-genes and 32 introns with a high number of homing endonucleases that represent approximately 54.1% of the mt-genome. However, the gene order of *nad6-rnl-atp6,* is conserved among members of Pleosporales (Stone et al., 2018). Kolesnikova et al. (2019) analyzed species of the genus *Armillaria* (Agaricales) and found that the mt-genome varied in size (98,896–122,167 bp) and arrangement. So, mobile genetic elements as well as homing endonucleases seem to be shaping the mt-genome architecture (Kolesnikova et al., 2019). However, several controversial findings remain regarding mt-genome plasticity. The mt-genome of *Rhizopogon* (*Agaricomycetes*), varied in length and base composition of proteins, rRNA, and tRNA genes, apparently due to switches that occurred between the mt and nuclear genomes and frequent intron loss/gain events that occur along with evolution. Also, in the mt-genome of *R. vinicolor* intronic regions contributed to expansion (Li et al., 2019c). On the other hand, representatives of *Hygrophorus* (Agaricales) and *Russula* (Russulales) have a conserved and reduced mt-genome within only three group I introns (Li et al., 2019d). The mt-genome of *Nectria cinnabarina* (Hypocreales), a plant pathogenic fungus that provokes cankers on many tree species and coral spot, presented a highly conserved gene composition and order compared to phylogenetically related fungi though they differed in the quantity as well as tRNAs order (Wang et al., 2016). While the organization of the *Phomopsis longicolla* mt-genome resembles that of other *Sordariomycetes*, unlike other genomes it has rearrangements of both tRNA and protein-coding genes (Kouvelis et al., 2005; Koloniuk et al., 2016). Other fungal pathogens of plants, such as *Pyricularia grisea* (Sordariomycetidae) the rice blast fungus (Xia et al., 2000) and *Ceratocystis fagacearum* (Microascales) the oak wilt pathogen (Kurdyla et al., 1995) have mt-genomes with a lower level of diversity than nuclear genomes, which is consistent with the hypothesis that in these fungi the nuclear genomes evolved at a slower rate than the mt-genome. Therefore, even though no relationship can be made between the genome arrangement, conservation, and gene composition with the environment where organisms develop, the evolution of mt-genomes within these organisms seems to evolve at a faster rate.

THE MITOGENOME, ITS ROLE IN FUNGAL VIRULENCE AND A TARGET OF SEVERAL FUNGICIDES

As a result of the widespread use of new generation sequencing technologies, high-quality genomes are available and this allowed researchers to study the molecular bases of fungal biology in terms of sexual reproduction, virulence, secondary metabolite production as well as to know their ability to detoxify antifungal compounds (Mac Aogáin et al., 2019). Mitochondrial functions are essential for eukaryotes, and in phytopathogenic fungi, they are particularly important during their interaction with the hosts, where frequently environments with low oxygen tension arise (She et al., 2013; Sun et al., 2013). Mitochondria play a key role in virulence since the expression of mt-genes regulates fungal growth, biofilm, and hyphal growth. In addition to this, mt-genomes play a crucial role in resistance to antimicrobial compounds (Sandor et al., 2018). All these functions make mitochondria a good target to control diseases. Plant pathogenic fungi use both mitochondrial as well as

nuclear-encoded proteins to infect plant hosts and provoke disease (Olson and Stenlid, 2001) and also their genomes carry genes coding for mechanisms of resistance (Joseph-Horne and Hollomon, 2000; Cowen et al., 2015), which is probably the reason they are frequent targets of some fungicides. However, any molecule targeted to mitochondrial proteins possesses a threat to eukaryotic organisms that share the biochemical functions and complexity of the genome (Brown et al., 2012). Therefore, it would be interesting to analyze the effects that recombination within the mt-genome might have on fungal virulence and also on pathogenesis.

Genes related to mitochondria and their replication seem to play a key role in growth and virulence of fungal pathogens of plants. In *Pyricularia oryzae,* the imperfect fission of mitochondria affects conidiation, growth, and virulence, while other changes in mt-genes affect the development of infection structures, invasion, and pathogenicity as well (Patkar et al., 2012; Khan et al., 2015). The mitochondrial fatty acid metabolism occurs through enoyl-CoA hydratase (*Ech1*), another enzyme that can be targeted to control fungal pathogens. If this metabolic pathway is blocked, the integrity as well as the morphology of the mitochondria is modified, and therefore, growth as well as, pathogenicity of the fungus, are affected (Mahlert et al., 2009). In this sense Mahlert et al. (2009) found that the loss of mitochondrial fission, which was related to a dynamin-related GTPase (*Dnm1*) gene, provoked a reduction in pathogenicity of *Ustilago maydis,* a maize pathogen (Mahlert et al., 2009). So, integrity as well as the functionality of the mt-genome are crucial for pathogens.

Virulence as well as host range of fungal plant pathogens also are affected by the architecture, arrangements, and modifications of the mt-genome. Populations of multilocus haplotypes of *Mycosphaerella graminicola* adapted to bread wheat (*Triticum aestivum*) and durum wheat (*T. turgidum,* Zhan et al., 2004) differed in haplotypes predominance. It was hypothesized that the low level of mitochondrial diversity within representatives of this pathogen is due to a selective sweep that is under the influence of both the host and natural selection (Zhan et al., 2004). Further evidence of the mitochondrial role on virulence was provided by hypovirulent mutants of *Cryphonectria parasitica* that happened to have plasmid-like elements interrupted by self-splicing introns (Monteiro-Vitorello et al., 1995; Baidyaroy et al., 2011). Also, in the *Heterobasidium annosum* species-complex, the causal agent of root and butt rot in conifers, virulence is under the control of the mt-genome. Olson and Stenlid (2001) found that virulence of both heterokaryons, as well as homokaryons of this fungus belonging to S and P intersterile groups, is due to uniparental transmission of mitochondria rather than the nucleus, being specifically the mitochondria of P origin related to a virulent phenotype (Olson and Stenlid, 2001). van de Vossenberg et al. (2018) found that a shift in the mitochondrial haplotypes, triggered within isolates of a community of *S. endobioticum* obtained from semi-resistant potato cultivars, resulted in changes in virulence. On the other hand, Moolhuijzen et al. (2018) found that a mutant of the wheat pathogen *Pyrenophora tritici-repentis* isolated from Australia containing an intron within the *cytochrome b* gene, lack the fungicide resistance site mutation observed in North American isolates. The effect of mt-genome recombination on the development and maintenance of virulence in plant pathogen populations is mostly due to their uniparental inheritance that is characterized by non-random segregation (Griffiths, 1996; Basse, 2010). Recently, it has been demonstrated that in *Fusarium zanthoxyli* and *F. continuum*, two canker-inducing pathogens of prickly ash (*Zanthoxylum bungeanum*), mitochondria only were maternally inherited (Zhou et al., 2019). Based on the effect of mt-genomes on virulence, their evolution should have a considerable impact on the epidemiology of diseases. Therefore, studies should be aimed at analyzing mt-genomes of pathogens populations to have a better understanding of mt-genes on virulence.

Due to the key role mitochondria play in microorganisms (Deacon, 2013), they have been and probably will be targeted by actual and future fungicides to prevent plant or cure plant diseases. The respiratory chain that leads to the synthesis of ATP has been a site targeted by fungicides, like compounds that uncouple the redox process and proton gradient from ATPases like carboxin and cyanide (I-V; Schuler and Casida, 2001). Many phytopathogenic fungi grow under an ample range of oxygen tensions that occur in diseased tissue, though necrotic tissues generate an extremely hostile environment for pathogens, since toxic compounds are released, which additionally might be accompanied by a reduction in nutrients. Alternative redox centers have been found in plant pathogenic fungi and their functions probably are associated with the adverse environmental conditions (Joseph-Horne and Hollomon, 2000). Because of this, theses complexes are alternative pathways to avoid the inhibitory activity of fungicides targeting respiratory redox centers.

Respiratory inhibitors that have been used as insecticides and miticides for more than 150 years were primarily targeted to the NAD(P)H dehydrogenase enzyme, known as complex I (Schuler and Casida, 2001). Piericidin A, bullatacin, thiangazole, and rotenone are natural products that block complex I, however, none of them have been released to the market. The explanation of this might be that alternative isozymes with NAD(P)H dehydrogenase activity were found in many fungal species (Joseph-Horne and Hollomon, 2000) and might therefore, provide an alternative pathway to evade the action of the fungicides that block complex I.

Complex II, which is known as succinate dehydrogenase or succinate-coenzyme Q reductase, also is the target of fungicides used against pathogens like *R. solani*, *Verticillium albo-atrum*, *U. maydis* and *Neurospora crassa* worldwide (Ragsdale and Sisler, 1970). An example of such compounds is carboxin that blocks the binding sites to ubiquinone, suppressing the citric acid cycle, inhibiting in this way fungal respiration by uncoupling the electron transport chain (Lyr, 1995).

Complex III, known as cytochrome *bc*, also is a target of fungicides like strobilurins that are known as the Qo inhibitors or QoIs (Becker et al., 1981). The latter ones were first introduced to the market in 1996 (Gisi et al., 2002). However, the development of resistance to strobilurins occurred in many different plant pathogens including fungi

like, *Blumeria graminis* f. sp. *tritici*, *Mycosphaerella fijiensis*, and *Venturia inaequalis* as well as the oomycete *Plasmopara viticola* (Fraaije et al., 2002; Balba, 2007). Such resistance is related to a mutation that occurred within the coding sequence of cytochrome b (*cob*), where a G143 glycine is substituted by an alanine. If phenylalanine is replaced by leucine at position 129, F129L, the level of resistance is reduced, compared to the G143A substitution (Grasso et al., 2006). In addition to this, it has been stated that evolution of resistance to QoI fungicides based on G143A is not likely to occur in pathogens carrying an intron directly after this codon since this probably leads to a lethal phenotype (Grasso et al., 2006; Fisher and Meunier, 2008). The increased resistance of plant pathogens to such fungicides is not only a problem for agriculture, but also suggests the importance of studying if the evolution of mt-genomes is under other influences than the evolutionary clock, like anthropogenic ones. Additionally, synthetic fungicides have been developed based on QoIs compounds like kresoximmethyl, azoxystrobin and other derivatives that were commercially successful, due to their exceptionally wide range of crop protection (Affourtit et al., 2000). But still, many fungi can express an alternative QH2-oxidase that bypasses complex III and IV and confer resistance to this type of blocking agent (Vanlerberghe and McIntosh, 1997). Metyltetraprole, the first member of a new generation of QoIs, has a stable efficiency both in greenhouses and in the fields, even in the presence of G143A resistant mutants (Matsuzaki et al., 2020).

Complex IV, or cytochrome *c* oxidase, is a heme/copper terminal oxidase that uses cytochrome *c* as an electron donor. Inhibitors of complex IV are heme-binding inhibitors like azide, cyanide and sulfide, and inhibitors that compete with oxygen such as CO and NO, as well as polycations that compete with cytochrome c and phosphate or alkaline pH (Wallace and Starkov, 2000). Besides, heme is an important cofactor of enzymes such as sterol 14-α-demethylase, which is a target of azoles (e.g., fluconazole, ketoconazole, or vorizonazole). This prosthetic group is partially synthesized in mitochondria and plays a key role in several enzymes involved in sterol biosynthesis, respiratory chain, and cytochrome P450 synthesis and several functions are impacted by changes in heme cellular concentration (Bossche et al., 1995; Francois et al., 2005). Fe-S coupling in mitochondria can also be a target to control phytopathogenic fungi, since compounds such as auranofin reacts with thiol and selenol protein groups (Sannella et al., 2008), which blocks mitochondrial processes, such as Mia 40 and the cytochrome *c* oxidase biogenesis factor, both essential proteins for mitochondrial activities (Thangamani et al., 2017).

The complex V is composed by the H^+-ATP synthetase that synthetizes ATP using the proton potential ($\Delta\mu_{H+}$). This complex is inhibited by several mycotoxins like aurovertins A-E, leucinostatins A and B, venturicidin, and by oligomycins A-D and others. Furthermore, compounds such as flavonoids, the beta-adrenergic receptor antagonist propanolol, some anesthesics, the herbicide paraquat, several pyrethroid insecticides, DDT and parathion, several cationic dyes and other compounds are also blocking agents of this complex (Wallace and Starkov, 2000), which also is targeted by carbodiimide that is formed during bioactivation of the thiourea insecticide diafenthiuron (Schuler and Casida, 2001).

The mt-genome impact on virulence and pathogenicity also is under the influence of the environment that causes epigenetic modifications. In a recent study, Kang et al. (2017) characterized the mt-genome of Ophocordiceps sinensis and showed that usually affect the enzymatic activity of oxidative phosphorilationn and then the respiratory rate.

Repetitive mobile elements within fungal mt-genomes like palindromic sequences, AT-rich intergenic spacers, MUSEs, introns associated with mt-genome defects, rearrangements and genetic diversity of sequences flanking introns as well as epigenetic modifications suggest that mt-genomes also are prone to mutate in response to fungicides, leading this to the development of resistance to such molecules. It would be interesting to analyze the effects of recombination as well as all the other causes of changes within the mt-genome on fungal virulence and pathogenesis.

Last but not least is the fungal pathogen control on inhibition of essential matrix proteins, i.e., the mitochondrial processing peptidase (MPP) that is a nuclear enzyme involved in mitochondrial protein import (Braun and Schmitz, 1997), turning this protein into a possible target for fungicides. Thus, there are very many different ways for the mt-genome of pathogenic organisms like fungi to be altered or modified, though much remains to be studied regarding the effect of such changes on biological responses.

CONCLUSION AND PERSPECTIVES

Data regarding the structural organization of mt-fungal genomes, reveal the importance of mitochondria and their activity in several different essential metabolic processes, however, they are plastic and dynamic but they still are used in studies of evolution within the kingdom fungi. Several processes occurring within mitochondria lead to a size reduction in their genomes.

It can be concluded that mt-genomes are plastic but still conserved which is good in terms of functionality, and in addition to this they harbor DNA repair mechanisms. Their relatively small size, circular-mapping topology, and multi-copy nature of the mt-DNA simplify sequencing and assembly, this enables researchers to make a robust comparative analysis to study evolution. Even though mobile elements play a crucial role in building the mt-genome architecture, reshuffling appears to be characteristic of an organism or a group of them. The degree of gene conservation and ordination within fungal mt-genome seemed to be dependent upon the fungal group studied. The mt-genomes of plant pathogenic fungi regarding order, number and gene orientation suggest they are plastic in part due to the action of homing endonucleases as well as repetitive elements, which provides more evidences of the crucial role these elements play in shaping the mt-genome architecture. Mt-genomes are prone to mutations due to their richness in repetitive mobile elements, AT-rich intergenic spacers, MUSEs, introns, rearrangements, and

genetic diversity of sequences flanking introns. In consequence, this could occasionally lead to the onset of adaptive mutants that are resistant to fungicide.

Since the degree of conservation and ordination of genes vary according to the group studied, a preliminary analysis should be done in order to select "*a priori*" reliable phylogenetic markers. Among mt-genomic features, those involved at increasing the synthesis of iron-sulfur clusters and heme cofactors are probably the most important ways, considering the role S and Fe play on fungal pathogenesis and other biological processes as well. However, information regarding the rate of mt-genome mutations is lacking as well as its impact on functions, maintenance, and evolution of these genomes.

Fungal phytopathogens mt-genomes also are related to virulence. Although the mt-genome of model phytopathogens have been structurally characterized it is crucial to increase their number in databases to establish if there is any particular pattern that might explain fungal virulence and pathogenesis. The mitochondrial mechanisms of mt-DNA maintenance and/or repair should be deepened further in order to better understand their biological significance and to develop new strategies to manage the threat of phytopathogenic fungi. A more profound understanding of fungal mt-genome regarding structure and function should provide the tools to manage phytopathogenic fungi and their virulence.

AUTHOR CONTRIBUTIONS

All authors contributed on the revision and conceptualization of this manuscript. RM, MS, and PB elaborated the manuscript. RM and MF made the figures.

ACKNOWLEDGMENTS

RM and MS are members of the Research Career of CONICET (Consejo Nacional de Investigaciones Científicas y Técnicas). LB and PB are researchers from CICPBA (Comisión de Investigaciones Científicas de la Provincia de Buenos Aires). VM belongs to the Universidad Nacional de La Plata.

REFERENCES

Adams, K. L., and Palmer, J. D. (2003). Evolution of mitochondrial gene content: gene loss and transfer to the nucleus. *Mol. Phylogenet. Evol.* 29, 380–395. doi: 10.1016/S1055-7903(03)00194-5

Affourtit, C., Heaney, S. P., and Moore, A. L. (2000). Mitochondrial electron transfer in the wheat pathogenic fungus *Septoria tritici*: on the role of alternative respiratory enzymes in fungicide resistance. *Biochim. Biophys. Acta Bioenerg.* 1459, 291–298. doi: 10.1016/S0005-2728(00)00157-2

Aguileta, G., De Vienne, D. M., Ross, O. N., Hood, M. E., Giraud, T., Petit, E., et al. (2014). High variability of mitochondrial gene order among fungi. *Genome Biol. Evol.* 6, 451–465. doi: 10.1093/gbe/evu028

Andersson, S. G., Zomorodipour, A., Andersson, J. O., Sicheritz-Pontén, T., Alsmark, U. C. M., Podowski, R. M., et al. (1998). The genome sequence of *Rickettsia prowazekii* and the origin of mitochondria. *Nature* 396:133. doi: 10.1038/24094

Arcilla, J. E. A., Arango, R. E., Torres, J. M., and Arias, T. (2019). Comparative genomics in plant fungal pathogens (Mycosphaerellaceae): variation in mitochondrial composition due to at least five independent intron invasions. *bioRxiv*. [Preprint] doi: 10.1101/694562

Baidyaroy, D., Hausner, G., Hafez, M., Michel, F., Fulbright, D. W., and Bertrand, H. (2011). A 971-bp insertion in the *rns* gene is associated with mitochondrial hypovirulence in a strain of *Cryphonectria parasitica* isolated from nature. *Fungal Genet. Biol.* 48, 775–783. doi: 10.1016/j.fgb.2011.05.006

Balba, H. (2007). Review of strobilurin fungicide chemicals. *J. Environ. Sci. Health Part B* 42, 441–451. doi: 10.1080/03601230701316465

Basse, C. W. (2010). Mitochondrial inheritance in fungi. *Curr. Opin. Microbiol.* 13, 712–719. doi: 10.1016/j.mib.2010.09.003

Beaudet, D., Terrat, Y., Halary, S., de la Providencia, I. E., and Hijri, M. (2013). Mitochondrial genome rearrangements in *Glomus* species triggered by homologous recombination between distinct mtDNA haplotypes. *Genome Biol. Evol.* 5, 1628–1643. doi: 10.1093/gbe/evt120

Becker, W. F., Von Jagow, G., Anke, T., and Steglich, W. (1981). Oudemansin, strobilurin A, strobilurin B and myxothiazol: new inhibitors of the bc_1 segment of the respiratory chain with an E−β−methoxyacrylate system as common structural element. *FEBS Lett.* 132, 329–333. doi: 10.1016/0014-5793(81)81190-8

Bendich, A. J. (1993). Reaching for the ring: the study of mitochondrial genome structure. *Curr. Genet.* 24, 279–290. doi: 10.1007/BF00336777

Bendich, A. J. (1996). Structural analysis of mitochondrial DNA molecules from fungi and plants using moving pictures and pulsed-field gel electrophoresis. *J. Mol. Biol.* 255, 564–588. doi: 10.1006/jmbi.1996.0048

Boore, J. L. (1999). Animal mitochondrial genomes. *Nucleic Acids Res.* 27, 1767–1780. doi: 10.1093/nar/27.8.1767

Bossche, H. V., Koymans, L., and Moereels, H. (1995). P450 inhibitors of use in medical treatment: focus on mechanisms of action. *Pharmacol. Ther.* 67, 79–100. doi: 10.1016/0163-7258(95)00011-5

Brankovics, B., van Dam, P., Rep, M., de Hoog, G. S., van der Lee, T. A., Waalwijk, C., et al. (2017). Mitochondrial genomes reveal recombination in the presumed asexual *Fusarium oxysporum* species complex. *BMC Genomics* 18:735. doi: 10.1186/s12864-017-4116-5

Braun, H. P., and Schmitz, U. K. (1997). The mitochondrial processing peptidase. *Int. J. Biochem. Cell Biol.* 29, 1043–1045. doi: 10.1016/S1357-2725(97)00032-0

Brown, G. D., Denning, D. W., Gow, N. A., Levitz, S. M., Netea, M. G., and White, T. C. (2012). Hidden killers: human fungal infections. *Sci. Transl. Med.* 4, rv13–rv165. doi: 10.1126/scitranslmed.3004404

Bullerwell, C. E., Forget, L., and Lang, B. F. (2003). Evolution of monoblepharidalean fungi based on complete mitochondrial genome sequences. *Nucleic Acids Res.* 31, 1614–1623. doi: 10.1093/nar/gkg264

Burger, G., Gray, M. W., and Lang, B. F. (2003). Mitochondrial genomes: anything goes. *Trends Genet.* 19, 709–716. doi: 10.1016/j.tig.2003.10.012

Burki, F. (2016). Mitochondrial evolution: going, going, gone. *Curr. Biol.* 26, R410–R412. doi: 10.1016/j.cub.2016.04.032

Burri, L., Williams, B. A., Bursac, D., Lithgow, T., and Keeling, P. J. (2006). Microsporidian mitosomes retain elements of the general mitochondrial targeting system. *Proc. Natl. Acad. Sci. U.S.A.* 103, 15916–15920. doi: 10.1073/pnas.0604109103

Cowen, L. E., Sanglard, D., Howard, S. J., Rogers, P. D., and Perlin, D. S. (2015). Mechanisms of antifungal drug resistance. *Cold Spring Harbor Perspect. Med.* 5:a019752. doi: 10.1101/cshperspect.a019752

Deacon, J. W. (2013). *Fungal Biology*, 4th Edn. Edinburgh: John Wiley & Sons.

Deng, Y., Hsiang, T., Li, S., Lin, R., and Xie, B. (2018). Comparison of the mitochondrial genome sequences of six *Annulohypoxylon stygium* isolates suggests short fragment insertions as a potential factor leading to larger genomic size. *Front. Microbiol.* 9:2079. doi: 10.3389/fmicb.2018.02079

Deng, Y., Zhang, Q., Ming, R., Lin, L., Lin, X., Lin, Y., et al. (2016). Analysis of the mitochondrial genome in *Hypomyces aurantius* reveals a novel twintron complex in fungi. *Int. J. Mol. Sci.* 17:1049. doi: 10.3390/ijms17071049

Doolittle, W. F. (1998). You are what you eat: a gene transfer ratchet could account for bacterial genes in eukaryotic nuclear genomes. *Trends Genet.* 14, 307–311. doi: 10.1016/S0168-9525(98)01494-2

Dujon, B., Beifort, M., Butow, R. A., Jacq, C., Lemieux, C., Perlman, P. S., et al. (1989). Mobile introns: definition of terms and recommended nomenclature. *Gene* 82, 115–118. doi: 10.1016/0378-1119(89)90035-8

Férandon, C., Moukha, S., Callac, P., Benedetto, J. P., Castroviejo, M., and Barroso, G. (2010). The *Agaricus bisporus cox1* gene: the longest mitochondrial gene and the largest reservoir of mitochondrial group I introns. *PLoS One* 5:e14048. doi: 10.1371/journal.pone.0014048

Férandon, C., Xu, J., and Barroso, G. (2013). The 135 kbp mitochondrial genome of *Agaricus bisporus* is the largest known eukaryotic reservoir of group I introns and plasmid-related sequences. *Fungal Genet. Biol.* 55, 85–91. doi: 10.1016/j.fgb.2013.01.009

Fisher, N., and Meunier, B. (2008). Molecular basis of resistance to cytochrome bc_1 inhibitors. *FEMS Yeast Res.* 8, 183–192. doi: 10.1111/j.1567-1364.2007.00328.x

Forget, L., Ustinova, J., Wang, Z., Huss, V. A., and Franz Lang, B. (2002). *Hyaloraphidium curvatum*: a linear mitochondrial genome, tRNA editing, and an evolutionary link to lower fungi. *Mol. Biol. Evol.* 19, 310–319. doi: 10.1093/oxfordjournals.molbev.a004084

Formey, D., Molès, M., Haouy, A., Savelli, B., Bouchez, O., Bécard, G., et al. (2012). Comparative analysis of mitochondrial genomes of *Rhizophagus irregularis* –syn. *Glomus irregulare*– reveals a polymorphism induced by variability generating elements. *New Phytol.* 196, 1217–1227. doi: 10.1111/j.1469-8137.2012.04283.x

Fraaije, B. A., Butters, J. A., Coelho, J. M., Jones, D. R., and Hollomon, D. W. (2002). Following the dynamics of strobilurin resistance in *Blumeria graminis* f. sp. *tritici* using quantitative allele—specific real—time PCR measurements with the fluorescent dye SYBR Green I. *Plant Pathol.* 51, 45–54. doi: 10.1046/j.0032-0862.2001.00650.x

Franco, M. E. E., López, S. M. Y., Medina, R., Lucentini, C. G., Troncozo, M. I., Pastorino, G. N., et al. (2017). The mitochondrial genome of the plant-pathogenic fungus *Stemphylium lycopersici* uncovers a dynamic structure due to repetitive and mobile elements. *PLoS One* 12:e0185545. doi: 10.1371/journal.pone.0185545

Francois, I. E., Aerts, A. M., Cammue, B., and Thevissen, K. (2005). Currently used antimycotics: spectrum, mode of action and resistance occurrence. *Curr. Drug Targets* 6, 895–907. doi: 10.2174/138945005774912744

Freel, K. C., Friedrich, A., Hou, J., and Schacherer, J. (2014). Population genomic analysis reveals highly conserved mitochondrial genomes in the yeast species *Lachancea thermotolerans*. *Genome Biol. Evol.* 6, 2586–2594. doi: 10.1093/gbe/evu203

Gaillardin, C., Neuvéglise, C., Kerscher, S., and Nicaud, J. M. (2012). Mitochondrial genomes of yeasts of the *Yarrowia* clade. *FEMS Yeast Res.* 12, 317–331. doi: 10.1111/j.1567-1364.2011.00782.x

Gisi, U., Sierotzki, H., Cook, A., and McCaffery, A. (2002). Mechanisms influencing the evolution of resistance to Qo inhibitor fungicides. *Pest. Manage. Sci.* 58, 859–867. doi: 10.1002/ps.565

Grasso, V., Palermo, S., Sierotzki, H., Garibaldi, A., and Gisi, U. (2006). Cytochrome *b* gene structure and consequences for resistance to Qo inhibitor fungicides in plant pathogens. *Pest. Manage. Sci.* 62, 465–472. doi: 10.1002/ps.1236

Gray, M. W. (2015). Mosaic nature of the mitochondrial proteome: Implications for the origin and evolution of mitochondria. *Proc. Natl. Acad. Sci. U.S.A.* 112, 10133–10138. doi: 10.1073/pnas.1421379112

Gray, M. W., and Spencer, D. F. (1996). "Organellar evolution," in *Evolution of Microbial Life*, eds D. M. Roberts, P. Sharp, G. Alderson, and M. Collins (Cambridge: Cambridge Univercity Press), 109–126.

Gray, M. W., Burger, G., and Lang, B. F. (1999). Mitochondrial evolution. *Science* 283, 1476–1482. doi: 10.1126/science.283.5407.1476

Greiner, S., Lehwark, P., and Bock, R. (2019). OrganellarGenomeDRAW (OGDRAW) version 1.3.1: expanded toolkit for the graphical visualization of organellar genomes. *Nucleic Acids Res.* 47, W59–W64. doi: 10.1093/nar/gkz238

Griffiths, A. J. (1996). Mitochondrial inheritance in filamentous fungi. *J. Genet.* 75, 403–414. doi: 10.1007/BF02966318

Gross, S. R., Levine, P. H., Metzger, S., and Glaser, G. (1989a). Recombination and replication of plasmid-like derivatives of a short section of the mitochondrial chromosome of *Neurospora crassa*. *Genetics* 121, 693–701.

Gross, S. R., Mary, A., and Levine, P. H. (1989b). Change in chromosome number associated with a double deletion in the *Neurospora crassa* mitochondrial chromosome. *Genetics* 121, 685–691.

Hackstein, J. H., Baker, S. E., van Hellemond, J. J., and Tielens, A. G. (2019). "Hydrogenosomes of anaerobic fungi: an alternative way to adapt to anaerobic environments," in *Hydrogenosomes and Mitosomes: Mitochondria of Anaerobic Eukaryotes. Microbiology Monographs*, Vol. 9, ed. J. Tachezy (Cham: Springer), doi: 10.1007/978-3-030-17941-0_7

Hadwiger, L. A., and Polashock, J. (2013). Fungal mitochondrial DNases: effectors with the potential to activate plant defenses in nonhost resistance. *Phytopathol* 103, 81–90. doi: 10.1094/PHYTO-04-12-0085-R

Hafez, M., and Hausner, G. (2012). Homing endonucleases: DNA scissors on a mission. *Genome* 55, 553–569. doi: 10.1139/g2012-049

Hausner, G. (2003). "Fungal mitochondrial genomes, plasmids, and introns," in *Fungal Genomics*, eds D. K. Arora and G. G. Khachatourians (Amsterdam: Elsevier), 101–131.

Hausner, G. (2012). "Introns, mobile elements, and plasmids," in *Organelle Genetics*, ed. C. Bullerwell (Berlin: Springer), doi: 10.1007/978-3-642-22380-8_13

Henze, K., Badr, A., Wettern, M., Cerff, R., and Martin, W. (1995). A nuclear gene of eubacterial origin in *Euglena gracilis* reflects cryptic endosymbioses during protist evolution. *Proc. Natl. Acad. Sci. U.S.A.* 92, 9122–9126. doi: 10.1073/pnas.92.20.9122

Joardar, V., Abrams, N. F., Hostetler, J., Paukstelis, P. J., Pakala, S., Pakala, S. B., et al. (2012). Sequencing of mitochondrial genomes of nine *Aspergillus* and *Penicillium* species identifies mobile introns and accessory genes as main sources of genome size variability. *BMC Genomics* 13:698. doi: 10.1186/1471-2164-13-698

Joseph-Horne, T., and Hollomon, D. W. (2000). Functional diversity within the mitochondrial electron transport chain of plant pathogenic fungi. *Pest Manage. Sci.* 56, 24–30. doi: 10.1002/(SICI)1526-4998(200001)56:1<24::AID-PS71<3.0.CO;2-Y

Kang, X., Hu, L., Shen, P., Li, R., and Liu, D. (2017). SMRT sequencing revealed mitogenome characteristics and mitogenome-wide DNA modification pattern in *Ophiocordyceps sinensis*. *Front. Microbiol.* 8:1422. doi: 10.3389/fmicb.2017.01422

Khan, I. A., Ning, G., Liu, X., Feng, X., Lin, F., and Lu, J. (2015). Mitochondrial fission protein MoFis1 mediates conidiation and is required for full virulence of the rice blast fungus *Magnaporthe oryzae*. *Microbiol. Res.* 178, 51–58. doi: 10.1016/j.micres.2015.06.002

Kim, J., Chubatsu, L. S., Admon, A., Stahl, J., Fellous, R., and Linn, S. (1995). Implication of mammalian ribosomal protein S3 in the processing of DNA damage. *J. Biol. Chem.* 270, 13620–13629. doi: 10.1074/jbc.270.23.13620

Kim, T. S., Kim, H. D., and Kim, J. (2009). PKCδ-dependent functional switch of rpS3 between translation and DNA repair. *Biochim. Biophys. Acta Mol. Cell Res.* 1793, 395–405. doi: 10.1016/j.bbamcr.2008.10.017

Kim, Y., Kim, H.D., Kim, J. (2013). Cytoplasmic ribosomal protein S3 (rpS3) plays a pivotal role in mitochondrial DNA damage surveillance. *Biochim. Biophys. Acta Mol. Cell Res.* 1833, 2943–2952.? doi: 10.1016/j.bbamcr.2013.07.015

Klöpper, T. H., Kienle, N., Fasshauer, D., and Munro, S. (2012). Untangling the evolution of Rab G proteins: implications of a comprehensive genomic analysis. *BMC Biol.* 10:71. doi: 10.1186/1741-7007-10-71

Kolesnikova, A. I., Putintseva, Y. A., Simonov, E. P., Biriukov, V. V., Oreshkova, N. V., Pavlov, I. N., et al. (2019). Mobile genetic elements explain size variation in the mitochondrial genomes of four closely-related *Armillaria* species. *BMC Genomics* 20:351. doi: 10.1186/s12864-019-5732-z

Koll, F., Boulay, J., Belcour, L., and d'Aubenton-Carafa, Y. (1996). Contribution of ultra-short invasive elements to the evolution of the mitochondrial genome in the genus *Podospora*. *Nucleic Acids Res.* 24, 1734–1741. doi: 10.1093/nar/24.9.1734

Koloniuk, I., Hrabakova, L., and Petrzik, K. (2016). The complete mitochondrial genome of the phytopathogenic fungus *Phomopsis longicolla*. *Mitochon. DNA Part A* 27, 3979–3980. doi: 10.3109/19401736.2014.989513

Koonin, E. V. (2010). The origin and early evolution of eukaryotes in the light of phylogenomics. *Genome Biol.* 11:209. doi: 10.1186/gb-2010-11-5-209

Kouvelis, V. N., Sialakouma, A., and Typas, M. A. (2005). Mitochondrial gene sequences alone or combined with ITS region sequences provide firm molecular

criteria for the classification of *Lecanicillium* species. *Mycol. Res.* 112, 829–844. doi: 10.1016/j.mycres.2008.01.016

Kurdyla, T. M., Guthrie, P. A. I., McDonald, B. A., and Appel, D. N. (1995). RFLPs in mitochondrial and nuclear DNA indicate low levels of genetic diversity in the oak wilt pathogen *Ceratocystis fagacearum*. *Curr. Genet.* 27, 373–378. doi: 10.1007/BF00352107

Laforest, M. J., Roewer, I., and Lang, B. F. (1997). Mitochondrial tRNAs in the Lower Fungus *Spizellomyces Punctatus* tRNA Editing and UAG 'Stop'Codons Recognized as Leucine. *Nucleic Acids Res.* 25, 626–632. doi: 10.1093/nar/25.3.626

Lang, B. F., Gray, M. W., and Burger, G. (1999). Mitochondrial genome evolution and the origin of eukaryotes. *Annu. Rev. Genet.* 33, 351–397. doi: 10.1146/annurev.genet.33.1.351

Lang, B. F., Laforest, M. J., and Burger, G. (2007). Mitochondrial introns: a critical view. *Trends Genet.* 23, 119–125. doi: 10.1016/j.tig.2007.01.006

Lee, H. H., Ke, H. M., Lin, C. Y. I., Lee, T. J., Chung, C. L., and Tsai, I. J. (2019). Evidence of extensive intraspecific noncoding reshuffling in a 169-kb mitochondrial genome of a basidiomycetous fungus. *Genome Biol. Evol.* 11, 2774–2788. doi: 10.1093/gbe/evz181

Li, Q., Chen, C., Xiong, C., Jin, X., Chen, Z., and Huang, W. (2018a). Comparative mitogenomics reveals large-scale gene rearrangements in the mitochondrial genome of two *Pleurotus* species. *Appl. Microbiol. Biotechnol.* 102, 6143–6153. doi: 10.1007/s00253-018-9082-6

Li, Q., Liao, M., Yang, M., Xiong, C., Jin, X., Chen, Z., et al. (2018b). Characterization of the mitochondrial genomes of three species in the ectomycorrhizal genus *Cantharellus* and phylogeny of *Agaricomycetes*. *Int. J. Biol. Macromol.* 118, 756–769. doi: 10.1016/j.ijbiomac.2018.06.129

Li, Q., Ren, Y., Shi, X., Peng, L., Zhao, J., Song, Y., et al. (2019a). Comparative mitochondrial genome analysis of two ectomycorrhizal fungi (*Rhizopogon*) reveals dynamic changes of intron and phylogenetic relationships of the subphylum Agaricomycotina. *Int. J. Mol. Sci.* 20:5167. doi: 10.3390/ijms20205167

Li, Q., Wang, Q., Jin, X., Chen, Z., Xiong, C., Li, P., et al. (2019b). Characterization and comparison of the mitochondrial genomes from two *Lyophyllum* fungal species and insights into phylogeny of *Agaricomycetes*. *Int. J. Biol. Macromol.* 121, 364–372. doi: 10.1016/j.ijbiomac.2018.10.037

Li, Q., Wang, Q., Jin, X., Chen, Z., Xiong, C., Li, P., et al. (2019c). The first complete mitochondrial genome from the family *Hygrophoraceae* (*Hygrophorus russula*) by next-generation sequencing and phylogenetic implications. *Int. J. Biol. Macromol.* 122, 1313–1320. doi: 10.1016/j.ijbiomac.2018.09.091

Li, Q., Xiang, D., Wan, Y., Wu, Q., Wu, X., Ma, C., et al. (2019d). The complete mitochondrial genomes of five important medicinal *Ganoderma* species: Features, evolution, and phylogeny. *Int. J. Biol. Macromol.* 139, 397–408. doi: 10.1016/j.ijbiomac.2019.08.003

Li, Q., Yang, M., Chen, C., Xiong, C., Jin, X., Pu, Z., et al. (2018c). Characterization and phylogenetic analysis of the complete mitochondrial genome of the medicinal fungus *Laetiporus sulphureus*. *Sci. Rep.* 8:9104. doi: 10.1038/s41598-018-27489-9

Li, Y., Hu, X. D., Yang, R. H., Hsiang, T., Wang, K., Liang, D. Q., et al. (2015). Complete mitochondrial genome of the medicinal fungus *Ophiocordyceps sinensis*. *Sci. Rep.* 5:13892. doi: 10.1038/srep13892

Ling, F., and Shibata, T. (2002). Recombination−dependent mtDNA partitioning: *in vivo* role of Mhr1p to promote pairing of homologous DNA. *EMBO J.* 21, 4730–4740. doi: 10.1093/emboj/cdf466

Liu, W., Cai, Y., Zhang, Q., Chen, L., Shu, F., Ma, X., et al. (2020). The mitochondrial genome of *Morchella importuna* (272.2 kb) is the largest among fungi and contains numerous introns, mitochondrial non-conserved open reading frames and repetitive sequences. *Int. J. Biol. Macromol.* 143, 373–381. doi: 10.1016/j.ijbiomac.2019.12.056

Losada, L., Pakala, S., Fedorova, N., Joardar, V., Shabalina, S., Hostetler, J., et al. (2014). Mobile elements and mitochondrial genome expansion in the soil fungus and potato pathogen *Rhizoctonia solani* AG-3. *FEMS Microbiol. Lett.* 352, 165–173. doi: 10.1111/1574-6968.12387

Lyr, H. (1995). "Aromatic hydrocarbon fungicides and their mechanism of action," in *Modern Selective Fungicides*, ed. H. Lyr (Jena: Gustav Fischer), 76–98.

Mac Aogáin, M., Chaturvedi, V., and Chotirmall, S. H. (2019). Mycopathologia GENOMES: the new 'home' for the publication of fungal genomes. *Mycopathologia* 184, 551–554. doi: 10.1007/s11046-019-00366-3

Mahlert, M., Vogler, C., Stelter, K., Hause, G., and Basse, C. W. (2009). The *a2* mating-type-locus gene *lga2* of *Ustilago maydis* interferes with mitochondrial dynamics and fusion, partially in dependence on a Dnm1-like fission component. *J. Cell. Sci.* 122, 2402–2412. doi: 10.1242/jcs.039354

Maleszka, R., and Clark-Walker, G. D. (1992). *In vivo* conformation of mitochondrial DNA in fungi and zoosporic moulds. *Curr. Genet.* 22, 341–344. doi: 10.1007/BF00317933

Maleszka, R., Skelly, P. J., and Clark−Walker, G. D. (1991). Rolling circle replication of DNA in yeast mitochondria. *EMBO J.* 10, 3923–3929. doi: 10.1002/j.1460-2075.1991.tb04962.x

Margulis, L. (1970). *Origin of Eukaryotic Cells*. New Haven, CT: Yale University Press, 349.

Martin, W., and Müller, M. (1998). The hydrogen hypothesis for the first eukaryote. *Nature* 392, 37–41. doi: 10.1038/32096

Matsuzaki, Y., Yoshimoto, Y., Arimori, S., Kiguchi, S., Harada, T., and Iwahashi, F. (2020). Discovery of metyltetraprole: Identification of tetrazolinone pharmacophore to overcome QoI resistance. *Bioorg. Med. Chem.* 28:115211. doi: 10.1016/j.bmc.2019.115211

Melnikov, S., Manakongtreecheep, K., Rivera, K., Makarenko, A., Pappin, D., and Söll, D. (2018). Muller's ratchet and ribosome degeneration in the obligate intracellular parasites *Microsporidia*. *Int. J. Mol. Sci.* 19:4125. doi: 10.3390/ijms19124125

Monteiro-Vitorello, C. B., Bell, J. A., Fulbright, D. W., and Bertrand, H. (1995). A cytoplasmically transmissible hypovirulence phenotype associated with mitochondrial DNA mutations in the chestnut blight fungus *Cryphonectria parasitica*. *Proc. Natl. Acad. Sci.U.S.A.* 92, 5935–5939. doi: 10.1073/pnas.92.13.5935

Moolhuijzen, P., See, P. T., Hane, J. K., Shi, G., Liu, Z., Oliver, R. P., et al. (2018). Comparative genomics of the wheat fungal pathogen *Pyrenophora tritici-repentis* reveals chromosomal variations and genome plasticity. *BMC Genomics* 19:279. doi: 10.1186/s12864-018-5059-1

Moran, N. A., and Bennett, G. M. (2014). The tiniest tiny genomes. *Annu. Rev. Microbiol.* 68, 195–215. doi: 10.1146/annurev-micro-091213-112901

Müller, M. (1997). Evolutionary origins of trichomonad hydrogenosomes. *Parasitol. Today* 13, 166–167. doi: 10.1016/s0169-4758(97)01036-3

Müller, M., Mentel, M., van Hellemond, J. J., Henze, K., Woehle, C., Gould, S. B., et al. (2012). Biochemistry and evolution of anaerobic energy metabolism in eukaryotes. *Microbiol. Mol. Biol. Rev.* 76, 444–495. doi: 10.1128/MMBR.05024-11

Muthabathula, P., Koduru, U. D., and Saragadam, S. (2019). Comparative mitochondrial genome analysis of Hypocrealean fungi with different lifestyles. *Res. J. Life. Sci. Bioinf. Pharm. Chem. Sci.* 5, 597–612. doi: 10.26479/2019.0501.50

Nedelcu, A. M., and Lee, R. M. (1998). A degenerate group II intron in the introless mitochondrial genome of Chlamydomonas reinhardtii: evolutionary implications. *Mol. Biol. Evol.* 15, 918–922. doi: 10.1093/oxfordjournals.molbev.a025996

O'Malley, M. A., Leger, M. M., Wideman, J. G., and Ruiz-Trillo, I. (2019). Concepts of the last eukaryotic common ancestor. *Nat. Ecol. Evol.* 3, 338–344. doi: 10.1038/s41559-019-0796-3

Olson, Å, and Stenlid, J. (2001). Plant pathogens: mitochondrial control of fungal hybrid virulence. *Nature* 411:438. doi: 10.1038/35078147

Pantou, M. P., Kouvelis, V. N., and Typas, M. A. (2006). The complete mitochondrial genome of the vascular wilt fungus *Verticillium dahliae*: a novel gene order for *Verticillium* and a diagnostic tool for species identification. *Curr. Genet.* 50, 125–136. doi: 10.1007/s00294-006-0079-9

Paquin, B., and Lang, B. F. (1996). The mitochondrial DNA of *Allomyces macrogynus*: the complete genomic sequence from an ancestral fungus. *J. Mol. Biol.* 255, 688–701. doi: 10.1006/jmbi.1996.0056

Paquin, B., Laforest, M. J., Forget, L., Roewer, I., Wang, Z., Longcore, J., et al. (1997). The fungal mitochondrial genome project: evolution of fungal mitochondrial genomes and their gene expression. *Curr. Genet.* 31, 380–395. doi: 10.1007/s002940050220

Patkar, R. N., Ramos−Pamplona, M., Gupta, A. P., Fan, Y., and Naqvi, N. I. (2012). Mitochondrial β−oxidation regulates organellar integrity and is necessary for conidial germination and invasive growth in *Magnaporthe oryzae*. *Mol. Microbiol.* 86, 1345–1363. doi: 10.1111/mmi.12060

Petrov, A. S., Wood, E. C., Bernier, C. R., Norris, A. M., Brown, A., and Amunts, A. (2018). Structural patching fosters divergence of mitochondrial ribosomes. *Mol. Biol. Evol.* 36, 207–219. doi: 10.1093/molbev/msy221

Pogoda, C. S., Keepers, K. G., Lendemer, J. C., Kane, N. C., and Tripp, E. A. (2018). Reductions in complexity of mitochondrial genomes in lichen−forming fungi shed light on genome architecture of obligate symbioses. *Mol. Ecol.* 27, 1155–1169. doi: 10.1111/mec.14519

Quandt, C. A., Beaudet, D., Corsaro, D., Walochnik, J., Michel, R., Corradi, N., et al. (2017). The genome of an intranuclear parasite, *Paramicrosporidium saccamoebae*, reveals alternative adaptations to obligate intracellular parasitism. *eLife* 6:e29594. doi: 10.7554/eLife.29594

Ragsdale, N. N., and Sisler, H. D. (1970). Metabolic effects related to fungitoxicity of carboxin. *Phytopathol* 60, 1422–1427. doi: 10.1094/phyto-60-1422

Repar, J., and Warnecke, T. (2017). Mobile introns shape the genetic diversity of their host genes. *Genetics* 205, 1641–1648. doi: 10.1534/genetics.116.199059

Roger, A. J., Muñoz-Gómez, S. A., and Kamikawa, R. (2017). The origin and diversification of mitochondria. *Curr. Biol.* 27, 1177–1192. doi: 10.1016/j.cub.2017.09.015

Rudel, T., Kepp, O., and Kozjak-Pavlovic, V. (2010). Interactions between bacterial pathogens and mitochondrial cell death pathways. *Nat. Rev. Microbiol.* 8, 693–705. doi: 10.1038/nrmicro2421

Russ, C., Lang, B. F., Chen, Z., Gujja, S., Shea, T., Zeng, Q., et al. (2016). Genome sequence of *Spizellomyces punctatus*. *Genome Announc.* 4, e849–e816. doi: 10.1128/genomeA.00849-16

Salavirta, H., Oksanen, I., Kuuskeri, J., Mäkelä, M., Laine, P., Paulin, L., et al. (2014). Mitochondrial genome of *Phlebia radiata* is the second largest (156 kbp) among fungi and features signs of genome flexibility and recent recombination events. *PLoS One* 9:e97141. doi: 10.1371/journal.pone.0097141

Sandor, S., Zhang, Y., and Xu, J. (2018). Fungal mitochondrial genomes and genetic polymorphisms. *Appl. Microbiol. Biotechnol.* 102, 9433–9448. doi: 10.1007/s00253-018-9350-5

Sannella, A. R., Casini, A., Gabbiani, C., Messori, L., Bilia, A. R., Vincieri, F. F., et al. (2008). New uses for old drugs. Auranofin, a clinically established antiarthritic metallodrug, exhibits potent antimalarial effects *in vitro*: mechanistic and pharmacological implications. *FEBS Lett.* 582, 844–847. doi: 10.1016/j.febslet.2008.02.028

Santamaria, M., Vicario, S., Pappadà, G., Scioscia, G., Scazzocchio, C., and Saccone, C. (2009). Towards barcode markers in Fungi: an intron map of Ascomycota mitochondria. *BMC Bioinf.* 10:S15. doi: 10.1186/1471-2105-10-S6-S15

Schäfer, B. (2003). Genetic conservation versus variability in mitochondria: the architecture of the mitochondrial genome in the petite-negative yeast *Schizosaccharomyces pombe*. *Curr. Genet.* 43, 311–326. doi: 10.1007/s00294-003-0404-5

Schuler, F., and Casida, J. E. (2001). The insecticide target in the PSST subunit of complex I. *Pest. Manage. Sci.* 57, 932–940. doi: 10.1002/ps.364

Schuster, A., Lopez, J. V., Becking, L. E., Kelly, M., Pomponi, S. A., Wörheide, G., et al. (2017). Evolution of group I introns in Porifera: new evidence for intron mobility and implications for DNA barcoding. *BMC Evol. Biol.* 17:82. doi: 10.1186/s12862-017-0928-9

Sengupta, S., Yang, X., and Higgs, P. G. (2007). The mechanisms of codon reassignments in mitochondrial genetic codes. *J. Mol. Evol.* 64, 662–688. doi: 10.1007/s00239-006-0284-7

Shao, R., Dowton, M., Murrell, A., and Barker, S. C. (2003). Rates of gene rearrangement and nucleotide substitution are correlated in the mitochondrial genomes of insects. *Mol. Biol. Evol.* 20, 1612–1619. doi: 10.1093/molbev/msg176

She, X., Zhang, L., Chen, H., Calderone, R., and Li, D. (2013). Cell surface changes in the *Candida albicans* mitochondrial mutant *goa1*Δ are associated with reduced recognition by innate immune cells. *Cell. Microbiol.* 15, 1572–1584. doi: 10.1111/cmi.12135

Simon, A., Liu, Y., Sérusiaux, E., and Goffinet, B. (2017). Complete mitogenome sequence of *Ricasolia amplissima* (Lobariaceae) reveals extensive mitochondrial DNA rearrangement within the Peltigerales (lichenized ascomycetes). *Bryologist* 120, 335–339. doi: 10.1639/0007-2745-120.3.335

Spanu, P. D., Abbott, J. C., Amselem, J., Burgis, T. A., Soanes, D. M., Stüber, K., et al. (2010). Genome expansion and gene loss in powdery mildew fungi reveal tradeoffs in extreme parasitism. *Science* 330, 1543–1546. doi: 10.1126/science.1194573

Spatafora, J. W., Sung, G. H., Johnson, D., Hesse, C., O'Rourke, B., Serdani, M., et al. (2006). A five-gene phylogeny of Pezizomycotina. *Mycologia* 98, 1018–1028. doi: 10.1080/15572536.2006.11832630

Stone, C. L., Frederick, R. D., Tooley, P. W., Luster, D. G., Campos, B., Winegar, R. A., et al. (2018). Annotation and analysis of the mitochondrial genome of *Coniothyrium glycines*, causal agent of red leaf blotch of soybean, reveals an abundance of homing endonucleases. *PLoS One* 13:e0207062. doi: 10.1371/journal.pone.0207062

Sun, N., Fonzi, W., Chen, H., She, X., Zhang, L., Zhang, L., et al. (2013). Azole susceptibility and transcriptome profiling in *Candida albicans* mitochondrial electron transport chain complex I mutants. *Antimicrob. Agents Chemother.* 57, 532–542. doi: 10.1128/AAC.01520-12

Szklarczyk, R., and Huynen, M. A. (2010). Mosaic origin of the mitochondrial proteome. *Proteomics* 10, 4012–4024. doi: 10.1002/pmic.201000329

Thangamani, S., Maland, M., Mohammad, H., Pascuzzi, P. E., Avramova, L., Koehler, C. M., et al. (2017). Repurposing approach identifies auranofin with broad spectrum antifungal activity that targets Mia40-Erv1 pathway. *Front. Cell. Infect. Microbiol.* 7:4. doi: 10.3389/fcimb.2017.00004

Timmis, J. N., Ayliffe, M. A., Huang, C. Y., and Martin, W. (2004). Endosymbiotic gene transfer: organelle genomes forge eukaryotic chromosomes. *Nat. Rev. Genet.* 5, 123–135. doi: 10.1038/nrg1271

Torriani, S. F., Penselin, D., Knogge, W., Felder, M., Taudien, S., Platzer, M., et al. (2014). Comparative analysis of mitochondrial genomes from closely related *Rhynchosporium* species reveals extensive intron invasion. *Fungal Genet. Biol.* 62, 34–42. doi: 10.1016/j.fgb.2013.11.001

van de Sande, W. W. (2012). Phylogenetic analysis of the complete mitochondrial genome of *Madurella mycetomatis* confirms its taxonomic position within the order Sordariales. *PLoS One* 7:e38654. doi: 10.1371/journal.pone.0038654

van de Vossenberg, B. T., Brankovics, B., Nguyen, H. D., van Gent-Pelzer, M. P., Smith, D., Dadej, K., et al. (2018). The linear mitochondrial genome of the quarantine chytrid *Synchytrium endobioticum*; insights into the evolution and recent history of an obligate biotrophic plant pathogen. *BMC Evol. Biol.* 18:136. doi: 10.1186/s12862-018-1246-6

Vanlerberghe, G. C., and McIntosh, L. (1997). Alternative oxidase: from gene to function. *Annu. Rev. Plant Biol.* 48, 703–734. doi: 10.1146/annurev.arplant.48.1.703

Verma, S., Shakya, V. P., and Idnurm, A. (2018). Exploring and exploiting the connection between mitochondria and the virulence of human pathogenic fungi. *Virulence* 9, 426–446. doi: 10.1080/21505594.2017.1414133

Wai, A., Shen, C., Carta, A., Dansen, A., Crous, P. W., and Hausner, G. (2019). Intron-encoded ribosomal proteins and N-acetyltransferases within the mitochondrial genomes of fungi: here today, gone tomorrow? *Mitochond. DNA Part A* 30, 573–584. doi: 10.1080/24701394.2019.1580272

Wallace, K. B., and Starkov, A. A. (2000). Mitochondrial targets of drug toxicity. *Annu. Rev. Pharmacol. Toxicol.* 40, 353–388. doi: 10.1146/annurev.pharmtox.40.1.353

Wang, G., Lin, J., Shi, Y., Chang, X., Wang, Y., Guo, L., et al. (2019). Mitochondrial genome in *Hypsizygus marmoreus* and its evolution in Dikarya. *BMC Genomics* 20:765. doi: 10.1186/s12864-019-6133-z

Wang, L., Zhang, S., Li, J. H., and Zhang, Y. J. (2018). Mitochondrial genome, comparative analysis and evolutionary insights into the entomopathogenic fungus *Hirsutella thompsonii*. *Environ. Microbiol.* 20, 3393–3405. doi: 10.1111/1462-2920.14379

Wang, X. C., Zeng, Z. Q., and Zhuang, W. Y. (2016). The complete mitochondrial genome of the important phytopathogen *Nectria cinnabarina* (Hypocreales, Ascomycota). *Mitochondrial DNA Part A.* 27, 4670–4671. doi: 10.3109/19401736.2015.1106495

Wang, Z., and Wu, M. (2014). Phylogenomic reconstruction indicates mitochondrial ancestor was an energy parasite. *PLoS One* 9:e110685. doi: 10.1371/journal.pone.0110685

Wool, I. G. (1996). Extraribosomal functions of ribosomal proteins. *Trends Biochem. Sci.* 21, 164–165. doi: 10.1016/S0968-0004(96)20011-8

Wu, B., and Hao, W. (2019). Mitochondria—encoded endonucleases drive recombination of protein coding genes in yeast. *Environ. Microbiol.* 21, 4233–4240. doi: 10.1111/1462-2920.14783

Wu, B., Buljic, A., and Hao, W. (2015). Extensive horizontal transfer and homologous recombination generate highly chimeric mitochondrial genomes in yeast. *Mol. Biol. Evol.* 32, 2559–2570. doi: 10.1093/molbev/msv127

Xia, J. Q., Correll, J. C., Lee, F. N., Ross, W. J., and Rhoads, D. D. (2000). Regional population diversity of *Pyricularia grisea* in Arkansas and the influence of host selection. *Plant Dis.* 84, 877–884. doi: 10.1094/PDIS.2000.84.8.877

Yin, S., Heckman, J., and RajBhandary, U. L. (1981). Highly conserved GC-rich palindromic DNA sequences flank tRNA genes in *Neurospora crassa* mitochondria. *Cell* 26, 325–332. doi: 10.1016/0092-8674(81)90201-4

Zhan, J., Kema, G. H., and McDonald, B. A. (2004). Evidence for natural selection in the mitochondrial genome of *Mycosphaerella graminicola*. *Phytopathology* 94, 261–267. doi: 10.1094/PHYTO.2004.94.3.261

Zhang, Y. J., Yang, X. Q., Zhang, S., Humber, R. A., and Xu, J. (2017). Genomic analyses reveal low mitochondrial and high nuclear diversity in the cyclosporin-producing fungus *Tolypocladium inflatum*. *Appl. Microbiol. Biotechnol.* 101, 8517–8531. doi: 10.1007/s00253-017-8574-0

Zhang, Y., Zhang, S., Zhang, G., Liu, X., Wang, C., and Xu, J. (2015). Comparison of mitochondrial genomes provides insights into intron dynamics and evolution in the caterpillar fungus *Cordyceps militaris*. *Fungal Genet. Biol.* 77, 95–107. doi: 10.1016/j.fgb.2015.04.009

Zhou, X., Cao, Z. M., Liu, X., Kim, H. S., Proctor, R. H., and O'Donnell, K. (2019). Maternal mitochondrial inheritance in two *Fusarium* pathogens of prickly ash (*Zanthoxylum bungeanum*) in northern China. *Mycologia* 111, 235–243. doi: 10.1080/00275514.2018.1562269

Zimmer, M., Krabusch, M., and Wolf, K. (1991). Characterization of a novel open reading frame, *urf a*, in the mitochondrial genome of fission yeast: correlation of *urf a* mutations with a mitochondrial mutator phenotype and a possible role of frameshifting in *urf a* expression. *Curr. Genet.* 19, 95–102. doi: 10.1007/BF00326289

Zubaer, A., Wai, A., and Hausner, G. (2018). The mitochondrial genome of *Endoconidiophora resinifera* is intron rich. *Sci. Rep.* 8:17591. doi: 10.1038/s41598-018-35926-y

Conflict of Interest: The authors declare that the research was conducted in the absence of any commercial or financial relationships that could be construed as a potential conflict of interest.

frontiers in Microbiology

ORIGINAL RESEARCH
published: 03 June 2020
doi: 10.3389/fmicb.2020.01092

Detecting Introgression Between Members of the *Fusarium fujikuroi* and *F. oxysporum* Species Complexes by Comparative Mitogenomics

Balázs Brankovics[1]*, *Anne D. van Diepeningen*[1], *G. Sybren de Hoog*[2,3], *Theo A. J. van der Lee*[1] *and Cees Waalwijk*[1]

[1] B.U. Biointeractions and Plant Health, Wageningen Plant Research, Wageningen University & Research, Wageningen, Netherlands, [2] Westerdijk Fungal Biodiversity Institute, KNAW, Utrecht, Netherlands, [3] Center of Expertise in Mycology, Radboud University Medical Center, Nijmegen, Netherlands

OPEN ACCESS

Edited by:
Levente Kiss,
University of Southern Queensland, Australia

Reviewed by:
Li-Jun Ma,
University of Massachusetts Amherst, United States
Ilias Kappas,
Aristotle University of Thessaloniki, Greece

***Correspondence:**
Balázs Brankovics
balazs.brankovics@wur.nl

Specialty section:
This article was submitted to Fungi and Their Interactions, a section of the journal Frontiers in Microbiology

Received: 30 January 2020
Accepted: 30 April 2020
Published: 03 June 2020

Citation:
Brankovics B, van Diepeningen AD, de Hoog GS, van der Lee TAJ and Waalwijk C (2020) Detecting Introgression Between Members of the Fusarium fujikuroi and F. oxysporum Species Complexes by Comparative Mitogenomics. Front. Microbiol. 11:1092. doi: 10.3389/fmicb.2020.01092

The *Fusarium fujikuroi* species complex (FFSC) and *F. oxysporum* species complex (FOSC) are two related groups of plant pathogens causing a wide diversity of diseases in agricultural crops world wide. The aims of this study are (1) to clarify the phylogeny of the FFSC, (2) to identify potential deviation from tree-like evolution, (3) to explore the value of using mitogenomes for these kinds of analyses, and (4) to better understand mitogenome evolution. In total, we have sequenced 24 species from the FFSC and a representative set of recently analyzed FOSC strains was chosen, while *F. redolens* was used as outgroup for the two species complexes. A species tree was constructed based on the concatenated alignment of seven nuclear genes and the mitogenome, which was contrasted to individual gene trees to identify potential conflicts. These comparisons indicated conflicts especially within the previously described African clade of the FFSC. Furthermore, the analysis of the mitogenomes revealed the presence of a variant of the large variable (LV) region in FFSC which was previously only reported for FOSC. The distribution of this variant and the results of sequence comparisons indicate horizontal genetic transfer between members of the two species complexes, most probably through introgression. In addition, a duplication of *atp9* was found inside an intron of *cob*, which suggests that even highly conserved mitochondrial genes can have paralogs. Paralogization in turn may lead to inaccurate single gene phylogenies. In conclusion, mitochondrial genomes provide a robust basis for phylogeny. Comparative phylogenetic analysis indicated that gene flow among and between members of FFSC and FOSC has played an important role in the evolutionary history of these two groups. Since mitogenomes show greater levels of conservation and synteny than nuclear regions, they are more likely to be compatible for recombination than nuclear regions. Therefore, mitogenomes can be used as indicators to detect interspecies gene flow.

Keywords: mitogenomics, introgression, *Fusarium oxysporum* species complex, *F. fujikuroi* species complex, phylogenetics, horizontal gene transfer

1. INTRODUCTION

Members of the *Fusarium fujikuroi* species complex (FFSC) are plant pathogens causing a wide diversity of diseases in agricultural crops worldwide. The species are difficult to distinguish by morphological characters and often share a high (90%) sequence similarity, but can differ in host plant specificity, lifestyle and secondary metabolite production (Niehaus et al., 2016). Based on a biogeographic hypothesis proposed from the phylogenetic evidence, three major clades have been described within the FFSC: named as the African, American, and Asian clades (O'Donnell et al., 1998). Although multilocus sequence analysis supports the recognition of the three biogeographic clades, several genetic markers appear to contradict this grouping, such as the ITS2 region (O'Donnell et al., 1998, 2000) and the fumonisin biosynthetic gene cluster (Proctor et al., 2013). Interspecies recombination was suggested within the FFSC based on comparative mitochondrial genome analysis that found conflicting mitochondrial gene trees (Fourie et al., 2013, 2018).

A gene tree may deviate from the species tree, because of recombination, incomplete lineage sorting (ILS) (Zhou et al., 2017) and horizontal gene transfer (HGT) (Arvestad et al., 2003). ILS is the result of allelic polymorphism that is maintained after speciation, although the polymorphism may be lost through fixation in the daughter species. ILS can be identified by comparing the putative species tree and the gene trees based on the different allelic groups (Ward et al., 2002; Brankovics et al., 2017). Concordance between the species tree and the allelic trees indicates ILS; however, this is only possible when the polymorphism is still present in all or most daughter species included. HGT transfer can be detected by comparing the pairwise genetic distances of the putative transferred region and the genomic genetic distance (average distance of multiple regions) (Novichkov et al., 2004). When the gene based genetic distance is significantly lower than the genome based one, it indicates a possible HGT event. A common mechanism for HGT is introgression (or "introgressive hybridization"). Introgression is the incorporation of genes or alleles through hybridization and backcrossing between two distinctive species (Anderson and Hubricht, 1938; Anderson, 1949).

We have recently identified incomplete lineage sorting in the case of the large variable region of the mitochondrial genome of the *F. oxysporum* species complex (FOSC) (Brankovics et al., 2017). The mitogenomes of *Fusarium* spp. contain a set of fourteen "standard" mitochondrial polypeptide-encoding genes, two rRNA-encoding genes, *rnl* (mtLSU) and *rns* (mtSSU), and more than twenty tRNA-encoding genes (Al-Reedy et al., 2012). The genes, their orientation and order are highly conserved within the FOSC, except for a region located between *rnl* and *nad2*. This exceptionally variable region is referred to as large variable (LV) region, which in most cases harbors a set of tRNA-encoding genes and a large open reading frame (ORF) with unknown function (LV-uORF) (Al-Reedy et al., 2012; Fourie et al., 2013; Brankovics et al., 2017). In the case of *F. oxysporum*, this region has at least three forms or variants that show low levels of similarity to each other. Two of the variants are present in two of the major clades, the trees based on nuclear and mitochondrial markers are congruent with trees based on each of the variants, which indicates ILS (Brankovics et al., 2017).

Previous comparative mitogenome analyses of *F. fujikuroi* species complex (FFSC) by Fourie et al. (2013, 2018) have indicated that mitochondrial recombination is happening between species within this complex. Unfortunately, the first study only included one representative for each of the three major lineages, while the second one did not include the LV region, which limited the resolution of the analyses and the strength of the conclusions. Furthermore, these studies focused only on the mitogenomes and did not examine the evolution of nuclear markers. The aims of this study are (1) to clarify the phylogeny of the *F. fujikuroi* species complex (FFSC), (2) to identify potential deviation from tree-like evolution, (3) to explore the value of using mitogenomes for these kinds of analyses, and (4) to better understand mitogenome evolution. In total, 36 strains were analyzed: 24 strains from the FFSC and 9 representative strains were chosen from the set of recently analyzed FOSC strains (Brankovics et al., 2017), two strains that are closely related the FOSC, and *F. redolens* that was used as the outgroup. A species tree was constructed based on the concatenated alignment of seven nuclear genes and the mitogenome to serve as a reference. Individual gene trees were then compared to the species tree identifying conflicts that may indicate hybridization events, incomplete lineage sorting or horizontal gene transfer. The comparative mitogenomic analyses identify two insertion events: the duplication of a conserved gene, *atp9*, into another gene's intron, and the insertion of variant 2 of the large variable (LV) region into a variant 1 of the LV region. In addition, the phylogeny of the LV variant 2 sequences is indicative of horizontal transfer within the FFSC and between the FFSC and the FOSC.

2. MATERIALS AND METHODS

2.1. Strains

In total 24 species belonging to the *F. fujikuroi* species complex (FFSC) were analyzed in this study, with 14 belonging to the African clade, 5 to the American clade, and 5 to the Asian clade of the FFSC (O'Donnell et al., 1998). In addition, nine strains were selected to represent the breadth and diversity of the *F. oxysporum* species complex (FOSC), and two sister species of the FOSC, *F. foetens* and *F. commune*, were analyzed. *F. redolens* was included as an outgroup to both the FFSC and the FOSC (**Table 1**).

2.2. Sequencing

For each strain a random sheared shotgun library was prepared using NEXTflex ChIP-seq Library prep kit with few adaptations for low input gDNA according to manufacturer's protocol (Bioscientific). The library was loaded on an Illumina paired-end flowcell for cluster generation using a cBot. Sequencing was done on an Illumina HiSeq2000 instrument using 125, 7, 125 flow cycles for forward, index, and reverse reads respectively. De-multiplexing of resulting data was carried out using Casava 1.8 software. The 26 strains sequenced for this study are

TABLE 1 | LV variant and intron presence in the analyzed strains.

Sp. complex	Clade	Strain	LV variant	Introns																										GenBank accession numbers
				atp6-i365	cob-i201	cob-i393	cob-i4	cob-i823	cox1-i218	cox1-i287	cox1-i392	cox1-i621	cox1-i715	cox1-i737	cox1-i873	cox1-i6	cox1-i1063	cox1-i1131	cox1-i1268	cox2-i228	cox3-i219	nad1-i636	nad2-i762	nad2-i1632	nad5-i717	nad5-i924	rnl-intron	
FFSC	African	***F. pseudoanthophilum* CBS414.97**	1		+	+	+		+	+	+	+	+		+		+		+		+			+		+	+	MT010924
		***F. brevicatenulatum* CBS404.97**	1		+	+	+		+	+	+	+	+		+		+		+	+	+			+		+	+	MT010923
		***F. napiforme* CBS748.97**	1		+	+	+			+	+	+	+		+		+		+					+		+	+	MT010918
		***F. ramigenum* CBS418.97**	2		+						+	+	+		+		+				+			+		+	+	MT010919
		***F. pseudonygamai* CBS417.97**	1		+	+	+	+			+	+	+		+		+		+					+			+	MT010925
		***F. ficicrescens* CBS125178**	2			+	+		+															+			+	MT010922
		***F. musae* CBS624.87**	1			+	+						+				+		+			+		+			+	MT010916
		***F. verticillioides* CBS576.78**	1										+				+					+		+			+	MT010915
		***F. andiyazi* CBS119857**	1									+												+			+	MT010917
		***F. nygamai* CBS749.97**	1												+				+			+		+			+	MT010926
		***F. lactis* CBS411.97**	2										+											+			+	MT010921
		***F. pseudocircinatum* CBS449.97**	1										+											+			+	MT010920
		***F. denticulatum* CBS407.97**	2			+							+	+	+		+	+						+			+	MT010934
	American	***F. guttiforme* CBS409.97**	1			+	+		+			+	+		+	+	+	+	+				+	+	+			+	MT010931
		***F. ananatum* CBS118516**	2			+	+		+			+	+		+	+	+		+				+	+	+			+	MT010930
		***F. begoniae* CBS452.97**	1[b]			+	+		+			+	+		+	+	+		+				+	+	+			+	MT010929
		***F. anthophilum* CBS119858**	1									+	+		+	+	+						+	+	+			+	MT010928
		***F. bactridioides* CBS100057**	1			+	+		+		+	+	+		+	+	+	+	+	+	+	+	+	+	+			+	MT010927
	Asian	***F. annulatum* CBS258.54**	2																									+	MT010912
		F. proliferatum ITEM2400	1																									+	LT841261
		***F. globosum* CBS428.97**	1																									+	MT010913
		***F. concentricum* CBS450.97**	1																									+	MT010911
		***F. sacchari* CBS147.25**	1			+	+		+		+		+	+										+			+	MT010910
	-[a]	***F. acutatum* CBS402.97**	1												+				+					+	+		+	MT010914
FOSC	3	*F. oxysporum* Fol4287	2			+																			+		+	LT6324
		F. oxysporum F11	1			+																			+		+	LT841205
		F. oxysporum FOSC3a	2			+	+																		+		+	LT6345
	4	***F. oxysporum* CBS130302**	1			+																			+		+	MT010933
	2	*F. oxysporum* Fom009	3																						+		+	LT6337
		F. oxysporum Fon013	2																						+		+	LT6337
		F. oxysporum N2	1																						+		+	LT6350
	1	*F. oxysporum* Il5	1	+		+	+																		+		+	LT6347
		F. oxysporum Foc011	1			+																			+		+	LT6308
		***F. foetens* CBS110286**	1																						+		+	MT010932
		F. commune JCM11502	1																			+			+		+	NC_036106
		***F. redolens* CBS743.97**	1											+			+			+							+	MT010909

*The strains are ordered according to the species tree (**Figure 6A**). F. acutatum belongs to the African clade sensu (O'Donnell et al., 1998), but it groups separately in the current analysis (shown as -[a]). The LV region of F. begoniae is variant 1 with a putative variant 2 insert (shown as 1[b]). Strains sequenced for this study are shown in bold.*

highlighted in Table 1. Sequencing data is available under the following accession number: PRJEB38038.

2.3. Assembly

The following (complete: from start to stop codon) nuclear protein coding genes were assembled from NGS data for all strains: γ-actin (*act*), β-tubulin II (*tub2*), calmodulin (*cal*), the largest and second largest subunit of DNA-dependent RNA polymerase II (*rpb1* and *rpb2*, respectively), translation elongation factor 1α (*tef1a*) and translation elongation factor 3 (*tef3*). These nuclear genes were selected for this study either because they are commonly used or have been suggested as good candidates for phylogeny and DNA barcoding for fungi (Stielow et al., 2015). Besides the nuclear protein coding genes, the complete mitochondrial genomes were also assembled for all strains.

The regions listed above were assembled from NGS reads using GRAbB (Genomic Region Assembly by Baiting; Brankovics et al., 2016) by specifying the appropriate reference sequence and employing SPAdes 3.6 (Bankevich et al., 2012; Nurk et al., 2013) as assembler.

2.4. Sequence Annotation

The initial mitogenome annotations were done using MFannot (http://megasun.bch.umontreal.ca/cgi-bin/mfannot/mfannotInterface.pl) and were manually improved: annotation of tRNA genes was improved using tRNAscan-SE (Pavesi et al., 1994), annotation of protein-coding genes and the *rnl* gene was corrected by aligning intronless homologs to the genome. Intron encoded proteins were identified using NCBI's ORF Finder (https://www.ncbi.nlm.nih.gov/orffinder/) and annotated using InterProScan (Mitchell et al., 2015).

2.5. Comparative Sequence Analysis

The nucleotide sequences were aligned using MUSCLE (Edgar, 2004a,b). Nuclear gene sequences were aligned per gene, while the mitochondrial sequences were aligned per region (exons, intergenic regions), and subsequently concatenated to yield the final alignment.

Genetic distances were calculated using the *ape* package (Paradis et al., 2004) of *R*: FASTA format sequence alignments were imported into *R*, pairwise distance were calculated using *dist.dna* function with standard settings. The *ggplot* function from the *ggplot2* package (Wickham, 2009) was used for plotting the distance data as a scatter plot. The *lm* function was used for linear regression, 0 intercept was used for the models.

In the mitogenome of *F. sacchari* a duplication was found involving *atp9*, therefore sequence repeats were identified using exonerate (Slater and Birney, 2005) by using the mitogenome of *F. sacchari* both as query and target. Hits were filtered, and repeats longer than 100 bp and scoring at least 80% of the possible maximal score were kept (settings were chosen for clarity of visualization). These hits were visualized using Circos (Krzywinski et al., 2009), which then was manually combined with the genetic map drawn using CLC Sequence Viewer.

2.6. Phylogenetic Analysis

Phylogenetic analyses were conducted using the ML method which was run using IQ-Tree (Nguyen et al., 2014) with model selection (Kalyaanamoorthy et al., 2017) and 1,000 ultrafast bootstraps (Hoang et al., 2017) and with the *F. redolens* as the outgroup. The phylogenetic trees were visualized using an in-house script *print-single-nwk.py* that is available on GitHub (https://github.com/b-brankovics/simple-nwk-tools). The comparison table between phylogenetic trees was generated using another in-house script *phylo-report.pl* that is available on GitHub (https://github.com/b-brankovics/phylo-report).

Clade monophyly was tested using the Shimodaira-Hasegawa (SH) test and the approximately unbiased (AU) test. In total, 34 constrain trees were specified: 33 trees with one branch from the reference tree specifying the constraint, also we added a constraint tree with the African clade. Each constrain tree was constructed for each alignment using IQ-tree. Then all the constrain trees per alignment were tested with the SH and AU tests built into IQ-tree. Finally, all results were collected and organized into **Table S1**.

3. RESULTS

3.1. Phylogeny

In order to get a robust estimate of the phylogeny of the analyzed strains, a concatenated alignment was used containing seven nuclear genes (*act*, *tub2*, *cal*, *rpb1*, *rpb2*, *tef1a*, and *tef3*) and the conserved region of the mitochondrial genome (excluding the large variable region and introns). The species tree (**Figure 1**) was estimated with maximum likelihood algorithm and 1,000 ultrafast bootstrap replicates using IQ-tree (Nguyen et al., 2014). Most of the clades on the tree received high bootstrap support except for two terminal branches (shown as Af32 and O27 in **Figure 1**). Interestingly, *F. acutatum* appeared as an early branching species within FFSC, instead of grouping with the other members from the African clade. In this study, we refer to the clade containing all the African clade member species except for *F. acutatum* as the "African" clade (shown as Af10 in **Figure 1**), in order to distinguish it from the African clade *sensu* (O'Donnell et al., 1998).

To identify conflicts between the species tree and trees based on subparts (concatenated nuclear genes, the conserved region of the mitogenome, concatenated mitochondrial coding sequences, concatenated protein coding sequence of the mitogenome, single nuclear and mitochondrial genes) of the alignment used for the estimation of the species tree, each tree was compared to the species tree. For the analysis, only internodes/clades that had at least 70% bootstrap support were considered, the rest were collapsed. **Figure 1** summarizes the results of this comparison by showing whether a given internode/clade (i) is present (S in **Figure 1**) with sufficient support (bootstrap $\geqslant$ 70) in the given tree, (ii) is contradicted (C in **Figure 1**) by a sufficiently supported clade, or (iii) neither (absent or insufficiently supported in the tree; (A in **Figure 1**). The FFSC, "African," American, Asian

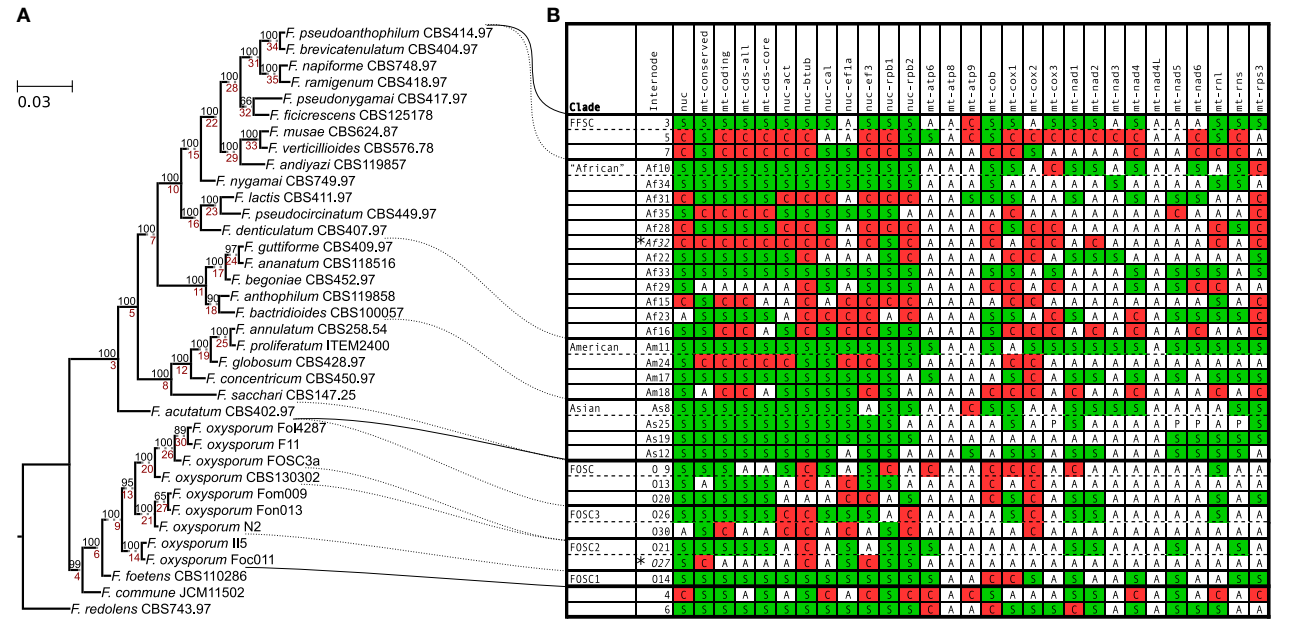

FIGURE 1 | Species tree and internode compatibility with individual trees. **(A)** Species tree estimated based on the concatenated sequence of the conserved region of the mitocgenome and seven nuclear protein coding genes; bootstrap values are shown above the branches, and internode labels are indicated below the branches (prefixes were added to some internodes based on their taxonomic position). These labels are unique numbers that are referred to by the internode column of the table. **(B)** The table summarizes the compatibility between the species tree and each of the other trees on internode level (the two internodes with insufficient support in the species tree are marked with asterisks). All insufficiently supported (BS $\geqslant$ 70) internodes were removed from the trees. Internode compatibility can be supported (S), absent (A) or conflicted/discordant (C). Internodes are ordered as they appear on the tree with the exception of ones that correspond to major clades. FFSC, *F. fujikuroi* species complex; The "African" (without *F. acutatum*), American & Asian clade of the FFSC; FOSC, *F. oxysporum* species complex). Column notations: nuc, concatenated nuclear genes; mt-conserved, conserved region of the mitogenome; mt-coding, concatenated coding sequences of the mitogenome (tRNA, rRNA, and protein coding); mt-cds-all, mitochondrial protein coding sequences; mt-cds-core, same as mt-cds-all, except *rps3* and *orf151* are not included; single genes have a prefix nuc for nuclear and mt for mitochondrial.

clades are supported by all concatenated trees, and show conflict with no more than one nuclear and a few mitochondrial gene trees. The FOSC clade was supported by three and conflicted by two nuclear single gene phylogenies. Two of the mitochondrial locus phylogenies (*atp8* and *nad4L*) lack well supported clades due to low levels of sequence variation in the alignments. All other phylogenies show at least one conflict (or discordance) with the species tree. These conflicts show the lack of concordance between the different gene genealogies which may be due to ancestral incomplete lineage sorting during the evolution of these groups or to horizontal gene transfer or the combination of the two.

In addition to comparing the species tree with individual phylogenies, the African clade *sensu* (O'Donnell et al., 1998) was also compared. It is contradicted by the tree based on the conserved region of the mitogenome, but supported by the rest of the concatenated trees. From the nuclear gene trees, *tub2* and *rpb1* support the clade, while the other nuclear gene trees are in conflict with it. Interestingly, *tub2* and *rpb1* are the two nuclear markers that contradict the FOSC clade. From the mitochondrial gene trees, *cox1*, *nad4*, and *nad6* support the clade, while *cox2*, *cox3*, *nad1*, *rns*, *rnl*, and *rps3* are in conflict with it. The clades of the species tree and the African clade were also tested using the Shimodaira-Hasegawa (SH) and the approximately unbiased (AU) tree topology tests implemented in IQ-tree (**Table S1**). The SH test has revealed that the only data set that significantly rejects the African clade is the conserved region of the mitogenome. The early branching of *F. acutatum* is significantly rejected by the *tub2* and *rpb1* genes and two of the concatenated mitochondrial data sets in the SH test. The AU test found more conflicts significant than the SH test. The AU test rejected the monophyly of the African clade based on the *rpb2* gene, which was the only nuclear gene that supported the early branching of *F. acutatum*.

Although the phylogenetic analysis based on the concatenated data set resulted in a well resolved tree with highly supported branches, examining the individual loci revealed several conflicts between the phylogenies that may indicate incomplete lineage sorting or horizontal gene transfer events in the evolution of the FFSC. Despite the conflicts in basal branches, all the phylogenies clearly separate FFSC and FOSC.

3.2. Mitochondrial Genome Assembly and Annotation

The mitogenomes of all strains were successfully assembled into single contigs with overlapping sequences at ends indicating circular topologies. Overlapping sequences were clipped before annotation and further analysis. The mitogenomes encoded for

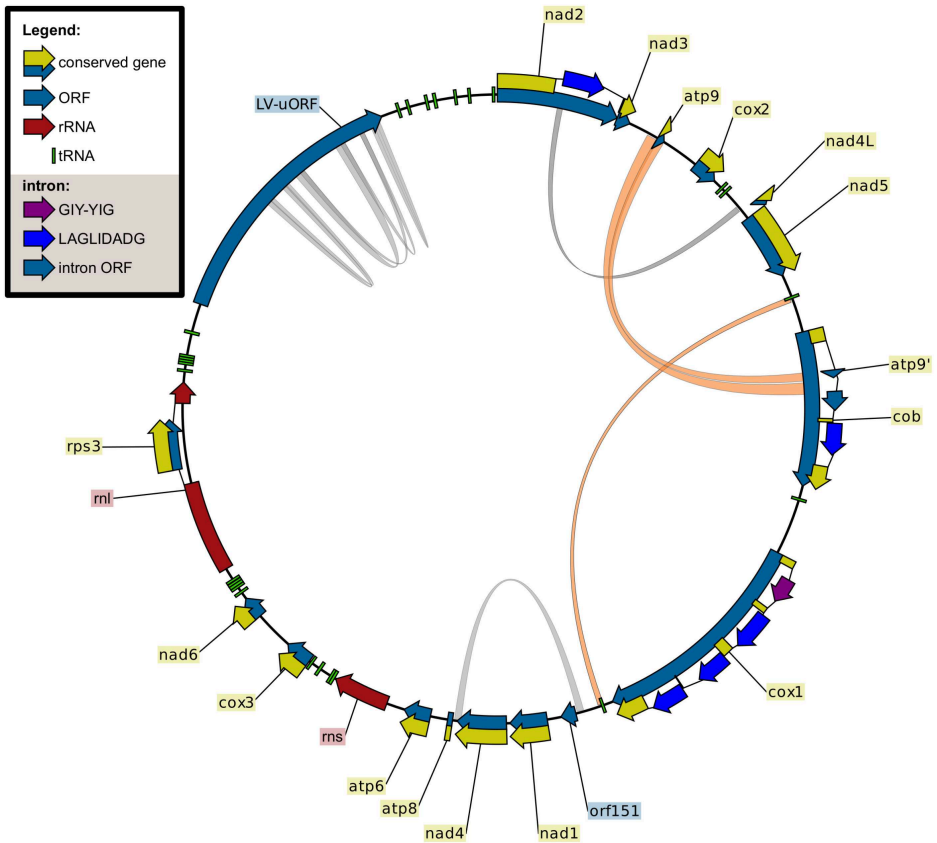

FIGURE 2 | Mitochondrial genome of *Fusarium sacchari* CBS 147.25. Genetic map created using CLC Sequence Viewer. Repeats larger than 100 bp were visualized using Circos, duplication of the *atp9* region into cob-i393 and the two copies of *trnR(tct)* are shown in orange.

the expected set of 14 "standard" mitochondrial polypeptide-encoding genes, a set of tRNA coding genes, two rRNA genes, and *rps3* located in an intron of the *rnl*. In addition, all genomes contained orf151 that has no functional prediction, and the large variable (LV) region. In accordance with earlier findings, gene content and order was conserved between species, and all genes and ORFs had the same orientation.

In total, 24 intron sites were found in the current data set in the following genes (**Table 1**): *atp6* (1), *cob* (4), *cox1* (11), *cox2* (1), *cox3* (1), *nad1* (1), *nad2* (2), *nad5* (2), and *rnl* (1). The only intron found in all strains analyzed was the intron of *rnl* harboring the *rps3* gene. The major clades of FFSC show different patterns of intron content: the American clade is intron rich, the Asian clade has a low intron content, while the African clade shows great variation. In the Asian clade, strains contain only the *rnl* intron, with the exception of *F. sacchari*. Interestingly, one of the introns of *cob*, cob-i393, in the mt sequence of *F. sacchari* contains a second copy of *atp9* (**Figures 2**, **3**). The analysis of this duplication is discussed in the next section.

One of the tRNA genes, *trnR(tct)*, was found to be duplicated in all strains analyzed (**Figure 2**). The duplicated gene shows great conservation, only two sequence variants with a single SNP difference were found in the genomes of the 36 strains. *F. redolens* contained two copies of variant A, while 32 out of 36 strains contained two copies of variant B. Curiously, *F. acutatum*, *F. commune* and *F. sacchari* contained both variants A and B of *trnR(tct)*. This might be the result of outcrossing of these groups with more distantly related species that contain variant A or it may be due to incomplete lineage sorting.

3.2.1. Duplication of *atp9* Into cob-i393 Intron

Comparing the sequence of cob-i393 intron of *F. sacchari* with that of the other species has revealed conservation of the first 0.7 kbp. The greatest similarity to the *F. sacchari* sequence was shown for the *F. ficicrescens* sequence (**Figure 3**). The region showing similarity did not contain any putative genes; however, MFannot and RNAweasel identified the intron based on this segment as a group ID intron, which matches the prediction for the other cob-i393 introns. Other ORFs identified in the cob-i393 introns of *F. sacchari* and *F. ficicrescens* had no functional annotation, neither CD-search nor IntreProScan did produce hits. The rest of the cob-i393 sequence of *F. sacchari* showed no similarity to intronic sequences found in the current data set.

The cob-i393 intron of *F. sacchari* contains a duplicate of *atp9* followed by a duplication of the upstream region of *atp9* and the first 24 bp of *atp9* (**Figure 3**). The *atp9* duplicate contained a codon insertion near the C-terminus and 3 SNPs, which were not found in any of the *atp9* sequences examined in this study.

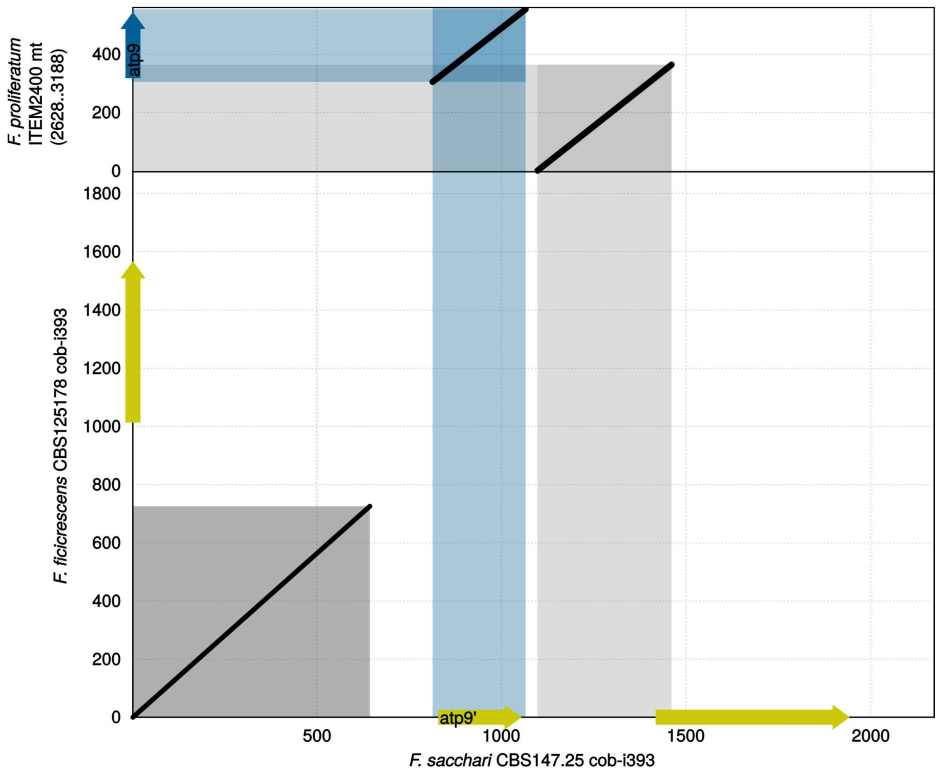

FIGURE 3 | Sequence comparison of cob-i393 of *F. sacchari* against cob-i393 of *F. ficicrescens* and mitogenome segment of *F. proliferatum* containing *atp9*. Conserved *atp9* shown as a blue arrow, while intronic coding sequences are shown as yellow arrows.

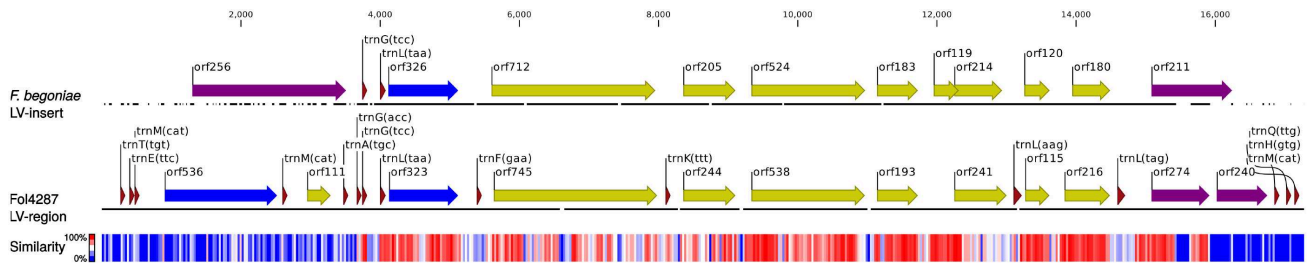

FIGURE 4 | Alignment between the insert in the LV region of *F. begoniae* and variant 2 of *F. oxysporum* Fol4287. Black lines: aligned sequences, gaps in the alignment are shown as gaps in the black lines; red triangles: tRNA genes; yellow arrows: ORFs; blue arrows: LAGLIDADG endonucleases; purple arrows: GIY-YIG endonucleases. Sequence similarity is indicated in color scale based on 30 bp segments. The scale above indicates position within the alignment.

Interestingly, the two duplicated sequence regions (*atp9* and its upstream region) showed greater similarity to other Asian clade strains than to *F. sacchari*. The corresponding regions are identical for all other Asian clade strains.

In conclusion, the duplicate of *atp9* and its upstream region found in the cob-i393 intron of *F. sacchari* has have probably originated from *F. sacchari* or another Asian clade species. During or after the duplication the sequence has mutated.

3.3. Large Variable Region

Most of the FFSC species analyzed contained variant 1 of the large variable (LV) region, typical of *Fusarium* spp. However, variant 2, which was previously reported only for *F. oxysporum*, was also found dispersed over the species complex in all three major clades: "African," American, and Asian. Furthermore, *F. begoniae* contained a LV-region that was a combination of variants 1 and 2.

3.3.1. Hybrid LV-Region in *F. begoniae*

The first 895 bp and the last 11,807 bp of the 25,064 bp long LV-region appeared to be an ortholog of variant 1 (**Figure S1**), while the 12,462 bp long sequence between these two segments showed high sequence similarity to a major part of variant 2 (**Figure 4** and **Figure S2**). These results indicate that the sequence segment similar to variant 2 represents a putative insert into the canonical variant 1 sequence.

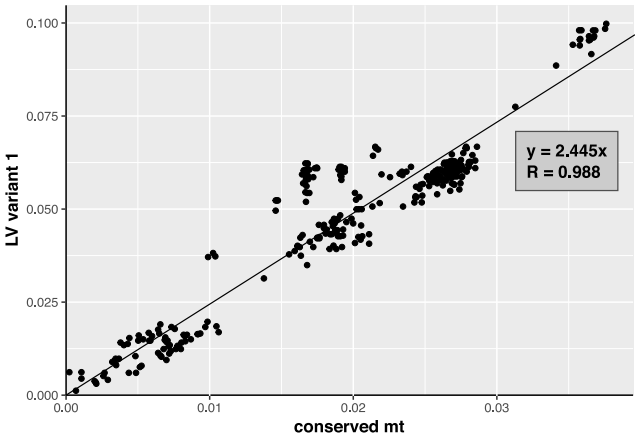

FIGURE 5 | Variant 1 of the LV region plotted against the mean genetic distance. The plot of genetic distance between strains based on variant 1 of LV-region against conserved mt region with trend line. Function of the trend line and *R* are shown on the plot.

The putative insert is located between two tRNA genes: the second copy of *trnM(cat)* and *trnG(tcc)*. Interestingly, the nucleotide preceding the insertion site is a thymidine and the last nucleotide of the insert is a guanosine which is the same as for typical mitochondrial introns. Although rnaweasel did not identify any intron specific motifs in the insert sequence both terminal regions of the insert contain ORFs that were predicted to be GIY-YIG homing endonucleases. The putative GIY-YIG endonuclease located near the upstream terminus of the insert showed no homology to any other sequence included in the current study, although it produced a partial hit with BLASTN to an ORF (orf275) in the mitogenome of *Beauveria caledonica* (GenBank accession: KT201150). The ORF is located in the intergenic region between *cox3* and *nad6* in *B. caledonica*. The putative GIY-YIG endonuclease located near the downstream terminus of the insert showed partial similarity to one of the GIY-YIG endonuclease found in the downstream region of variant 2 (**Figure 4**). The insert contains mostly ORFs with unknown functions, no hits were obtained with CD-Search or InterProScan, the size and positions of these ORFs are similar to the ones found in variant 2 sequences. Both the insert and variant 2 have the same two tRNA genes located upstream of a putative LAGLIDADG endonuclease. However, the insert contains no other tRNA genes in contrast to variant 2 of the LV region.

The inserted region shows several characteristics that are similar to mitochondrial regions: the preceding thymidine and the terminal guanosine nucleotide, also the presence of homing endonuclease genes. In addition, one of the endonucleases is similar to homing endonuclease that is located in intergenic region of *B. caledonica*. The insertion may have occurred following the same mechanism as introns are spread with a homing endonuclease that may recognize an intergenic target.

3.3.2. LV Variant 2 Shows Signs of Horizontal Transfer

To investigate whether the distribution of variants 1 and 2 within the FFSC is the result of incomplete lineage sorting or horizontal transfer of sequences, we compared the pairwise sequence distances based on the LV variant sequences and those based on the conserved part of the mitochondrial genomes, which excluded the LV-region and intron sequences. The two distances, based on variant sequence and based on the conserved region, were plotted against each other using a scatter plot. A trend line, representing the correlation between the two distances, was estimated for each of the plots. For this analysis three alignments were created: for variant 1, for variant 2, and for the conserved region. The putative insert in the LV-region of *F. begoniae* was excluded from this analysis, by removing it from the LV sequence; the resulting sequence was included as a variant 1 sequence.

The pairwise genetic distances estimated based on variant 1 sequences showed good correlation with those based on the conserved mt region ($R = 0.988$; **Figure 5**). In contrast, correlation between the pairwise genetic distances estimated based on variant 2 and the conserved region showed weaker correlation ($R = 0.898$; **Figure 6B**). The variant 2 sequence of *F. ramigenum* was more similar to that of strains belonging to the FOSC than to strains belonging to the FFSC (**Figure 6B**). The topology of the maximum likelihood tree calculated based on variant 2 (**Figure S3**) showed several conflicts with the conserved region or the species tree, most notably: (i) *F. ramigenum* was clustered inside the FOSC with high support, and (ii) *F. annulatum* (Asian clade) and *F. ficicrescens* ("African" clade) grouped together in a well-supported (bootstrap=100) clade separate from the rest of the FFSC strains.

In conclusion, the variant 1 of the LV region appears to follow the evolution of the conserved parts of the mitogenome, while the variant 2 shows several deviations from the expected pattern. Variant 2 is distributed across the FFSC and FOSC and its genealogy deviates from those of other markers that suggests the pattern is the result of horizontal transfer, most probably due to introgression.

4. DISCUSSION

Three biogeographic clades (African, American, and Asian) have been described within the *F. fujikuroi* species complex (FFSC) based on phylogenetic data (O'Donnell et al., 1998). Although multilocus sequence analysis supports the recognition of the three clades, several genetic markers produce topologies that appear to contradict this grouping, such markers include the ITS2 region (O'Donnell et al., 1998, 2000) and the fumonisin biosynthetic gene (FUM) cluster (Proctor et al., 2013). Comparative mitochondrial genome analyses have indicated possible recombination events in the evolutionary history of the *F. fujikuroi* species complex (FFSC) based on conflicting single gene tree topologies (Fourie et al., 2013, 2018). In this study, a large set (24 species) of FFSC and a representative set of FOSC strains were sequenced to compare their mitochondrial genome, and to contrast phylogenetic results of concatenated regions

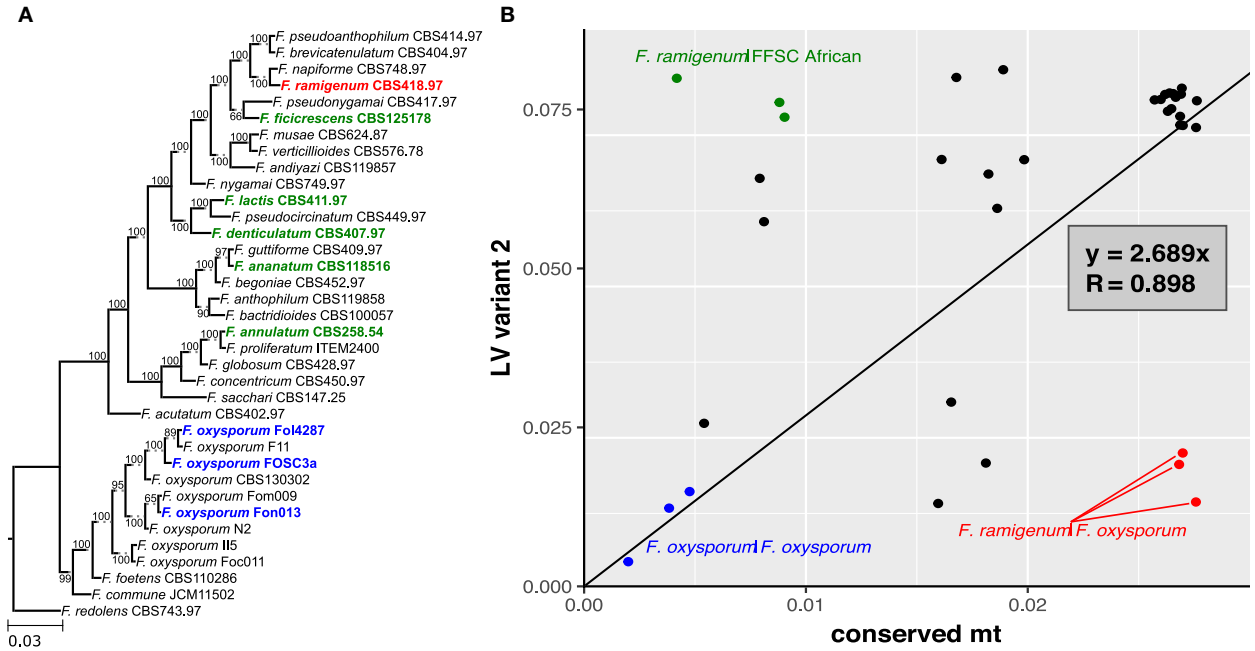

FIGURE 6 | LV region of *F. ramigenum* is most similar to that of *F. oxysporum*. **(A)** Species tree with bootstrap support, strains with variant 2 of the LV region are shown in boldface. **(B)** The plot of genetic distance between strains based on variant 2 of LV-region against conserved mt region with trend line. Function of the trend line and *R* are shown on the plot. FFSC vs. *F. ramigenum* are shown in green, while FOSC vs. *F. ramigenum* is shown in red. The three FOSC comparisons are shown in blue.

and individual genes, both nuclear and mitochondrial, in order to investigate the evolutionary relationship between and within these groups.

The phylogenetic analysis indicated that *F. acutatum* clusters separately from the three biogeographic clades, while it should group within the African clade (O'Donnell et al., 1998). The monophyly of the African clade was supported by only five of the markers, but was conflicted by eleven loci analyzed. The weak support for the clustering of *F. acutatum* within the African clade is in agreement with earlier findings (O'Donnell et al., 2000). However, the other two clades (American and Asian) were robustly supported by the majority of loci, and even the "African" clade (African clade = *F. acutatum* ∪ "African" clade) was robustly supported. The "African" clade contained the largest number of clades with extensive conflicts with the individual gene trees. In addition, the "African" clade had the most diverse intron pattern, while the other two clades had a more homogeneous intron distribution. Both of these facts suggest that incomplete lineage sorting or recombination is confounding the phylogenetic reconstruction in this group.

The comparative analysis of the mitochondrial genome sequences provided further evidence for deviation from the classical tree-like model of evolution for the FFSC. Variant 2 of the LV-region was found in representatives of all three major clades of the FFSC. This variant was previously known only for clades 1 and 2 of the *F. oxysporum* species complex (FOSC), where the most probable explanation for the distribution of the variant across both clades was shown to be incomplete lineage sorting (Brankovics et al., 2017). In order to identify whether the distribution of the variant within the FFSC can be explained by horizontal transfer or incomplete lineage sorting, the genetic distance calculated based on the LV variants was compared to that calculated based on the conserved region of the mitogenome. The genetic distances based on variant 1, the predominant variant in the genus, showed strong correlation with those based on the conserved regions. However, the results for variant 2 significantly deviated from the pattern expected for vertical inheritance. The variant 2 sequence of *F. ramigenum* showed greater similarity to variant 2 sequences of FOSC strains than to that of other FFSC strains, indicating horizontal transfer of this region between members of the two species complexes. Besides horizontal transfer between the two species complexes, the sequence evolution of variant 2 is suggestive of horizontal transfer between the different clades within the FFSC.

Interfertility of species belonging to the Asian clade of the FFSC has been demonstrated under laboratory conditions (Leslie et al., 2004). The viability of the progeny of interspecies crosses was shown to be significantly lower than for within species crosses, indicating only partial genetic incompatibility between these species. Although the genetic distance between *F. oxysporum* and FFSC is greater than the genetic distance between any two FFSC species, both *F. oxysporum* and FFSC species have 12 core chromosomes, which show large levels of synteny to each other (Ma et al., 2010). This similarity on chromosome level may allow low levels of cross-fertility even between the two species complexes. Although *F. oxysporum* is usually considered asexual, based on the phenomenon of horizontal chromosome transfer between strains

and comparative mitogenome analysis it supposed to have a cryptic sexual or (para)sexual cycle (Brankovics et al., 2017). The possibility of (rare) out-crossing between the two complexes is supported by phylogenetic data of the ITS2 region (O'Donnell et al., 1998) and of the FUM cluster (Proctor et al., 2013). In the case of ITS2, both species complexes have been shown to have two divergent types of the region (O'Donnell et al., 1998). While for the FUM cluster, the two FOSC strains that carry the cluster group within the FFSC based on FUM gene trees (Proctor et al., 2013). These findings show that introgression between the FFSC and FOSC has played an important role in the evolutionary history of these two complexes.

In the mitochondrial genomes, the conserved genes show complete synteny and the coding sequences show very high levels of sequence similarity, whereas the nuclear chromosomes show occasional rearrangements. Thus, recombination between mitogenomes would be less likely to lead to lower fitness than nuclear recombination, because it is less likely to lead to rearrangements or deletions. Cytoplasmic fusion without karyogamy between hyphae of FFSC and FOSC strains could allow for mitochondrial recombination as well as transfer of genetic information between the nuclei through mobile elements or other genetic mechanisms. Accordingly, mitogenomes could be used as indicators for detecting interspecies gene flow.

Besides the phylogenetic value of the mitogenomes assembled for this study, their comparative analysis provides insights into the evolution of these organellar genomes. Analysis of mitogenomes of the FOSC has already indicated that homing endonucleases (HE) may have played an important role in the origin of variants 2 and 3 of the LV region (Brankovics et al., 2017). Homing endonucleases are frequently associated with group I mitochondrial introns; they are able to specifically cleave double stranded DNA and introduce their genes into the target region (Burt and Koufopanou, 2004). In the current study, a putative insert was identified in the LV region of *F. begoniae* that contained HE genes at both termini, providing further support for the importance of HE genes in mitochondrial genome rearrangements. Since HEs have a driving role in gene conversion events, the most likely sites for introgression events are the target sequences of HEs and their vicinity.

Another interesting finding of the mitogenome analysis is the identification of the duplication of *atp9* into an intron of *cob* in *F. sacchari*. The resulting intron contains no HE genes, which is similar to the intron in *rnl* that contains the *rps3* gene only. The translocation of *rps3* into the intron of *rnl* happened in the ancestor of the *Pezizomycotina* (Ghikas et al., 2006). The duplication of *atp9* indicates that the same or similar mechanisms are still active on the mitogenome of the FFSC. The intronization of genes and intergenic segments, like that of *atp9* and its upstream intergenic region, may allow the evolution of rearranged regions that afterwards could replace the original region through recombination. This could be the mechanism behind the evolution of the new variants of the LV region. The intronic origin would also explain why HE genes are present in this region, since they are typically intron encoded.

5. CONCLUSIONS

Complete mitogenome sequences can provide a robust basis for phylogeny. In contrast, the duplication of *atp9* suggests that single mitochondrial genes may lead to inaccurate phylogenetic estimates, due to possible paralogs.

Mitogenomes could be used as indicators for detecting interspecies gene flow, since mitogenomes show greater levels of conservation and synteny than nuclear regions. Introgression among and between members of *Fusarium oxysporum* and *F. fujikuroi* species complexes has played an important role in the evolutionary history of these two complexes, which has to be taken into consideration when analyzing gene genealogies for these groups.

DATA AVAILABILITY STATEMENT

The datasets generated for this study can be found in the NCBI's GenBank database (MT010857-MT011064) and in the SRA (NCBI/ENA) database (PRJEB38038).

AUTHOR CONTRIBUTIONS

BB, AD, TL, and CW designed the study. AD, TL, and CW sequenced large part of the strains used for this study. BB carried out the analysis. BB wrote the first draft. All authors helped shaping the manuscript and approved the final version of the manuscript.

FUNDING

The investigations were supported by the Division for Earth and Life Sciences (ALW) with financial aid from the Netherlands Organization for Scientific Research (NWO, http://www.nwo.nl/) under grant number 833.13.006. This work was further supported by the MycoKey project (EU Project H2020-E.U.3.2-678781). The funding organizations had no role in study design, data collection and analysis, decision to publish, or preparation of the manuscript.

SUPPLEMENTARY MATERIAL

The Supplementary Material for this article can be found online at: https://www.frontiersin.org/articles/10.3389/fmicb.2020.01092/full#supplementary-material

Figure S1 | LV region of *F. begoniae* and of *F. anthophilum* (variant 1). Gray area represents the insert region in the LV-region of *F. begoniae*.

Figure S2 | LV region of *F. begoniae* and of *F. oxysporum* Fol4287 (variant 2). Gray area represents the insert region in the LV-region of *F. begoniae*.

Figure S3 | Unrooted maximum likelihood tree based on LV variant 2 sequences. Bootsptrap values (based on 1,000 replicates) are indicated below the branches.

Table S1 | The *p*-values for the topology constrain analysis. The internodes are the same that were used for **Figure 1B** with the addition of the African clade.

REFERENCES

Al-Reedy, R. M., Malireddy, R., Dillman, C. B., and Kennell, J. C. (2012). Comparative analysis of *Fusarium* mitochondrial genomes reveals a highly variable region that encodes an exceptionally large open reading frame. *Fungal Genet. Biol.* 49, 2–14. doi: 10.1016/j.fgb.2011.11.008

Anderson, E. (1949). *Introgressive Hybridization*. New York, NY; London: John Wiley and Sons, Inc.; Chapman and Hall, Ltd. doi: 10.5962/bhl.title.4553

Anderson, E., and Hubricht, L. (1938). Hybridization in tradescantia. III. The evidence for introgressive hybridization. *Am. J. Bot.* 25, 396–402. doi: 10.1002/j.1537-2197.1938.tb09237.x

Arvestad, L., Berglund, A.-C., Lagergren, J., and Sennblad, B. (2003). Bayesian gene/species tree reconciliation and orthology analysis using MCMC. *Bioinformatics* 19(Suppl. 1), 7–15. doi: 10.1093/bioinformatics/btg1000

Bankevich, A., Nurk, S., Antipov, D., Gurevich, A. A., Dvorkin, M., Kulikov, A. S., et al. (2012). SPAdes: A new genome assembly algorithm and its applications to single-cell sequencing. *J. Comput. Biol.* 19, 455–477. doi: 10.1089/cmb.2012.0021

Brankovics, B., van Dam, P., Rep, M., de Hoog, G. S., van der Lee, T. A. J., Waalwijk, C., et al. (2017). Mitochondrial genomes reveal recombination in the presumed asexual *Fusarium oxysporum* species complex. *BMC Genomics* 18:735. doi: 10.1186/s12864-017-4116-5

Brankovics, B., Zhang, H., van Diepeningen, A. D., van der Lee, T. A. J., Waalwijk, C., and de Hoog, G. S. (2016). GRAbB: Selective assembly of genomic regions, a new niche for genomic research. *PLoS Comput. Biol.* 12:e1004753. doi: 10.1371/journal.pcbi.1004753

Burt, A., and Koufopanou, V. (2004). Homing endonuclease genes: the rise and fall and rise again of a selfish element. *Curr. Opin. Genet. Dev.* 14, 609–615. doi: 10.1016/j.gde.2004.09.010

Edgar, R. C. (2004a). MUSCLE: a multiple sequence alignment method with reduced time and space complexity. *BMC Bioinformatics* 19:113. doi: 10.1186/1471-2105-5-113

Edgar, R. C. (2004b). MUSCLE: multiple sequence alignment with high accuracy and high throughput. *Nucleic Acids Res.* 32, 1792–1797. doi: 10.1093/nar/gkh340

Fourie, G., van der Merwe, N. A., Wingfield, B. D., Bogale, M., Tudzynski, B., Wingfield, M. J., et al. (2013). Evidence for inter-specific recombination among the mitochondrial genomes of *Fusarium* species in the *Gibberella fujikuroi* complex. *BMC Genomics* 14:605. doi: 10.1186/1471-2164-14-605

Fourie, G., van der Merwe, N. A., Wingfield, B. D., Bogale, M., Wingfield, M. J., and Steenkamp, E. T. (2018). Mitochondrial introgression and interspecies recombination in the *Fusarium fujikuroi* species complex. *IMA Fungus* 9, 37–48. doi: 10.5598/imafungus.2018.09.01.04

Ghikas, D. V., Kouvelis, V. N., and Typas, M. A. (2006). The complete mitochondrial genome of the entomopathogenic fungus *Metarhizium anisopliae* var. anisopliae: gene order and trn gene clusters reveal a common evolutionary course for all Sordariomycetes, while intergenic regions show variation. *Arch. Microbiol.* 185, 393–401. doi: 10.1007/s00203-006-0104-x

Hoang, D. T., Chernomor, O., von Haeseler, A., Minh, B. Q., and Vinh, L. S. (2017). UFBoot2: improving the ultrafast bootstrap approximation. *Mol. Biol. Evol.* 35, 518–522. doi: 10.1093/molbev/msx281

Kalyaanamoorthy, S., Minh, B. Q., Wong, T. K. F., von Haeseler, A., and Jermiin, L. S. (2017). ModelFinder: fast model selection for accurate phylogenetic estimates. *Nat. Methods* 14, 587–589. doi: 10.1038/nmeth.4285

Krzywinski, M., Schein, J., Birol, I., Connors, J., Gascoyne, R., Horsman, D., et al. (2009). Circos: an information esthetic for comparative genomics. *Genome Res.* 19, 1639–1645. doi: 10.1101/gr.092759.109

Leslie, J. F., Zeller, K. A., Wohler, M., and Summerell, B. A. (2004). Interfertility of two mating populations in the *Gibberella fujikuroi* species complex. *Eur. J. Plant Pathol.* 110, 611–618. doi: 10.1023/B:EJPP.0000032400.55446.d8

Ma, L.-J., van der Does, H. C., Borkovich, K. A., Coleman, J. J., Daboussi, M.-J., Di Pietro, A., et al. (2010). Comparative genomics reveals mobile pathogenicity chromosomes in *Fusarium*. *Nature* 464, 367–373. doi: 10.1038/nature08850

Mitchell, A., Chang, H.-Y., Daugherty, L., Fraser, M., Hunter, S., Lopez, R., et al. (2015). The InterPro protein families database: the classification resource after 15 years. *Nucleic Acids Res.* 43, D213–D221. doi: 10.1093/nar/gku1243

Nguyen, L.-T., Schmidt, H. A., von Haeseler, A., and Minh, B. Q. (2014). IQ-TREE: a fast and effective stochastic algorithm for estimating maximum-likelihood phylogenies. *Mol. Biol. Evol.* 32, 268–274. doi: 10.1093/molbev/msu300

Niehaus, E.-M., Münsterkötter, M., Proctor, R. H., Brown, D. W., Sharon, A., Idan, Y., et al. (2016). Comparative "omics" of the *Fusarium fujikuroi* species complex highlights differences in genetic potential and metabolite synthesis. *Genome Biol. Evol.* 8, 3574–3599. doi: 10.1093/gbe/evw259

Novichkov, P. S., Omelchenko, M. V., Gelfand, M. S., Mironov, A. A., Wolf, Y. I., and Koonin, E. V. (2004). Genome-wide molecular clock and horizontal gene ransfer in bacterial evolution. *J. Bacteriol.* 186, 6575–6585. doi: 10.1128/JB.186.19.6575-6585.2004

Nurk, S., Bankevich, A., Antipov, D., Gurevich, A. A., Korobeynikov, A., Lapidus, A., et al. (2013). Assembling single-cell genomes and mini-metagenomes from chimeric MDA products. *J. Comput. Biol.* 20, 714–737. doi: 10.1089/cmb.2013.0084

O'Donnell, K., Cigelnik, E., and Nirenberg, H. I. (1998). Molecular systematics and phylogeography of the *Gibberella fujikuroi* species complex. *Mycologia* 90, 465–493. doi: 10.1080/00275514.1998.12026933

O'Donnell, K., Nirenberg, H. I., Aoki, T., and Cigelnik, E. (2000). A multigene phylogeny of the *Gibberella fujikuroi* species complex: detection of additional phylogenetically distinct species. *Mycoscience* 41, 61–78. doi: 10.1007/BF02464387

Paradis, E., Claude, J., and Strimmer, K. (2004). APE: analyses of phylogenetics and evolution in R language. *Bioinformatics* 20, 289–290. doi: 10.1093/bioinformatics/btg412

Pavesi, A., Conterio, F., Bolchi, A., Dieci, G., and Ottonello, S. (1994). Identification of new eukaryotic tRNA genes in genomic DNA databases by a multistep weight matrix analysis of transcriptional control regions. *Nucleic Acids Res.* 22, 1247–1256. doi: 10.1093/nar/22.7.1247

Proctor, R. H., Van Hove, F., Susca, A., Stea, G., Busman, M., van der Lee, T., et al. (2013). Birth, death and horizontal transfer of the fumonisin biosynthetic gene cluster during the evolutionary diversification of *Fusarium*. *Mol. Microbiol.* 90, 290–306. doi: 10.1111/mmi.12362

Slater, G. S. C., and Birney, E. (2005). Automated generation of heuristics for biological sequence comparison. *BMC Bioinformatics* 6:31. doi: 10.1186/1471-2105-6-31

Stielow, J. B., Lévesque, C. A., Seifert, K. A., Meyer, W., Irinyi, L., Smits, D., et al. (2015). One fungus, which genes? Development and assessment of universal primers for potential secondary fungal DNA barcodes. *Persoonia* 35, 242–263. doi: 10.3767/003158515X689135

Ward, T. J., Bielawski, J. P., Kistler, H. C., Sullivan, E., and O'Donnell, K. (2002). Ancestral polymorphism and adaptive evolution in the trichothecene mycotoxin gene cluster of phytopathogenic *Fusarium*. *Proc. Natl. Acad. Sci. U.S.A.* 99, 9278–9283. doi: 10.1073/pnas.142307199

Wickham, H. (2009). *ggplot2: Elegant Graphics for Data Analysis*. New York, NY: Springer-Verlag. doi: 10.1007/978-0-387-98141-3

Zhou, Y., Duvaux, L., Ren, G., Zhang, L., Savolainen, O., and Liu, J. (2017). Importance of incomplete lineage sorting and introgression in the origin of shared genetic variation between two closely related pines with overlapping distributions. *Heredity* 118, 211–220. doi: 10.1038/hdy.2016.72

Conflict of Interest: The authors declare that the research was conducted in the absence of any commercial or financial relationships that could be construed as a potential conflict of interest.

Advantages of publishing in Frontiers

OPEN ACCESS
Articles are free to read for greatest visibility and readership

FAST PUBLICATION
Around 90 days from submission to decision

HIGH QUALITY PEER-REVIEW
Rigorous, collaborative, and constructive peer-review

TRANSPARENT PEER-REVIEW
Editors and reviewers acknowledged by name on published articles

Frontiers
Avenue du Tribunal-Fédéral 34
1005 Lausanne | Switzerland

Visit us: www.frontiersin.org
Contact us: frontiersin.org/about/contact

REPRODUCIBILITY OF RESEARCH
Support open data and methods to enhance research reproducibility

DIGITAL PUBLISHING
Articles designed for optimal readership across devices

FOLLOW US
@frontiersin

IMPACT METRICS
Advanced article metrics track visibility across digital media

EXTENSIVE PROMOTION
Marketing and promotion of impactful research

LOOP RESEARCH NETWORK
Our network increases your article's readership